INVESTIGATING SECRETION OF EFFECTORS TO HOST RED BLOOD CELLS BY *PLASMODIUM FALCIPARUM*

by

DAVID ANAGUANO-PILLAJO

(Under the Direction of Vasant Muralidharan)

ABSTRACT

Malaria is a deadly disease caused by *Plasmodium falciparum* parasites. The clinical manifestations of malaria are closely tied to parasite proliferation within human red blood cells (RBCs). Intracellular development initiates by merozoite invasion of RBCs, which is subsequently followed by parasite remodeling of the host RBC to establish successful infection. Secretion of parasite proteins into the RBC plays a crucial role for the development of both processes. In this manuscript, I present a study focusing on these two processes, which include screening interactors of proteins associated with protein export and investigating the role of a protein essential for merozoite invasion.

Protein export is essential for remodeling RBCs. However, the process by which membrane proteins are extracted from the parasite's plasma membrane (PPM) for export remains a mystery. In the first study, we addressed this question by fusing the exported membrane protein SBP1 with TurboID, a highly efficient biotin ligase. Through time-resolved proximity biotinylation and quantitative proteomics, we identified two groups of $SBP1^{TbID}$ interactors: early (pre-export) and late (post-export) interactors. Significantly, two membrane-associated proteins emerged as pre-export interactors, one harboring a predicted translocon domain, potentially facilitating the export

of membrane proteins. Conditional mutants of these candidates were found essential for asexual growth and localized at the host-parasite interface during early ring stages, suggesting a potential interaction with membrane proteins at the PPM for export to the host RBC.

Invasion of RBCs involves effectors secreted from specialized organelles like the rhoptries. Our work focused on Rhoptry Neck Protein 11 (RON11), which contains seven transmembrane domains and a calcium-binding EF-hand domain. RON11 knockdown mutants inhibited parasite growth by preventing merozoite invasion of RBCs. Utilizing ultrastructure expansion microscopy (U-ExM), we observed unique phenotypes, with RON11 depletion leading to fully developed merozoites featuring single rhoptries. Surprisingly, RON11 loss did not affect attachment or rhoptry effector release but blocked merozoite internalization. Furthermore, we demonstrated RON11 involvement in forming the second rhoptry pair after the initiation of merozoite segregation. In summary, RON11 is a key player in generating two rhoptries and is critical for merozoite internalization into RBCs, shedding light on the invasion mechanisms of *P. falciparum*.

INDEX WORDS: *Plasmodium falciparum*, malaria, protein export, proximity labeling, rhoptry biogenesis, invasion, Ultrastructure expansion microscopy

INVESTIGATING SECRETION OF EFFECTORS TO HOST RED BLOOD CELLS BY *PLASMODIUM FALCIPARUM*

by

DAVID ANAGUANO-PILLAJO

B.S., Universidad de las Fuerzas Armadas-ESPE, Ecuador, 2014

M.Sc., University of Massachusetts-Amherst, 2018

A Dissertation Submitted to the Graduate Faculty of The University of Georgia in Partial Fulfillment of the Requirements for the Degree

DOCTOR OF PHILOSOPHY

ATHENS, GEORGIA

2023

INVESTIGATING SECRETION OF EFFECTORS TO HOST RED BLOOD CELLS BY *PLASMODIUM FALCIPARUM*

by

DAVID ANAGUANO-PILLAJO

Major Professor:	Vasant Muralidharan
Committee:	Belen Cassera
	Tania De Koning-Ward
	Roberto Docampo
	Karl F. Lechtreck

Electronic Version Approved:

Ron Walcott
Vice Provost for Graduate Education and Dean of the Graduate School
The University of Georgia
December 2023

DEDICATION

Para Marcelino y Blanca. Gracias por guiarme a ser la persona que soy ahora y por siempre dejarme soñar en grande. Por ustedes y para ustedes.

ACKNOWLEDGEMENTS

First, I want to thank my family. Thanks for being a great support through my career and personal life. I could not see you as often as I would have wanted to, but I know you are always there cheering for me.

To my mentors throughout my short scientific career. Thanks for trusting in me and giving me opportunities to grow, and especially for showing me that you can be a successful scientist while caring about mentees.

At last but not least, to the friends I have made through graduate school. Thanks for making this journey that is coming to an end, enjoyable and worth it to remember. It is never the place, but the people you share with.

TABLE OF CONTENTS

Page

LIST OF TABLES

Page

LIST OF FIGURES

Page

CHAPTER 1

1. INTRODUCTION AND LITERATURE REVIEW

1.1. Malaria and *Plasmodium falciparum*

Malaria is a life-threatening disease caused by the apicomplexan parasite of the genus *Plasmodium* and transmitted by the insect vector of the genus *Anopheles*. Malaria is a major global health issue with nearly half of the world population in risk of contracting the disease, especially in regions between the tropics (Cowman et al. 2016). In 2021, an estimated of 247 million cases, resulting in 619 000 deaths, were attributed to the disease (World Health Organization 2022). Out of the five *Plasmodium* species known to infect humans, *Plasmodium falciparum* is the most virulent, lethal, and widely distributed, accounting for 98% of the cases worldwide, especially in Africa where is responsible for almost the entirety of cases and deaths by malaria. The majority of the deaths are in children under the age of five, making malaria one of the global leading causes of child mortality, just after pneumonia and diarrhea, especially in sub-Saharan Africa (Liu et al. 2012, 2016; Sarfo et al. 2023).

Global efforts on malaria burden reduction resulted on a steady decline of cases and deaths by 2019 of 232 million cases and 568 000 deaths, however the COVID-19 pandemic resulted in an increase of numbers due to disruptions of prevention campaigns and other essential malaria services, especially in countries with higher malaria impact (World Health Organization 2022). Efforts towards the development of vaccines have also been substantial, with the approval of the

first vaccine, RTS,S, in 2021 (World Health Organization 2021). While RTS,S vaccine efficacy was moderate during the first year, protection wore off over time (S. C. T. P. (2014) Rts 2014; S. Rts and Others 2015). Under these premises, and with the recent alarming development of artemisinin resistance on regions of Southeast Asia and East Africa (Ahorhorlu et al. 2023; Balikagala et al. 2021; Uwimana et al. 2021), it is essential to understand better the mechanisms *P. falciparum* utilizes to infect and develop within red blood cells. This would help us to find new effectors that can be targeted for drug development.

The complex life cycle of *P. falciparum* alternates between two hosts: female mosquitoes of the *Anopheles* genus and humans. Sporozoites injected after the bite of an infected mosquito are transported through the skin to the lymphatics and into the liver. There they infect hepatocytes, where a single sporozoite can asexually replicate into tens of thousands of merozoites. These merozoites are released into the blood stream, and there they infect red blood cells (RBC) to start a 48-hour intraerythrocytic life cycle, where the parasites undergo repeated rounds of growth, replication, egress, and invasion. This cycle is associated with the generation of clinical symptoms and the mortality of malaria infections. Eventually, a subset of parasites will develop into female and male gametocytes, to undergo sexual replication within the Anopheles mosquito, after the mosquito takes a blood meal from an infected human host. These parasites will replicate and develop into sporozoites within the mosquito, before being injected again into a human host to start the cycle again.

This intraerythrocytic cycle is associated with the generation of clinical symptoms, such as headaches, myalgia, high fevers, severe anemia, pulmonary and renal failure, vascular obstruction, and cerebral damage. These disorders could persist even after parasite clearance and are a

consequence of the development of the parasite within human RBCs. Untreated, or non- promptly treated infections can lead to severe illness or death.

1.2. Protein export

During its asexual life cycle, *P. falciparum* parasites invade RBCs and enclose themselves in invaginations predominantly composed of the erythrocyte membrane, resulting in the formation of the parasitophorous vacuole (PV) (Lingelbach and Joiner 1998; Geoghegan et al. 2021). Red blood cells provide an unfavorable environment for parasite development. The absence of a major histocompatibility complex provides an ideal intracellular hideout for parasites. However, this environment also exposes them to adverse conditions, such as the absence of essential biosynthetic pathways, subcellular organelles, and nutritional resources that could otherwise be exploited by the parasite for growth and replication. To generate a successful infection withing RBCs, *P. falciparum* parasites extensively remodel their host cells to generate a more suitable niche.

Among the modifications made by the parasites, the formation of Maurer's cleft, knobs, and new permeability pathways (NPPs) are noteworthy. The Maurer's clefts are flattened subcellular organelles localized in the RBC cytoplasm, functioning as transport hubs for proteins exported to the host cell membrane (Mundwiler-Pachlatko and Beck 2013). Notably, they are involved in the transport of members of the *P. falciparum* erythrocyte membrane protein 1 (PfEMP1) family, that are the main ligands responsible for cytoadherence and antigenic variation (Rug et al. 2014; McHugh et al. 2020; Carmo et al. 2022; Maier et al. 2007). The knobs are structures protruding from the RBC surface that facilitate the cytoadherence of infected RBCs to the endothelium. These structures consist mostly of the knob-associated histidine-rich protein (KAHRP) (Crabb et al. 1997; Rug et al. 2014; Looker et al. 2019) and are loaded with proteins

from the family PfEMP1(K. L. Waller et al. 1999; Oh et al. 2000). Finally, the NPPs are modifications in the RBC membrane acting as channels to enable nutrient uptake and waste efflux from hemoglobin digestion (Desai, Krogstad, and McCleskey 1993; Counihan, Modak, and de Koning-Ward 2021). The gene family known as RhopH1, which is comprised by the clag2, clag3.1, clag3.2, clag8 and clag9 genes primarily constitutes the NPPs involved on solute transport (Nguitragool et al. 2011; Pillai et al. 2012; Osamu Kaneko et al. 2005; O. Kaneko et al. 2001; Ling et al. 2004).

This remodeling of RBCs involves the export of approximately 500 parasite proteins – equivalent to 10% of the parasite proteome – towards the host cell (Boddey et al. 2013; Hiller et al. 2004; Jonsdottir et al. 2021; van Ooij et al. 2008). During this process, exported proteins traverse various membranes, such as the parasite plasma membrane (PPM) and the parasitophorous vacuole membrane (PVM), to reach their final destination in the RBC cytoplasm or membrane.

The initial proteins secreted into the RBC are factors secreted during invasion from merozoite secretory organelles, namely dense granules and rhoptries. These factors play essential roles in attachment, invasion and subsequent development within the RBC (Cova, Lamarque, and Lebrun 2022; Riglar et al. 2011).

1.1.1. Protein processing at the ER

In *P. falciparum*, all proteins destined for export to the various subcellular organelles, including the PV, must start their journey at the endoplasmic reticulum (ER). Like most eukaryotic organisms, secreted proteins utilize the ER-Golgi secretory pathway for their transport. Typically, proteins initiate their secretory journey through co-translational import to the ER via the SEC61 complex (Florentin et al. 2020; Marapana et al. 2018), where a conserved N-terminal hydrophobic

signal peptide (SP) is recognized and processed by a parasite ER peptidase (Adisa et al. 2003; R. F. Waller et al. 2000). Subsequently, proteins are distributed from the Golgi apparatus to their final compartments. Depending on the presence of specific organelle-targeting signals, mature proteins may take different routes or require distinct prerequisites for their transit.

ER-resident proteins possess a C-terminal retrieval sequence (KDEL and variants) that is recognized at the Golgi by the ERD2 protein, which then redirects them back to the ER via coat protein complex (COP) I vesicles (Elmendorf and Haldar 1993; Kudyba et al. 2019; Fierro et al. 2020; David W. Cobb et al. 2021; Külzer, Gehde, and Przyborski 2009; Fierro, Hussain, et al. 2023). Proteins targeted to the unique parasite organelle, the apicoplast, also contain an N-terminal sequence known as the transit peptide (TP), situated immediately downstream of the SP (Foth et al. 2003). This non-conserved sequence resembles a plant chloroplast transit peptide and is suggested to be recognized by ER chaperones for the sorting and transport of specific apicoplast proteins (Foth et al. 2003; Ramya, Surolia, and Surolia 2006; Ramya et al. 2007; Gallagher, Matthews, and Prigge 2011).

In contrast, proteins transported to the different secretory organelles, such as the rhoptries, micronemes, exonemes and dense granules, have not been associated with any distinct or conserved motif. Although these proteins commence their journey through the common ER-Golgi pathway, the mechanism directing them to different organelles remains unknown. For rhoptry proteins, it has been shown that certain regions are required for localization, as well as for the interaction with other rhoptry proteins (Richard et al. 2009; Hallée, Boddey, et al. 2018; A. Ghoneim et al. 2007; Sherling et al. 2017; Baldi et al. 2000; Morse et al. 2016). However, little is known about the trafficking of proteins to other secretory organelles.

1.1.2. Export control in the ER

Proteins designated for export to the RBC utilize a more complex system to reach their final locations at the host cell. These proteins enter the ER through a different SEC translocon complex, compared to the classical secretory pathway, which includes the SEC61 channel and the non-catalytic subunit SPC25 (Marapana et al. 2018). The majority of exported proteins contain a conserved motif known as the Plasmodium Exporting Element (PEXEL), or host-targeting signal, localized downstream of the SP sequence (Hiller et al. 2004; Marti et al. 2004). The PEXEL motif mainly consists of the canonical amino acid sequence RxLxE/Q/D, although other functional non-canonical sequences have also been identified (Boddey et al. 2013; Schulze et al. 2015). Upon entering the ER, the PEXEL motif is recognized and cleaved after the leucine residue by the aspartic protease Plasmepsin 5 (PMV). Subsequently, the new residue is acetylated and then the processed protein is transported to the PV through vesicular trafficking (Marapana et al. 2018; Boddey et al. 2010; Russo et al. 2010; Chang et al. 2008). While it was previously assumed that processing of the PEXEL motif by PMV was required for protein trafficking to the RBC, recent research shows that the PEXEL motif is dispensable for export, as long as the mature N-termini of the protein is produced, suggesting that cleavage and export might be two independent events (Hasan et al. 2023). In agreement with these findings, it was also found that some PEXEL-positive proteins processed by PMV remain confined within the PV, corroborating PMV might have a broader role beyond licensing proteins for export to the RBC (Fierro, Muheljic, et al. 2023; Ressurreição, Fréville, and van Ooij 2023).

In addition to PEXEL proteins, *P. falciparum* exports another smaller group of proteins to the RBC called PEXEL-negative exported proteins (PNEPs). These proteins are characterized by the absence of an identifiable conserved motif necessary for export. Their only shared feature is

the presence of a SP and the requirement of their N-terminal region for export (Heiber et al. 2013; Haase et al. 2009; Zhu et al. 2013; Gruring et al. 2012). Due to their unique nature, PNEPs are not processed by PMV and, as most of them contain transmembrane domains, they are inserted into the parasite plasma membrane (PPM) through vesicular trafficking (Mesén-Ramírez et al. 2016). How membrane proteins are extracted from the PPM and released into the PV remains still a major question, however it is clear that this process requires the activity of an unidentified unfoldase or translocon complex (K. M. Matthews, Kalanon, and de Koning-Ward 2019; Gruring et al. 2012).

1.1.3. PV translocation

Regardless of their ER processing, both PEXEL proteins and PNEPs converge within the PV and are translocated across the PVM through the *Plasmodium* Translocon of Exported proteins (PTEX) complex (Beck et al. 2014; de Koning-Ward et al. 2009; Elsworth et al. 2014; Bullen et al. 2012; Ho et al. 2018). This large translocon complex comprises three principal components: Heat shock protein 101 (Hsp101), PTEX150, and exported protein 2 (EXP2). Hsp101, a AAA+ unfoldase chaperone, forms an asymmetric spiral hexamer. It utilizes ATP hydrolysis to unfold exported proteins and transport them to the host cell cytosol (Ho et al. 2018). Unfolded proteins are shielded by the rim-like complex formed by a PTEX150 heptamer, which connects the Hsp101 motor with the EXP2 pore complex (Ho et al. 2018). EXP2 forms a heptameric membrane-spanning pore complex at the PVM. Besides facilitating the translocation of proteins to the host cell cytosol, this complex also operates as a non-selective channel enabling solute movement between the PV and the RBC cytosol, such as nutrients and waste products (Krugliak, Zhang, and Ginsburg 2002; Marchetti et al. 2015; Garten et al. 2018; Charnaud et al. 2018). Recent findings indicate that Hsp101 also localizes to the ER and might serve as a chaperone by selecting and

transporting PEXEL exported proteins from the ER to the PTEX complex (Fierro, Hussain, et al. 2023; Gabriela et al. 2022).

Several other proteins have been shown to interact with the PTEX complex, although their dispensability during protein export renders them as accessory proteins. Thioredoxin 2 (TRX2) and PTEX88 were among the first accessory proteins identified alongside the core PTEX complex (de Koning-Ward et al. 2009). TRX2, an active thioredoxin, may participate in the sulfide bond remodeling that facilitates unfolding of cargo proteins (Sharma et al. 2011; Peng, Cascio, and Egea 2015; K. Matthews et al. 2013). PTEX88, while lacking a known function in protein trafficking, has been interestingly linked to an indirect role in parasite sequestration (Chisholm et al. 2016). Additionally, PTEX88 appears to interact more closely with Hsp101 than other PTEX components, and with other PV-resident proteins, such as the components of the exported protein-interacting complex (EPIC) (Chisholm et al. 2018). The EPIC complex, situated at the PVM, is formed by three main proteins: the parasitophorous vacuole protein 1 (PV1), parasitophorous vacuole protein 2 (PV2) and exported protein 3 (EXP3). While EXP3 and PV2 are dispensable for parasite growth, PV1 knockdown results in reduced protein export and parasite virulence (Batinovic et al. 2017). This suggests that PV1 might function as an Hsp101 co-chaperone, delivering proteins from the PV to the PTEX complex (Hakamada et al. 2020; Batinovic et al. 2017). Lastly, Pf113 is another accessory protein identified. It is a GPI-anchored surface protein that interacts with membrane proteins and the PTEX complex, implying a participation in membrane protein trafficking (Miyazaki et al. 2021; Elsworth et al. 2016). While these proteins may be dispensable during in vitro culture, they appear to be crucial for in vivo infections.

1.1.4. Transport within the RBC

Following PVM translocation, it is presumed that exported proteins undergo refolding before being transported to their final locations within the RBC cytosol or membrane. Nevertheless, the mechanisms governing this process remain unclear. Chaperones are expected to participate in this post-translocation phase, similar to other translocon systems. However, the nature of these factors is still unknown. For instance, certain members of the family of parasite-encoded co-chaperones HSP40/DnaJ are predicted to be exported and some have been shown to be essential for PfEMP1 transport or to interact with exported factors within the RBC cytosol (Külzer et al. 2012; Petersen et al. 2016; Acharya et al. 2012; Zhang et al. 2017; Maier et al. 2008). The parasite HSP70 chaperone, HSP70x, is also exported to the RBC cytosol and it has been implicated in parasite cytoadherence. However, no role in protein trafficking has been observed (Külzer et al. 2012; D. W. Cobb et al. 2017; Charnaud et al. 2017). An example of unusual trafficking by parasite-derived chaperones is the mechanism of the RhopH complex. The RhopH complex consists of three main proteins: CLAG3, RhopH2, and RhopH3. These proteins are essential for establishing the *Plasmodium* surface anion channel (PSAC), a NPP localized at the RBC membrane (Nguitragool et al. 2011). The RhopH complex components reside within the rhoptries during schizont stages and are secreted into the RBC during invasion. Interestingly, during invasion Clag3 is secreted into the RBC cytoplasm, while RhopH2 and RhopH3 stay within the PV until late ring-stages when they are translocated through the PTEX complex (Osamu Kaneko et al. 2005; Ling et al. 2004; Schureck et al. 2021; Ito, Schureck, and Desai 2017; Counihan et al. 2017; Pasternak et al. 2022). Once RhopH2 and RhopH3 reach the RBC cytoplasm, the RhopH complex is formed with CLAG3 TM domains concealed within the complex (Ho et al. 2021; Ito, Schureck, and Desai 2017; Schureck et al. 2021; Pasternak et al. 2022), indicating that

RhopH2 and RhopH3 might serve as chaperones specifically for the transport of the PSAC component, CLAG3, into the RBC membrane. Finally, another mechanism used by *P. falciparum* to traffic proteins within the host cell is the utilization of the host chaperone network. For example, host-derived HSP70s have been identified to interact with PTEX components through pull-downs assays, or with parasite-encoded HSP40s through yeast 2-hybrid assays (Banumathy, Singh, and Tatu 2002; de Koning-Ward et al. 2009). The host-derived type II chaperonin TCP1 ring complex (TRiC), known for its role in ATP-dependent protein folding, has been found to interact with exported proteins like PfEMP1 within the RBC cytoplasm (Batinovic et al. 2017). These observations raise the possibility of host-derived chaperones playing a role in protein transport post-PVM translocation.

1.2.Merozoite invasion

P. falciparum merozoites are the erythrocytic infective form, with a small size of around 1-2 μM. Their sole purpose is to infect new erythrocytes to ensure parasite's survival. The invasion of RBCs is a rapid and complex multi-step process that takes approximately 60 seconds (Gilson and Crabb 2009). This process is mediated by the interaction between parasite-secreted proteins and RBC receptors. Merozoite proteins that facilitate invasion are primarily contained within apically localized organelles, such as micronemes and rhoptries. Micronemes store adhesins that play a role in erythrocyte binding, while rhoptries contain proteins that promote the invasion process and the formation of the PV.

1.2.1. Initial attachment

Invasion begins when a merozoite recognizes an erythrocyte and initiates a low-affinity and reversible interaction. This initial interaction is thought to be mediated by a group of integral and peripheral proteins that completely coat the merozoite surface, known as merozoite surface proteins (MSPs) (Beeson et al. 2016). MSP1, the most abundant of these proteins, forms a large complex with other MSP proteins at the merozoite membrane and is linked to it through glycosylphosphatidylinositol (GPI) anchors (Sanders et al. 2006). MSP1 has been shown to interact with the erythrocyte surface proteins glycophorin A (GPA) (Baldwin et al. 2015) and band 3 (Li et al. 2004), as well as the cytoskeleton protein spectrin (Herrera et al. 1993; Das et al. 2015). However, other studies have reported no direct interaction between MSP1 and the erythrocyte surface. Instead, they suggest that other MSP1 interactors within the MSP1 complex, such as MSP6, MSP9, MSP Duffy binding-like 1 (MSPDBL1) and MSPDBL2 may be responsible for these interactions (Lin et al. 2016, 2014; G. Paul et al. 2018; Li et al. 2004).

The initial interaction progresses into a stronger interaction that causes a deformation on the RBC surface, increasing the surface of contact between the merozoite and the erythrocyte. This deformation is associated with ligand-receptor interactions and the ability of merozoites to glide over RBCs, powered by their actin-myosin motor (Hart et al. 2023; Yahata et al. 2021). The tighter interaction is mediated by two main parasites adhesins secreted by the micronemes: the reticulocyte binding-like (RBL/Rh) proteins and the Duffy binding proteins (DBP/EBA) (Tham, Healer, and Cowman 2012; Weiss et al. 2015).

In *P. falciparum*, four DBP orthologs have been identified: erythrocyte binding antigen (EBA) 175, which binds to GPA; EBA-140, which binds glycophorin C; EBA-181, with an unknown receptor; and erythrocyte binding ligand (EBL) 1, which binds to glycophorin B

(Cowman et al. 2017). On the other hand, five RBL orthologs have been identified: Rh1, Rh2a and Rh2b with unknown receptors; Rh4, which binds to the complement receptor 1 (CD35); and Rh5, which binds to basigin (CD147) (Cowman et al. 2017). RBL and DBP receptors appear to work in conjunction at different stages during merozoite invasion (Weiss et al. 2015; Hart et al. 2023), except for Rh5, the only non-transmembrane protein, which has been shown to act downstream of the other ligands and is individually necessary for completing invasion (Volz et al. 2016; Weiss et al. 2015). Moreover, beyond their roles as receptors, the cytoplasmic tails of these ligands have been shown to participate in downstream signaling during invasion, particularly in rhoptry secretion (Tham et al. 2015).

Initially, RBL and DBP receptors were thought to have redundant functions during merozoite attachment. However, recent studies in *P. knowlesi* and *P. falciparum* have demonstrated that RBL and DBP proteins have different localization after microneme secretion and might act at different steps of merozoite attachment (Hart et al. 2023; Tham et al. 2015).

1.2.2. Reorientation and tight junction formation

Merozoites that successfully initiate an interaction with erythrocytes start reorienting their apical end towards the host membrane. This reorientation seems to be induced by the RBC wrapping around the merozoite and the interaction of Rh5 with the host cell receptor basigin (Crosnier et al. 2011; Dasgupta et al. 2014). Rh5 forms a complex with two other proteins: Rh5 interacting protein (Ripr) and cysteine-rich protective protein (CyRPA), all of which are essential for parasite invasion (Volz et al. 2016; Wong et al. 2018; Baum et al. 2009).

Since all three components lack a transmembrane domain or GPI anchor, the Rh5 complex needs to be firmly attached to the merozoite membrane by other anchoring proteins (Volz et al.

2016). Pf113, an abundant GPI-anchored protein, was shown to bind to the N-terminal region of Rh5 and interacts with CyRPA. However, it was not shown to directly interact with Ripr nor basigin (Galaway et al. 2017). Interestingly, Pf113 has also been associated with the PTEX complex and may play a role in regulating the export of proteins (Elsworth et al. 2016).

Recently, two additional proteins have been found to interact with the three proteins, forming a pentameric complex: *Plasmodium* thrombospondin-related apical merozoite protein (PTRAMP) and cysteine-rich small secreted (CSS) protein (Scally et al. 2022). According to this model, PTRAMP is anchored to the merozoite membrane and connects to the tripartite complex, specifically with Ripr, through CSS. This novel complex, referred to as PCRCR, plays a vital role in merozoite invasion, and its binding to BSG necessitates processing by Plasmepsin X (PMX) (Scally et al. 2022; Triglia et al. 2023).

The formation of the Rh5 complex at the merozoite's apical tip has also been associated with the creation of a pore at the merozoite-RBC interface. This pore allows the passage of calcium from the parasite into the host cell (Weiss et al. 2015; Geoghegan et al. 2021; Volz et al. 2016) and possibly facilitating the movement of secreted rhoptry proteins. However, there are conflicting data regarding the capacity of Rh5 alone or in complex to insert into membranes and generate a pore.

The interaction between Rh5 and basigin leads to the formation of the RON complex, a group of parasite proteins secreted from the rhoptries and inserted into the RBC surface. The RON complex consists of RON2, RON4, and RON5. After secretion, both RON2 and RON5 localizes to the cytoplasmic side of the RBC, while RON2 embeds into the membrane to serve as a receptor for the merozoite surface protein AMA1 (Alexander et al. 2006; Cao et al. 2009; Lamarque et al. 2011; Riglar et al. 2011; Vulliez-Le Normand et al. 2012). The binding of AMA1 to the RON

complex forms a strong and irreversible interaction known as the tight or moving junction, which dictates the commitment of the merozoites to internalization (Srinivasan et al. 2011). Although the AMA1-RON2 binding has been shown to be essential for invasion (Collins et al. 2009; Richard et al. 2010), echinocytosis is still observed after blocking the interaction, suggesting that the earlier step of Rh5-basigin interaction is what triggers the release of rhoptry proteins (Weiss et al. 2015).

1.2.3. Rhoptry secretion

The rhoptries are a pair of club-shaped organelles localized at the apical end of the merozoite, whose contents are secreted into the RBC during invasion. They are the largest of the secretory organelles, measuring approximately 500 nm in total length and 200 nm at their widest point, occupying an estimated 2-7% of the total merozoite volume (Hanssen et al. 2013).

Rhoptries are divided into two distinct regions: a narrow tubular duct at the anterior end, known as neck, and a posterior sac-like body known as the bulb (Hanssen et al. 2013; Bannister et al. 2000a). Each region comprises different groups of proteins, and since no membrane has been identified to separate them, it remains unclear how effectors localize to each specific region (Zuccala et al. 2012). Proteins in the rhoptry neck typically play a role in facilitating early interactions with the host RBC, such as Rh5 and proteins of the RON complex, which are involved in early attachment and tight junction formation respectively (Volz et al. 2016; Weiss et al. 2015). Conversely, rhoptry bulb proteins are usually secreted into the RBC cytosol to facilitate later stages of invasion and development, such as RAP1 and RhopH2, which are involved in formation of the PV and the establishment of the NPPs, respectively (Counihan et al. 2017; Ghosh et al. 2017). Little is known about how rhoptries maintain their shape and dimorphism, but mutants that lose this organization have lost their ability to invade host RBCs (Sherling et al. 2019).

During the invasion process, the rhoptries undergo various dynamic structural changes that might be involved in rhoptry exocytosis. Rhoptry discharge is suggested to be triggered by the interaction of merozoite surface ligands and host RBC receptors, as shown in the calcium-dependent binding of EBA175 and GPA (Singh et al. 2010).

To enable the secretion of rhoptry proteins, first an unknown signal triggers the fusion of the rhoptry neck with the PPM (Hanssen et al. 2013). Recently, it was discovered that rhoptries are indirectly docked to the parasite PPM through an intermediate vesicle known as the apical vesicle (AV). This vesicle connects the tip of the rhoptry neck with the apicomplexan-conserved rhoptry secretion apparatus (RSA), marking the docking site for rhoptry exocytosis at the PPM (Aquilini et al. 2021; Martinez et al. 2022). Upon signaling exposure, the AV first fuses with one rhoptry, which is then docked directly to the RSA. This is followed by the fusion of the second rhoptry neck to the docked one, resulting an structure with two bulbs and a single neck connected to the RSA (Hanssen et al. 2013; Martinez et al. 2022). After the initial fusion events are completed, neck proteins are secreted into the RBC membrane (Hanssen et al. 2013). Finally, as the merozoite begins active invasion, both bulbs start fusing while proteins and lipids are secreted into the RBC, resulting in a single rhoptry with a reduced size (Hanssen et al. 2013). Little is known about how these fusion events are regulated, but it has been shown that rhoptry apical surface protein 2 (RASP2) could play a role in this process due to its essentially in rhoptry secretion and subsequent invasion (Suarez et al. 2019).

Once merozoites complete invasion, the single rhoptry structure is maintained, suggesting that rhoptry structure might be supported by an unidentified scaffold (Hanssen et al. 2013). Since rhoptries are not present during ring-stage parasites, it is assumed that they are rapidly disassembled after completing invasion, in mechanism that remains largely unexplored.

1.2.4. Internalization

Once the tight junction correctly forms at the merozoite-RBC interface, the junction subsequently opens like a ring while as the parasite internalizes the RBC (Riglar et al. 2011; Srinivasan et al. 2011; Geoghegan et al. 2021). During active invasion, it is suggested that the actinomyosin motor provides the force necessary to pull different membrane ligands through the RBC surface to the rear of the merozoite. This process results in the internalization of the merozoite within the PV, primarily composed of RBC-derived membrane (Geoghegan et al. 2021; Perrin et al. 2018).

During internalization, two structures have been shown to be essential for the process: the unique apicomplexan double membrane organelle, known as the inner membrane complex (IMC), and the merozoite motor, known as the glideosome. The IMC consists of a series of flattened vesicles that forms de novo during merozoite segregation and localizes beneath the PPM (Bannister et al. 2000b; Liffner et al. 2023). Its primary function is to act as a scaffold for the formation of daughter cells (Kono et al. 2012, 2016) and to anchoring the glideosome, which resides in the space generated between the IMC and the PPM (Ferreira et al. 2020). Approximately 45 proteins within the *P. falciparum* IMC have been identified, each with different localizations and functions within the complex (Ferreira et al. 2020). However a recent report using proximity labeling identified approximately 300 proteins that might be localized to the IMC, revealing also the crucial role of palmitoylation in regulating some of these proteins (Qian et al. 2022; Wang et al. 2020). During schizogony, the IMC begins forming at the apical end of each new daughter merozoite, associating with newly formed microtubule organization centers (MTOCs) (Kono et al. 2012; Liffner et al. 2023). The IMC continues to grow into a ring shape led by the basal complex until it completely envelops the new cell, reaching the basal pole (Kono et al. 2016; Liffner et al.

2023). Several proteins, such as MORN1, BTP1, BTP2, BCP1, HAD2a and CINCH, have been used to track IMC formation through the localization at the basal complex (Ferreira et al. 2020). However, only HAD2 (Engelberg et al. 2016) and CINCH (Rudlaff et al. 2019) have been demonstrated to be essential for parasite development.

On the other hand, the glideosome is a protein complex suggested to act as a bridge, connecting the IMC with membrane ligands, while also maintaining the IMC and the PPM in close proximity (Frénal et al. 2010). Its primarily role is to serve as a scaffold for the unique actinomyosin-based contractile system, which powers various mechanisms, including transmigration, gliding and invasion (Frénal et al. 2010, 2017; Yahata et al. 2021). Multiple proteins forming the glideosome have been identified, such as the glideosome-associated proteins (GAP40, GAP45, GAP50, GAP70), the glideosome-associated proteins with multiple membrane spans (GAPM1, GAPM2, GAPM3), myosin A (MyoA), the myosin A tail-interacting protein (MTIP) and the essential light chain 1 (ELC1) protein (Ferreira et al. 2020). While most of these proteins have been shown to be essential, their precise roles within the glideosome are still under investigation.

The central component of the actinomyosin motor is MyoA, whose C-terminal region interacts with MTIP and ELC1 to form the lever arm of the motor and provide stability to it (Bergman et al. 2003; Green et al. 2006; Pazicky et al. 2020; J. C. Thomas et al. 2010). In the early stages of parasite development, GAP45, an essential protein spanning the whole IMC-PPM space, forms a soluble complex with MyoA and MTIP through its C-terminal region (Frénal et al. 2010; Gaskins et al. 2004; Perrin et al. 2018). Subsequently, GAP45 attaches to the IMC membrane-associated proteins GAP40 and GAP50, anchoring the motor to the IMC (Frénal et al. 2010; He Lu et al. 2023; Yeoman et al. 2011). Following this, myristoylation and palitoylation of the GAP45

N-terminal results in its anchoring to the PPM (Frénal et al. 2010; Rees-Channer et al. 2006; Ridzuan et al. 2012). Ultimately, MyoA displaces actin filament rearward, generating the force needed for the merozoite to move inside the host RBC (Frénal et al. 2017).

Actin filaments in apicomplexans form in the absence of actin-stabilizing proteins, resulting in short, unstable filaments that undergo rapid treadmilling (Skillman et al. 2013; Vahokoski et al. 2014; Skillman et al. 2011). Only two proteins, the formin proteins FRM1 and FRM2, have been identified to play a role in actin filament assembly and growth (Baum et al. 2008), with FRM1 localizing to the merozoite apical end and associating with actin filament formation and actinomyosin motor function (Baum et al. 2008; Collier et al. 2023). Additionally, the protein cofilin has been shown to act in depolymerizing actin filaments (Mehta and Sibley 2011).

After being internalized within the newly formed PV, merozoites exhibit a twisting motion thought to mechanically seal the PVM and complete scission of the PV from the RBC membrane (Blake, Haase, and Baum 2020; Geoghegan et al. 2021). Recent findings also highlight the essential role of the membrane-associated protease SUB2 in PVM sealing (Collins et al. 2020). Finally, after invasion is completed, the process of echinocytosis, initiated earlier during invasion, continues until the RBC returns to its original shape.

After the invasion is completed, an intriguing question pertains to the disassembly of the IMC. Previous data showed that disassembly can occur as early as 15 min post-invasion (Riglar et al. 2013); however, recent data suggests that the glideosome protein GAPM1 can still be observed until 4 hours post-infection in the parasite periphery (Anaguano et al. 2023). This raises questions about the regulation and mechanisms involved in this process.

1.2.5. Role of calcium during invasion

Fluctuations in calcium intracellular levels strongly regulate critical biological processes in *P. falciparum*, such as microneme secretion, motility, egress, invasion and differentiation (Lourido and Moreno 2015; de Oliveira et al. 2021). Calcium signaling is tightly regulated by its influx and efflux from subcellular compartments, such as the ER, acidocalcisomes and even the food vacuoles.

In the specific context of invasion, the precise role of calcium and the mechanisms of its release remain not completely understood. Primarily, calcium functions as a secondary messenger for the secretion of microneme proteins onto the merozoite surface and rhoptry proteins into the RBC. When merozoites sense low K^+ levels, as the ones found in blood, a rise in cytoplasmic calcium is triggered in a cAMP-dependent manner, leading to the activation of protein kinase A (PKA) and the subsequent translocation of microneme proteins to the merozoite surface (Dawn et al. 2014; Kumar et al. 2017; Singh et al. 2010). Subsequently, the binding of the EBA175 ligand to its RBC receptor GPA restores calcium to basal levels, thereby triggering rhoptry protein secretion (Siddiqui et al. 2013; Singh et al. 2010).

Another calcium-regulated protein essential for microneme secretion is double C2 (DOC2) protein. Presumably, this protein works by recruiting the membrane fusion machinery necessary for exocytosis upon binding to calcium (Farrell et al. 2012; Jean et al. 2014).

Calcium has also been linked with signaling cascades involving protein phosphorylation during invasion (Lasonder et al. 2012). Some members of the group of plant-like calcium-dependent protein kinases (CDPKs) have been shown to regulate invasion. For instance, CDPK1 has been shown to be essential for invasion (Azevedo et al. 2013; Bansal et al. 2013) and appears to work in conjunction with protein kinase B (PKB) to phosphorylate glideosome associated

protein 45 (GAP45) in response to calcium signaling (Green et al. 2008; D. C. Thomas et al. 2012). Other CDPK1 substrates have been identified at the IMC and glideosome, two structures crucial for merozoite invasion (Kumar et al. 2017). Interestingly, two kinases, CDPK5 and CDPK6, seem to play a compensatory role in the absence of a functional CDPK1 (Bansal et al. 2016), suggesting CDPKs might act in a collaboratively manner.

Another calcium-activated protein essential for invasion is the parasite phosphatase, calcineurin. Following merozoite-erythrocyte contact, calcium release activates calcineurin, which strengthens the interactions between RBL/DBP ligands and host receptors resulting in improved attachment and invasion. Interestingly, this occurs independently of microneme-secretion. (A. S. Paul et al. 2015).

Finally, despite a substantial body of research supporting the essential role of calcium in invasion, recent findings in *P. knowlesi* suggest that calcium might not be required for merozoite invasion (Hart et al. 2023).

1.3. Rhoptry biogenesis

Rhoptries are absent during the early stages of intraerythrocytic development and start assembling *de novo* during early schizogony (Liffner et al. 2023). They are formed from Golgi-derived vesicles (Bannister et al. 2000a) and are observed associated with microtubule organization centers (MTOCs) during the different rounds of mitosis in schizogony (Liffner et al. 2023; Rudlaff et al. 2020). During early schizogony, rhoptries maintain a uniform bulb shape, with the formation of the neck occurring only after merozoite segmentation has started (Bannister et al. 2000a; Liffner et al. 2023).

Rhoptry-resident proteins are trafficked through the classical secretory pathway, as most of them contain a signal peptide, and disruption of these pathways prevent rhoptry formation (A. Ghoneim et al. 2007; A. M. Ghoneim 2013; Howard and Schmidt 1995). To date, only two proteins have been implicated in rhoptry biogenesis: sortilin and the rhoptry apical membrane antigen (RAMA) protein. Sortilin is involved in chaperoning proteins from different secretory organelles, including the rhoptries (Hallée, Boddey, et al. 2018; Hallée, Counihan, et al. 2018). On the other hand, RAMA has been shown to be essential in parasite development because its absence results in mislocalization of rhoptry proteins and the formation of rhoptries lacking a distinctive neck (Sherling et al. 2019).

Very little is known about the formation of rhoptries during schizogony, including the factors that trigger their biogenesis, or the regulators that control rhoptry duality, as these numbers vary among apicomplexans.

1.4. References

Acharya, Pragyan, Shweta Chaubey, Manish Grover, and Utpal Tatu. 2012. "An Exported Heat Shock Protein 40 Associates with Pathogenesis-Related Knobs in Plasmodium Falciparum Infected Erythrocytes." *PloS One* 7 (9): e44605.

Adisa, Akinola, Melanie Rug, Nectarios Klonis, Michael Foley, Alan F. Cowman, and Leann Tilley. 2003. "The Signal Sequence of Exported Protein-1 Directs the Green Fluorescent Protein to the Parasitophorous Vacuole of Transfected Malaria Parasites." *The Journal of Biological Chemistry* 278 (8): 6532–42.

Ahorhorlu, Samuel Yao, Neils Ben Quashie, Rasmus Weisel Jensen, William Kudzi, Edmund Tetteh Nartey, Nancy Odurowah Duah-Quashie, Felix Zoiku, et al. 2023. "Assessment of Artemisinin Tolerance in Plasmodium Falciparum Clinical Isolates in Children with Uncomplicated Malaria in Ghana." *Malaria Journal* 22 (1): 58.

Alexander, David L., Shirin Arastu-Kapur, Jean-Francois Dubremetz, and John C. Boothroyd. 2006. "Plasmodium Falciparum AMA1 Binds a Rhoptry Neck Protein Homologous to TgRON4, a Component of the Moving Junction in Toxoplasma Gondii." *Eukaryotic Cell* 5 (7): 1169–73.

Anaguano, David, Watcharatip Dedkhad, Carrie F. Brooks, David W. Cobb, and Vasant Muralidharan. 2023. "Time-Resolved Proximity Biotinylation Implicates a Porin Protein in Export of Transmembrane Malaria Parasite Effectors." *Journal of Cell Science*, September. https://doi.org/10.1242/jcs.260506.

Aquilini, Eleonora, Marta Mendonça Cova, Shrawan Kumar Mageswaran, Nicolas Dos Santos Pacheco, Daniela Sparvoli, Diana Marcela Penarete-Vargas, Rania Najm, et al. 2021.

"An Alveolata Secretory Machinery Adapted to Parasite Host Cell Invasion." *Nature Microbiology* 6 (4): 425–34.

Azevedo, Mauro F., Paul R. Sanders, Efrosinia Krejany, Catherine Q. Nie, Ping Fu, Leon A. Bach, Gerhard Wunderlich, Brendan S. Crabb, and Paul R. Gilson. 2013. "Inhibition of Plasmodium Falciparum CDPK1 by Conditional Expression of Its J-Domain Demonstrates a Key Role in Schizont Development." *Biochemical Journal* 452 (3): 433–41.

Baldi, D. L., K. T. Andrews, R. F. Waller, D. S. Roos, R. F. Howard, B. S. Crabb, and A. F. Cowman. 2000. "RAP1 Controls Rhoptry Targeting of RAP2 in the Malaria Parasite Plasmodium Falciparum." *The EMBO Journal* 19 (11): 2435–43.

Baldwin, Michael R., Xuerong Li, Toshihiko Hanada, Shih-Chun Liu, and Athar H. Chishti. 2015. "Merozoite Surface Protein 1 Recognition of Host Glycophorin A Mediates Malaria Parasite Invasion of Red Blood Cells." *Blood* 125 (17): 2704–11.

Balikagala, Betty, Naoyuki Fukuda, Mie Ikeda, Osbert T. Katuro, Shin-Ichiro Tachibana, Masato Yamauchi, Walter Opio, et al. 2021. "Evidence of Artemisinin-Resistant Malaria in Africa." *The New England Journal of Medicine* 385 (13): 1163–71.

Bannister, L. H., J. M. Hopkins, R. E. Fowler, S. Krishna, and G. H. Mitchell. 2000a. "Ultrastructure of Rhoptry Development in Plasmodium Falciparum Erythrocytic Schizonts." *Parasitology* 121 (Pt 3) (September): 273–87.

———. 2000b. "A Brief Illustrated Guide to the Ultrastructure of Plasmodium Falciparum Asexual Blood Stages." *Parasitology Today* 16 (10): 427–33.

Bansal, Abhisheka, Kayode K. Ojo, Jianbing Mu, Dustin J. Maly, Wesley C. Van Voorhis, and Louis H. Miller. 2016. "Reduced Activity of Mutant Calcium-Dependent Protein Kinase

1 Is Compensated in Plasmodium Falciparum through the Action of Protein Kinase G." *MBio* 7 (6). https://doi.org/10.1128/mBio.02011-16.

Bansal, Abhisheka, Shailja Singh, Kunal R. More, Dhiraj Hans, Kuldeep Nangalia, Manickam Yogavel, Amit Sharma, and Chetan E. Chitnis. 2013. "Characterization of Plasmodium Falciparum Calcium-Dependent Protein Kinase 1 (PfCDPK1) and Its Role in Microneme Secretion during Erythrocyte Invasion." *The Journal of Biological Chemistry* 288 (3): 1590–1602.

Banumathy, Gowrishankar, Varsha Singh, and Utpal Tatu. 2002. "Host Chaperones Are Recruited in Membrane-Bound Complexes ByPlasmodium Falciparum*." *The Journal of Biological Chemistry* 277 (6): 3902–12.

Batinovic, Steven, Emma McHugh, Scott A. Chisholm, Kathryn Matthews, Boiyin Liu, Laure Dumont, Sarah C. Charnaud, et al. 2017. "An Exported Protein-Interacting Complex Involved in the Trafficking of Virulence Determinants in Plasmodium-Infected Erythrocytes." *Nature Communications* 8 (July): 16044.

Baum, Jake, Lin Chen, Julie Healer, Sash Lopaticki, Michelle Boyle, Tony Triglia, Florian Ehlgen, Stuart A. Ralph, James G. Beeson, and Alan F. Cowman. 2009. "Reticulocyte-Binding Protein Homologue 5 - an Essential Adhesin Involved in Invasion of Human Erythrocytes by Plasmodium Falciparum." *International Journal for Parasitology* 39 (3): 371–80.

Baum, Jake, Christopher J. Tonkin, Aditya S. Paul, Melanie Rug, Brian J. Smith, Sven B. Gould, Dave Richard, Thomas D. Pollard, and Alan F. Cowman. 2008. "A Malaria Parasite Formin Regulates Actin Polymerization and Localizes to the Parasite-Erythrocyte Moving Junction during Invasion." *Cell Host & Microbe* 3 (3): 188–98.

Beck, Josh R., Vasant Muralidharan, Anna Oksman, and Daniel E. Goldberg. 2014. “PTEX Component HSP101 Mediates Export of Diverse Malaria Effectors into Host Erythrocytes.” *Nature* 511 (7511): 592–95.

Beeson, James G., Damien R. Drew, Michelle J. Boyle, Gaoqian Feng, Freya J. I. Fowkes, and Jack S. Richards. 2016. “Merozoite Surface Proteins in Red Blood Cell Invasion, Immunity and Vaccines against Malaria.” *FEMS Microbiology Reviews* 40 (3): 343–72.

Bergman, Lawrence W., Karine Kaiser, Hisashi Fujioka, Isabelle Coppens, Thomas M. Daly, Sarah Fox, Kai Matuschewski, Victor Nussenzweig, and Stefan H. I. Kappe. 2003. “Myosin A Tail Domain Interacting Protein (MTIP) Localizes to the Inner Membrane Complex of Plasmodium Sporozoites.” *Journal of Cell Science* 116 (Pt 1): 39–49.

Blake, Thomas C. A., Silvia Haase, and Jake Baum. 2020. “Actomyosin Forces and the Energetics of Red Blood Cell Invasion by the Malaria Parasite Plasmodium Falciparum.” *PLoS Pathogens* 16 (10): e1009007.

Boddey, Justin A., Teresa G. Carvalho, Anthony N. Hodder, Tobias J. Sargeant, Brad E. Sleebs, Danushka Marapana, Sash Lopaticki, Thomas Nebl, and Alan F. Cowman. 2013. “Role of Plasmepsin V in Export of Diverse Protein Families from the Plasmodium Falciparum Exportome.” *Traffic* 14 (5): 532–50.

Boddey, Justin A., Anthony N. Hodder, Svenja Günther, Paul R. Gilson, Heather Patsiouras, Eugene A. Kapp, J. Andrew Pearce, et al. 2010. “An Aspartyl Protease Directs Malaria Effector Proteins to the Host Cell.” *Nature* 463 (7281): 627–31.

Bullen, Hayley E., Sarah C. Charnaud, Ming Kalanon, David T. Riglar, Chaitali Dekiwadia, Niwat Kangwanrangsan, Motomi Torii, et al. 2012. “Biosynthesis, Localization, and

Macromolecular Arrangement of the Plasmodium Falciparum Translocon of Exported Proteins (PTEX)." *The Journal of Biological Chemistry* 287 (11): 7871–84.

Cao, Jun, Osamu Kaneko, Amporn Thongkukiatkul, Mayumi Tachibana, Hitoshi Otsuki, Qi Gao, Takafumi Tsuboi, and Motomi Torii. 2009. "Rhoptry Neck Protein RON2 Forms a Complex with Microneme Protein AMA1 in Plasmodium Falciparum Merozoites." *Parasitology International* 58 (1): 29–35.

Carmo, Olivia M. S., Gerald J. Shami, Dezerae Cox, Boyin Liu, Adam J. Blanch, Snigdha Tiash, Leann Tilley, and Matthew W. A. Dixon. 2022. "Deletion of the Plasmodium Falciparum Exported Protein PTP7 Leads to Maurer's Clefts Vesiculation, Host Cell Remodeling Defects, and Loss of Surface Presentation of EMP1." *PLoS Pathogens* 18 (8): e1009882.

Chang, Henry H., Arnold M. Falick, Peter M. Carlton, John W. Sedat, Joseph L. DeRisi, and Michael A. Marletta. 2008. "N-Terminal Processing of Proteins Exported by Malaria Parasites." *Molecular and Biochemical Parasitology* 160 (2): 107–15.

Charnaud, Sarah C., Matthew W. A. Dixon, Catherine Q. Nie, Lia Chappell, Paul R. Sanders, Thomas Nebl, Eric Hanssen, et al. 2017. "The Exported Chaperone Hsp70-x Supports Virulence Functions for Plasmodium Falciparum Blood Stage Parasites." *PloS One* 12 (7): e0181656.

Charnaud, Sarah C., Rasika Kumarasingha, Hayley E. Bullen, Brendan S. Crabb, and Paul R. Gilson. 2018. "Knockdown of the Translocon Protein EXP2 in Plasmodium Falciparum Reduces Growth and Protein Export." *PloS One* 13 (11): e0204785.

Chisholm, Scott A., Ming Kalanon, Thomas Nebl, Paul R. Sanders, Kathryn M. Matthews, Benjamin K. Dickerman, Paul R. Gilson, and Tania F. de Koning-Ward. 2018. "The

Malaria PTEX Component PTEX88 Interacts Most Closely with HSP101 at the Host-Parasite Interface." *The FEBS Journal* 285 (11): 2037–55.

Chisholm, Scott A., Emma McHugh, Rachel Lundie, Matthew W. A. Dixon, Sreejoyee Ghosh, Meredith O'Keefe, Leann Tilley, Ming Kalanon, and Tania F. de Koning-Ward. 2016. "Contrasting Inducible Knockdown of the Auxiliary PTEX Component PTEX88 in P. Falciparum and P. Berghei Unmasks a Role in Parasite Virulence." *PloS One* 11 (2): e0149296.

Cobb, D. W., A. Florentin, M. A. Fierro, M. Krakowiak, J. M. Moore, and V. Muralidharan. 2017. "The Exported Chaperone PfHsp70x Is Dispensable for the Plasmodium Falciparum Intraerythrocytic Life Cycle." *MSphere* 2 (5). https://doi.org/10.1128/mSphere.00363-17.

Cobb, David W., Heather M. Kudyba, Alejandra Villegas, Michael R. Hoopmann, Rodrigo P. Baptista, Baylee Bruton, Michelle Krakowiak, Robert L. Moritz, and Vasant Muralidharan. 2021. "A Redox-Active Crosslinker Reveals an Essential and Inhibitable Oxidative Folding Network in the Endoplasmic Reticulum of Malaria Parasites." *PLoS Pathogens* 17 (2): e1009293.

Collier, Sophie, Emma Pietsch, Madeline Dans, Dawson Ling, Tatyana A. Tavella, Sash Lopaticki, Danushka S. Marapana, et al. 2023. "Plasmodium Falciparum Formins Are Essential for Invasion and Sexual Stage Development." *Communications Biology* 6 (1): 1–15.

Collins, Christine R., Fiona Hackett, Steven A. Howell, Ambrosius P. Snijders, Matthew R. G. Russell, Lucy M. Collinson, and Michael J. Blackman. 2020. "The Malaria Parasite

Sheddase SUB2 Governs Host Red Blood Cell Membrane Sealing at Invasion." *ELife* 9 (December): e61121.

Collins, Christine R., Chrislaine Withers-Martinez, Fiona Hackett, and Michael J. Blackman. 2009. "An Inhibitory Antibody Blocks Interactions between Components of the Malarial Invasion Machinery." *PLoS Pathogens* 5 (1): e1000273.

Counihan, Natalie A., Scott A. Chisholm, Hayley E. Bullen, Anubhav Srivastava, Paul R. Sanders, Thorey K. Jonsdottir, Greta E. Weiss, et al. 2017. "Plasmodium Falciparum Parasites Deploy RhopH2 into the Host Erythrocyte to Obtain Nutrients, Grow and Replicate." *ELife* 6 (March). https://doi.org/10.7554/eLife.23217.

Counihan, Natalie A., Joyanta K. Modak, and Tania F. de Koning-Ward. 2021. "How Malaria Parasites Acquire Nutrients From Their Host." *Frontiers in Cell and Developmental Biology* 9 (March): 649184.

Cova, Marta Mendonça, Mauld H. Lamarque, and Maryse Lebrun. 2022. "How Apicomplexa Parasites Secrete and Build Their Invasion Machinery." *Annual Review of Microbiology* 76 (1): 619–40.

Cowman, Alan F., Julie Healer, Danushka Marapana, and Kevin Marsh. 2016. "Malaria: Biology and Disease." *Cell* 167 (3): 610–24.

Cowman, Alan F., Christopher J. Tonkin, Wai-Hong Tham, and Manoj T. Duraisingh. 2017. "The Molecular Basis of Erythrocyte Invasion by Malaria Parasites." *Cell Host & Microbe* 22 (2): 232–45.

Crabb, Brendan S., Brian M. Cooke, John C. Reeder, Ross F. Waller, Sonia R. Caruana, Kathleen M. Davern, Mark E. Wickham, Graham V. Brown, Ross L. Coppel, and Alan F.

Cowman. 1997. “Targeted Gene Disruption Shows That Knobs Enable Malaria-Infected Red Cells to Cytoadhere under Physiological Shear Stress.” *Cell* 89 (2): 287–96.

Crosnier, Cécile, Leyla Y. Bustamante, S. Josefin Bartholdson, Amy K. Bei, Michel Theron, Makoto Uchikawa, Souleymane Mboup, et al. 2011. “Basigin Is a Receptor Essential for Erythrocyte Invasion by Plasmodium Falciparum.” *Nature* 480 (7378): 534–37.

Das, Sujaan, Nadine Hertrich, Abigail J. Perrin, Chrislaine Withers-Martinez, Christine R. Collins, Matthew L. Jones, Jean M. Watermeyer, et al. 2015. “Processing of Plasmodium Falciparum Merozoite Surface Protein MSP1 Activates a Spectrin-Binding Function Enabling Parasite Egress from RBCs.” *Cell Host & Microbe* 18 (4): 433–44.

Dasgupta, Sabyasachi, Thorsten Auth, Nir S. Gov, Timothy J. Satchwell, Eric Hanssen, Elizabeth S. Zuccala, David T. Riglar, et al. 2014. “Membrane-Wrapping Contributions to Malaria Parasite Invasion of the Human Erythrocyte.” *Biophysical Journal* 107 (1): 43–54.

Dawn, Amrita, Shailja Singh, Kunal R. More, Faiza Amber Siddiqui, Niseema Pachikara, Ghania Ramdani, Gordon Langsley, and Chetan E. Chitnis. 2014. “The Central Role of CAMP in Regulating Plasmodium Falciparum Merozoite Invasion of Human Erythrocytes.” *PLoS Pathogens* 10 (12): e1004520.

Desai, S. A., D. J. Krogstad, and E. W. McCleskey. 1993. “A Nutrient-Permeable Channel on the Intraerythrocytic Malaria Parasite.” *Nature* 362 (6421): 643–46.

Elmendorf, H. G., and K. Haldar. 1993. “Identification and Localization of ERD2 in the Malaria Parasite Plasmodium Falciparum: Separation from Sites of Sphingomyelin Synthesis and Implications for Organization of the Golgi.” *The EMBO Journal* 12 (12): 4763–73.

Elsworth, Brendan, Kathryn Matthews, Catherine Q. Nie, Ming Kalanon, Sarah C. Charnaud, Paul R. Sanders, Scott A. Chisholm, et al. 2014. “PTEX Is an Essential Nexus for Protein Export in Malaria Parasites.” *Nature* 511 (7511): 587–91.

Elsworth, Brendan, Paul R. Sanders, Thomas Nebl, Steven Batinovic, Ming Kalanon, Catherine Q. Nie, Sarah C. Charnaud, et al. 2016. “Proteomic Analysis Reveals Novel Proteins Associated with the Plasmodium Protein Exporter PTEX and a Loss of Complex Stability upon Truncation of the Core PTEX Component, PTEX150.” *Cellular Microbiology* 18 (11): 1551–69.

Engelberg, Klemens, F. Douglas Ivey, Angela Lin, Maya Kono, Alexander Lorestani, Dave Faugno-Fusci, Tim-Wolf Gilberger, Michael White, and Marc-Jan Gubbels. 2016. “A MORN1-Associated HAD Phosphatase in the Basal Complex Is Essential for Toxoplasma Gondii Daughter Budding.” *Cellular Microbiology* 18 (8): 1153–71.

Farrell, Andrew, Sivasakthivel Thirugnanam, Alexander Lorestani, Jeffrey D. Dvorin, Keith P. Eidell, David J. P. Ferguson, Brooke R. Anderson-White, Manoj T. Duraisingh, Gabor T. Marth, and Marc-Jan Gubbels. 2012. “A DOC2 Protein Identified by Mutational Profiling Is Essential for Apicomplexan Parasite Exocytosis.” *Science* 335 (6065): 218–21.

Ferreira, Josie Liane, Dorothee Heincke, Jan Stephan Wichers, Benjamin Liffner, Danny W. Wilson, and Tim-Wolf Gilberger. 2020. “The Dynamic Roles of the Inner Membrane Complex in the Multiple Stages of the Malaria Parasite.” *Frontiers in Cellular and Infection Microbiology* 10: 611801.

Fierro, Manuel A., Beejan Asady, Carrie F. Brooks, David W. Cobb, Alejandra Villegas, Silvia N. J. Moreno, and Vasant Muralidharan. 2020. “An Endoplasmic Reticulum CREC

Family Protein Regulates the Egress Proteolytic Cascade in Malaria Parasites." *MBio* 11 (1). https://doi.org/10.1128/mBio.03078-19.

Fierro, Manuel A., Tahir Hussain, Liam J. Campin, and Josh R. Beck. 2023. "Knock-Sideways by Inducible ER Retrieval Enables a Unique Approach for Studying Plasmodium-Secreted Proteins." *Proceedings of the National Academy of Sciences of the United States of America* 120 (33): e2308676120.

Fierro, Manuel A., Ajla Muheljic, Jihui Sha, James A. Wohlschlegel, and Josh R. Beck. 2023. "PEXEL Is a Proteolytic Maturation Site for Both Exported and Non-Exported Plasmodium Proteins." *BioRxiv : The Preprint Server for Biology*, July. https://doi.org/10.1101/2023.07.12.548774.

Florentin, Anat, David W. Cobb, Heather M. Kudyba, and Vasant Muralidharan. 2020. "Directing Traffic: Chaperone-Mediated Protein Transport in Malaria Parasites." *Cellular Microbiology* 22 (7): e13215.

Foth, Bernardo J., Stuart A. Ralph, Christopher J. Tonkin, Nicole S. Struck, Martin Fraunholz, David S. Roos, Alan F. Cowman, and Geoffrey I. McFadden. 2003. "Dissecting Apicoplast Targeting in the Malaria Parasite Plasmodium Falciparum." *Science* 299 (5607): 705–8.

Frénal, Karine, Jean-François Dubremetz, Maryse Lebrun, and Dominique Soldati-Favre. 2017. "Gliding Motility Powers Invasion and Egress in Apicomplexa." *Nature Reviews. Microbiology* 15 (11): 645–60.

Frénal, Karine, Valérie Polonais, Jean-Baptiste Marq, Rolf Stratmann, Julien Limenitakis, and Dominique Soldati-Favre. 2010. "Functional Dissection of the Apicomplexan Glideosome Molecular Architecture." *Cell Host & Microbe* 8 (4): 343–57.

Gabriela, Mikha, Kathryn M. Matthews, Cas Boshoven, Betty Kouskousis, Thorey K. Jonsdottir, Hayley E. Bullen, Joyanta Modak, et al. 2022. “A Revised Mechanism for How Plasmodium Falciparum Recruits and Exports Proteins into Its Erythrocytic Host Cell.” *PLoS Pathogens* 18 (2): e1009977.

Galaway, Francis, Laura G. Drought, Maria Fala, Nadia Cross, Alison C. Kemp, Julian C. Rayner, and Gavin J. Wright. 2017. “P113 Is a Merozoite Surface Protein That Binds the N Terminus of Plasmodium Falciparum RH5.” *Nature Communications* 8 (1): 1–11.

Gallagher, John R., Krista A. Matthews, and Sean T. Prigge. 2011. “Plasmodium Falciparum Apicoplast Transit Peptides Are Unstructured in Vitro and during Apicoplast Import.” *Traffic* 12 (9): 1124–38.

Garten, Matthias, Armiyaw S. Nasamu, Jacquin C. Niles, Joshua Zimmerberg, Daniel E. Goldberg, and Josh R. Beck. 2018. “EXP2 Is a Nutrient-Permeable Channel in the Vacuolar Membrane of Plasmodium and Is Essential for Protein Export via PTEX.” *Nature Microbiology* 3 (10): 1090–98.

Gaskins, Elizabeth, Stacey Gilk, Nicolette DeVore, Tara Mann, Gary Ward, and Con Beckers. 2004. “Identification of the Membrane Receptor of a Class XIV Myosin in Toxoplasma Gondii.” *The Journal of Cell Biology* 165 (3): 383–93.

Geoghegan, Niall D., Cindy Evelyn, Lachlan W. Whitehead, Michal Pasternak, Phoebe McDonald, Tony Triglia, Danushka S. Marapana, et al. 2021. “4D Analysis of Malaria Parasite Invasion Offers Insights into Erythrocyte Membrane Remodeling and Parasitophorous Vacuole Formation.” *Nature Communications* 12 (1): 1–16.

Ghoneim, Ahmed, Osamu Kaneko, Takafumi Tsuboi, and Motomi Torii. 2007. “The Plasmodium Falciparum RhopH2 Promoter and First 24 Amino Acids Are Sufficient to Target Proteins to the Rhoptries.” *Parasitology International* 56 (1): 31–43.

Ghoneim, Ahmed M. 2013. “Trafficking of Plasmodium Falciparum Chimeric Rhoptry Protein with Brefeldin A.” *Folia Parasitologica* 60 (1): 75–78.

Ghosh, Sreejoyee, Kit Kennedy, Paul Sanders, Kathryn Matthews, Stuart A. Ralph, Natalie A. Counihan, and Tania F. de Koning-Ward. 2017. “The Plasmodium Rhoptry Associated Protein Complex Is Important for Parasitophorous Vacuole Membrane Structure and Intraerythrocytic Parasite Growth.” *Cellular Microbiology* 19 (8). https://doi.org/10.1111/cmi.12733.

Gilson, Paul R., and Brendan S. Crabb. 2009. “Morphology and Kinetics of the Three Distinct Phases of Red Blood Cell Invasion by Plasmodium Falciparum Merozoites.” *International Journal for Parasitology* 39 (1): 91–96.

Green, Judith L., Stephen R. Martin, Jeremy Fielden, Asimina Ksagoni, Munira Grainger, Brian Y. S. Yim Lim, Justin E. Molloy, and Anthony A. Holder. 2006. “The MTIP-Myosin A Complex in Blood Stage Malaria Parasites.” *Journal of Molecular Biology* 355 (5): 933–41.

Green, Judith L., Roxanne R. Rees-Channer, Stephen A. Howell, Stephen R. Martin, Ellen Knuepfer, Helen M. Taylor, Munira Grainger, and Anthony A. Holder. 2008. “The Motor Complex of Plasmodium Falciparum: Phosphorylation by a Calcium-Dependent Protein Kinase.” *The Journal of Biological Chemistry* 283 (45): 30980–89.

Gruring, C., A. Heiber, F. Kruse, S. Flemming, G. Franci, S. F. Colombo, E. Fasana, et al. 2012. "Uncovering Common Principles in Protein Export of Malaria Parasites." *Cell Host & Microbe* 12 (5): 717–29.

Haase, Silvia, Susann Herrmann, Christof Grüring, Arlett Heiber, Pascal W. Jansen, Christine Langer, Moritz Treeck, et al. 2009. "Sequence Requirements for the Export of the Plasmodium Falciparum Maurer's Clefts Protein REX2." *Molecular Microbiology* 71 (4): 1003–17.

Hakamada, Kazuaki, Manami Nakamura, Rio Midorikawa, Kyosuke Shinohara, Keiichi Noguchi, Hikaru Nagaoka, Eizo Takashima, et al. 2020. "PV1 Protein from Plasmodium Falciparum Exhibits Chaperone-Like Functions and Cooperates with Hsp100s." *International Journal of Molecular Sciences* 21 (22). https://doi.org/10.3390/ijms21228616.

Hallée, Stéphanie, Justin A. Boddey, Alan F. Cowman, and Dave Richard. 2018. "Evidence That the Plasmodium Falciparum Protein Sortilin Potentially Acts as an Escorter for the Trafficking of the Rhoptry-Associated Membrane Antigen to the Rhoptries." *MSphere* 3 (1). https://doi.org/10.1128/mSphere.00551-17.

Hallée, Stéphanie, Natalie A. Counihan, Kathryn Matthews, Tania F. de Koning-Ward, and Dave Richard. 2018. "The Malaria Parasite Plasmodium Falciparum Sortilin Is Essential for Merozoite Formation and Apical Complex Biogenesis." *Cellular Microbiology* 20 (8): e12844.

Hanssen, Eric, Chaitali Dekiwadia, David T. Riglar, Melanie Rug, Leandro Lemgruber, Alan F. Cowman, Marek Cyrklaff, et al. 2013. "Electron Tomography of Plasmodium Falciparum

Merozoites Reveals Core Cellular Events That Underpin Erythrocyte Invasion." *Cellular Microbiology* 15 (9): 1457–72.

Hart, Melissa N., Franziska Mohring, Sophia M. DonVito, James A. Thomas, Nicole Muller-Sienerth, Gavin J. Wright, Ellen Knuepfer, Helen R. Saibil, and Robert W. Moon. 2023. "Sequential Roles for Red Blood Cell Binding Proteins Enable Phased Commitment to Invasion for Malaria Parasites." *Nature Communications* 14 (1): 4619.

Hasan, Muhammad M., Alexander J. Polino, Sumit Mukherjee, Barbara Vaupel, and Daniel E. Goldberg. 2023. "The Mature N-Termini of Plasmodium Effector Proteins Confer Specificity of Export." *MBio*, August, e0121523.

He Lu, Qiu Yue, Pang Geping, Li Siqi, Wang Jingjing, Feng Yonghui, Chen Lumeng, et al. 2023. "Plasmodium Falciparum GAP40 Plays an Essential Role in Merozoite Invasion and Gametocytogenesis." *Microbiology Spectrum* 11 (3): e01434-23.

Heiber, Arlett, Florian Kruse, Christian Pick, Christof Grüring, Sven Flemming, Alexander Oberli, Hanno Schoeler, et al. 2013. "Identification of New PNEPs Indicates a Substantial Non-PEXEL Exportome and Underpins Common Features in Plasmodium Falciparum Protein Export." *PLoS Pathogens* 9 (8): e1003546.

Herrera, S., W. Rudin, M. Herrera, P. Clavijo, L. Mancilla, C. de Plata, H. Matile, and U. Certa. 1993. "A Conserved Region of the MSP-1 Surface Protein of Plasmodium Falciparum Contains a Recognition Sequence for Erythrocyte Spectrin." *The EMBO Journal* 12 (4): 1607–14.

Hiller, N. Luisa, Souvik Bhattacharjee, Christiaan van Ooij, Konstantinos Liolios, Travis Harrison, Carlos Lopez-Estraño, and Kasturi Haldar. 2004. "A Host-Targeting Signal in

Virulence Proteins Reveals a Secretome in Malarial Infection." *Science* 306 (5703): 1934–37.

Ho, Chi-Min, Josh R. Beck, Mason Lai, Yanxiang Cui, Daniel E. Goldberg, Pascal F. Egea, and Z. Hong Zhou. 2018. "Malaria Parasite Translocon Structure and Mechanism of Effector Export." *Nature* 561 (7721): 70–75.

Ho, Chi-Min, Jonathan Jih, Mason Lai, Xiaorun Li, Daniel E. Goldberg, Josh R. Beck, and Z. Hong Zhou. 2021. "Native Structure of the RhopH Complex, a Key Determinant of Malaria Parasite Nutrient Acquisition." *Proceedings of the National Academy of Sciences* 118 (35): e2100514118.

Howard, Randall F., and Cheryl M. Schmidt. 1995. "The Secretory Pathway of Plasmodium Falciparum Regulates Transport of P82/RAP-1 to the Rhoptries." *Molecular and Biochemical Parasitology* 74 (1): 43–54.

Ito, Daisuke, Marc A. Schureck, and Sanjay A. Desai. 2017. "An Essential Dual-Function Complex Mediates Erythrocyte Invasion and Channel-Mediated Nutrient Uptake in Malaria Parasites." *ELife* 6 (February). https://doi.org/10.7554/eLife.23485.

Jean, Sophonie, Mónica A. Zapata-Jenks, Julie M. Farley, Erin Tracy, and D. C. Ghislaine Mayer. 2014. "Plasmodium Falciparum Double C2 Domain Protein, PfDOC2, Binds to Calcium When Associated with Membranes." *Experimental Parasitology* 144 (September): 91–95.

Jonsdottir, Thorey K., Mikha Gabriela, Brendan S. Crabb, Tania F de Koning-Ward, and Paul R. Gilson. 2021. "Defining the Essential Exportome of the Malaria Parasite." *Trends in Parasitology* 37 (7): 664–75.

Kaneko, O., T. Tsuboi, I. T. Ling, S. Howell, M. Shirano, M. Tachibana, Y. M. Cao, A. A. Holder, and M. Torii. 2001. “The High Molecular Mass Rhoptry Protein, RhopH1, Is Encoded by Members of the Clag Multigene Family in Plasmodium Falciparum and Plasmodium Yoelii.” *Molecular and Biochemical Parasitology* 118 (2): 223–31.

Kaneko, Osamu, Brian Y. S. Yim Lim, Hideyuki Iriko, Irene T. Ling, Hitoshi Otsuki, Munira Grainger, Takafumi Tsuboi, et al. 2005. “Apical Expression of Three RhopH1/Clag Proteins as Components of the Plasmodium Falciparum RhopH Complex.” *Molecular and Biochemical Parasitology* 143 (1): 20–28.

Koning-Ward, Tania F. de, Paul R. Gilson, Justin A. Boddey, Melanie Rug, Brian J. Smith, Anthony T. Papenfuss, Paul R. Sanders, et al. 2009. “A Newly Discovered Protein Export Machine in Malaria Parasites.” *Nature* 459 (7249): 945–49.

Kono, Maya, Dorothee Heincke, Louisa Wilcke, Tatianna Wai Ying Wong, Caroline Bruns, Susann Herrmann, Tobias Spielmann, and Tim W. Gilberger. 2016. “Pellicle Formation in the Malaria Parasite.” *Journal of Cell Science* 129 (4): 673–80.

Kono, Maya, Susann Herrmann, Noeleen B. Loughran, Ana Cabrera, Klemens Engelberg, Christine Lehmann, Dipto Sinha, et al. 2012. “Evolution and Architecture of the Inner Membrane Complex in Asexual and Sexual Stages of the Malaria Parasite.” *Molecular Biology and Evolution* 29 (9): 2113–32.

Krugliak, Miriam, Jianmin Zhang, and Hagai Ginsburg. 2002. “Intraerythrocytic Plasmodium Falciparum Utilizes Only a Fraction of the Amino Acids Derived from the Digestion of Host Cell Cytosol for the Biosynthesis of Its Proteins.” *Molecular and Biochemical Parasitology* 119 (2): 249–56.

Kudyba, Heather M., David W. Cobb, Manuel A. Fierro, Anat Florentin, Dragan Ljolje, Balwan Singh, Naomi W. Lucchi, and Vasant Muralidharan. 2019. “The Endoplasmic Reticulum Chaperone PfGRP170 Is Essential for Asexual Development and Is Linked to Stress Response in Malaria Parasites.” *Cellular Microbiology* 21 (9): e13042.

Külzer, Simone, Sarah Charnaud, Tal Dagan, Jan Riedel, Pradipta Mandal, Eva R. Pesce, Gregory L. Blatch, Brendan S. Crabb, Paul R. Gilson, and Jude M. Przyborski. 2012. “Plasmodium Falciparum-Encoded Exported Hsp70/Hsp40 Chaperone/Co-Chaperone Complexes within the Host Erythrocyte.” *Cellular Microbiology* 14 (11): 1784–95.

Külzer, Simone, Nina Gehde, and Jude M. Przyborski. 2009. “Return to Sender: Use of Plasmodium ER Retrieval Sequences to Study Protein Transport in the Infected Erythrocyte and Predict Putative ER Protein Families.” *Parasitology Research* 104 (6): 1535–41.

Kumar, Sudhir, Manish Kumar, Roseleen Ekka, Jeffrey D. Dvorin, Aditya S. Paul, Anil K. Madugundu, Tim Gilberger, et al. 2017. “PfCDPK1 Mediated Signaling in Erythrocytic Stages of Plasmodium Falciparum.” *Nature Communications* 8 (1): 63.

Lamarque, Mauld, Sébastien Besteiro, Julien Papoin, Magali Roques, Brigitte Vulliez-Le Normand, Juliette Morlon-Guyot, Jean-François Dubremetz, et al. 2011. “The RON2-AMA1 Interaction Is a Critical Step in Moving Junction-Dependent Invasion by Apicomplexan Parasites.” *PLoS Pathogens* 7 (2): e1001276.

Lasonder, Edwin, Judith L. Green, Grazia Camarda, Hana Talabani, Anthony A. Holder, Gordon Langsley, and Pietro Alano. 2012. “The Plasmodium Falciparum Schizont Phosphoproteome Reveals Extensive Phosphatidylinositol and CAMP-Protein Kinase A Signaling.” *Journal of Proteome Research* 11 (11): 5323–37.

Li, Xuerong, Huiqing Chen, Thein H. Oo, Thomas M. Daly, Lawrence W. Bergman, Shih-Chun Liu, Athar H. Chishti, and Steven S. Oh. 2004. “A Co-Ligand Complex Anchors Plasmodium Falciparum Merozoites to the Erythrocyte Invasion Receptor Band 3.” *The Journal of Biological Chemistry* 279 (7): 5765–71.

Liffner, Benjamin, Ana Karla Cepeda Diaz, James Blauwkamp, David Anaguano, Sonja Frölich, Vasant Muralidharan, Danny W. Wilson, Jeffrey Dvorin, and Sabrina Absalon. 2023. “Atlas of Plasmodium Falciparum Intraerythrocytic Development Using Expansion Microscopy.” eLife Sciences Publications, Ltd. https://doi.org/10.7554/elife.88088.1.

Lin, Clara S., Alessandro D. Uboldi, Christian Epp, Hermann Bujard, Takafumi Tsuboi, Peter E. Czabotar, and Alan F. Cowman. 2016. “Multiple Plasmodium Falciparum Merozoite Surface Protein 1 Complexes Mediate Merozoite Binding to Human Erythrocytes.” *The Journal of Biological Chemistry* 291 (14): 7703–15.

Lin, Clara S., Alessandro D. Uboldi, Danushka Marapana, Peter E. Czabotar, Christian Epp, Hermann Bujard, Nicole L. Taylor, Matthew A. Perugini, Anthony N. Hodder, and Alan F. Cowman. 2014. “The Merozoite Surface Protein 1 Complex Is a Platform for Binding to Human Erythrocytes by Plasmodium Falciparum.” *The Journal of Biological Chemistry* 289 (37): 25655–69.

Ling, Irene T., Laurence Florens, Anton R. Dluzewski, Osamu Kaneko, Munira Grainger, Brian Y. S. Yim Lim, Takafumi Tsuboi, et al. 2004. “The Plasmodium Falciparum Clag9 Gene Encodes a Rhoptry Protein That Is Transferred to the Host Erythrocyte upon Invasion.” *Molecular Microbiology* 52 (1): 107–18.

Lingelbach, K., and K. A. Joiner. 1998. “The Parasitophorous Vacuole Membrane Surrounding Plasmodium and Toxoplasma: An Unusual Compartment in Infected Cells.” *Journal of Cell Science* 111 (Pt 11) (June): 1467–75.

Liu, Li, Hope L. Johnson, Simon Cousens, Jamie Perin, Susana Scott, Joy E. Lawn, Igor Rudan, et al. 2012. “Global, Regional, and National Causes of Child Mortality: An Updated Systematic Analysis for 2010 with Time Trends since 2000.” *The Lancet* 379 (9832): 2151–61.

Liu, Li, Shefali Oza, Dan Hogan, Yue Chu, Jamie Perin, Jun Zhu, Joy E. Lawn, Simon Cousens, Colin Mathers, and Robert E. Black. 2016. “Global, Regional, and National Causes of under-5 Mortality in 2000-15: An Updated Systematic Analysis with Implications for the Sustainable Development Goals.” *The Lancet* 388 (10063): 3027–35.

Looker, Oliver, Adam J. Blanch, Boyin Liu, Juan Nunez-Iglesias, Paul J. McMillan, Leann Tilley, and Matthew W. A. Dixon. 2019. “The Knob Protein KAHRP Assembles into a Ring-Shaped Structure That Underpins Virulence Complex Assembly.” *PLoS Pathogens* 15 (5): e1007761.

Lourido, Sebastian, and Silvia N. J. Moreno. 2015. “The Calcium Signaling Toolkit of the Apicomplexan Parasites Toxoplasma Gondii and Plasmodium Spp.” *Cell Calcium* 57 (3): 186–93.

Maier, Alexander G., Melanie Rug, Matthew T. O’Neill, James G. Beeson, Matthias Marti, John Reeder, and Alan F. Cowman. 2007. “Skeleton-Binding Protein 1 Functions at the Parasitophorous Vacuole Membrane to Traffic PfEMP1 to the Plasmodium Falciparum-Infected Erythrocyte Surface.” *Blood* 109 (3): 1289–97.

Maier, Alexander G., Melanie Rug, Matthew T. O'Neill, Monica Brown, Srabasti Chakravorty, Tadge Szestak, Joanne Chesson, et al. 2008. "Exported Proteins Required for Virulence and Rigidity of Plasmodium Falciparum-Infected Human Erythrocytes." *Cell* 134 (1): 48–61.

Marapana, Danushka S., Laura F. Dagley, Jarrod J. Sandow, Thomas Nebl, Tony Triglia, Michał Pasternak, Benjamin K. Dickerman, et al. 2018. "Plasmepsin V Cleaves Malaria Effector Proteins in a Distinct Endoplasmic Reticulum Translocation Interactome for Export to the Erythrocyte." *Nature Microbiology* 3 (9): 1010–22.

Marchetti, Rosa V., Adele M. Lehane, Sarah H. Shafik, Markus Winterberg, Rowena E. Martin, and Kiaran Kirk. 2015. "A Lactate and Formate Transporter in the Intraerythrocytic Malaria Parasite, Plasmodium Falciparum." *Nature Communications* 6 (1): 1–7.

Marti, Matthias, Robert T. Good, Melanie Rug, Ellen Knuepfer, and Alan F. Cowman. 2004. "Targeting Malaria Virulence and Remodeling Proteins to the Host Erythrocyte." *Science* 306 (5703): 1930–33.

Martinez, Matthew, William David Chen, Marta Mendonça Cova, Petra Molnár, Shrawan Kumar Mageswaran, Amandine Guérin, Audrey R. Odom John, Maryse Lebrun, and Yi-Wei Chang. 2022. "Rhoptry Secretion System Structure and Priming in Plasmodium Falciparum Revealed Using in Situ Cryo-Electron Tomography." *Nature Microbiology*. https://doi.org/10.1038/s41564-022-01171-3.

Matthews, Kathryn, Ming Kalanon, Scott A. Chisholm, Angelika Sturm, Christopher D. Goodman, Matthew W. A. Dixon, Paul R. Sanders, et al. 2013. "The Plasmodium Translocon of Exported Proteins (PTEX) Component Thioredoxin-2 Is Important for Maintaining Normal Blood-Stage Growth." *Molecular Microbiology* 89 (6): 1167–86.

Matthews, Kathryn M., Ming Kalanon, and Tania F. de Koning-Ward. 2019. “Uncoupling the Threading and Unfoldase Actions of Plasmodium HSP101 Reveals Differences in Export between Soluble and Insoluble Proteins.” *MBio* 10 (3). https://doi.org/10.1128/mBio.01106-19.

McHugh, Emma, Olivia M. S. Carmo, Adam Blanch, Oliver Looker, Boyin Liu, Snigdha Tiash, Dean Andrew, et al. 2020. “Role of Plasmodium Falciparum Protein GEXP07 in Maurer’s Cleft Morphology, Knob Architecture, and P. Falciparum EMP1 Trafficking.” *MBio* 11 (2). https://doi.org/10.1128/mBio.03320-19.

Mehta, Simren, and L. David Sibley. 2011. “Actin Depolymerizing Factor Controls Actin Turnover and Gliding Motility in Toxoplasma Gondii.” *Molecular Biology of the Cell* 22 (8): 1290–99.

Mesén-Ramírez, Paolo, Ferdinand Reinsch, Alexandra Blancke Soares, Bärbel Bergmann, Ann-Katrin Ullrich, Stefan Tenzer, and Tobias Spielmann. 2016. “Stable Translocation Intermediates Jam Global Protein Export in Plasmodium Falciparum Parasites and Link the PTEX Component EXP2 with Translocation Activity.” *PLoS Pathogens* 12 (5): e1005618.

Miyazaki, Shinya, Ben-Yeddy Abel Chitama, Wataru Kagaya, Amuza Byaruhanga Lucky, Xiaotong Zhu, Kazuhide Yahata, Masayuki Morita, Eizo Takashima, Takafumi Tsuboi, and Osamu Kaneko. 2021. “Plasmodium Falciparum SURFIN4.1 Forms an Intermediate Complex with PTEX Components and Pf113 during Export to the Red Blood Cell.” *Parasitology International* 83 (August): 102358.

Morse, David, Wesley Webster, Ming Kalanon, Gordon Langsley, and Geoffrey I. McFadden. 2016. “Plasmodium Falciparum Rab1A Localizes to Rhoptries in Schizonts.” *PloS One* 11 (6): e0158174.

Mundwiler-Pachlatko, Esther, and Hans-Peter Beck. 2013. “Maurer’s Clefts, the Enigma of Plasmodium Falciparum.” *Proceedings of the National Academy of Sciences of the United States of America* 110 (50): 19987–94.

Nguitragool, Wang, Abdullah A. B. Bokhari, Ajay D. Pillai, Kempaiah Rayavara, Paresh Sharma, Brad Turpin, L. Aravind, and Sanjay A. Desai. 2011. “Malaria Parasite Clag3 Genes Determine Channel-Mediated Nutrient Uptake by Infected Red Blood Cells.” *Cell* 145 (5): 665–77.

Oh, S. S., S. Voigt, D. Fisher, S. J. Yi, P. J. LeRoy, L. H. Derick, S. Liu, and A. H. Chishti. 2000. “Plasmodium Falciparum Erythrocyte Membrane Protein 1 Is Anchored to the Actin-Spectrin Junction and Knob-Associated Histidine-Rich Protein in the Erythrocyte Skeleton.” *Molecular and Biochemical Parasitology* 108 (2): 237–47.

Oliveira, Lucas Silva de, Marcos Rodrigo Alborghetti, Renata Garcia Carneiro, Izabela Marques Dourado Bastos, Rogerio Amino, Philippe Grellier, and Sébastien Charneau. 2021. “Calcium in the Backstage of Malaria Parasite Biology.” *Frontiers in Cellular and Infection Microbiology* 11 (July): 708834.

Ooij, Christiaan van, Pamela Tamez, Souvik Bhattacharjee, N. Luisa Hiller, Travis Harrison, Konstantinos Liolios, Taco Kooij, et al. 2008. “The Malaria Secretome: From Algorithms to Essential Function in Blood Stage Infection.” *PLoS Pathogens* 4 (6): e1000084.

Pasternak, Michał, Julie M. J. Verhoef, Wilson Wong, Tony Triglia, Michael J. Mlodzianoski, Niall Geoghegan, Cindy Evelyn, Ahmad Z. Wardak, Kelly Rogers, and Alan F. Cowman.

2022. “RhopH2 and RhopH3 Export Enables Assembly of the RhopH Complex on P. Falciparum-Infected Erythrocyte Membranes.” *Communications Biology* 5 (1). https://doi.org/10.1038/s42003-022-03290-3.

Paul, Aditya S., Sudeshna Saha, Klemens Engelberg, Rays H. Y. Jiang, Bradley I. Coleman, Aziz L. Kosber, Chun-Ti Chen, et al. 2015. “Parasite Calcineurin Regulates Host Cell Recognition and Attachment by Apicomplexans.” *Cell Host & Microbe* 18 (1): 49–60.

Paul, Gourab, Arunaditya Deshmukh, Bishwanath Kumar Chourasia, Kalamuddin, Ashutosh Panda, Susheel Kumar Singh, Puneet K. Gupta, et al. 2018. “Protein–Protein Interaction Studies Reveal the Plasmodium Falciparum Merozoite Surface Protein-1 Region Involved in a Complex Formation That Binds to Human Erythrocytes.” *Biochemical Journal* 475 (6): 1197–1209.

Pazicky, Samuel, Karthikeyan Dhamotharan, Karol Kaszuba, Haydyn D. T. Mertens, Tim Gilberger, Dmitri Svergun, Jan Kosinski, Ulrich Weininger, and Christian Löw. 2020. “Structural Role of Essential Light Chains in the Apicomplexan Glideosome.” *Communications Biology* 3 (1): 1–14.

Peng, Mindy, Duilio Cascio, and Pascal F. Egea. 2015. “Crystal Structure and Solution Characterization of the Thioredoxin-2 from Plasmodium Falciparum, a Constituent of an Essential Parasitic Protein Export Complex.” *Biochemical and Biophysical Research Communications* 456 (1): 403–9.

Perrin, Abigail J., Christine R. Collins, Matthew R. G. Russell, Lucy M. Collinson, David A. Baker, and Michael J. Blackman. 2018. “The Actinomyosin Motor Drives Malaria Parasite Red Blood Cell Invasion but Not Egress.” *MBio* 9 (4). https://doi.org/10.1128/mBio.00905-18.

Petersen, Wiebke, Simone Külzer, Sonja Engels, Qi Zhang, Alyssa Ingmundson, Melanie Rug, Alexander G. Maier, and Jude M. Przyborski. 2016. “J-Dot Targeting of an Exported HSP40 in Plasmodium Falciparum-Infected Erythrocytes.” *International Journal for Parasitology* 46 (8): 519–25.

Pillai, Ajay D., Wang Nguitragool, Brian Lyko, Keithlee Dolinta, Michelle M. Butler, Son T. Nguyen, Norton P. Peet, Terry L. Bowlin, and Sanjay A. Desai. 2012. “Solute Restriction Reveals an Essential Role for Clag3-Associated Channels in Malaria Parasite Nutrient Acquisition.” *Molecular Pharmacology* 82 (6): 1104–14.

Qian, Pengge, Xu Wang, Chuan-Qi Zhong, Jiaxu Wang, Mengya Cai, Wang Nguitragool, Jian Li, Huiting Cui, and Jing Yuan. 2022. “Inner Membrane Complex Proteomics Reveals a Palmitoylation Regulation Critical for Intraerythrocytic Development of Malaria Parasite.” *ELife* 11 (July). https://doi.org/10.7554/eLife.77447.

Ramya, T. N. C., Krishanpal Karmodiya, Avadhesha Surolia, and Namita Surolia. 2007. “15-Deoxyspergualin Primarily Targets the Trafficking of Apicoplast Proteins in Plasmodium Falciparum.” *The Journal of Biological Chemistry* 282 (9): 6388–97.

Ramya, T. N. C., Namita Surolia, and Avadhesha Surolia. 2006. “15-Deoxyspergualin Modulates Plasmodium Falciparum Heat Shock Protein Function.” *Biochemical and Biophysical Research Communications* 348 (2): 585–92.

Rees-Channer, Roxanne R., Stephen R. Martin, Judith L. Green, Paul W. Bowyer, Munira Grainger, Justin E. Molloy, and Anthony A. Holder. 2006. “Dual Acylation of the 45 KDa Gliding-Associated Protein (GAP45) in Plasmodium Falciparum Merozoites.” *Molecular and Biochemical Parasitology* 149 (1): 113–16.

Ressurreição, Margarida, Aline Fréville, and Christiaan van Ooij. 2023. “Identification of a Non-Exported Plasmepsin V Substrate That Functions in the Parasitophorous Vacuole of Malaria Parasites.” *BioRxiv*. https://doi.org/10.1101/2023.05.15.540838.

Richard, Dave, Lev M. Kats, Christine Langer, Casilda G. Black, Khosse Mitri, Justin A. Boddey, Alan F. Cowman, and Ross L. Coppel. 2009. “Identification of Rhoptry Trafficking Determinants and Evidence for a Novel Sorting Mechanism in the Malaria Parasite Plasmodium Falciparum.” *PLoS Pathogens* 5 (3): e1000328.

Richard, Dave, Christopher A. MacRaild, David T. Riglar, Jo-Anne Chan, Michael Foley, Jake Baum, Stuart A. Ralph, Raymond S. Norton, and Alan F. Cowman. 2010. “Interaction between Plasmodium Falciparum Apical Membrane Antigen 1 and the Rhoptry Neck Protein Complex Defines a Key Step in the Erythrocyte Invasion Process of Malaria Parasites.” *The Journal of Biological Chemistry* 285 (19): 14815–22.

Ridzuan, Mohd A. Mohd, Robert W. Moon, Ellen Knuepfer, Sally Black, Anthony A. Holder, and Judith L. Green. 2012. “Subcellular Location, Phosphorylation and Assembly into the Motor Complex of GAP45 during Plasmodium Falciparum Schizont Development.” *PloS One* 7 (3): e33845.

Riglar, David T., Dave Richard, Danny W. Wilson, Michelle J. Boyle, Chaitali Dekiwadia, Lynne Turnbull, Fiona Angrisano, et al. 2011. “Super-Resolution Dissection of Coordinated Events during Malaria Parasite Invasion of the Human Erythrocyte.” *Cell Host & Microbe* 9 (1): 9–20.

Riglar, David T., Kelly L. Rogers, Eric Hanssen, Lynne Turnbull, Hayley E. Bullen, Sarah C. Charnaud, Jude Przyborski, et al. 2013. “Spatial Association with PTEX Complexes

Defines Regions for Effector Export into Plasmodium Falciparum-Infected Erythrocytes." *Nature Communications* 4: 1415.

Rts, S. Clinical Trials Partnership (2014). 2014. "Efficacy and Safety of the RTS, S/AS01 Malaria Vaccine during 18 Months after Vaccination: A Phase 3 Randomized, Controlled Trial in Children and Young Infants at 11 African Sites." *PLoS Medicine* 11 (7): e1001685.

Rts, Sctp, and Others. 2015. "Efficacy and Safety of RTS, S/AS01 Malaria Vaccine with or without a Booster Dose in Infants and Children in Africa: Final Results of a Phase 3, Individually Randomised, Controlled Trial." *The Lancet* 386 (9988): 31–45.

Rudlaff, Rachel M., Stephan Kraemer, Jeffrey Marshman, and Jeffrey D. Dvorin. 2020. "Three-Dimensional Ultrastructure of Plasmodium Falciparum throughout Cytokinesis." *PLoS Pathogens* 16 (6): e1008587.

Rudlaff, Rachel M., Stephan Kraemer, Vincent A. Streva, and Jeffrey D. Dvorin. 2019. "An Essential Contractile Ring Protein Controls Cell Division in Plasmodium Falciparum." *Nature Communications* 10 (1): 1–13.

Rug, Melanie, Marek Cyrklaff, Antti Mikkonen, Leandro Lemgruber, Simone Kuelzer, Cecilia P. Sanchez, Jennifer Thompson, et al. 2014. "Export of Virulence Proteins by Malaria-Infected Erythrocytes Involves Remodeling of Host Actin Cytoskeleton." *Blood* 124 (23): 3459–68.

Russo, Ilaria, Shalon Babbitt, Vasant Muralidharan, Tamira Butler, Anna Oksman, and Daniel E. Goldberg. 2010. "Plasmepsin V Licenses Plasmodium Proteins for Export into the Host Erythrocyte." *Nature* 463 (7281): 632–36.

Sanders, Paul R., Lev M. Kats, Damien R. Drew, Rebecca A. O'Donnell, Matthew O'Neill, Alexander G. Maier, Ross L. Coppel, and Brendan S. Crabb. 2006. "A Set of Glycosylphosphatidyl Inositol-Anchored Membrane Proteins of Plasmodium Falciparum Is Refractory to Genetic Deletion." *Infection and Immunity* 74 (7): 4330–38.

Sarfo, Jacob Owusu, Mustapha Amoadu, Peace Yaa Kordorwu, Abdul Karim Adams, Thomas Boateng Gyan, Abdul-Ganiyu Osman, Immanuel Asiedu, and Edward Wilson Ansah. 2023. "Malaria amongst Children under Five in Sub-Saharan Africa: A Scoping Review of Prevalence, Risk Factors and Preventive Interventions." *European Journal of Medical Research* 28 (1): 80.

Scally, Stephen W., Tony Triglia, Cindy Evelyn, Benjamin A. Seager, Michał Pasternak, Pailene S. Lim, Julie Healer, et al. 2022. "PCRCR Complex Is Essential for Invasion of Human Erythrocytes by Plasmodium Falciparum." *Nature Microbiology* 7 (12): 2039–53.

Schulze, Jana, Marcel Kwiatkowski, Janus Borner, Hartmut Schlüter, Iris Bruchhaus, Thorsten Burmester, Tobias Spielmann, and Christian Pick. 2015. "The Plasmodium Falciparum Exportome Contains Non-Canonical PEXEL/HT Proteins." *Molecular Microbiology* 97 (2): 301–14.

Schureck, Marc A., Joseph E. Darling, Alan Merk, Jinfeng Shao, Geervani Daggupati, Prakash Srinivasan, Paul Dominic B. Olinares, et al. 2021. "Malaria Parasites Use a Soluble RhopH Complex for Erythrocyte Invasion and an Integral Form for Nutrient Uptake." *ELife* 10 (January): e65282.

Sharma, Ashwani, Arvind Sharma, Sameer Dixit, and Amit Sharma. 2011. "Structural Insights into Thioredoxin-2: A Component of Malaria Parasite Protein Secretion Machinery." *Scientific Reports* 1 (December): 179.

Sherling, Emma S., Ellen Knuepfer, Joseph A. Brzostowski, Louis H. Miller, Michael J. Blackman, and Christiaan van Ooij. 2017. “The Plasmodium Falciparum Rhoptry Protein RhopH3 Plays Essential Roles in Host Cell Invasion and Nutrient Uptake.” *ELife* 6 (March). https://doi.org/10.7554/eLife.23239.

Sherling, Emma S., Abigail J. Perrin, Ellen Knuepfer, Matthew R. G. Russell, Lucy M. Collinson, Louis H. Miller, and Michael J. Blackman. 2019. “The Plasmodium Falciparum Rhoptry Bulb Protein RAMA Plays an Essential Role in Rhoptry Neck Morphogenesis and Host Red Blood Cell Invasion.” *PLoS Pathogens* 15 (9): e1008049.

Siddiqui, Faiza Amber, Shikha Dhawan, Shailja Singh, Bijender Singh, Pankaj Gupta, Alok Pandey, Asif Mohmmed, Deepak Gaur, and Chetan E. Chitnis. 2013. “A Thrombospondin Structural Repeat Containing Rhoptry Protein from Plasmodium Falciparum Mediates Erythrocyte Invasion.” *Cellular Microbiology* 15 (8): 1341–56.

Singh, Shailja, M. Mahmood Alam, Ipsita Pal-Bhowmick, Joseph A. Brzostowski, and Chetan E. Chitnis. 2010. “Distinct External Signals Trigger Sequential Release of Apical Organelles during Erythrocyte Invasion by Malaria Parasites.” *PLoS Pathogens* 6 (2): e1000746.

Skillman, Kristen M., Karthikeyan Diraviyam, Asis Khan, Keliang Tang, David Sept, and L. David Sibley. 2011. “Evolutionarily Divergent, Unstable Filamentous Actin Is Essential for Gliding Motility in Apicomplexan Parasites.” *PLoS Pathogens* 7 (10): e1002280.

Skillman, Kristen M., Christopher I. Ma, Daved H. Fremont, Karthikeyan Diraviyam, John A. Cooper, David Sept, and L. David Sibley. 2013. “The Unusual Dynamics of Parasite Actin Result from Isodesmic Polymerization.” *Nature Communications* 4 (1): 1–8.

Srinivasan, Prakash, Wandy L. Beatty, Ababacar Diouf, Raul Herrera, Xavier Ambroggio, J. Kathleen Moch, Jessica S. Tyler, et al. 2011. “Binding of Plasmodium Merozoite

Proteins RON2 and AMA1 Triggers Commitment to Invasion." *Proceedings of the National Academy of Sciences of the United States of America* 108 (32): 13275–80.

Suarez, Catherine, Gaëlle Lentini, Raghavendran Ramaswamy, Marjorie Maynadier, Eleonora Aquilini, Laurence Berry-Sterkers, Michael Cipriano, et al. 2019. "A Lipid-Binding Protein Mediates Rhoptry Discharge and Invasion in Plasmodium Falciparum and Toxoplasma Gondii Parasites." *Nature Communications* 10 (1): 4041.

Tham, Wai-Hong, Julie Healer, and Alan F. Cowman. 2012. "Erythrocyte and Reticulocyte Binding-like Proteins of Plasmodium Falciparum." *Trends in Parasitology* 28 (1): 23–30.

Tham, Wai-Hong, Nicholas T. Y. Lim, Greta E. Weiss, Sash Lopaticki, Brendan R. E. Ansell, Megan Bird, Isabelle Lucet, et al. 2015. "Plasmodium Falciparum Adhesins Play an Essential Role in Signalling and Activation of Invasion into Human Erythrocytes." *PLoS Pathogens* 11 (12): e1005343.

Thomas, Divya Catherine, Anwar Ahmed, Tim Wolf Gilberger, and Pushkar Sharma. 2012. "Regulation of Plasmodium Falciparum Glideosome Associated Protein 45 (PfGAP45) Phosphorylation." *PloS One* 7 (4): e35855.

Thomas, Jemima C., Judith L. Green, Ronald I. Howson, Peter Simpson, David K. Moss, Stephen R. Martin, Anthony A. Holder, Ernesto Cota, and Edward W. Tate. 2010. "Interaction and Dynamics of the Plasmodium Falciparum MTIP-MyoA Complex, a Key Component of the Invasion Motor in the Malaria Parasite." *Molecular BioSystems* 6 (3): 494–98.

Triglia, Tony, Stephen W. Scally, Benjamin A. Seager, Michał Pasternak, Laura F. Dagley, and Alan F. Cowman. 2023. "Plasmepsin X Activates the PCRCR Complex of Plasmodium

Falciparum by Processing PfRh5 for Erythrocyte Invasion." *Nature Communications* 14 (1): 2219.

Uwimana, Aline, Noella Umulisa, Meera Venkatesan, Samaly S. Svigel, Zhiyong Zhou, Tharcisse Munyaneza, Rafiki M. Habimana, et al. 2021. "Association of Plasmodium Falciparum Kelch13 R561H Genotypes with Delayed Parasite Clearance in Rwanda: An Open-Label, Single-Arm, Multicentre, Therapeutic Efficacy Study." *The Lancet Infectious Diseases* 21 (8): 1120–28.

Vahokoski, Juha, Saligram Prabhakar Bhargav, Ambroise Desfosses, Maria Andreadaki, Esa-Pekka Kumpula, Silvia Muñico Martinez, Alexander Ignatev, et al. 2014. "Structural Differences Explain Diverse Functions of Plasmodium Actins." *PLoS Pathogens* 10 (4): e1004091.

Volz, Jennifer C., Alan Yap, Xavier Sisquella, Jenn K. Thompson, Nicholas T. Y. Lim, Lachlan W. Whitehead, Lin Chen, et al. 2016. "Essential Role of the PfRh5/PfRipr/CyRPA Complex during Plasmodium Falciparum Invasion of Erythrocytes." *Cell Host & Microbe* 20 (1): 60–71.

Vulliez-Le Normand, Brigitte, Michelle L. Tonkin, Mauld H. Lamarque, Susann Langer, Sylviane Hoos, Magali Roques, Frederick A. Saul, et al. 2012. "Structural and Functional Insights into the Malaria Parasite Moving Junction Complex." *PLoS Pathogens* 8 (6): e1002755.

Waller, K. L., B. M. Cooke, W. Nunomura, N. Mohandas, and R. L. Coppel. 1999. "Mapping the Binding Domains Involved in the Interaction between the Plasmodium Falciparum Knob-Associated Histidine-Rich Protein (KAHRP) and the Cytoadherence Ligand P.

Falciparum Erythrocyte Membrane Protein 1 (PfEMP1).” *The Journal of Biological Chemistry* 274 (34): 23808–13.

Waller, R. F., M. B. Reed, A. F. Cowman, and G. I. McFadden. 2000. “Protein Trafficking to the Plastid of Plasmodium Falciparum Is via the Secretory Pathway.” *The EMBO Journal* 19 (8): 1794–1802.

Wang, Xu, Pengge Qian, Huiting Cui, Luming Yao, and Jing Yuan. 2020. “A Protein Palmitoylation Cascade Regulates Microtubule Cytoskeleton Integrity in Plasmodium.” *The EMBO Journal* 39 (13): e104168.

Weiss, Greta E., Paul R. Gilson, Tana Taechalertpaisarn, Wai-Hong Tham, Nienke W. M. de Jong, Katherine L. Harvey, Freya J. I. Fowkes, et al. 2015. “Revealing the Sequence and Resulting Cellular Morphology of Receptor-Ligand Interactions during Plasmodium Falciparum Invasion of Erythrocytes.” *PLoS Pathogens* 11 (2): e1004670.

Wong, Wilson, Rick Huang, Sebastien Menant, Chuan Hong, Jarrod J. Sandow, Richard W. Birkinshaw, Julie Healer, et al. 2018. “Structure of Plasmodium Falciparum Rh5–CyRPA–Ripr Invasion Complex.” *Nature* 565 (7737): 118–21.

World Health Organization. 2021. “WHO Recommends Groundbreaking Malaria Vaccine for Children at Risk,” October 6, 2021. https://www.who.int/news/item/06-10-2021-who-recommends-groundbreaking-malaria-vaccine-for-children-at-risk.

———. 2022. *World Malaria Report 2022*. World Health Organization.

Yahata, Kazuhide, Melissa N. Hart, Heledd Davies, Masahito Asada, Samuel C. Wassmer, Thomas J. Templeton, Moritz Treeck, Robert W. Moon, and Osamu Kaneko. 2021. “Gliding Motility of *Plasmodium* Merozoites.” *Proceedings of the National Academy of*

Sciences of the United States of America 118 (48). https://doi.org/10.1073/pnas.2114442118.

Yeoman, Jeffrey A., Eric Hanssen, Alexander G. Maier, Nectarios Klonis, Bohumil Maco, Jake Baum, Lynne Turnbull, Cynthia B. Whitchurch, Matthew W. A. Dixon, and Leann Tilley. 2011. "Tracking Glideosome-Associated Protein 50 Reveals the Development and Organization of the Inner Membrane Complex of Plasmodium Falciparum." *Eukaryotic Cell* 10 (4): 556–64.

Zhang, Qi, Cheng Ma, Alexander Oberli, Astrid Zinz, Sonja Engels, and Jude M. Przyborski. 2017. "Proteomic Analysis of Exported Chaperone/Co-Chaperone Complexes of P. Falciparum Reveals an Array of Complex Protein-Protein Interactions." *Scientific Reports* 7 (1): 1–15.

Zhu, Xiaotong, Kazuhide Yahata, Jean Semé Fils Alexandre, Takafumi Tsuboi, and Osamu Kaneko. 2013. "The N-Terminal Segment of Plasmodium Falciparum SURFIN4.1 Is Required for Its Trafficking to the Red Blood Cell Cytosol through the Endoplasmic Reticulum." *Parasitology International* 62 (2): 215–29.

Zuccala, Elizabeth S., Alexander M. Gout, Chaitali Dekiwadia, Danushka S. Marapana, Fiona Angrisano, Lynne Turnbull, David T. Riglar, et al. 2012. "Subcompartmentalisation of Proteins in the Rhoptries Correlates with Ordered Events of Erythrocyte Invasion by the Blood Stage Malaria Parasite." *PloS One* 7 (9): e46160.

1.5. Figures

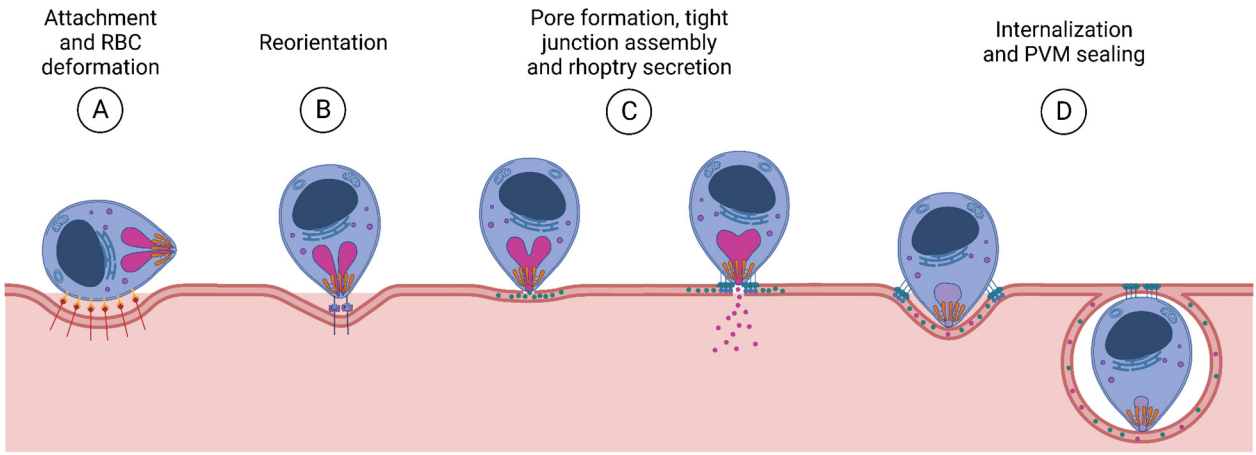

Figure 1.1. *Plasmodium falciparum* invasion of host RBCs. A) A merozoite recognizes an RBC and initiates a weak early attachment mediated by the interaction of merozoite ligands with host cell receptors. This is followed by merozoite gliding over the RBC, which causes RBC deformation. B) Subsequently, binding of the Rh5 complex to basigin in conjunction with RBC deformation seems to lead to the reorientation of the merozoite's apical end towards the RBC. C) At this point, a pore is formed at the RBC-merozoite site of contact (likely caused by the RH5-basigin interaction). This leads to the secretion of rhoptry proteins, insertion of the rhoptry complex into the RBC membrane, and the formation of the tight junction, marking an irreversible point of commitment to invasion. D) Finally, the merozoite utilizes its actinomyosin motor to move through the opening tight junction, pulling the RBC membrane around itself to form the PVM. Once the merozoite has been internalized, motor-driven merozoite twisting and SUB2 activity lead to PVM sealing, resulting in fully merozoite invasion.

CHAPTER 2

2. TIME-RESOLVED PROXIMITY BIOTINYLATION IMPLICATES A PORIN PROTEIN IN EXPORT OF TRANSMEMBRANE MALARIA PARASITE EFFECTORS

David Anaguano, Watcharatip Dedkhad, Carrie F. Brooks, David W. Cobb, Vasant Muralidharan. 2023. Time-Resolved Proximity Biotinylation Implicates a Porin Protein in Export of Transmembrane Malaria Parasite Effectors. *Journal of Cell Science*, September. doi:10.1242/jcs.260506. Reprinted here with permission of the publisher.

2.1. Abstract

The malaria-causing parasite, Plasmodium falciparum completely remodels its host red blood cell (RBC) through the export of several hundred parasite proteins, including transmembrane proteins, across multiple membranes to the RBC. However, the process by which these exported membrane proteins are extracted from the parasite plasma membrane for export remains unknown. To address this question, we fused the exported membrane protein, skeleton binding protein 1 (SBP1), with TurboID, a rapid, efficient, and promiscuous biotin ligase ($SBP1^{TbID}$). Using time-resolved, proximity biotinylation, and label-free quantitative proteomics, we identified two groups of $SBP1^{TbID}$ interactors: early interactors (pre-export) and late interactors (post-export). Notably, two promising membrane-associated proteins were identified as pre-export interactors, one of which possesses a predicted translocon domain, that could facilitate the export of membrane proteins. Further investigation using conditional mutants of these candidate proteins showed that these proteins were essential for asexual growth and localize to the host-parasite interface during early stages of the intraerythrocytic cycle. These data suggest that they might play a role in ushering membrane proteins from the parasite plasma membrane for export to the host RBC.

2.2. Introduction

Malaria is a major global health issue, with an estimated 241 million cases and 627,000 deaths reported during 2021 (Organization and Others 2021). This life-threatening disease is caused by *Plasmodium* parasites, belonging to the apicomplexan phylum. Among these parasites *Plasmodium falciparum* is the most virulent and lethal, accounting for 95% of all malaria-related deaths (Moxon et al. 2020). Malaria symptoms include headaches, myalgia, high fevers, severe anemia, pulmonary and renal failure, vascular obstruction, and cerebral damage. These disorders can persist even after parasite clearance and result from the proliferation of parasites within human red blood cells (RBC) (Moxon et al. 2020; Ashley, Pyae Phyo, and Woodrow 2018).

To establish infection during their intraerythrocytic cycle, *P. falciparum* parasites extensively remodel the morphology and physiology of the RBCs. This transformation requires the export of several hundred proteins (approximately 10% of the parasite proteome) across the unique parasitophorous vacuole (PV), a membrane surrounding the parasite, into the cytoplasm and membrane of RBCs (Spillman, Beck, and Goldberg 2015; Spielmann and Gilberger 2015; K. M. Matthews, Pitman, and de Koning-Ward 2019; de Koning-Ward et al. 2016). This process leads to increased permeability, loss of cell deformability, and the formation of virulence-associated knobs at the RBC membrane (Maier et al. 2009; Sanjay A. Desai 2014). These multi-step transformations are crucial for parasite survival and pathogenesis, conferring *P. falciparum* its ability to maintain chronic infections in humans. A large fraction of exported proteins is recognizable by the presence of a 5-amino-acid motif, known as the *Plasmodium* export element or PEXEL (Hiller et al. 2004; Marti et al. 2004), whereas others lack a discernable primary sequence motif and are termed as PEXEL-negative exported proteins or PNEPs (Heiber et al. 2013). Most PNEPs possess a transmembrane (TM) domain that serves to target them to the

endoplasmic reticulum (ER) and the secretory pathway (Heiber et al. 2013). Several of these PNEPs play critical roles in malaria pathogenesis, such as skeleton-binding protein 1 (SBP1) (Blisnick et al. 2000; Saridaki et al. 2009; Maier et al. 2007), membrane-associated histidine-rich protein (MAHRP1) (C. Spycher et al. 2003; Cornelia Spycher et al. 2008) and erythrocyte membrane protein 1 (PfEMP1) (Su et al. 1995; Baruch et al. 1995, 1997).

Exported membrane proteins are inserted into ER membrane during their synthesis (Heiber et al. 2013; Spielmann et al. 2006; Gruring et al. 2012). These membrane proteins are transported via vesicles from the ER and inserted into the parasite plasma membrane (PPM) when the transport vesicles fuse to the PPM (Gruring et al. 2012). Although it has been established that all exported proteins require the *Plasmodium* translocon of exported proteins (PTEX) complex to cross the PV membrane (PVM) (Josh R. Beck et al. 2014; Elsworth et al. 2014), the mechanism by which membrane proteins are extracted from the PPM and delivered to the PTEX complex remains unknown. It has been postulated that a putative *Plasmodium* translocon of exported membrane proteins (which we term as PTEM) (J. R. Beck and Ho 2021; Garten and Beck 2021) is necessary for the extraction of membrane proteins from the PPM, either alone or in cooperation with the PTEX unfoldase HSP101 (Kathryn M. Matthews, Kalanon, and de Koning-Ward 2019; Gabriela et al. 2022) (Fig. 2.1A). However, the identity of proteins in this putative PTEM complex is unknown, and no candidates have been identified using bioinformatic approaches within the *P. falciparum* genome. To address this knowledge gap, we attempted to utilize an unbiased proteomic approach to identify proteins potentially constituting the putative PTEM complex.

Immunoprecipitation (IP)-based proteomic approaches have been used previously to identify the exported-protein interacting complex (EPIC) at the PV, which is thought to be required for protein export (Batinovic et al. 2017). Similar approaches using *Plasmodium* exported proteins

have identified stable complexes at the Maurer's clefts (MC), a parasite-generated protein sorting organelle in the RBC (Jonsdottir, Counihan, et al. 2021; Carmo et al. 2022; Takano et al. 2019; McHugh et al. 2020b). However, the identification of the putative PTEM has proven elusive because its interaction with exported membrane proteins will be transient and therefore, unlikely to be captured using IP assays which are heavily biased towards identifying stable complexes. Therefore, we used a rapid, proximity-labeling approach to attempt to identify a putative PTEM complex and to our knowledge, this approach has not yet been used in a time-resolved manner to capture transient interactions in the secretory pathway.

We chose to tag the endogenous SBP1 gene (PF3D7_0501300) with a new iteration of the promiscuous biotin ligase BirA, known as TurboID (generating SBP1^{TbID}) (Branon et al., 2018). SBP1 is a PNEP with a single TM domain and is exported in early ring-stage parasites to the MC (Blisnick et al. 2000). TurboID is a highly efficient enzyme that is able to biotinylate proteins in close proximity within 10 minutes (Branon et al., 2018). Therefore, we hypothesized that SBP1^{TbID} will biotinylate proteins, even those transiently interacting with SBP1^{TbID} along the secretory pathway during its export to the MC. Given that SBP1^{TbID} should rapidly biotinylate proximal proteins, we further reasoned that we could differentiate early (pre-export) interactors from late (post-export) interactors of SBP1^{TbID}. Our data show that the SBP1^{TbID} fusion protein is exported to the MC efficiently and with similar kinetics to another MC protein, MAHRP1. Crucially, SBP1^{TbID} is able to rapidly biotinylate proximal proteins prior to its export from the PV as well as after export at the MC. Using label-free quantitative proteomics, we compared pre-export interactors and post-export interactors of SBP1^{TbID}. This approach led to the identification of two membrane-associated proteins that might play a role in the export of transmembrane malaria parasite effectors to the host RBC.

2.3. Results

2.3.1. SBP1 fused TurboID is exported to Maurer's Clefts

Using CRISPR/Cas9 gene editing we generated mutants of SBP1 (Fig. 2.1B), where the endogenous gene was tagged with the TurboID biotin ligase ($SBP1^{TbID}$) (Branon et al. 2018; May et al. 2020). We chose TurboID because it is an optimized version of the biotin ligase BirA (Branon et al., 2018). TurboID is a highly active mutant of BirA with an increased biotinylation radius and faster biotinylation kinetics (Branon et al. 2018; May et al. 2020). PCR analysis of genomic DNA isolated from the $SBP1^{TbID}$ parasite line showed the correct integration of the TurboID biotin ligase and a V5 tag at the endogenous locus of SBP1 (Fig. 2.1C). We detected expression of the $SBP1^{TbID}$ in the mutant line at the expected size, but not in the parental line (Fig. 2.1D). To ensure that the expression of TurboID is not detrimental to the parasite, we observed the growth of $SBP1^{TbID}$ and the parental parasite line ($NF54^{attB}$) (Nkrumah et al., 2006), over several asexual cycles using flow cytometry (Fig. 2.1E). These data show no difference in the asexual growth of $SBP1^{TbID}$ compared to that of the parental parasites, demonstrating that expression of TurboID or its fusion to SBP1 does not inhibit parasite growth.

SBP1 is an exported protein with a single TM domain synthesized in the parasite ER and transported to the MC in the RBC cytoplasm(Mundwiler-Pachlatko and Beck 2013; Cooke et al. 2006). Therefore, we wanted to ensure that the fusion of TurboID to SBP1 did not inhibit its export to the MC. Using immunofluorescence microscopy (IFA), we tested whether $SBP1^{TbID}$ colocalized with another MC resident protein, MAHRP1 (Spycher et al., 2008). These data show that $SBP1^{TbID}$ was exported from the parasite to the MC and that it colocalized with MAHRP1 in trophozoite and schizont stage parasites (Fig. 2.1F and 2.1G). By contrast, in early ring stage parasites, these data

show that SBP1^{TbID}, as well as MAHRP1, localize to the periphery of the parasite, probably in the PV prior to export (Fig. 2.1F). This has been previously observed by electron microscopy, where SBP1 accumulated in electron-dense regions within the parasite plasma membrane (PPM) before being transported through the PV membrane (Iriko et al., 2020). These data suggest that SBP1 and possibly other MC resident proteins accumulate in the PV before being exported to the infected RBC. Together, the data show that tagging SBP1 with the TbID biotin ligase did not alter the asexual growth or development of the parasite, nor did it inhibit the export of SBP1 to the host RBC and MC (Fig. 2.1).

2.3.2. Biotin-dependent proximity labeling by SBP1^{TbID}

Given that our data show that the SBP1^{TbID} fusion protein was exported to MC, we wanted to examine the capacity of TurboID to biotinylate proximal proteins in SBP1^{TbID} parasites. TurboID is an extremely efficient enzyme and we found it could utilize the minimal amount of biotin present in the media used to grow SBP1^{TbID} parasites (Fig. 2.2). The normal asexual development of *P. falciparum* does not require biotin (Dellibovi-Ragheb et al. 2018). To test whether SBP1^{TbID} biotinylation is dependent upon the presence of exogenous biotin, we analyzed protein extracts of asynchronous parasites in the presence or absence of biotin by streptavidin blotting. We observed that efficient biotinylation of proximal proteins occurs only in the presence of biotin in SBP1^{TbID} parasites (Fig. 2.3A). Self-biotinylation in SBP1^{TbID} parasites was observed in the presence or absence of biotin (Fig. 2.3A, lane 3 and 4, see asterisk), in agreement with what has been previously reported when tagging proteins with TurboID (Branon et al. 2018; Larochelle et al. 2019). No endogenous biotinylation was detected in the parental line NF54^{attB}, showing that biotinylation occurs only when TurboID is being expressed by the parasite line (Fig. 2.3A, lanes

1 and 2). These data show that SBP1^{TbID} efficiently biotinylated proteins and its activity is dependent upon the presence of biotin in the growth medium.

TurboID is a highly active enzyme (Branon et al., 2018) that offers the possibility of rapid and time-resolved labeling approaches in contrast to previous proximity-labeling methods with much longer incubation times, usually greater than 12 hours (Roux et al. 2012; Kim et al. 2016; Kudyba et al. 2019). Thus, we wanted to assess the biotinylation activity of SBP1^{TbID} and test whether this fusion protein can rapidly biotinylate proximal proteins. SBP1^{TbID} parasites were incubated with biotin for 1, 2, or 6 hours and the biotinylation of proteins was observed using western blots probed with streptavidin (Fig. 2.3B). We also tested biotinylation in response to different concentrations of biotin, 25, 50 and 100 μM (Fig. 2.3C). Biotinylated proteins were observed at all time points and biotin concentrations, and the observable difference in the extent of protein biotinylation between the time points and concentrations was minimal (Fig. 2.3B and 2.3C).

The SBP1^{TbID} fusion protein has to traverse several membranes during its export to the MC, and therefore, it is likely to unfold and then refold during this transport process. In the case of exported membrane proteins, it is not known whether they are kept unfolded during their transport, although all proteins have to unfold while crossing the PV membrane using the PTEX complex at the PV membrane (Josh R. Beck et al. 2014; Ho et al. 2018; Elsworth et al. 2014). Furthermore, to our knowledge, TurboID has not yet been utilized in a time-resolved manner to identify transient interactors as proteins are transported through the secretory pathway. Therefore, we wanted to determine whether SBP1^{TbID} parasites could biotinylate proteins proximal to SBP1 at different cellular locations during the export of SBP1^{TbID} from the parasite ER to the MC. Synchronized early ring and trophozoite stage parasites were observed by IFAs after the addition

of biotin for 2 h. We observed biotinylation at the parasite periphery, possibly when SBP1^{TbID} accumulates at the PV (Iriko et al., 2020) (Fig. 2.3D, top panels). Biotinylation was also observed when SBP1^{TbID} had been exported to the MC (Fig. 2.3D, bottom panels). The observed biotinylation was dependent upon the addition of biotin. Together, these data demonstrate that SBP1^{TbID} was highly active, efficient, rapid, and labeled proximal proteins at different subcellular locations during its export from the parasite ER to the final location at the MC (Fig. 2.3).

2.3.3. Early interactors of SBP1^{TbID} identified by proximity labeling

Given that our data show that SBP1^{TbID} biotinylated proximal proteins during its transit via the secretory pathway to the RBC cytoplasm (Fig. 2.3D), we next wanted to identify the *P. falciparum* effectors that interact with SBP1 at the host-parasite interface. To do so, we wanted to define the kinetics of SBP1^{TbID} transport from its site of synthesis in the parasite ER to its export to the MC and test whether we could reproducibly detect SBP1 at the host-parasite interface. As described above (Fig. 2.1E, 2.3D), SBP1^{TbID} and proteins biotinylated by SBP1^{TbID} could be detected at the parasite-RBC interface. To assess whether we could reproducibly observe SBP1^{TbID} within the parasite prior to its export to the host RBC, we used tightly synchronized cultures and observed the subcellular localization of SBP1^{TbID} with respect to EXP2, a PVM resident protein (Garten et al. 2018; Charnaud et al. 2018), at different time points after parasite invasion. SBP1 has been detected at the MCs as early as 4-6 hours post-invasion (hpi) (Grüring et al. 2011), therefore, we observed the subcellular location of SBP1^{TbID} in parasites at 3, 4 and 5 hpi. In some SBP1^{TbID} parasites, SBP1 was either not detectable or not expressed (Fig. 2.4B, top panels). As expected, we found parasites where SBP1^{TbID} was within the PV periphery and others where the protein was already exported to the RBC cytoplasm (Fig. 2.4B, mid and bottom panels). We

quantified these three events over several biological replicates. At 4hpi, SBP1^{TbID} was not expressed in about 30% of the parasites, exported in ~10% of observed parasites, and at the host-parasite interface in the vast majority (60%) of all parasites (Fig. 2.4C). These data showed us that harvesting proteins biotinylated by SBP1^{TbID} at the host-parasite interface was feasible.

To identify early interactors of SBP1, especially those at the host-parasite interface, we opted for a quantitative and comparative approach. We wanted to differentiate these early interactors from SBP1 interactors at the MC, which have been previously identified (Takano et al. 2019), as well as those being co-transported with SBP1 to the MC. We hypothesized that using label-free quantitative proteomics and comparing interactors isolated from 4 hpi and 20 hpi would allow us to identify the early interactors of SBP1. By 20 hpi, all SBP1 is at the MCs and no more SBP1 is synthesized (Fig. 2.3D) (McMillan et al. 2013). Label-free proteomics has been shown to offer a large dynamic range and high proteome coverage for the identification of biotinylated proteins (Lobingier et al. 2017; Mair et al. 2019; Santos-Barriopedro, van Mierlo, and Vermeulen 2021; Larochelle et al. 2019).

First, tightly synchronized late-stage schizonts were collected. These parasites were then split into two samples. One sample was incubated with biotin for 4 h until 4 hpi (Fig. 2.4A, blue box), after which it was collected for further processing. Based on our data, which indicate that SBP1^{TbID} is predominantly localized at the host-parasite interface during the 4-hour ring stage (Fig. 2.4C), parasites were incubated with biotin for 4 h to maximize the labeling of proximal proteins and capture a larger fraction of the pre-export interactors. To collect the post-export sample, SBP1^{TbID} parasites were allowed to develop until 16 hpi, as by this time, all SBP1 is localized to the Maurer's clefts (MC) and is no longer synthesized. Thus, the other sample was allowed to develop without biotin for 16h and then incubated with biotin for 4 h until 20 hpi (Fig. 2.4A, red

box).

Biotinylated proteins were isolated from parasite lysates using streptavidin-affinity pulldown. The streptavidin-captured proteins were identified via mass spectrometry (MS) and quantified over several biological replicates (Lobingier et al. 2017; Larochelle et al. 2019; Mair et al. 2019) (Fig. 2.5A). In total, 1,122 proteins were identified in at least one of the replicates. We then compared the proteins identified in the 4h sample with those identified in the 20h sample (Fig. 2.5B). We defined the putative pre-export interactors of SBP1 from our dataset using three stringent criteria. Proteins that exhibited more than 10-fold enrichment compared to the 20h samples, with a p-value cut-off of 0.05, and were present in all three biological replicates, were considered as differentially labeled interactors at 4 hpi. Using these criteria, we identified 24 protein candidates as putative pre-export interactors of SBP1^{TbID} during its transport at the parasite-RBC interface (Fig. 2.5B). Among the identified proteins, only 2 were specific to *P. falciparum*, whereas the remaining 22 had homologs in other *Plasmodium* species. Interestingly, the majority of proteins with unknown functions were exclusive to *Plasmodium*, and 9 proteins had homologs in other Apicomplexans (Fig. 2.5B and Table 2.1).

The identified proteins were classified into subgroups based on their predicted functions and subcellular locations (Amos et al. 2022). Of the 24 identified proteins, 11 were uncharacterized proteins with no predicted function. As expected, this approach identified proteins known to be involved in protein and vesicle transport (5/24). One of the statistically significant interactors of SBP1 was EXP3 (3-fold enriched at 4hpi), which has been localized to the PV and functions in protein export (Batinovic et al. 2017). The experiment worked as designed because SBP1 (star, Fig. 2.5B) and other MC localized as well exported proteins were also identified but were not enriched at either time point or enriched in the 20 hpi samples (Fig. 2.5B). Identification of

exported proteins, including MC proteins, only in the post-export (20 hpi) samples further suggests that the proteomic approach using SBP1^{TbID} worked as designed (Table 2.2). Together these data showed that our approach successfully identified a group of proteins differentially biotinylated by SBP1^{TbID} prior to its export to the MC.

2.3.4. Early interactors of SBP1^{TbID} localize to the host-parasite interface

Given that we were interested in identifying proteins that facilitate the export of transmembrane proteins through the PPM, we reasoned that membrane-associated proteins among pre-export SBP1 interactors could function in this role. Thus, based on membrane association, high statistical score, and fold enrichment, we selected the Glideosome-associated protein with multiple membrane spans 1 (GAPM1, PF3D7_1323700) as one putative candidate. GAPM1 is a membrane protein associated with the biogenesis of the Inner Membrane Complex (IMC) in asexual and sexual stages. GAPM1, as part of the IMC, is suggested to have a role in merozoite invasion (Kono et al. 2013, 2012; Bullen et al. 2009). Using these criteria, another putative candidate was the channel protein Voltage-dependent anion-selective channel protein (VAC, PF3D7_1432100). VAC is a soluble protein with a translocon of the outer mitochondrial membrane (TOM40) domain but no mitochondria-targeting signal. Recent work has shown that VAC is a putative membrane protein that does not localize to the mitochondrial membrane(Lamb et al., 2022). Nothing is known about the function of VAC in *P. falciparum*.

To characterize these proteins, we used CRISPR/Cas9 gene editing to generate the conditional mutants, termed VAC^{apt} and GAPM1$^{mNG\text{-}apt}$. In these parasite lines, their endogenous loci were tagged with the *tetR* aptamer system, which results in anhydrotetracycline (aTc)-

dependent expression of the protein (Fig. 2.6A and 2.6B) (Rajaram et al., 2020). PCR analysis of genomic DNA from VAC^{apt} and GAPM1$^{mNG\text{-}apt}$ parasite lines showed correct integration of the knockdown system at the endogenous loci (Fig. 2.6C). To assess the efficiency of the knockdown system, we measured protein expression in the presence or absence of aTc by Western blotting. For both proteins, there is a clear reduction of protein expression (Fig. 2.6D), which in the case of GAPM1$^{mNG\text{-}apt}$ was detrimental, as parasites were not able to progress into a second life cycle. Knockdown of VAC inhibited the asexual expansion of VAC^{apt} parasites (Fig. 2.6E).

Our data confirms that GAPM1^{mNG} localizes to the IMC in schizonts (Fig. 2.7) (Bullen et al, 2009). However, the localization of GAPM1 post-invasion in the early ring stages is not known. Similarly, the subcellular localization of VAC during the early stages of the asexual life cycle was unknown. The proteomic data suggest that these proteins are in close proximity to SBP1^{TbID} when SBP1 is in the PV (Fig. 2.5B). Therefore, we used IFAs to localize both proteins in tightly synchronized parasites at 4 hpi with respect to the PV marker EXP2. VAC^{apt} localizes to the parasite periphery and is closely juxtaposed with the known PV marker, EXP2, but it also partially overlaps with the mitochondria (Fig. 2.8A, top panels), suggesting that it might be localized to both subcellular organelles. GAPM1$^{mNG\text{-}apt}$ localizes to the parasite periphery at 4 hpi and shows colocalization with EXP2 (Fig. 2.8A, bottom panels). To corroborate our observations by IFAs, we used light-sheet microscopy (LSM) to determine the subcellular localization of VAC and GAPM1 with respect to EXP2 and MAHRP1 (Fig. 2.8A and 2.8C), which is another exported membrane protein that is trafficked to Maurer's clefts (Fig. 2.1F). Both proteins show a high degree of colocalization with EXP2, strengthening our previous observation. Additionally, colocalization of VAC and GAPM1 was observed with respect to the exported protein MAHRP1, confirming that all three proteins are localized to the host-parasite interface at 4-hpi parasites (Fig 2.8B and

2.8D). Despite both proteins showing a high degree of colocalization with the PVM marker EXP2, our observations using structured illumination microscopy (SIM) (Fig. 2.9) showed a more juxtaposed but not completely overlapping localization. This suggests VAC and GAPM1 do not localize to the PVM but rather to a different membrane such as the PPM.

The limited resolution provided by conventional microscopy, together with the lack of available PPM markers and the narrow space between the PPM and PVM, makes it challenging to determine the precise localization of VAC and GAPM1 within the membranes. In an effort to overcome these limitations, we employed ultrastructural expansion microscopy (U-ExM) in combination with NHS-ester immunostaining, which has been demonstrated to allow visualization of various membranes, such as the nuclear membrane and the PPM (Liffner and Absalon 2021; Liffner et al. 2023). We co-localized GAPM1 and VAC with the PV lumen marker, Rhoptry associated protein 1 (RAP1, Fig. 2.10A) (Riglar et al. 2011). Our observations indicate that VAC and GAPM1 are localized within the PVM, overlapping with the PV lumen marker RAP1 (Fig. 2.10A). However, based on the U-ExM data, it remains unclear whether these proteins are localized in the PPM (Fig. 2.10A). Interestingly, VAC exhibits an additional focal localization towards the cytoplasmic side of the parasites, which supports our previous observation suggesting a dual localization of the protein in early-stage parasites (Fig. 2.10A, top panels). Finally, we utilized live-cell microscopy to track the localization of GAPM1, which is tagged with mNeonGreen, after invasion of RBCs (Fig. 2.10B). These data show that GAPM1 remains present for at least 15 min post-invasion (Fig. 2.10B). Together with our previous data, this suggests that the IMC might not completely disappear until later during ring-stage development, contrary to what was previously suggested (Riglar et al. 2013). Another possibility, consistent with prior

observations, is that GAPM1 relocalizes from the IMC to the PPM. Our observations cannot distinguish between these possibilities.

Together these results show that both GAPM1 and VAC localize to the parasite periphery together with SBP1^{TbID} at the PV at 4 hpi, as suggested by the proximity labeling data.

2.4. Discussion

The protein-protein interactions that usher exported proteins to their final destinations in the RBC via the secretory pathway are transient in nature. Previously, IP-based methods have been used to identify proteins required for the export of *P. falciparum* proteins, such as the PTEX complex (de Koning-Ward et al. 2009) and the EPIC complex (Batinovic et al. 2017). Although IP-based approaches are well-suited for identifying stable complexes, they are unlikely to identify transient interactions. A putative additional translocon at the PPM required for extracting exported membrane proteins that are inserted into the PPM during transport has long been proposed (J. R. Beck and Ho 2021; Garten and Beck 2021). As yet, no candidates for this putative complex have been identified (Fig. 2.1).

In our study, we used time-resolved biotinylation to identify transient interactions of an exported membrane protein, SBP1, during its export. This approach uses a rapid and promiscuous biotin ligase to biotinylate proximal proteins (Branon et al., 2018). It is important to note that TurboID is a highly efficient enzyme and can utilize a minimal amount of biotin in the media. Hence, to ensure that TurboID is active only at specific times we utilized biotin-free medium for this time-resolved approach to identify transient interactors of SBP1 during its trafficking in the infected RBC. As biotinylation is a permanent modification, even transient interactions can be

potentially identified. Using this approach, we found putative candidates localized at the parasite periphery that could help extract membrane exported proteins from the PPM for transport into the RBC. Our data show that fusion of TurboID to the exported transmembrane-containing protein, SBP1, did not alter its trafficking to the MC nor did it have any effect on parasite growth. These data also suggest that TurboID is enzymatically active during transit in the parasite secretory pathway. This property of TurboID might be useful in many contexts to resolve protein trafficking pathways in other organisms.

A previous study on the SBP1 interactome at their final location at the MC identified 88 parasite proteins as putative interactors (Takano et al. 2019). Most of their top-ranked hit proteins were also identified in our study such as PfEMP1, Pf332, PIESP2, REX1, MAHRP1, PTP1 and vapA. However, these were not highly enriched (≤10-fold) in the post-export interactors fraction. This could be because some of these proteins are co-transported with SBP1 and thus, are identified in the pre-export fraction as well. Members of the PTEX complex such as EXP2, HSP101, and Trx2, were also identified in the pre-export fraction, albeit at levels below statistical significance. In addition, PTP2 and PfG174, which have been previously shown to localize as residents (Maier et al. 2008), or transient interactors (Vincensini et al. 2005) of the MCs, were more than 10-fold enriched at the post-export time point, demonstrating the reliability of our approach for identification of SBP1 interactors. Another subset of proteins identified in our study as post export interactors of SBP1 are ribosomal proteins, which have been previously observed to be exported to the *P. falciparum* infected RBC (Sudipta Das et al. 2012). Together, these data strongly suggest that the time-resolved, rapid biotinylation approach was working as designed. Given that our focus was to identify pre-export interactors, we did not pursue these proteins for further study.

Using label-free quantitative proteomics, we identified a group of 24 putative candidates that are proximal to SBP1 prior to its export to the RBC. Several of the proteins identified (14/24) were uncharacterized proteins or nuclear proteins. Because we undertook this approach to identify the putative translocon complex required for extraction of exported membrane proteins from the plasma membrane, we did not pursue the function of these proteins in this study. Translocons function to transport proteins across membranes and therefore, we hypothesized that membrane-associated proteins in this list could putatively function as translocons. There were two putative candidates in the pre-export interactors of SBP1 that were membrane-associated, VAC, and GAPM1. However, their localization in early ring-stage parasites was unknown. Therefore, to study the function of VAC and GAPM1 in early ring-stage parasites, we successfully generated conditional mutants. The data show that both VAC and GAPM1 play important functions in parasite survival within the infected RBC. Knockdown of these proteins inhibits parasite growth. However, achieving protein knockdown takes about 24-48 hours and results in parasite death prior to invasion of the RBC. Proteins transported to the MC are synthesized and transported early in the asexual lifecycle (2-8hpi). Therefore, this prevents the characterization of their role in export, as the knockdown takes effect after proteins are exported to the MC and parasites die prior to reaching the next life cycle. Similar to what was found for the PTEX translocon, EXP2 (Garten et al. 2018), it is likely that both GAPM1 and VAC have other essential functions in the asexual life cycle. Defining their function in export will require using a more rapid knockdown approach that has similar kinetics to that of SBP1 export, such as degradation-domain-based tools (Josh R. Beck et al. 2014; Muralidharan et al. 2012) or rapid mislocalization-based methods (Birnbaum et al., 2017).

VAC has a β-barrel porin domain that can form an aqueous channel in the membrane and function as a translocon in mitochondria and other plastids (Lamb et al., 2022). In a recent proximity-biotinylation-based proteomic screen to catalog mitochondrial proteins in *P. falciparum*, VAC was pulled down in the membrane fraction of parasite lysates, and not in the mitochondrial fraction (Lamb et al., 2022). In addition, VAC is predicted to not contain a mitochondrial targeting sequence, in contrast to its *Plasmodium* ortholog, TOM40 (PF3D7_0617000), which has a mitochondrial targeting sequence, suggesting that VAC might not be localized to the mitochondria (Claros and Vincens 1996). Our data reveal that VAC localizes at the host-parasite interface in early ring stages. Although there is some overlap of VAC with the mitochondria, there is a stronger overlap between the PVM marker, EXP2, and VAC in lower-resolution IFAs. It is also possible that VAC is dually localized both to the mitochondria as well as to the host-parasite interface. Super resolution microscopy suggests that EXP2 and VAC are closely juxtaposed but with minimal overlap. This suggests that VAC localizes to a compartment in close proximity to the PVM, most likely the PPM. By contrast, GAPM1 has seven TM domains and is from an apicomplexan-specific family of proteins (Bullen et al. 2009). GAPM1 has been localized to the inner membrane complex (IMC) in schizont-stage parasites (Bullen et al. 2009). The IMC plays an essential role in the invasion of merozoites into the RBC, however, it is unclear what happens to the IMC proteins post-invasion (Ferreira et al. 2020). Lower resolution IFAs show that GAPM1 co-localizes with the PVM-localized EXP2 in early ring-stage parasites. Using both U-ExM and SIM we observe that, like VAC, GAPM1 is in close juxtaposition with EXP2, but does not completely overlap it, suggesting that GAPM1 might also localize to the PPM in early rings. These data further suggest that the IMC could fuse to the parasite plasma membrane after merozoite invasion or that GAPM1 relocalizes to the PPM. Our data is consistent with both models and cannot distinguish between

them. Cryo-EM studies of during and after parasite invasion might illuminate the fate of the IMC in newly invaded rings. Using U-ExM allowed us to observe the localization of VAC and GAPM1 at a better resolution and supports our observations that they are localized at the parasite periphery in early ring stage parasites. However, we were unable to differentiate between the PV lumen using RAP1 (Riglar et al. 2011) and the PPM where GAPM1 and VAC might localize. Although our extensive microscopy data show that both EXP2 and RAP1 are in close proximity to both GAPM1 and VAC, neither EXP2 nor RAP1 was reproducibly identified in our mass spectrometry experiments. Together these strongly suggest the proximity labeling approach worked to identify specific interactors of SBP1 prior to its export from the parasite. These findings are consistent with the model that VAC and GAPM1 transiently interact with SBP1 prior to its export at the parasite periphery, perhaps as members of a putative translocon complex.

Several mechanistic aspects of this model remain to be resolved but similar to the PTEX complex, which was first identified as a putative complex at the PV membrane (de Koning-Ward et al. 2009), both VAC and GAPM1 are at the right place at the right time. Furthermore, VAC has a porin translocon domain which could function in a manner analogous to the mitochondrial outer membrane translocon to extract membrane-anchored exported proteins from the parasite plasma membrane. This hints that this ancient porin domain protein has been repurposed by *Plasmodium* parasites on the PPM to facilitate export of membrane proteins to the infected RBC.

2.5. Materials and methods

2.5.1. Construction of SBP1 plasmids

Genomic DNA was isolated from *P. falciparum* NF54^{attB} cultures using the QIAamp DNA blood kit (Qiagen). PCR products were inserted into the respective plasmids using ligation-independent cloning (SLIC), as described previously (D. W. Cobb et al. 2017), or the NEBuilder HiFi DNA Assembly system (NEB). All constructs used in this study were confirmed by sequencing. All primers used in this study are in Table 2.3.

For generation of the plasmid pTOPO-SBP1-TbID, sequences of approximately 500 bp of homology to the SBP1 C-terminus and 3'UTR were amplified using primer pairs P1-P2 and P3-P4, respectively, and the sequence of V5-tagged TurboID was amplified using primers P5 and P6. For expression of a SBP1 gRNA, oligos P17-P18 were inserted into cut pUF1-Cas9.

For generation of the plasmid pKD-VAC-Apt, sequences of approximately 450 bp of homology to the Pf1432100 C-terminus and 3'UTR were amplified using primer pairs P7-P8 and P9-P10, respectively. Amplicons were then inserted into pKD (D. W. Cobb et al. 2017; Rajaram, Liu, and Prigge 2020) digested with AatII and AscI. For expression of a Pf1432100 gRNA, oligo P19 was inserted into cut PUF1-Cas9.

For generation of the plasmid pKD-GAPM1-mNG-Apt, sequences of approximately 500 bp of homology to the PfGAPM1 C-terminus and 3'UTR were amplified using primer pairs P11-P12 and P13-P14, respectively, and the sequence of mNeonGreen was amplified using primers P15 and P16. Amplicons were then inserted into pKD (Rajaram et al., 2020) digested with AatII and AscI. For expression of PfGAPM1 gRNA, oligo P20 was inserted into cut PUF1-Cas9.

2.5.2. Parasite culture and transfections

Plasmodium parasites were cultured in RPMI 1640 medium (NF54^{attB}, VAC^{apt} and GAPM1$^{mNG\text{-}apt}$) or in biotin-free medium (SBP1^{TbID}) (Zimbres et al., 2020) supplemented with AlbuMAX I (Gibco), and transfected as described earlier (Kudyba et al., 2018).

For generation of SBP1^{TbID} parasites, a mix of two plasmids (50 µg each) were transfected into NF54^{attB} parasites in duplicate. The plasmid mix contained the plasmid pUF1-Cas9-SBP1gRNA, which contains the DHOD resistance gene, and the marker-free plasmid pTOPO-SBP1-TbID. Drug pressure was applied 48 h after transfection, using 1µM DSM1 (Ganesan et al., 2011) and selecting for Cas9 expression. After parasites grew back from transfection, integration was confirmed by PCR, and then cloned using limiting dilution. After clonal selection, cultures were transferred to biotin-free medium without DSM1.

For generation of VAC^{apt} and GAPM1$^{mNG\text{-}apt}$ parasites, the pKD-VAC-Apt and pKD-GAPM1-mNG-Apt plasmids (20 µg) and the respective pUF1-Cas9 plasmid (50 µg) were transfected into NF54^{attB} parasites in duplicate. Before transfection pKD plasmids were digested overnight with EcoRV (NEB). The enzyme was then subjected to heat inactivation for 20 min at 65 °C and then mixed with the pUF1-Cas9 plasmid. Transfected parasites were grown in 0.5 µM anhydrous tetracycline (aTc) (Cayman Chemical). Drug pressure was applied 48 h after transfection, using blasticidin (BSD) at a concentration of 2.5 µg/mL, selecting for pKD-VAC-Apt and pKD-GAPM1-mNG-Apt expression. After parasites grew back from transfection, integration was confirmed by PCR, and then cloned using limiting dilution. Clones were maintained in mediums containing 0.5 µM aTc and 2.5 µg/mL BSD.

2.5.3. Growth assays

For all assays, aliquots of parasite cultures were incubated in 8 µM Hoechst 33342 (ThermoFisher Scientific) for 20 min at room temperature and then fluorescence was measured using a CytoFlex S (Beckman Coulter) flow-cytometer. Flow cytometry data were analyzed using FlowJo software (Tree Star, Inc.) and plotted using Prism (GraphPad Software, Inc.).

For the SBP1^{TbID} growth assay, asynchronous parasites were transferred to a 96-well plate at 0.5% parasitemia and grown for 4 days. Parasitemia was monitored every 24 h.

For the VAC^{apt} and GAPM1$^{mNG\text{-}apt}$ growth assays, synchronous ring-stage parasites were washed 5 times with RPMI 1640 medium and split into two cultures, one resuspended in medium containing 0.5 µM aTc and 2.5 µg/mL BSD, and the other one in medium containing only 2.5 µg/mL BSD. Then cultures were transferred to a 96-well plate at 0.2% parasitemia and grown for 6 days. Parasitemia was monitored every 48 h.

2.5.4. Western blotting

For SBP1^{TbID} parasites, RIPA buffer (150 mM NaCl, 20mM Tris-HCl pH 7.5, 1mM EDTA, 1% SDS, 0.1% Triton X-100) and sonication was used to lyse parasite pellets conserving all exported proteins. Briefly, late-stage parasites were first isolated using a Percoll gradient (Genesee Scientific). The resulting pellets were then resuspended in RIPA buffer and sonicated three times at 20% amplitude for 20 seconds each. Protein supernatants were solubilized in protein loading dye with Beta-mercaptoethanol (LI-COR Biosciences) and used for SDS-PAGE.

For VAC^{apt} and GAPM1$^{mNG\text{-}apt}$ parasites, ice-cold 0.04% saponin in 1x PBS was used to isolate parasites from host cells. The parasite pellets were subsequently solubilized in protein loading dye with Beta-mercaptoethanol (LI-COR Biosciences) and used for SDS-PAGE.

Primary antibodies used in this study included mouse-anti-V5 (Cell Signaling Technology, 1:1000), rabbit-anti-PfEF1α (from D. Goldberg, 1:2000), and mouse-anti-HA 6E2 (Cell Signaling Technology, 1:2000). Secondary antibodies used were IRDye 680 CW goat-anti-rabbit IgG, IRDye 800CW goat-anti-mouse IgG, and IRDye 800CW Streptavidin (Li-COR Biosciences, 1:20 000 and 1:10 000). Membranes were imaged using the Odyssey Clx Li-COR infrared imaging system (Li-COR Biosciences). Images were processed and analyzed using ImageStudio (Li-COR Biosciences).

2.5.5. Immunofluorescence microscopy

For IFAs, cells were fixed following the previously described protocol (D. W. Cobb et al. 2017). The SBP1^{TbID} cell line was smeared onto a slide and fixed with acetone. The VAC^{apt} and GAPM1^{apt} cell lines were fixed with 4% paraformaldehyde (PFA) (Electron Microscopy Sciences) and 0.03% glutaraldehyde.

Primary antibodies used in the IFAs included mouse-anti-V5 TCM5 (eBioscience, 1:100), rabbit-anti-V5 D3H8Q (Cell Signaling technology, 1:100), rabbit-anti-HA 71550 (ThermoFisher Scientific, 1:100), rabbit-anti-MAHRP (from H. Beck, 1:500), mouse-anti-EXP2 7.7 and mouse-anti-KAHRP (from D. Cavanagh; 1:1000, 1:500 respectively). Secondary antibodies used were Alexa Fluor 488, Alexa Fluor 546, and Streptavidin Alexa Fluor 488 (Life Technologies, 1:1000).

After mounting the cells using ProLong Diamond with 4’,6’-diamidino-2-phenylindole (DAPI) (Invitrogen), they were imaged using a DeltaVision II microscope system with an

Olympus Ix-71 inverted microscope. Images were collected as a Z-stack and deconvolved using SoftWorx (GE Healthcare), then displayed as a maximum intensity projection. Adjustments to brightness and contrast were made for display purposes using Adobe Photoshop.

2.5.6. Synchronization assays

To detect SBP1 during export, SBP1^{TbID} parasites were synchronized using two rounds of 5% sorbitol treatment. Subsequently, schizont-stage parasites were isolated using a Percoll gradient (Genesee Scientific) and promptly transferred to freshly pre-warmed fresh red blood cells at a hematocrit of 1%. Parasites were then allowed to undergo egress and invade new red blood cells, and samples were collected at various time points for IFAs.

2.5.7. SBP1^{TbID} proximity biotinylation and mass spectrometry

To confirm the biotinylation of proteins by TbID-tagged SBP1, SBP1^{TbID} parasites were collected for Western blotting and IFAs after a 2-hour incubation in biotin-free media supplemented with 50 μM biotin.

For the detection of SBP1 during export, SBP1^{TbID} parasites were synchronized with two series of 5% sorbitol treatment. Late-schizont-stage parasites were isolated by performing a Percoll (Genesee Scientific) gradient separation. The isolated parasites were then splitted into two samples and immediately transferred to red blood cells at a hematocrit of 1% in warm medium, one sample without biotin and the other group with biotin (50 μM). Both parasite cultures were incubated for 4 hours at 37°C with shaking to allow egress and invasion of new red blood cells. Afterward, cultures were treated with 5% sorbitol to remove any remaining late-stage parasites.

The biotinylated culture was washed with 1X PBS, incubated on ice for 10 min to inactivate the biotinylation process, and then stored at -80 °C until further processing. The non-biotinylated culture was incubated for 16 h at 37°C with shaking, followed by a 4-hour incubation in medium containing biotin. Finally, the parasites were collected as described previously.

To isolate biotinylated proteins, parasite pellets were lysed using an extraction buffer containing 40 mM Tris-HCL pH 7.6, 150 mM KCl, 1mM EDTA, 5% NP-40 and 1X HALT (Thermo Scientific) protease inhibitor cocktail. Sonication was performed three times at 10% amplitude with 20-second pulses. Streptavidin MagneSphere Paramagnetic Particle beads (Promega) were used to capture biotinylated proteins. The beads were washed three times in 1 mL of 1X PBS. Protein lysates were then incubated with the streptavidin beads for 1 hour at room temperature. After removing the unbound fraction, the magnetic beads were washed twice with an extraction buffer and once with 1X PBS. The biotinylated proteins bound to the magnetic beads were digested and analyzed at the Proteomics and Metabolomics shared resource at Fred Hutchinson Cancer Research Center using a Orbitrap Fusion with ETD Mass Spectrometer. The mass spectrometry proteomic data have been deposited to the ProteomeXchange consortium via the MassIVE partner repository with the dataset identified PXD034946 (Project name: Rapid proximity biotinylation of the *Plasmodium falciparum* exported protein, SBP1).

2.5.8. Ultrastructural expansion microscopy (U-ExM)

Cultures for U-ExM were synchronized to 4-hour rings, following the previous described synchronization assay. Ultrastructure expansion microscopy (U-ExM) was performed as described previously (Liffner and Absalon 2021), with minor modifications.

To start, 12 mm round coverslips were treated with poly-D-lysine for 1 hour at 37 °C. They were then washed three times with MilliQ water and placed in a 24-well plate. Parasite cultures with approximately 5% parasitemia were adjusted to 0.5% hematocrit. Then, 1 mL of parasite culture was added to the well containing the treated coverslip and incubated for 1 h at 37 °C.

After the incubation, the supernatant was carefully removed, and a fixative solution (4% v/v PFA in PBS) was added, followed by a 20 min incubation at 37 °C. The coverslips were washed three times with 1X PBS and incubated overnight at 37 °C in 500 µL of 1.4% formaldehyde/2% acrylamide (FA/AA) in PBS.

The monomer solution (19% sodium acrylate, 10% acrylamide, 0.1% N,N'-methylenebisacrylamide in PBS) was prepared a day prior and stored at -20 °C. Before gelation, coverslips were removed from FA/AA solution and washed three times in 1X PBS.

For gelation, 5 µL of 10% tetramethylenediamine (TEMED) and 5 µL of 10% ammonium persulfate (APS) were added to 90 µL of the monomer solution, briefly vortexed, and 35 µL of the monomer mixture were pipetted onto parafilm. The coverslips were placed on top with the cell-side facing down, and the gels were incubated at 37 °C for 30 min.

Next, the gels were transferred into a 6-well plate containing denaturing buffer (200 mM sodium dodecyl sulfate (SDS), 200 mM NaCl, 50 mM Tris, pH 9) and incubated for 15 min incubation at room temperature. Afterward, the gels were separated from the coverslips and transferred to 1.5 mL tubes with the denaturing buffer for 90-min incubation at 95 °C.

Subsequently, the gels were incubated with secondary antibodies diluted in 1X PBS for 2.5 hours. After denaturation, gels were transferred to Petri dishes containing 25 mL of MilliQ water and incubated three times for 30 min at room temperature with shaking, changing the water in between. The gels were measured and subsequently shrunk using two washes with 1X PBS. They

were then transferred to a 24-well plate for blocking in 3% BSA in PBS at room temperature for 30 min. After blocking gels were incubated with primary antibodies diluted in 3% BSA overnight at room temperature.

Following primary antibody incubation, the gels were washed three times in 0.5% PBS with 0.1% Tween 20 for 10 min before incubation with secondary antibodies diluted in 1X PBS for 2.5 hours.

After secondary antibody staining, the gels were washed three times with 0.5% PBS with 0.1% Tween 20. Then, gels were transferred back to 10 cm Petri dishes for the second round of expansion, involving three incubations with MilliQ water. After re-expansion, the gels were either imaged immediately or stored in 0.2% propyl gallate in water until imaging.

The primary antibodies used were rat-anti-HA 3F10 (Roche, 1:50) and mouse-anti-RAP1 2.29 (from J. McBride, 1:500) (Hall et al. 1983). The secondary antibodies used were Alexa Fluor 488 and Alexa Fluor 546 (Life Technologies, 1:500), NHS-ester 405 (Thermofisher, 1:250). The gels were imaged using a Zeiss LSM 980 microscope with Airyscan 2. Images were collected as a Z-stack, processed by Airyscan, and then displayed as a maximum intensity projection. Adjustments to brightness and contrast were made using ZEN Blue software for display purposes.

2.5.9. Live microscopy

Parasites were initially synchronized using a Percoll gradient and 5% sorbitol treatment. Schizont-stage parasites were then enriched using magnetic separation with LD columns (MACS - Miltenyi Biotec). Subsequently, the enriched parasites were incubated for 4 hours at 37 °C in pre-warmed RPMI media supplemented with 25 nM ML10 compound (obtained from S. Osborne, BEI resources) as described previously (Ressurreição et al. 2020).

After the 4-hour incubation, parasites were washed once with pre-warmed RPMI media and immediately transferred to pre-warmed fresh red blood cells at a hematocrit of 0.25%.

For live cell imaging, a sample of the parasite culture was transferred to a 35 mm glass bottom dish at 1.5 hours post wash, and observed using a DeltaVision II microscope system with an Olympus Ix-71 inverted microscope. The imaging process involved capturing images for 15 minutes with a frame interval of 15 seconds, starting from the observation of parasite invasion. Imaging was conducted within environmental chambers set at 37 °C and 5% CO2. Images and videos were processed using the FIJI software.

2.6. Acknowledgements

We thank Dan Goldberg for anti-EF1α; Hans-Peter Beck for anti-MAHRP1; The European Malaria Reagent Repository for anti-EXP2 and anti-RAP1; Julie Nelson at the CTEGD Cytometry Shared Resource Laboratory for help with flow cytometry and analysis; and Muthugapatti Kandasamy at the Biomedical Microscopy Core at the University of Georgia for help with microscopy. We acknowledge the assistance of Phil Gafken at the Proteomics Resource at Fred Hutchinson Cancer Research Center for mass spectrometry and data analysis. The study was funded by NIH/NIAID R01AI130139 (V.M.), T32AI060546 (D.W.C.), and the Office of the Vice-President for Research at UGA (D.A.).

2.7. References

Acharya, Pragyan, Shweta Chaubey, Manish Grover, and Utpal Tatu. 2012. "An Exported Heat Shock Protein 40 Associates with Pathogenesis-Related Knobs in Plasmodium Falciparum Infected Erythrocytes." *PloS One* 7 (9): e44605.

Adisa, Akinola, Melanie Rug, Nectarios Klonis, Michael Foley, Alan F. Cowman, and Leann Tilley. 2003. "The Signal Sequence of Exported Protein-1 Directs the Green Fluorescent Protein to the Parasitophorous Vacuole of Transfected Malaria Parasites." *The Journal of Biological Chemistry* 278 (8): 6532–42.

Alexander, David L., Shirin Arastu-Kapur, Jean-Francois Dubremetz, and John C. Boothroyd. 2006. "Plasmodium Falciparum AMA1 Binds a Rhoptry Neck Protein Homologous to TgRON4, a Component of the Moving Junction in Toxoplasma Gondii." *Eukaryotic Cell* 5 (7): 1169–73.

Amos, Beatrice, Cristina Aurrecoechea, Matthieu Barba, Ana Barreto, Evelina Y. Basenko, Wojciech Bażant, Robert Belnap, et al. 2022. "VEuPathDB: The Eukaryotic Pathogen, Vector and Host Bioinformatics Resource Center." *Nucleic Acids Research* 50 (D1): D898–911.

Anaguano, David, Watcharatip Dedkhad, Carrie F. Brooks, David W. Cobb, and Vasant Muralidharan. 2023. "Time-Resolved Proximity Biotinylation Implicates a Porin Protein in Export of Transmembrane Malaria Parasite Effectors." *Journal of Cell Science*, September. https://doi.org/10.1242/jcs.260506.

Aquilini, Eleonora, Marta Mendonça Cova, Shrawan Kumar Mageswaran, Nicolas Dos Santos

Pacheco, Daniela Sparvoli, Diana Marcela Penarete-Vargas, Rania Najm, et al. 2021. "An Alveolata Secretory Machinery Adapted to Parasite Host Cell Invasion." *Nature Microbiology* 6 (4): 425–34.

Ashley, Elizabeth A., Aung Pyae Phyo, and Charles J. Woodrow. 2018. "Malaria." *The Lancet* 391 (10130): 1608–21.

Azevedo, Mauro F., Paul R. Sanders, Efrosinia Krejany, Catherine Q. Nie, Ping Fu, Leon A. Bach, Gerhard Wunderlich, Brendan S. Crabb, and Paul R. Gilson. 2013. "Inhibition of Plasmodium Falciparum CDPK1 by Conditional Expression of Its J-Domain Demonstrates a Key Role in Schizont Development." *Biochemical Journal* 452 (3): 433–41.

Baldi, D. L., K. T. Andrews, R. F. Waller, D. S. Roos, R. F. Howard, B. S. Crabb, and A. F. Cowman. 2000. "RAP1 Controls Rhoptry Targeting of RAP2 in the Malaria Parasite Plasmodium Falciparum." *The EMBO Journal* 19 (11): 2435–43.

Baldwin, Michael R., Xuerong Li, Toshihiko Hanada, Shih-Chun Liu, and Athar H. Chishti. 2015. "Merozoite Surface Protein 1 Recognition of Host Glycophorin A Mediates Malaria Parasite Invasion of Red Blood Cells." *Blood* 125 (17): 2704–11.

Bannister, L. H., J. M. Hopkins, R. E. Fowler, S. Krishna, and G. H. Mitchell. 2000a. "Ultrastructure of Rhoptry Development in Plasmodium Falciparum Erythrocytic Schizonts." *Parasitology* 121 (Pt 3) (September): 273–87.

———. 2000b. "A Brief Illustrated Guide to the Ultrastructure of Plasmodium Falciparum Asexual Blood Stages." *Parasitology Today* 16 (10): 427–33.

Bansal, Abhisheka, Kayode K. Ojo, Jianbing Mu, Dustin J. Maly, Wesley C. Van Voorhis, and Louis H. Miller. 2016. “Reduced Activity of Mutant Calcium-Dependent Protein Kinase 1 Is Compensated in Plasmodium Falciparum through the Action of Protein Kinase G.” *MBio* 7 (6). https://doi.org/10.1128/mBio.02011-16.

Bansal, Abhisheka, Shailja Singh, Kunal R. More, Dhiraj Hans, Kuldeep Nangalia, Manickam Yogavel, Amit Sharma, and Chetan E. Chitnis. 2013. “Characterization of Plasmodium Falciparum Calcium-Dependent Protein Kinase 1 (PfCDPK1) and Its Role in Microneme Secretion during Erythrocyte Invasion.” *The Journal of Biological Chemistry* 288 (3): 1590–1602.

Bantuchai, Sirasate, Mamoru Nozaki, Amporn Thongkukiatkul, Natcha Lorsuwannarat, Mayumi Tachibana, Minami Baba, Kazuhiro Matsuoka, Takafumi Tsuboi, Motomi Torii, and Tomoko Ishino. 2019. “Rhoptry Neck Protein 11 Has Crucial Roles during Malaria Parasite Sporozoite Invasion of Salivary Glands and Hepatocytes.” *International Journal for Parasitology* 49 (9): 725–35.

Banumathy, Gowrishankar, Varsha Singh, and Utpal Tatu. 2002. “Host Chaperones Are Recruited in Membrane-Bound Complexes ByPlasmodium Falciparum*.” *The Journal of Biological Chemistry* 277 (6): 3902–12.

Baruch, D. I., X. C. Ma, H. B. Singh, X. Bi, B. L. Pasloske, and R. J. Howard. 1997. “Identification of a Region of PfEMP1 That Mediates Adherence of Plasmodium Falciparum Infected Erythrocytes to CD36: Conserved Function with Variant Sequence.” *Blood* 90 (9): 3766–75.

Baruch, D. I., B. L. Pasloske, H. B. Singh, X. Bi, X. C. Ma, M. Feldman, T. F. Taraschi, and R. J. Howard. 1995. “Cloning the P. Falciparum Gene Encoding PfEMP1, a Malarial Variant Antigen and Adherence Receptor on the Surface of Parasitized Human Erythrocytes.” *Cell* 82 (1): 77–87.

Batinovic, Steven, Emma McHugh, Scott A. Chisholm, Kathryn Matthews, Boiyin Liu, Laure Dumont, Sarah C. Charnaud, et al. 2017. “An Exported Protein-Interacting Complex Involved in the Trafficking of Virulence Determinants in Plasmodium-Infected Erythrocytes.” *Nature Communications* 8 (July): 16044.

Baum, Jake, Lin Chen, Julie Healer, Sash Lopaticki, Michelle Boyle, Tony Triglia, Florian Ehlgen, Stuart A. Ralph, James G. Beeson, and Alan F. Cowman. 2009. “Reticulocyte-Binding Protein Homologue 5 - an Essential Adhesin Involved in Invasion of Human Erythrocytes by Plasmodium Falciparum.” *International Journal for Parasitology* 39 (3): 371–80.

Baum, Jake, Christopher J. Tonkin, Aditya S. Paul, Melanie Rug, Brian J. Smith, Sven B. Gould, Dave Richard, Thomas D. Pollard, and Alan F. Cowman. 2008. “A Malaria Parasite Formin Regulates Actin Polymerization and Localizes to the Parasite-Erythrocyte Moving Junction during Invasion.” *Cell Host & Microbe* 3 (3): 188–98.

Beck, J. R., and C. M. Ho. 2021. “Transport Mechanisms at the Malaria Parasite-Host Cell Interface.” *PLoS Pathogens* 17 (4): e1009394.

Beck, Josh R., Vasant Muralidharan, Anna Oksman, and Daniel E. Goldberg. 2014. “PTEX Component HSP101 Mediates Export of Diverse Malaria Effectors into Host

Erythrocytes." *Nature* 511 (7511): 592–95.

Beeson, James G., Damien R. Drew, Michelle J. Boyle, Gaoqian Feng, Freya J. I. Fowkes, and Jack S. Richards. 2016. "Merozoite Surface Proteins in Red Blood Cell Invasion, Immunity and Vaccines against Malaria." *FEMS Microbiology Reviews* 40 (3): 343–72.

Bergman, Lawrence W., Karine Kaiser, Hisashi Fujioka, Isabelle Coppens, Thomas M. Daly, Sarah Fox, Kai Matuschewski, Victor Nussenzweig, and Stefan H. I. Kappe. 2003. "Myosin A Tail Domain Interacting Protein (MTIP) Localizes to the Inner Membrane Complex of Plasmodium Sporozoites." *Journal of Cell Science* 116 (Pt 1): 39–49.

Birnbaum, Jakob, Sven Flemming, Nick Reichard, Alexandra Blancke Soares, Paolo Mesén-Ramírez, Ernst Jonscher, Bärbel Bergmann, and Tobias Spielmann. 2017. "A Genetic System to Study Plasmodium Falciparum Protein Function." *Nature Methods* 14 (4): 450–56.

Blake, Thomas C. A., Silvia Haase, and Jake Baum. 2020. "Actomyosin Forces and the Energetics of Red Blood Cell Invasion by the Malaria Parasite Plasmodium Falciparum." *PLoS Pathogens* 16 (10): e1009007.

Blisnick, Thierry, Maria Eugenia Morales Betoulle, Jean-Christophe Barale, Pierrick Uzureau, Laurence Berry, Sarah Desroses, Hisashi Fujioka, Denise Mattei, and Catherine Braun Breton. 2000. "Pfsbp1, a Maurer's Cleft Plasmodium Falciparum Protein, Is Associated with the Erythrocyte Skeleton." *Molecular and Biochemical Parasitology* 111 (1): 107–21.

Boddey, Justin A., Teresa G. Carvalho, Anthony N. Hodder, Tobias J. Sargeant, Brad E. Sleebs,

Danushka Marapana, Sash Lopaticki, Thomas Nebl, and Alan F. Cowman. 2013. “Role of Plasmepsin V in Export of Diverse Protein Families from the Plasmodium Falciparum Exportome.” *Traffic* 14 (5): 532–50.

Boddey, Justin A., Anthony N. Hodder, Svenja Günther, Paul R. Gilson, Heather Patsiouras, Eugene A. Kapp, J. Andrew Pearce, et al. 2010. “An Aspartyl Protease Directs Malaria Effector Proteins to the Host Cell.” *Nature* 463 (7281): 627–31.

Branon, Tess C., Justin A. Bosch, Ariana D. Sanchez, Namrata D. Udeshi, Tanya Svinkina, Steven A. Carr, Jessica L. Feldman, Norbert Perrimon, and Alice Y. Ting. 2018. “Efficient Proximity Labeling in Living Cells and Organisms with TurboID.” *Nature Biotechnology* 36 (9): 880–87.

Bullen, Hayley E., Sarah C. Charnaud, Ming Kalanon, David T. Riglar, Chaitali Dekiwadia, Niwat Kangwanrangsan, Motomi Torii, et al. 2012. “Biosynthesis, Localization, and Macromolecular Arrangement of the Plasmodium Falciparum Translocon of Exported Proteins (PTEX).” *The Journal of Biological Chemistry* 287 (11): 7871–84.

Bullen, Hayley E., Christopher J. Tonkin, Rebecca A. O’Donnell, Wai-Hong Tham, Anthony T. Papenfuss, Sven Gould, Alan F. Cowman, Brendan S. Crabb, and Paul R. Gilson. 2009. “A Novel Family of Apicomplexan Glideosome-Associated Proteins with an Inner Membrane-Anchoring Role.” *Journal of Biological Chemistry*. https://doi.org/10.1074/jbc.m109.036772.

Cao, Jun, Osamu Kaneko, Amporn Thongkukiatkul, Mayumi Tachibana, Hitoshi Otsuki, Qi Gao, Takafumi Tsuboi, and Motomi Torii. 2009. “Rhoptry Neck Protein RON2 Forms a

Complex with Microneme Protein AMA1 in Plasmodium Falciparum Merozoites." *Parasitology International* 58 (1): 29–35.

Carmo, Olivia M. S., Gerald J. Shami, Dezerae Cox, Boyin Liu, Adam J. Blanch, Snigdha Tiash, Leann Tilley, and Matthew W. A. Dixon. 2022. "Deletion of the Plasmodium Falciparum Exported Protein PTP7 Leads to Maurer's Clefts Vesiculation, Host Cell Remodeling Defects, and Loss of Surface Presentation of EMP1." *PLoS Pathogens* 18 (8): e1009882.

Chang, Henry H., Arnold M. Falick, Peter M. Carlton, John W. Sedat, Joseph L. DeRisi, and Michael A. Marletta. 2008. "N-Terminal Processing of Proteins Exported by Malaria Parasites." *Molecular and Biochemical Parasitology* 160 (2): 107–15.

Charnaud, Sarah C., Matthew W. A. Dixon, Catherine Q. Nie, Lia Chappell, Paul R. Sanders, Thomas Nebl, Eric Hanssen, et al. 2017. "The Exported Chaperone Hsp70-x Supports Virulence Functions for Plasmodium Falciparum Blood Stage Parasites." *PloS One* 12 (7): e0181656.

Charnaud, Sarah C., Rasika Kumarasingha, Hayley E. Bullen, Brendan S. Crabb, and Paul R. Gilson. 2018. "Knockdown of the Translocon Protein EXP2 in Plasmodium Falciparum Reduces Growth and Protein Export." *PloS One* 13 (11): e0204785.

Chisholm, Scott A., Ming Kalanon, Thomas Nebl, Paul R. Sanders, Kathryn M. Matthews, Benjamin K. Dickerman, Paul R. Gilson, and Tania F. de Koning-Ward. 2018. "The Malaria PTEX Component PTEX88 Interacts Most Closely with HSP101 at the Host-Parasite Interface." *The FEBS Journal* 285 (11): 2037–55.

Chisholm, Scott A., Emma McHugh, Rachel Lundie, Matthew W. A. Dixon, Sreejoyee Ghosh,

Meredith O'Keefe, Leann Tilley, Ming Kalanon, and Tania F. de Koning-Ward. 2016. "Contrasting Inducible Knockdown of the Auxiliary PTEX Component PTEX88 in P. Falciparum and P. Berghei Unmasks a Role in Parasite Virulence." *PloS One* 11 (2): e0149296.

Claros, M. G., and P. Vincens. 1996. "Computational Method to Predict Mitochondrially Imported Proteins and Their Targeting Sequences." *European Journal of Biochemistry / FEBS* 241 (3): 779–86.

Cobb, D. W., A. Florentin, M. A. Fierro, M. Krakowiak, J. M. Moore, and V. Muralidharan. 2017. "The Exported Chaperone PfHsp70x Is Dispensable for the Plasmodium Falciparum Intraerythrocytic Life Cycle." *MSphere* 2 (5). https://doi.org/10.1128/mSphere.00363-17.

Cobb, David W., Heather M. Kudyba, Alejandra Villegas, Michael R. Hoopmann, Rodrigo P. Baptista, Baylee Bruton, Michelle Krakowiak, Robert L. Moritz, and Vasant Muralidharan. 2021. "A Redox-Active Crosslinker Reveals an Essential and Inhibitable Oxidative Folding Network in the Endoplasmic Reticulum of Malaria Parasites." *PLoS Pathogens* 17 (2): e1009293.

Collier, Sophie, Emma Pietsch, Madeline Dans, Dawson Ling, Tatyana A. Tavella, Sash Lopaticki, Danushka S. Marapana, et al. 2023. "Plasmodium Falciparum Formins Are Essential for Invasion and Sexual Stage Development." *Communications Biology* 6 (1): 1–15.

Collins, Christine R., Fiona Hackett, Steven A. Howell, Ambrosius P. Snijders, Matthew R. G.

Russell, Lucy M. Collinson, and Michael J. Blackman. 2020. “The Malaria Parasite Sheddase SUB2 Governs Host Red Blood Cell Membrane Sealing at Invasion.” *ELife* 9 (December): e61121.

Collins, Christine R., Chrislaine Withers-Martinez, Fiona Hackett, and Michael J. Blackman. 2009. “An Inhibitory Antibody Blocks Interactions between Components of the Malarial Invasion Machinery.” *PLoS Pathogens* 5 (1): e1000273.

Cooke, Brian M., Donna W. Buckingham, Fiona K. Glenister, Kate M. Fernandez, Lawrence H. Bannister, Matthias Marti, Narla Mohandas, and Ross L. Coppel. 2006. “A Maurer’s Cleft-Associated Protein Is Essential for Expression of the Major Malaria Virulence Antigen on the Surface of Infected Red Blood Cells.” *The Journal of Cell Biology* 172 (6): 899–908.

Counihan, Natalie A., Scott A. Chisholm, Hayley E. Bullen, Anubhav Srivastava, Paul R. Sanders, Thorey K. Jonsdottir, Greta E. Weiss, et al. 2017. “Plasmodium Falciparum Parasites Deploy RhopH2 into the Host Erythrocyte to Obtain Nutrients, Grow and Replicate.” *ELife* 6 (March). https://doi.org/10.7554/eLife.23217.

Counihan, Natalie A., Ming Kalanon, Ross L. Coppel, and Tania F. de Koning-Ward. 2013. “Plasmodium Rhoptry Proteins: Why Order Is Important.” *Trends in Parasitology* 29 (5): 228–36.

Counihan, Natalie A., Joyanta K. Modak, and Tania F. de Koning-Ward. 2021. “How Malaria Parasites Acquire Nutrients From Their Host.” *Frontiers in Cell and Developmental Biology* 9 (March): 649184.

Cova, Marta Mendonça, Mauld H. Lamarque, and Maryse Lebrun. 2022. “How Apicomplexa Parasites Secrete and Build Their Invasion Machinery.” *Annual Review of Microbiology* 76 (1): 619–40.

Cowman, Alan F., Julie Healer, Danushka Marapana, and Kevin Marsh. 2016. “Malaria: Biology and Disease.” *Cell* 167 (3): 610–24.

Cowman, Alan F., Christopher J. Tonkin, Wai-Hong Tham, and Manoj T. Duraisingh. 2017. “The Molecular Basis of Erythrocyte Invasion by Malaria Parasites.” *Cell Host & Microbe* 22 (2): 232–45.

Crabb, Brendan S., Brian M. Cooke, John C. Reeder, Ross F. Waller, Sonia R. Caruana, Kathleen M. Davern, Mark E. Wickham, Graham V. Brown, Ross L. Coppel, and Alan F. Cowman. 1997. “Targeted Gene Disruption Shows That Knobs Enable Malaria-Infected Red Cells to Cytoadhere under Physiological Shear Stress.” *Cell* 89 (2): 287–96.

Crosnier, Cécile, Leyla Y. Bustamante, S. Josefin Bartholdson, Amy K. Bei, Michel Theron, Makoto Uchikawa, Souleymane Mboup, et al. 2011. “Basigin Is a Receptor Essential for Erythrocyte Invasion by Plasmodium Falciparum.” *Nature* 480 (7378): 534–37.

Das, Sudipta, Himanish Basu, Reshma Korde, Rita Tewari, and Shobhona Sharma. 2012. “Arrest of Nuclear Division in Plasmodium through Blockage of Erythrocyte Surface Exposed Ribosomal Protein P2.” *PLoS Pathogens* 8 (8): e1002858.

Das, Sujaan, Nadine Hertrich, Abigail J. Perrin, Chrislaine Withers-Martinez, Christine R. Collins, Matthew L. Jones, Jean M. Watermeyer, et al. 2015. “Processing of Plasmodium Falciparum Merozoite Surface Protein MSP1 Activates a Spectrin-Binding Function

Enabling Parasite Egress from RBCs." *Cell Host & Microbe* 18 (4): 433–44.

Dasgupta, Sabyasachi, Thorsten Auth, Nir S. Gov, Timothy J. Satchwell, Eric Hanssen, Elizabeth S. Zuccala, David T. Riglar, et al. 2014. "Membrane-Wrapping Contributions to Malaria Parasite Invasion of the Human Erythrocyte." *Biophysical Journal* 107 (1): 43–54.

Dawn, Amrita, Shailja Singh, Kunal R. More, Faiza Amber Siddiqui, Niseema Pachikara, Ghania Ramdani, Gordon Langsley, and Chetan E. Chitnis. 2014. "The Central Role of CAMP in Regulating Plasmodium Falciparum Merozoite Invasion of Human Erythrocytes." *PLoS Pathogens* 10 (12): e1004520.

Dellibovi-Ragheb, Teegan A., Hugo Jhun, Christopher D. Goodman, Maroya S. Walters, Daniel R. T. Ragheb, Krista A. Matthews, Krithika Rajaram, et al. 2018. "Host Biotin Is Required for Liver Stage Development in Malaria Parasites." *Proceedings of the National Academy of Sciences* 115 (11): E2604–13.

Desai, S. A., D. J. Krogstad, and E. W. McCleskey. 1993. "A Nutrient-Permeable Channel on the Intraerythrocytic Malaria Parasite." *Nature* 362 (6421): 643–46.

Desai, Sanjay A. 2014. "Why Do Malaria Parasites Increase Host Erythrocyte Permeability?" *Trends in Parasitology* 30 (3): 151–59.

Elmendorf, H. G., and K. Haldar. 1993. "Identification and Localization of ERD2 in the Malaria Parasite Plasmodium Falciparum: Separation from Sites of Sphingomyelin Synthesis and Implications for Organization of the Golgi." *The EMBO Journal* 12 (12): 4763–73.

Elsworth, Brendan, Kathryn Matthews, Catherine Q. Nie, Ming Kalanon, Sarah C. Charnaud,

Paul R. Sanders, Scott A. Chisholm, et al. 2014. “PTEX Is an Essential Nexus for Protein Export in Malaria Parasites.” *Nature* 511 (7511): 587–91.

Elsworth, Brendan, Paul R. Sanders, Thomas Nebl, Steven Batinovic, Ming Kalanon, Catherine Q. Nie, Sarah C. Charnaud, et al. 2016. “Proteomic Analysis Reveals Novel Proteins Associated with the Plasmodium Protein Exporter PTEX and a Loss of Complex Stability upon Truncation of the Core PTEX Component, PTEX150.” *Cellular Microbiology* 18 (11): 1551–69.

Engelberg, Klemens, F. Douglas Ivey, Angela Lin, Maya Kono, Alexander Lorestani, Dave Faugno-Fusci, Tim-Wolf Gilberger, Michael White, and Marc-Jan Gubbels. 2016. “A MORN1-Associated HAD Phosphatase in the Basal Complex Is Essential for Toxoplasma Gondii Daughter Budding.” *Cellular Microbiology* 18 (8): 1153–71.

Farrell, Andrew, Sivasakthivel Thirugnanam, Alexander Lorestani, Jeffrey D. Dvorin, Keith P. Eidell, David J. P. Ferguson, Brooke R. Anderson-White, Manoj T. Duraisingh, Gabor T. Marth, and Marc-Jan Gubbels. 2012. “A DOC2 Protein Identified by Mutational Profiling Is Essential for Apicomplexan Parasite Exocytosis.” *Science* 335 (6065): 218–21.

Ferreira, Josie Liane, Dorothee Heincke, Jan Stephan Wichers, Benjamin Liffner, Danny W. Wilson, and Tim-Wolf Gilberger. 2020. “The Dynamic Roles of the Inner Membrane Complex in the Multiple Stages of the Malaria Parasite.” *Frontiers in Cellular and Infection Microbiology* 10: 611801.

Fierro, Manuel A., Beejan Asady, Carrie F. Brooks, David W. Cobb, Alejandra Villegas, Silvia N. J. Moreno, and Vasant Muralidharan. 2020. “An Endoplasmic Reticulum CREC

Family Protein Regulates the Egress Proteolytic Cascade in Malaria Parasites." *MBio* 11 (1). https://doi.org/10.1128/mBio.03078-19.

Fierro, Manuel A., Tahir Hussain, Liam J. Campin, and Josh R. Beck. 2023. "Knock-Sideways by Inducible ER Retrieval Enables a Unique Approach for Studying Plasmodium-Secreted Proteins." *Proceedings of the National Academy of Sciences of the United States of America* 120 (33): e2308676120.

Fierro, Manuel A., Ajla Muheljic, Jihui Sha, James A. Wohlschlegel, and Josh R. Beck. 2023. "PEXEL Is a Proteolytic Maturation Site for Both Exported and Non-Exported Plasmodium Proteins." *BioRxiv : The Preprint Server for Biology*, July. https://doi.org/10.1101/2023.07.12.548774.

Florentin, Anat, David W. Cobb, Heather M. Kudyba, and Vasant Muralidharan. 2020. "Directing Traffic: Chaperone-Mediated Protein Transport in Malaria Parasites." *Cellular Microbiology* 22 (7): e13215.

Foth, Bernardo J., Stuart A. Ralph, Christopher J. Tonkin, Nicole S. Struck, Martin Fraunholz, David S. Roos, Alan F. Cowman, and Geoffrey I. McFadden. 2003. "Dissecting Apicoplast Targeting in the Malaria Parasite Plasmodium Falciparum." *Science* 299 (5607): 705–8.

Frénal, Karine, Jean-François Dubremetz, Maryse Lebrun, and Dominique Soldati-Favre. 2017. "Gliding Motility Powers Invasion and Egress in Apicomplexa." *Nature Reviews. Microbiology* 15 (11): 645–60.

Frénal, Karine, Valérie Polonais, Jean-Baptiste Marq, Rolf Stratmann, Julien Limenitakis, and

Dominique Soldati-Favre. 2010. “Functional Dissection of the Apicomplexan Glideosome Molecular Architecture.” *Cell Host & Microbe* 8 (4): 343–57.

Gabriela, Mikha, Kathryn M. Matthews, Cas Boshoven, Betty Kouskousis, Thorey K. Jonsdottir, Hayley E. Bullen, Joyanta Modak, et al. 2022. “A Revised Mechanism for How Plasmodium Falciparum Recruits and Exports Proteins into Its Erythrocytic Host Cell.” *PLoS Pathogens* 18 (2): e1009977.

Galaway, Francis, Laura G. Drought, Maria Fala, Nadia Cross, Alison C. Kemp, Julian C. Rayner, and Gavin J. Wright. 2017. “P113 Is a Merozoite Surface Protein That Binds the N Terminus of Plasmodium Falciparum RH5.” *Nature Communications* 8 (1): 1–11.

Gallagher, John R., Krista A. Matthews, and Sean T. Prigge. 2011. “Plasmodium Falciparum Apicoplast Transit Peptides Are Unstructured in Vitro and during Apicoplast Import.” *Traffic* 12 (9): 1124–38.

Ganesan, Suresh M., Joanne M. Morrisey, Hangjun Ke, Heather J. Painter, Kamal Laroiya, Margaret A. Phillips, Pradipsinh K. Rathod, Michael W. Mather, and Akhil B. Vaidya. 2011. “Yeast Dihydroorotate Dehydrogenase as a New Selectable Marker for Plasmodium Falciparum Transfection.” *Molecular and Biochemical Parasitology* 177 (1): 29–34.

Garten, Matthias, and Josh R. Beck. 2021. “Structured to Conquer: Transport across the Plasmodium Parasitophorous Vacuole.” *Current Opinion in Microbiology* 63 (October): 181–88.

Garten, Matthias, Armiyaw S. Nasamu, Jacquin C. Niles, Joshua Zimmerberg, Daniel E.

Goldberg, and Josh R. Beck. 2018. “EXP2 Is a Nutrient-Permeable Channel in the Vacuolar Membrane of Plasmodium and Is Essential for Protein Export via PTEX.” *Nature Microbiology* 3 (10): 1090–98.

Gaskins, Elizabeth, Stacey Gilk, Nicolette DeVore, Tara Mann, Gary Ward, and Con Beckers. 2004. “Identification of the Membrane Receptor of a Class XIV Myosin in Toxoplasma Gondii.” *The Journal of Cell Biology* 165 (3): 383–93.

Geoghegan, Niall D., Cindy Evelyn, Lachlan W. Whitehead, Michal Pasternak, Phoebe McDonald, Tony Triglia, Danushka S. Marapana, et al. 2021. “4D Analysis of Malaria Parasite Invasion Offers Insights into Erythrocyte Membrane Remodeling and Parasitophorous Vacuole Formation.” *Nature Communications* 12 (1): 1–16.

Ghoneim, Ahmed, Osamu Kaneko, Takafumi Tsuboi, and Motomi Torii. 2007. “The Plasmodium Falciparum RhopH2 Promoter and First 24 Amino Acids Are Sufficient to Target Proteins to the Rhoptries.” *Parasitology International* 56 (1): 31–43.

Ghoneim, Ahmed M. 2013. “Trafficking of Plasmodium Falciparum Chimeric Rhoptry Protein with Brefeldin A.” *Folia Parasitologica* 60 (1): 75–78.

Ghosh, Sreejoyee, Kit Kennedy, Paul Sanders, Kathryn Matthews, Stuart A. Ralph, Natalie A. Counihan, and Tania F. de Koning-Ward. 2017. “The Plasmodium Rhoptry Associated Protein Complex Is Important for Parasitophorous Vacuole Membrane Structure and Intraerythrocytic Parasite Growth.” *Cellular Microbiology* 19 (8). https://doi.org/10.1111/cmi.12733.

Gilson, Paul R., and Brendan S. Crabb. 2009. “Morphology and Kinetics of the Three Distinct

Phases of Red Blood Cell Invasion by Plasmodium Falciparum Merozoites." *International Journal for Parasitology* 39 (1): 91–96.

González-Sanz, Marta, Pedro Berzosa, and Francesca F. Norman. 2023. "Updates on Malaria Epidemiology and Prevention Strategies." *Current Infectious Disease Reports*, June, 1–9.

Green, Judith L., Stephen R. Martin, Jeremy Fielden, Asimina Ksagoni, Munira Grainger, Brian Y. S. Yim Lim, Justin E. Molloy, and Anthony A. Holder. 2006. "The MTIP-Myosin A Complex in Blood Stage Malaria Parasites." *Journal of Molecular Biology* 355 (5): 933–41.

Green, Judith L., Roxanne R. Rees-Channer, Stephen A. Howell, Stephen R. Martin, Ellen Knuepfer, Helen M. Taylor, Munira Grainger, and Anthony A. Holder. 2008. "The Motor Complex of Plasmodium Falciparum: Phosphorylation by a Calcium-Dependent Protein Kinase." *The Journal of Biological Chemistry* 283 (45): 30980–89.

Groomes, Patrice V., Usheer Kanjee, and Manoj T. Duraisingh. 2022. "RBC Membrane Biomechanics and Plasmodium Falciparum Invasion: Probing beyond Ligand-Receptor Interactions." *Trends in Parasitology* 38 (4): 302–15.

Gruring, C., A. Heiber, F. Kruse, S. Flemming, G. Franci, S. F. Colombo, E. Fasana, et al. 2012. "Uncovering Common Principles in Protein Export of Malaria Parasites." *Cell Host & Microbe* 12 (5): 717–29.

Grüring, Christof, Arlett Heiber, Florian Kruse, Johanna Ungefehr, Tim-Wolf Gilberger, and Tobias Spielmann. 2011. "Development and Host Cell Modifications of Plasmodium Falciparum Blood Stages in Four Dimensions." *Nature Communications* 2 (January):

165.

Haase, Silvia, Susann Herrmann, Christof Grüring, Arlett Heiber, Pascal W. Jansen, Christine Langer, Moritz Treeck, et al. 2009. “Sequence Requirements for the Export of the Plasmodium Falciparum Maurer’s Clefts Protein REX2.” *Molecular Microbiology* 71 (4): 1003–17.

Hakamada, Kazuaki, Manami Nakamura, Rio Midorikawa, Kyosuke Shinohara, Keiichi Noguchi, Hikaru Nagaoka, Eizo Takashima, et al. 2020. “PV1 Protein from Plasmodium Falciparum Exhibits Chaperone-Like Functions and Cooperates with Hsp100s.” *International Journal of Molecular Sciences* 21 (22). https://doi.org/10.3390/ijms21228616.

Hall, Roger, Jana McBride, Gillian Morgan, Andrew Tait, J. Werner Zolg, David Walliker, and John Scaife. 1983. “Antigens of the Erythrocytic Stages of the Human Malaria Parasite Plasmodium Falciparum Detected by Monoclonal Antibodies.” *Molecular and Biochemical Parasitology* 7 (3): 247–65.

Hallée, Stéphanie, Justin A. Boddey, Alan F. Cowman, and Dave Richard. 2018. “Evidence That the Plasmodium Falciparum Protein Sortilin Potentially Acts as an Escorter for the Trafficking of the Rhoptry-Associated Membrane Antigen to the Rhoptries.” *MSphere* 3 (1). https://doi.org/10.1128/mSphere.00551-17.

Hallée, Stéphanie, Natalie A. Counihan, Kathryn Matthews, Tania F. de Koning-Ward, and Dave Richard. 2018. “The Malaria Parasite Plasmodium Falciparum Sortilin Is Essential for Merozoite Formation and Apical Complex Biogenesis.” *Cellular Microbiology* 20 (8):

e12844.

Hanssen, Eric, Chaitali Dekiwadia, David T. Riglar, Melanie Rug, Leandro Lemgruber, Alan F. Cowman, Marek Cyrklaff, et al. 2013. “Electron Tomography of Plasmodium Falciparum Merozoites Reveals Core Cellular Events That Underpin Erythrocyte Invasion.” *Cellular Microbiology* 15 (9): 1457–72.

Hart, Melissa N., Franziska Mohring, Sophia M. DonVito, James A. Thomas, Nicole Muller-Sienerth, Gavin J. Wright, Ellen Knuepfer, Helen R. Saibil, and Robert W. Moon. 2023. “Sequential Roles for Red Blood Cell Binding Proteins Enable Phased Commitment to Invasion for Malaria Parasites.” *Nature Communications* 14 (1): 4619.

Hasan, Muhammad M., Alexander J. Polino, Sumit Mukherjee, Barbara Vaupel, and Daniel E. Goldberg. 2023. “The Mature N-Termini of Plasmodium Effector Proteins Confer Specificity of Export.” *MBio*, August, e0121523.

He Lu, Qiu Yue, Pang Geping, Li Siqi, Wang Jingjing, Feng Yonghui, Chen Lumeng, et al. 2023. “Plasmodium Falciparum GAP40 Plays an Essential Role in Merozoite Invasion and Gametocytogenesis.” *Microbiology Spectrum* 11 (3): e01434-23.

Heiber, Arlett, Florian Kruse, Christian Pick, Christof Grüring, Sven Flemming, Alexander Oberli, Hanno Schoeler, et al. 2013. “Identification of New PNEPs Indicates a Substantial Non-PEXEL Exportome and Underpins Common Features in Plasmodium Falciparum Protein Export.” *PLoS Pathogens* 9 (8): e1003546.

Herrera, S., W. Rudin, M. Herrera, P. Clavijo, L. Mancilla, C. de Plata, H. Matile, and U. Certa. 1993. “A Conserved Region of the MSP-1 Surface Protein of Plasmodium Falciparum

Contains a Recognition Sequence for Erythrocyte Spectrin." *The EMBO Journal* 12 (4): 1607–14.

Hiller, N. Luisa, Souvik Bhattacharjee, Christiaan van Ooij, Konstantinos Liolios, Travis Harrison, Carlos Lopez-Estraño, and Kasturi Haldar. 2004. "A Host-Targeting Signal in Virulence Proteins Reveals a Secretome in Malarial Infection." *Science* 306 (5703): 1934–37.

Ho, Chi-Min, Josh R. Beck, Mason Lai, Yanxiang Cui, Daniel E. Goldberg, Pascal F. Egea, and Z. Hong Zhou. 2018. "Malaria Parasite Translocon Structure and Mechanism of Effector Export." *Nature* 561 (7721): 70–75.

Ho, Chi-Min, Jonathan Jih, Mason Lai, Xiaorun Li, Daniel E. Goldberg, Josh R. Beck, and Z. Hong Zhou. 2021. "Native Structure of the RhopH Complex, a Key Determinant of Malaria Parasite Nutrient Acquisition." *Proceedings of the National Academy of Sciences* 118 (35): e2100514118.

Howard, Randall F., and Cheryl M. Schmidt. 1995. "The Secretory Pathway of Plasmodium Falciparum Regulates Transport of P82/RAP-1 to the Rhoptries." *Molecular and Biochemical Parasitology* 74 (1): 43–54.

Iriko, Hideyuki, Tomoko Ishino, Mayumi Tachibana, Ayaka Omoda, Motomi Torii, and Takafumi Tsuboi. 2020. "Skeleton Binding Protein 1 (SBP1) of Plasmodium Falciparum Accumulates in Electron-Dense Material before Passing through the Parasitophorous Vacuole Membrane." *Parasitology International* 75 (April): 102003.

Ito, Daisuke, Marc A. Schureck, and Sanjay A. Desai. 2017. "An Essential Dual-Function

Complex Mediates Erythrocyte Invasion and Channel-Mediated Nutrient Uptake in Malaria Parasites." *ELife* 6 (February). https://doi.org/10.7554/eLife.23485.

Jean, Sophonie, Mónica A. Zapata-Jenks, Julie M. Farley, Erin Tracy, and D. C. Ghislaine Mayer. 2014. "Plasmodium Falciparum Double C2 Domain Protein, PfDOC2, Binds to Calcium When Associated with Membranes." *Experimental Parasitology* 144 (September): 91–95.

Jonsdottir, Thorey K., Natalie A. Counihan, Joyanta K. Modak, Betty Kouskousis, Paul R. Sanders, Mikha Gabriela, Hayley E. Bullen, Brendan S. Crabb, Tania F. de Koning-Ward, and Paul R. Gilson. 2021. "Characterisation of Complexes Formed by Parasite Proteins Exported into the Host Cell Compartment of Plasmodium Falciparum Infected Red Blood Cells." *Cellular Microbiology* 23 (8): e13332.

Jonsdottir, Thorey K., Mikha Gabriela, Brendan S. Crabb, Tania F de Koning-Ward, and Paul R. Gilson. 2021. "Defining the Essential Exportome of the Malaria Parasite." *Trends in Parasitology* 37 (7): 664–75.

Kaneko, O., T. Tsuboi, I. T. Ling, S. Howell, M. Shirano, M. Tachibana, Y. M. Cao, A. A. Holder, and M. Torii. 2001. "The High Molecular Mass Rhoptry Protein, RhopH1, Is Encoded by Members of the Clag Multigene Family in Plasmodium Falciparum and Plasmodium Yoelii." *Molecular and Biochemical Parasitology* 118 (2): 223–31.

Kaneko, Osamu, Brian Y. S. Yim Lim, Hideyuki Iriko, Irene T. Ling, Hitoshi Otsuki, Munira Grainger, Takafumi Tsuboi, et al. 2005. "Apical Expression of Three RhopH1/Clag Proteins as Components of the Plasmodium Falciparum RhopH Complex." *Molecular*

and Biochemical Parasitology 143 (1): 20–28.

Kim, Dae In, Samuel C. Jensen, Kyle A. Noble, Birendra Kc, Kenneth H. Roux, Khatereh Motamedchaboki, and Kyle J. Roux. 2016. "An Improved Smaller Biotin Ligase for BioID Proximity Labeling." *Molecular Biology of the Cell* 27 (8): 1188–96.

Koning-Ward, Tania F. de, Matthew W. A. Dixon, Leann Tilley, and Paul R. Gilson. 2016. "Plasmodium Species: Master Renovators of Their Host Cells." *Nature Reviews. Microbiology* 14 (8): 494–507.

Koning-Ward, Tania F. de, Paul R. Gilson, Justin A. Boddey, Melanie Rug, Brian J. Smith, Anthony T. Papenfuss, Paul R. Sanders, et al. 2009. "A Newly Discovered Protein Export Machine in Malaria Parasites." *Nature* 459 (7249): 945–49.

Kono, Maya, Dorothee Heincke, Louisa Wilcke, Tatianna Wai Ying Wong, Caroline Bruns, Susann Herrmann, Tobias Spielmann, and Tim W. Gilberger. 2016. "Pellicle Formation in the Malaria Parasite." *Journal of Cell Science* 129 (4): 673–80.

Kono, Maya, Susann Herrmann, Noeleen B. Loughran, Ana Cabrera, Klemens Engelberg, Christine Lehmann, Dipto Sinha, et al. 2012. "Evolution and Architecture of the Inner Membrane Complex in Asexual and Sexual Stages of the Malaria Parasite." *Molecular Biology and Evolution* 29 (9): 2113–32.

Kono, Maya, Dhaneswar Prusty, John Parkinson, and Tim W. Gilberger. 2013. "The Apicomplexan Inner Membrane Complex." *Frontiers in Bioscience* 18 (3): 982–92.

Krai, Priscilla, Seema Dalal, and Michael Klemba. 2014. "Evidence for a Golgi-to-Endosome Protein Sorting Pathway in Plasmodium Falciparum." *PloS One* 9 (2): e89771.

Krugliak, Miriam, Jianmin Zhang, and Hagai Ginsburg. 2002. “Intraerythrocytic Plasmodium Falciparum Utilizes Only a Fraction of the Amino Acids Derived from the Digestion of Host Cell Cytosol for the Biosynthesis of Its Proteins.” *Molecular and Biochemical Parasitology* 119 (2): 249–56.

Kudyba, Heather M., David W. Cobb, Manuel A. Fierro, Anat Florentin, Dragan Ljolje, Balwan Singh, Naomi W. Lucchi, and Vasant Muralidharan. 2019. “The Endoplasmic Reticulum Chaperone PfGRP170 Is Essential for Asexual Development and Is Linked to Stress Response in Malaria Parasites.” *Cellular Microbiology* 21 (9): e13042.

Kudyba, Heather M., David W. Cobb, Anat Florentin, Michelle Krakowiak, and Vasant Muralidharan. 2018. “CRISPR/Cas9 Gene Editing to Make Conditional Mutants of Human Malaria Parasite P. Falciparum.” *Journal of Visualized Experiments: JoVE*, no. 139 (January): 1–10.

Külzer, Simone, Sarah Charnaud, Tal Dagan, Jan Riedel, Pradipta Mandal, Eva R. Pesce, Gregory L. Blatch, Brendan S. Crabb, Paul R. Gilson, and Jude M. Przyborski. 2012. “Plasmodium Falciparum-Encoded Exported Hsp70/Hsp40 Chaperone/Co-Chaperone Complexes within the Host Erythrocyte.” *Cellular Microbiology* 14 (11): 1784–95.

Külzer, Simone, Nina Gehde, and Jude M. Przyborski. 2009. “Return to Sender: Use of Plasmodium ER Retrieval Sequences to Study Protein Transport in the Infected Erythrocyte and Predict Putative ER Protein Families.” *Parasitology Research* 104 (6): 1535–41.

Kumar, Sudhir, Manish Kumar, Roseleen Ekka, Jeffrey D. Dvorin, Aditya S. Paul, Anil K.

Madugundu, Tim Gilberger, et al. 2017. “PfCDPK1 Mediated Signaling in Erythrocytic Stages of Plasmodium Falciparum.” *Nature Communications* 8 (1): 63.

Lamarque, Mauld, Sébastien Besteiro, Julien Papoin, Magali Roques, Brigitte Vulliez-Le Normand, Juliette Morlon-Guyot, Jean-François Dubremetz, et al. 2011. “The RON2-AMA1 Interaction Is a Critical Step in Moving Junction-Dependent Invasion by Apicomplexan Parasites.” *PLoS Pathogens* 7 (2): e1001276.

Lamb, Ian M., Kelly T. Rios, Anurag Shukla, Avantika I. Ahiya, Joanne Morrisey, Joshua C. Mell, Scott E. Lindner, Michael W. Mather, and Akhil B. Vaidya. 2022. “Mitochondrially Targeted Proximity Biotinylation and Proteomic Analysis in Plasmodium Falciparum.” *PloS One* 17 (8): e0273357.

Larochelle, M., D. Bergeron, B. Arcand, and F. Bachand. 2019. “Proximity-Dependent Biotinylation Mediated by TurboID to Identify Protein-Protein Interaction Networks in Yeast.” *Journal of Cell Science* 132 (11). https://doi.org/10.1242/jcs.232249.

Lasonder, Edwin, Judith L. Green, Grazia Camarda, Hana Talabani, Anthony A. Holder, Gordon Langsley, and Pietro Alano. 2012. “The Plasmodium Falciparum Schizont Phosphoproteome Reveals Extensive Phosphatidylinositol and CAMP-Protein Kinase A Signaling.” *Journal of Proteome Research* 11 (11): 5323–37.

Lasonder, Edwin, Chris J. Janse, Geert-Jan van Gemert, Gunnar R. Mair, Adriaan M. W. Vermunt, Bruno G. Douradinha, Vera van Noort, et al. 2008. “Proteomic Profiling of Plasmodium Sporozoite Maturation Identifies New Proteins Essential for Parasite Development and Infectivity.” *PLoS Pathogens* 4 (10): e1000195.

Li, Xuerong, Huiqing Chen, Thein H. Oo, Thomas M. Daly, Lawrence W. Bergman, Shih-Chun Liu, Athar H. Chishti, and Steven S. Oh. 2004. “A Co-Ligand Complex Anchors Plasmodium Falciparum Merozoites to the Erythrocyte Invasion Receptor Band 3.” *The Journal of Biological Chemistry* 279 (7): 5765–71.

Liffner, Benjamin, and Sabrina Absalon. 2021. “Expansion Microscopy Reveals Plasmodium Falciparum Blood-Stage Parasites Undergo Anaphase with A Chromatin Bridge in the Absence of Mini-Chromosome Maintenance Complex Binding Protein.” *Microorganisms* 9 (11): 2306.

Liffner, Benjamin, Juan Miguel Balbin, Jan Stephan Wichers, Tim-Wolf Gilberger, and Danny W. Wilson. 2021. “The Ins and Outs of Plasmodium Rhoptries, Focusing on the Cytosolic Side.” *Trends in Parasitology* 37 (7): 638–50.

Liffner, Benjamin, Ana Karla Cepeda Diaz, James Blauwkamp, David Anaguano, Sonja Frölich, Vasant Muralidharan, Danny W. Wilson, Jeffrey Dvorin, and Sabrina Absalon. 2023. “Atlas of Plasmodium Falciparum Intraerythrocytic Development Using Expansion Microscopy.” eLife Sciences Publications, Ltd. https://doi.org/10.7554/elife.88088.1.

Lin, Clara S., Alessandro D. Uboldi, Christian Epp, Hermann Bujard, Takafumi Tsuboi, Peter E. Czabotar, and Alan F. Cowman. 2016. “Multiple Plasmodium Falciparum Merozoite Surface Protein 1 Complexes Mediate Merozoite Binding to Human Erythrocytes.” *The Journal of Biological Chemistry* 291 (14): 7703–15.

Lin, Clara S., Alessandro D. Uboldi, Danushka Marapana, Peter E. Czabotar, Christian Epp, Hermann Bujard, Nicole L. Taylor, Matthew A. Perugini, Anthony N. Hodder, and Alan

F. Cowman. 2014. “The Merozoite Surface Protein 1 Complex Is a Platform for Binding to Human Erythrocytes by Plasmodium Falciparum.” *The Journal of Biological Chemistry* 289 (37): 25655–69.

Ling, Irene T., Laurence Florens, Anton R. Dluzewski, Osamu Kaneko, Munira Grainger, Brian Y. S. Yim Lim, Takafumi Tsuboi, et al. 2004. “The Plasmodium Falciparum Clag9 Gene Encodes a Rhoptry Protein That Is Transferred to the Host Erythrocyte upon Invasion.” *Molecular Microbiology* 52 (1): 107–18.

Lingelbach, K., and K. A. Joiner. 1998. “The Parasitophorous Vacuole Membrane Surrounding Plasmodium and Toxoplasma: An Unusual Compartment in Infected Cells.” *Journal of Cell Science* 111 (Pt 11) (June): 1467–75.

Liu, Li, Hope L. Johnson, Simon Cousens, Jamie Perin, Susana Scott, Joy E. Lawn, Igor Rudan, et al. 2012. “Global, Regional, and National Causes of Child Mortality: An Updated Systematic Analysis for 2010 with Time Trends since 2000.” *The Lancet* 379 (9832): 2151–61.

Liu, Li, Shefali Oza, Dan Hogan, Yue Chu, Jamie Perin, Jun Zhu, Joy E. Lawn, Simon Cousens, Colin Mathers, and Robert E. Black. 2016. “Global, Regional, and National Causes of under-5 Mortality in 2000-15: An Updated Systematic Analysis with Implications for the Sustainable Development Goals.” *The Lancet* 388 (10063): 3027–35.

Lobingier, Braden T., Ruth Hüttenhain, Kelsie Eichel, Kenneth B. Miller, Alice Y. Ting, Mark von Zastrow, and Nevan J. Krogan. 2017. “An Approach to Spatiotemporally Resolve Protein Interaction Networks in Living Cells.” *Cell* 169 (2): 350-360.e12.

Looker, Oliver, Adam J. Blanch, Boyin Liu, Juan Nunez-Iglesias, Paul J. McMillan, Leann Tilley, and Matthew W. A. Dixon. 2019. “The Knob Protein KAHRP Assembles into a Ring-Shaped Structure That Underpins Virulence Complex Assembly.” *PLoS Pathogens* 15 (5): e1007761.

Lourido, Sebastian, and Silvia N. J. Moreno. 2015. “The Calcium Signaling Toolkit of the Apicomplexan Parasites Toxoplasma Gondii and Plasmodium Spp.” *Cell Calcium* 57 (3): 186–93.

Maier, Alexander G., Brian M. Cooke, Alan F. Cowman, and Leann Tilley. 2009. “Malaria Parasite Proteins That Remodel the Host Erythrocyte.” *Nature Reviews. Microbiology* 7 (5): 341–54.

Maier, Alexander G., Melanie Rug, Matthew T. O’Neill, James G. Beeson, Matthias Marti, John Reeder, and Alan F. Cowman. 2007. “Skeleton-Binding Protein 1 Functions at the Parasitophorous Vacuole Membrane to Traffic PfEMP1 to the Plasmodium Falciparum-Infected Erythrocyte Surface.” *Blood* 109 (3): 1289–97.

Maier, Alexander G., Melanie Rug, Matthew T. O’Neill, Monica Brown, Srabasti Chakravorty, Tadge Szestak, Joanne Chesson, et al. 2008. “Exported Proteins Required for Virulence and Rigidity of Plasmodium Falciparum-Infected Human Erythrocytes.” *Cell* 134 (1): 48–61.

Mair, Andrea, Shou-Ling Xu, Tess C. Branon, Alice Y. Ting, and Dominique C. Bergmann. 2019. “Proximity Labeling of Protein Complexes and Cell-Type-Specific Organellar Proteomes in Arabidopsis Enabled by TurboID.” *ELife* 8 (September).

https://doi.org/10.7554/eLife.47864.

Marapana, Danushka S., Laura F. Dagley, Jarrod J. Sandow, Thomas Nebl, Tony Triglia, Michał Pasternak, Benjamin K. Dickerman, et al. 2018. “Plasmepsin V Cleaves Malaria Effector Proteins in a Distinct Endoplasmic Reticulum Translocation Interactome for Export to the Erythrocyte.” *Nature Microbiology* 3 (9): 1010–22.

Marchetti, Rosa V., Adele M. Lehane, Sarah H. Shafik, Markus Winterberg, Rowena E. Martin, and Kiaran Kirk. 2015. “A Lactate and Formate Transporter in the Intraerythrocytic Malaria Parasite, Plasmodium Falciparum.” *Nature Communications* 6 (1): 1–7.

Marti, Matthias, Robert T. Good, Melanie Rug, Ellen Knuepfer, and Alan F. Cowman. 2004. “Targeting Malaria Virulence and Remodeling Proteins to the Host Erythrocyte.” *Science* 306 (5703): 1930–33.

Martinez, Matthew, William David Chen, Marta Mendonça Cova, Petra Molnár, Shrawan Kumar Mageswaran, Amandine Guérin, Audrey R. Odom John, Maryse Lebrun, and Yi-Wei Chang. 2022. “Rhoptry Secretion System Structure and Priming in Plasmodium Falciparum Revealed Using in Situ Cryo-Electron Tomography.” *Nature Microbiology*. https://doi.org/10.1038/s41564-022-01171-3.

Matthews, K. M., E. L. Pitman, and T. F. de Koning-Ward. 2019. “Illuminating How Malaria Parasites Export Proteins into Host Erythrocytes.” *Cellular Microbiology* 21 (4): e13009.

Matthews, Kathryn, Ming Kalanon, Scott A. Chisholm, Angelika Sturm, Christopher D. Goodman, Matthew W. A. Dixon, Paul R. Sanders, et al. 2013. “The Plasmodium Translocon of Exported Proteins (PTEX) Component Thioredoxin-2 Is Important for

Maintaining Normal Blood-Stage Growth." *Molecular Microbiology* 89 (6): 1167–86.

Matthews, Kathryn M., Ming Kalanon, and Tania F. de Koning-Ward. 2019. "Uncoupling the Threading and Unfoldase Actions of Plasmodium HSP101 Reveals Differences in Export between Soluble and Insoluble Proteins." *MBio* 10 (3). https://doi.org/10.1128/mBio.01106-19.

May, D. G., K. L. Scott, A. R. Campos, and K. J. Roux. 2020. "Comparative Application of BioID and TurboID for Protein-Proximity Biotinylation." *Cells* 9 (5). https://doi.org/10.3390/cells9051070.

McBride, J. S., C. I. Newbold, and R. Anand. 1985. "Polymorphism of a High Molecular Weight Schizont Antigen of the Human Malaria Parasite Plasmodium Falciparum." *The Journal of Experimental Medicine* 161 (1): 160–80.

McHugh, Emma, Olivia M. S. Carmo, Adam Blanch, Oliver Looker, Boyin Liu, Snigdha Tiash, Dean Andrew, et al. 2020a. "Role of Plasmodium Falciparum Protein GEXP07 in Maurer's Cleft Morphology, Knob Architecture, and P. Falciparum EMP1 Trafficking." *MBio* 11 (2). https://doi.org/10.1128/mBio.03320-19.

———. 2020b. "Role of Plasmodium FalciparumProtein GEXP07 in Maurer's Cleft Morphology, Knob Architecture, and P. FalciparumEMP1 Trafficking." *MBio* 11 (2): 479.

McMillan, Paul J., Coralie Millet, Steven Batinovic, Mauro Maiorca, Eric Hanssen, Shannon Kenny, Rebecca A. Muhle, et al. 2013. "Spatial and Temporal Mapping of the PfEMP1 Export Pathway in Plasmodium Falciparum." *Cellular Microbiology* 15 (8): 1401–18.

Mehta, Simren, and L. David Sibley. 2011. “Actin Depolymerizing Factor Controls Actin Turnover and Gliding Motility in Toxoplasma Gondii.” *Molecular Biology of the Cell* 22 (8): 1290–99.

Mesén-Ramírez, Paolo, Ferdinand Reinsch, Alexandra Blancke Soares, Bärbel Bergmann, Ann-Katrin Ullrich, Stefan Tenzer, and Tobias Spielmann. 2016. “Stable Translocation Intermediates Jam Global Protein Export in Plasmodium Falciparum Parasites and Link the PTEX Component EXP2 with Translocation Activity.” *PLoS Pathogens* 12 (5): e1005618.

Miyazaki, Shinya, Ben-Yeddy Abel Chitama, Wataru Kagaya, Amuza Byaruhanga Lucky, Xiaotong Zhu, Kazuhide Yahata, Masayuki Morita, Eizo Takashima, Takafumi Tsuboi, and Osamu Kaneko. 2021. “Plasmodium Falciparum SURFIN4.1 Forms an Intermediate Complex with PTEX Components and Pf113 during Export to the Red Blood Cell.” *Parasitology International* 83 (August): 102358.

Morse, David, Wesley Webster, Ming Kalanon, Gordon Langsley, and Geoffrey I. McFadden. 2016. “Plasmodium Falciparum Rab1A Localizes to Rhoptries in Schizonts.” *PloS One* 11 (6): e0158174.

Moxon, Christopher A., Matthew P. Gibbins, Dagmara McGuinness, Danny A. Milner Jr, and Matthias Marti. 2020. “New Insights into Malaria Pathogenesis.” *Annual Review of Pathology* 15 (January): 315–43.

Mundwiler-Pachlatko, Esther, and Hans-Peter Beck. 2013. “Maurer’s Clefts, the Enigma of Plasmodium Falciparum.” *Proceedings of the National Academy of Sciences of the*

United States of America 110 (50): 19987–94.

Muralidharan, Vasant, Anna Oksman, Priya Pal, Susan Lindquist, and Daniel E. Goldberg. 2012. "Plasmodium Falciparum Heat Shock Protein 110 Stabilizes the Asparagine Repeat-Rich Parasite Proteome during Malarial Fevers." *Nature Communications* 3: 1310.

Nguitragool, Wang, Abdullah A. B. Bokhari, Ajay D. Pillai, Kempaiah Rayavara, Paresh Sharma, Brad Turpin, L. Aravind, and Sanjay A. Desai. 2011. "Malaria Parasite Clag3 Genes Determine Channel-Mediated Nutrient Uptake by Infected Red Blood Cells." *Cell* 145 (5): 665–77.

Nkrumah, Louis J., Rebecca A. Muhle, Pedro A. Moura, Pallavi Ghosh, Graham F. Hatfull, William R. Jacobs Jr, and David A. Fidock. 2006. "Efficient Site-Specific Integration in Plasmodium Falciparum Chromosomes Mediated by Mycobacteriophage Bxb1 Integrase." *Nature Methods* 3 (8): 615–21.

Oh, S. S., S. Voigt, D. Fisher, S. J. Yi, P. J. LeRoy, L. H. Derick, S. Liu, and A. H. Chishti. 2000. "Plasmodium Falciparum Erythrocyte Membrane Protein 1 Is Anchored to the Actin-Spectrin Junction and Knob-Associated Histidine-Rich Protein in the Erythrocyte Skeleton." *Molecular and Biochemical Parasitology* 108 (2): 237–47.

Oliveira, Lucas Silva de, Marcos Rodrigo Alborghetti, Renata Garcia Carneiro, Izabela Marques Dourado Bastos, Rogerio Amino, Philippe Grellier, and Sébastien Charneau. 2021. "Calcium in the Backstage of Malaria Parasite Biology." *Frontiers in Cellular and Infection Microbiology* 11 (July): 708834.

Ooij, Christiaan van, Pamela Tamez, Souvik Bhattacharjee, N. Luisa Hiller, Travis Harrison,

Konstantinos Liolios, Taco Kooij, et al. 2008. “The Malaria Secretome: From Algorithms to Essential Function in Blood Stage Infection.” *PLoS Pathogens* 4 (6): e1000084.

Organization, World Health, and Others. 2021. “World Malaria Report 2021.” https://apps.who.int/iris/bitstream/handle/10665/350147/9789240040496-eng.pdf?sequence=1.

Pasternak, Michał, Julie M. J. Verhoef, Wilson Wong, Tony Triglia, Michael J. Mlodzianoski, Niall Geoghegan, Cindy Evelyn, Ahmad Z. Wardak, Kelly Rogers, and Alan F. Cowman. 2022. “RhopH2 and RhopH3 Export Enables Assembly of the RhopH Complex on P. Falciparum-Infected Erythrocyte Membranes.” *Communications Biology* 5 (1). https://doi.org/10.1038/s42003-022-03290-3.

Paul, Aditya S., Sudeshna Saha, Klemens Engelberg, Rays H. Y. Jiang, Bradley I. Coleman, Aziz L. Kosber, Chun-Ti Chen, et al. 2015. “Parasite Calcineurin Regulates Host Cell Recognition and Attachment by Apicomplexans.” *Cell Host & Microbe* 18 (1): 49–60.

Paul, Gourab, Arunaditya Deshmukh, Bishwanath Kumar Chourasia, Kalamuddin, Ashutosh Panda, Susheel Kumar Singh, Puneet K. Gupta, et al. 2018. “Protein–Protein Interaction Studies Reveal the Plasmodium Falciparum Merozoite Surface Protein-1 Region Involved in a Complex Formation That Binds to Human Erythrocytes.” *Biochemical Journal* 475 (6): 1197–1209.

Pazicky, Samuel, Karthikeyan Dhamotharan, Karol Kaszuba, Haydyn D. T. Mertens, Tim Gilberger, Dmitri Svergun, Jan Kosinski, Ulrich Weininger, and Christian Löw. 2020. “Structural Role of Essential Light Chains in the Apicomplexan Glideosome.”

Communications Biology 3 (1): 1–14.

Peng, Mindy, Duilio Cascio, and Pascal F. Egea. 2015. "Crystal Structure and Solution Characterization of the Thioredoxin-2 from Plasmodium Falciparum, a Constituent of an Essential Parasitic Protein Export Complex." *Biochemical and Biophysical Research Communications* 456 (1): 403–9.

Perrin, Abigail J., Christine R. Collins, Matthew R. G. Russell, Lucy M. Collinson, David A. Baker, and Michael J. Blackman. 2018. "The Actinomyosin Motor Drives Malaria Parasite Red Blood Cell Invasion but Not Egress." *MBio* 9 (4). https://doi.org/10.1128/mBio.00905-18.

Perrin Abigail J., Collins Christine R., Russell Matthew R. G., Collinson Lucy M., Baker David A., and Blackman Michael J. 2018. "The Actinomyosin Motor Drives Malaria Parasite Red Blood Cell Invasion but Not Egress." *MBio* 9 (4): 10.1128/mbio.00905-18.

Petersen, Wiebke, Simone Külzer, Sonja Engels, Qi Zhang, Alyssa Ingmundson, Melanie Rug, Alexander G. Maier, and Jude M. Przyborski. 2016. "J-Dot Targeting of an Exported HSP40 in Plasmodium Falciparum-Infected Erythrocytes." *International Journal for Parasitology* 46 (8): 519–25.

Pillai, Ajay D., Wang Nguitragool, Brian Lyko, Keithlee Dolinta, Michelle M. Butler, Son T. Nguyen, Norton P. Peet, Terry L. Bowlin, and Sanjay A. Desai. 2012. "Solute Restriction Reveals an Essential Role for Clag3-Associated Channels in Malaria Parasite Nutrient Acquisition." *Molecular Pharmacology* 82 (6): 1104–14.

Qian, Pengge, Xu Wang, Chuan-Qi Zhong, Jiaxu Wang, Mengya Cai, Wang Nguitragool, Jian

Li, Huiting Cui, and Jing Yuan. 2022. “Inner Membrane Complex Proteomics Reveals a Palmitoylation Regulation Critical for Intraerythrocytic Development of Malaria Parasite.” *ELife* 11 (July). https://doi.org/10.7554/eLife.77447.

Rajaram, Krithika, Hans B. Liu, and Sean T. Prigge. 2020. “Redesigned TetR-Aptamer System To Control Gene Expression in Plasmodium Falciparum.” *MSphere* 5 (4). https://doi.org/10.1128/mSphere.00457-20.

Ramya, T. N. C., Krishanpal Karmodiya, Avadhesha Surolia, and Namita Surolia. 2007. “15-Deoxyspergualin Primarily Targets the Trafficking of Apicoplast Proteins in Plasmodium Falciparum.” *The Journal of Biological Chemistry* 282 (9): 6388–97.

Ramya, T. N. C., Namita Surolia, and Avadhesha Surolia. 2006. “15-Deoxyspergualin Modulates Plasmodium Falciparum Heat Shock Protein Function.” *Biochemical and Biophysical Research Communications* 348 (2): 585–92.

Rees-Channer, Roxanne R., Stephen R. Martin, Judith L. Green, Paul W. Bowyer, Munira Grainger, Justin E. Molloy, and Anthony A. Holder. 2006. “Dual Acylation of the 45 KDa Gliding-Associated Protein (GAP45) in Plasmodium Falciparum Merozoites.” *Molecular and Biochemical Parasitology* 149 (1): 113–16.

Ressurreição, Margarida, Aline Fréville, and Christiaan van Ooij. 2023. “Identification of a Non-Exported Plasmepsin V Substrate That Functions in the Parasitophorous Vacuole of Malaria Parasites.” *BioRxiv*. https://doi.org/10.1101/2023.05.15.540838.

Ressurreição, Margarida, James A. Thomas, Stephanie D. Nofal, Christian Flueck, Robert W. Moon, David A. Baker, and Christiaan van Ooij. 2020. “Use of a Highly Specific Kinase

Inhibitor for Rapid, Simple and Precise Synchronization of Plasmodium Falciparum and Plasmodium Knowlesi Asexual Blood-Stage Parasites." *PloS One* 15 (7): e0235798.

Richard, Dave, Lev M. Kats, Christine Langer, Casilda G. Black, Khosse Mitri, Justin A. Boddey, Alan F. Cowman, and Ross L. Coppel. 2009. "Identification of Rhoptry Trafficking Determinants and Evidence for a Novel Sorting Mechanism in the Malaria Parasite Plasmodium Falciparum." *PLoS Pathogens* 5 (3): e1000328.

Richard, Dave, Christopher A. MacRaild, David T. Riglar, Jo-Anne Chan, Michael Foley, Jake Baum, Stuart A. Ralph, Raymond S. Norton, and Alan F. Cowman. 2010. "Interaction between Plasmodium Falciparum Apical Membrane Antigen 1 and the Rhoptry Neck Protein Complex Defines a Key Step in the Erythrocyte Invasion Process of Malaria Parasites." *The Journal of Biological Chemistry* 285 (19): 14815–22.

Ridzuan, Mohd A. Mohd, Robert W. Moon, Ellen Knuepfer, Sally Black, Anthony A. Holder, and Judith L. Green. 2012. "Subcellular Location, Phosphorylation and Assembly into the Motor Complex of GAP45 during Plasmodium Falciparum Schizont Development." *PloS One* 7 (3): e33845.

Riglar, David T., Dave Richard, Danny W. Wilson, Michelle J. Boyle, Chaitali Dekiwadia, Lynne Turnbull, Fiona Angrisano, et al. 2011. "Super-Resolution Dissection of Coordinated Events during Malaria Parasite Invasion of the Human Erythrocyte." *Cell Host & Microbe* 9 (1): 9–20.

Riglar, David T., Kelly L. Rogers, Eric Hanssen, Lynne Turnbull, Hayley E. Bullen, Sarah C. Charnaud, Jude Przyborski, et al. 2013. "Spatial Association with PTEX Complexes

Defines Regions for Effector Export into Plasmodium Falciparum-Infected Erythrocytes." *Nature Communications* 4: 1415.

Roux, Kyle J., Dae In Kim, Manfred Raida, and Brian Burke. 2012. "A Promiscuous Biotin Ligase Fusion Protein Identifies Proximal and Interacting Proteins in Mammalian Cells." *The Journal of Cell Biology* 196 (6): 801–10.

Rts, S. Clinical Trials Partnership (2014). 2014. "Efficacy and Safety of the RTS, S/AS01 Malaria Vaccine during 18 Months after Vaccination: A Phase 3 Randomized, Controlled Trial in Children and Young Infants at 11 African Sites." *PLoS Medicine* 11 (7): e1001685.

Rts, Sctp, and Others. 2015. "Efficacy and Safety of RTS, S/AS01 Malaria Vaccine with or without a Booster Dose in Infants and Children in Africa: Final Results of a Phase 3, Individually Randomised, Controlled Trial." *The Lancet* 386 (9988): 31–45.

Rudlaff, Rachel M., Stephan Kraemer, Jeffrey Marshman, and Jeffrey D. Dvorin. 2020. "Three-Dimensional Ultrastructure of Plasmodium Falciparum throughout Cytokinesis." *PLoS Pathogens* 16 (6): e1008587.

Rudlaff, Rachel M., Stephan Kraemer, Vincent A. Streva, and Jeffrey D. Dvorin. 2019. "An Essential Contractile Ring Protein Controls Cell Division in Plasmodium Falciparum." *Nature Communications* 10 (1): 1–13.

Rug, Melanie, Marek Cyrklaff, Antti Mikkonen, Leandro Lemgruber, Simone Kuelzer, Cecilia P. Sanchez, Jennifer Thompson, et al. 2014. "Export of Virulence Proteins by Malaria-Infected Erythrocytes Involves Remodeling of Host Actin Cytoskeleton." *Blood* 124 (23):

3459–68.

Russo, Ilaria, Shalon Babbitt, Vasant Muralidharan, Tamira Butler, Anna Oksman, and Daniel E. Goldberg. 2010. “Plasmepsin V Licenses Plasmodium Proteins for Export into the Host Erythrocyte.” *Nature* 463 (7281): 632–36.

Sanders, Paul R., Lev M. Kats, Damien R. Drew, Rebecca A. O’Donnell, Matthew O’Neill, Alexander G. Maier, Ross L. Coppel, and Brendan S. Crabb. 2006. “A Set of Glycosylphosphatidyl Inositol-Anchored Membrane Proteins of Plasmodium Falciparum Is Refractory to Genetic Deletion.” *Infection and Immunity* 74 (7): 4330–38.

Santos-Barriopedro, Irene, Guido van Mierlo, and Michiel Vermeulen. 2021. “Off-the-Shelf Proximity Biotinylation for Interaction Proteomics.” *Nature Communications* 12 (1): 5015.

Sarfo, Jacob Owusu, Mustapha Amoadu, Peace Yaa Kordorwu, Abdul Karim Adams, Thomas Boateng Gyan, Abdul-Ganiyu Osman, Immanuel Asiedu, and Edward Wilson Ansah. 2023. “Malaria amongst Children under Five in Sub-Saharan Africa: A Scoping Review of Prevalence, Risk Factors and Preventive Interventions.” *European Journal of Medical Research* 28 (1): 80.

Saridaki, T., K. S. Frohlich, C. Braun-Breton, and M. Lanzer. 2009. “Export of PfSBP1 to the Plasmodium Falciparum Maurer’s Clefts.” *Traffic* 10 (2): 137–52.

Scally, Stephen W., Tony Triglia, Cindy Evelyn, Benjamin A. Seager, Michał Pasternak, Pailene S. Lim, Julie Healer, et al. 2022. “PCRCR Complex Is Essential for Invasion of Human Erythrocytes by Plasmodium Falciparum.” *Nature Microbiology* 7 (12): 2039–53.

Schulze, Jana, Marcel Kwiatkowski, Janus Borner, Hartmut Schlüter, Iris Bruchhaus, Thorsten Burmester, Tobias Spielmann, and Christian Pick. 2015. “The Plasmodium Falciparum Exportome Contains Non-Canonical PEXEL/HT Proteins.” *Molecular Microbiology* 97 (2): 301–14.

Schureck, Marc A., Joseph E. Darling, Alan Merk, Jinfeng Shao, Geervani Daggupati, Prakash Srinivasan, Paul Dominic B. Olinares, et al. 2021. “Malaria Parasites Use a Soluble RhopH Complex for Erythrocyte Invasion and an Integral Form for Nutrient Uptake.” *ELife* 10 (January): e65282.

Sharma, Ashwani, Arvind Sharma, Sameer Dixit, and Amit Sharma. 2011. “Structural Insights into Thioredoxin-2: A Component of Malaria Parasite Protein Secretion Machinery.” *Scientific Reports* 1 (December): 179.

Sherling, Emma S., Ellen Knuepfer, Joseph A. Brzostowski, Louis H. Miller, Michael J. Blackman, and Christiaan van Ooij. 2017. “The Plasmodium Falciparum Rhoptry Protein RhopH3 Plays Essential Roles in Host Cell Invasion and Nutrient Uptake.” *ELife* 6 (March). https://doi.org/10.7554/eLife.23239.

Sherling, Emma S., Abigail J. Perrin, Ellen Knuepfer, Matthew R. G. Russell, Lucy M. Collinson, Louis H. Miller, and Michael J. Blackman. 2019. “The Plasmodium Falciparum Rhoptry Bulb Protein RAMA Plays an Essential Role in Rhoptry Neck Morphogenesis and Host Red Blood Cell Invasion.” *PLoS Pathogens* 15 (9): e1008049.

Siddiqui, Faiza Amber, Shikha Dhawan, Shailja Singh, Bijender Singh, Pankaj Gupta, Alok Pandey, Asif Mohmmed, Deepak Gaur, and Chetan E. Chitnis. 2013. “A

Thrombospondin Structural Repeat Containing Rhoptry Protein from Plasmodium Falciparum Mediates Erythrocyte Invasion." *Cellular Microbiology* 15 (8): 1341–56.

Singh, Shailja, M. Mahmood Alam, Ipsita Pal-Bhowmick, Joseph A. Brzostowski, and Chetan E. Chitnis. 2010. "Distinct External Signals Trigger Sequential Release of Apical Organelles during Erythrocyte Invasion by Malaria Parasites." *PLoS Pathogens* 6 (2): e1000746.

Skillman, Kristen M., Karthikeyan Diraviyam, Asis Khan, Keliang Tang, David Sept, and L. David Sibley. 2011. "Evolutionarily Divergent, Unstable Filamentous Actin Is Essential for Gliding Motility in Apicomplexan Parasites." *PLoS Pathogens* 7 (10): e1002280.

Skillman, Kristen M., Christopher I. Ma, Daved H. Fremont, Karthikeyan Diraviyam, John A. Cooper, David Sept, and L. David Sibley. 2013. "The Unusual Dynamics of Parasite Actin Result from Isodesmic Polymerization." *Nature Communications* 4 (1): 1–8.

Spielmann, T., and T. W. Gilberger. 2015. "Critical Steps in Protein Export of Plasmodium Falciparum Blood Stages." *Trends in Parasitology* 31 (10): 514–25.

Spielmann, T., P. L. Hawthorne, M. W. Dixon, M. Hannemann, K. Klotz, D. J. Kemp, N. Klonis, L. Tilley, K. R. Trenholme, and D. L. Gardiner. 2006. "A Cluster of Ring Stage-Specific Genes Linked to a Locus Implicated in Cytoadherence in Plasmodium Falciparum Codes for PEXEL-Negative and PEXEL-Positive Proteins Exported into the Host Cell." *Molecular Biology of the Cell* 17 (8): 3613–24.

Spillman, Natalie J., Josh R. Beck, and Daniel E. Goldberg. 2015. "Protein Export into Malaria Parasite-Infected Erythrocytes: Mechanisms and Functional Consequences." *Annual Review of Biochemistry* 84 (1): 813–41.

Spycher, C., N. Klonis, T. Spielmann, E. Kump, S. Steiger, L. Tilley, and H. P. Beck. 2003. "MAHRP-1, a Novel Plasmodium Falciparum Histidine-Rich Protein, Binds Ferriprotoporphyrin IX and Localizes to the Maurer's Clefts." *The Journal of Biological Chemistry* 278 (37): 35373–83.

Spycher, Cornelia, Melanie Rug, Esther Pachlatko, Eric Hanssen, David Ferguson, Alan F. Cowman, Leann Tilley, and Hans-Peter Beck. 2008. "The Maurer's Cleft Protein MAHRP1 Is Essential for Trafficking of PfEMP1 to the Surface of Plasmodium Falciparum-infected Erythrocytes." *Molecular Microbiology* 68 (5): 1300–1314.

Srinivasan, Prakash, Wandy L. Beatty, Ababacar Diouf, Raul Herrera, Xavier Ambroggio, J. Kathleen Moch, Jessica S. Tyler, et al. 2011. "Binding of Plasmodium Merozoite Proteins RON2 and AMA1 Triggers Commitment to Invasion." *Proceedings of the National Academy of Sciences of the United States of America* 108 (32): 13275–80.

Su, X. Z., V. M. Heatwole, S. P. Wertheimer, F. Guinet, J. A. Herrfeldt, D. S. Peterson, J. A. Ravetch, and T. E. Wellems. 1995. "The Large Diverse Gene Family Var Encodes Proteins Involved in Cytoadherence and Antigenic Variation of Plasmodium Falciparum-Infected Erythrocytes." *Cell* 82 (1): 89–100.

Suarez, Catherine, Gaëlle Lentini, Raghavendran Ramaswamy, Marjorie Maynadier, Eleonora Aquilini, Laurence Berry-Sterkers, Michael Cipriano, et al. 2019. "A Lipid-Binding Protein Mediates Rhoptry Discharge and Invasion in Plasmodium Falciparum and Toxoplasma Gondii Parasites." *Nature Communications* 10 (1): 4041.

Takano, Ryo, Hiroko Kozuka-Hata, Daisuke Kondoh, Hiroki Bochimoto, Masaaki Oyama, and

Kentaro Kato. 2019. “A High-Resolution Map of SBP1 Interactomes in Plasmodium Falciparum-Infected Erythrocytes.” *IScience* 19 (September): 703–14.

Tham, Wai-Hong, Julie Healer, and Alan F. Cowman. 2012. “Erythrocyte and Reticulocyte Binding-like Proteins of Plasmodium Falciparum.” *Trends in Parasitology* 28 (1): 23–30.

Tham, Wai-Hong, Nicholas T. Y. Lim, Greta E. Weiss, Sash Lopaticki, Brendan R. E. Ansell, Megan Bird, Isabelle Lucet, et al. 2015. “Plasmodium Falciparum Adhesins Play an Essential Role in Signalling and Activation of Invasion into Human Erythrocytes.” *PLoS Pathogens* 11 (12): e1005343.

Thomas, Divya Catherine, Anwar Ahmed, Tim Wolf Gilberger, and Pushkar Sharma. 2012. “Regulation of Plasmodium Falciparum Glideosome Associated Protein 45 (PfGAP45) Phosphorylation.” *PloS One* 7 (4): e35855.

Thomas, Jemima C., Judith L. Green, Ronald I. Howson, Peter Simpson, David K. Moss, Stephen R. Martin, Anthony A. Holder, Ernesto Cota, and Edward W. Tate. 2010. “Interaction and Dynamics of the Plasmodium Falciparum MTIP-MyoA Complex, a Key Component of the Invasion Motor in the Malaria Parasite.” *Molecular BioSystems* 6 (3): 494–98.

Triglia, Tony, Stephen W. Scally, Benjamin A. Seager, Michał Pasternak, Laura F. Dagley, and Alan F. Cowman. 2023. “Plasmepsin X Activates the PCRCR Complex of Plasmodium Falciparum by Processing PfRh5 for Erythrocyte Invasion.” *Nature Communications* 14 (1): 2219.

Vahokoski, Juha, Saligram Prabhakar Bhargav, Ambroise Desfosses, Maria Andreadaki, Esa-

Pekka Kumpula, Silvia Muñico Martinez, Alexander Ignatev, et al. 2014. “Structural Differences Explain Diverse Functions of Plasmodium Actins.” *PLoS Pathogens* 10 (4): e1004091.

Vincensini, Laetitia, Sophie Richert, Thierry Blisnick, Alain Van Dorsselaer, Emmanuelle Leize-Wagner, Thierry Rabilloud, and Catherine Braun Breton. 2005. “Proteomic Analysis Identifies Novel Proteins of the Maurer’s Clefts, a Secretory Compartment Delivering Plasmodium Falciparum Proteins to the Surface of Its Host Cell.” *Molecular & Cellular Proteomics: MCP* 4 (4): 582–93.

Volz, Jennifer C., Alan Yap, Xavier Sisquella, Jenn K. Thompson, Nicholas T. Y. Lim, Lachlan W. Whitehead, Lin Chen, et al. 2016. “Essential Role of the PfRh5/PfRipr/CyRPA Complex during Plasmodium Falciparum Invasion of Erythrocytes.” *Cell Host & Microbe* 20 (1): 60–71.

Vulliez-Le Normand, Brigitte, Michelle L. Tonkin, Mauld H. Lamarque, Susann Langer, Sylviane Hoos, Magali Roques, Frederick A. Saul, et al. 2012. “Structural and Functional Insights into the Malaria Parasite Moving Junction Complex.” *PLoS Pathogens* 8 (6): e1002755.

Waller, K. L., B. M. Cooke, W. Nunomura, N. Mohandas, and R. L. Coppel. 1999. “Mapping the Binding Domains Involved in the Interaction between the Plasmodium Falciparum Knob-Associated Histidine-Rich Protein (KAHRP) and the Cytoadherence Ligand P. Falciparum Erythrocyte Membrane Protein 1 (PfEMP1).” *The Journal of Biological Chemistry* 274 (34): 23808–13.

Waller, R. F., M. B. Reed, A. F. Cowman, and G. I. McFadden. 2000. “Protein Trafficking to the Plastid of Plasmodium Falciparum Is via the Secretory Pathway.” *The EMBO Journal* 19 (8): 1794–1802.

Wang, Xu, Pengge Qian, Huiting Cui, Luming Yao, and Jing Yuan. 2020. “A Protein Palmitoylation Cascade Regulates Microtubule Cytoskeleton Integrity in Plasmodium.” *The EMBO Journal* 39 (13): e104168.

Weiss, Greta E., Paul R. Gilson, Tana Taechalertpaisarn, Wai-Hong Tham, Nienke W. M. de Jong, Katherine L. Harvey, Freya J. I. Fowkes, et al. 2015. “Revealing the Sequence and Resulting Cellular Morphology of Receptor-Ligand Interactions during Plasmodium Falciparum Invasion of Erythrocytes.” *PLoS Pathogens* 11 (2): e1004670.

Wong, Wilson, Rick Huang, Sebastien Menant, Chuan Hong, Jarrod J. Sandow, Richard W. Birkinshaw, Julie Healer, et al. 2018. “Structure of Plasmodium Falciparum Rh5–CyRPA–Ripr Invasion Complex.” *Nature* 565 (7737): 118–21.

World Health Organization. 2021. “WHO Recommends Groundbreaking Malaria Vaccine for Children at Risk,” October 6, 2021. https://www.who.int/news/item/06-10-2021-who-recommends-groundbreaking-malaria-vaccine-for-children-at-risk.

———. 2022. *World Malaria Report 2022*. World Health Organization.

Yahata, Kazuhide, Melissa N. Hart, Heledd Davies, Masahito Asada, Samuel C. Wassmer, Thomas J. Templeton, Moritz Treeck, Robert W. Moon, and Osamu Kaneko. 2021. “Gliding Motility of *Plasmodium* Merozoites.” *Proceedings of the National Academy of Sciences of the United States of America* 118 (48).

https://doi.org/10.1073/pnas.2114442118.

Yeoman, Jeffrey A., Eric Hanssen, Alexander G. Maier, Nectarios Klonis, Bohumil Maco, Jake Baum, Lynne Turnbull, Cynthia B. Whitchurch, Matthew W. A. Dixon, and Leann Tilley. 2011. "Tracking Glideosome-Associated Protein 50 Reveals the Development and Organization of the Inner Membrane Complex of Plasmodium Falciparum." *Eukaryotic Cell* 10 (4): 556–64.

Zhang, Qi, Cheng Ma, Alexander Oberli, Astrid Zinz, Sonja Engels, and Jude M. Przyborski. 2017. "Proteomic Analysis of Exported Chaperone/Co-Chaperone Complexes of P. Falciparum Reveals an Array of Complex Protein-Protein Interactions." *Scientific Reports* 7 (1): 1–15.

Zhu, Xiaotong, Kazuhide Yahata, Jean Semé Fils Alexandre, Takafumi Tsuboi, and Osamu Kaneko. 2013. "The N-Terminal Segment of Plasmodium Falciparum SURFIN4.1 Is Required for Its Trafficking to the Red Blood Cell Cytosol through the Endoplasmic Reticulum." *Parasitology International* 62 (2): 215–29.

Zimbres, Flavia M., Ana Lisa Valenciano, Emilio F. Merino, Anat Florentin, Nicole R. Holderman, Guijuan He, Katarzyna Gawarecka, et al. 2020. "Metabolomics Profiling Reveals New Aspects of Dolichol Biosynthesis in Plasmodium Falciparum." *Scientific Reports* 10 (1): 401.

Zuccala, Elizabeth S., Alexander M. Gout, Chaitali Dekiwadia, Danushka S. Marapana, Fiona Angrisano, Lynne Turnbull, David T. Riglar, et al. 2012. "Subcompartmentalisation of Proteins in the Rhoptries Correlates with Ordered Events of Erythrocyte Invasion by the

Blood Stage Malaria Parasite." *PloS One* 7 (9): e46160.

2.8. Tables

Table 2.1. List of putative interactors of SBP1^{TbID} at 4hpi with their homology in other Apicomplexans and their identified domains.

Gene ID	Only in *P. falciparum*	Other *Plasmodium* sp	Toxoplasma	Cryptosporidium	Eukaryotes	Domains
PF3D7_0208100		X	X		X	C2 domain
PF3D7_0815800		X	X	X	X	VPS9 domain (RABX5)
PF3D7_1432100		X				Porin domain
PF3D7_1401600	X					PHIST domain
PF3D7_0215700		X	X	X	X	RNA polymerase RPB2 domain
PF3D7_1227600		X				Trimeric LpxA-like domain
PF3D7_0803400		X	X	X	X	SNF2-like, N-terminal domain
PF3D7_0817700		X	X			--
PF3D7_1332200		X	X	X		--
PF3D7_1323700		X	X	X		DUF3273 (Not known function)
PF3D7_0304100		X	X	X		Inner membrane domain
PF3D7_1324800		X	X		X	Mur-like catalytic domain
PF3D7_0705100		X				--
PF3D7_0321100		X				Leucine-rich repeat domain
PF3D7_0308700		X				--
PF3D7_1026600	X					--
PF3D7_0723800		X				Serralysin-like metalloprotease
PF3D7_0308100		X	X	X	X	B-box-type zinc finger domain
PF3D7_0704300		X				--
PF3D7_0612200		X				Leucine-rich repeat domain
PF3D7_1138000		X				Sox, C-terminal
PF3D7_1239800		X				--
PF3D7_1025900		X				--
PF3D7_1014900		X				--

Table 2.2. List of putative interactors of SBP1^{TbID} at 20hpi with their essentiality and homology in other Apicomplexans.

Gene ID	Description	Predicted essentiality	Homology		References (PMID)
			Plasmodium spp.	Apicomplexans	
PF3D7_0915600	Uncharacterized protein	Yes	Yes	No	
PF3D7_0420100	Serine/threonine protein kinase, RIO2	Yes	Yes	Yes	22949065, 27150807
PF3D7_1247900	U3 small nucleolar RNA-associated protein 11	Yes	Yes	Yes	
PF3D7_1348200	Pre-mRNA-splicing factor SLU7	Yes	Yes	Yes	
PF3D7_0113700	Heat shock protein 40, type II	No	Yes	No	30804381, 26845441, 34614006
PF3D7_0827000	ATP-dependent RNA helicase DBP10, putative	Yes	Yes	Yes	20949012, 26525978
PF3D7_0731300	Plasmodium exported protein (PHISTb), unknown function	Yes	No	No	15671043
PF3D7_0731100	EMP1-trafficking protein, PTP2	No	Yes	No	18614010
PF3D7_1134200	Uncharacterized protein	Yes	Yes	No	
PF3D7_1358800	40S ribosomal protein S15	Yes	Yes	Yes	
PF3D7_1109400	Essential nuclear protein 1, putative	Yes/No	Yes	Yes	19200392
PF3D7_0501300	Skeleton-binding protein 1, SBP1	No	No	No	34843584, 31669509, 27193441
PF3D7_0113000	Glutamic acid-rich protein, GARP	No	No	No	2903445, 27777305
PF3D7_0830500	Sporozoite and liver stage tryptophan-rich protein, putative	Yes	Yes	No	
PF3D7_0519700	FoP domain-containing protein, putative	Yes/No	Yes	Yes	
PF3D7_1001900	Plasmodium exported protein (hyp16), PfJ23	No	Yes	No	30576479
PF3D7_0705500	Inositol-phosphate phosphatase, putative	Yes	Yes	Yes	
PF3D7_0730800.1	Uncharacterized protein	No	No	No	
PF3D7_0603000	Sde2_N_Ubi domain-containing protein	Yes	Yes	No	
PF3D7_1142500	60S ribosomal protein L28	Yes	Yes	No	24913268
PF3D7_1302000	EMP1-trafficking protein, PTP6	Yes	Yes	No	18614010
PF3D7_0606100	Negative elongation factor E	No	Yes	Yes	
PF3D7_0705700	40S ribosomal protein S29, putative	Yes	Yes	Yes	24913268
PF3D7_0730900	EMP1-trafficking protein, PTP4	No	No	No	18614010
PF3D7_0424500	Serine/threonine protein kinase, FIKK4.1	No	No	No	32284562, 17181785
PF3D7_0813900	40S ribosomal protein S16, RPS16	Yes	Yes	Yes	24913268
PF3D7_0519400	40S ribosomal protein S24, RPS24	No	Yes	Yes	24913268
PF3D7_1107700	Pescadillo homolog, PES	Yes	Yes	Yes	14698441
PF3D7_1408500	Uncharacterized protein	Yes	Yes	No	
PF3D7_1307800	Centrosomal protein CEP170	No	Yes	Yes	23181666
PF3D7_1460300	60S ribosomal protein L29, RPL29	Yes/No	-	-	24913268
PF3D7_0322900	40S ribosomal protein S3a, RPS3a	Yes	Yes	Yes	
PF3D7_0935900	Ring-exported protein 1, REX1	No	No	No	29324251, 15481109, 18573183, 26304012
PF3D7_1149400	Uncharacterized protein	Yes/No	No	No	
PF3D7_0202200	EMP1-trafficking protein, PTP1	Yes/No	No	No	18614010, 25139348, 23683579
PF3D7_0618300	60S ribosomal protein L27a, putative	Yes	Yes	Yes	
PF3D7_0611700	60S ribosomal protein L39, RPL39	Yes	Yes	Yes	24913268
PF3D7_1105400	40S ribosomal protein S4, RPS4	Yes	Yes	Yes	
PF3D7_0403200	Pre-mRNA splicing factor, putative	No	Yes	No	
PF3D7_1401200	Uncharacterized protein	Yes	No	No	
PF3D7_1110400	RNA-binding protein, putative	Yes/No	Yes	No	
PF3D7_0601900	Uncharacterized protein	Yes/No	No	No	23950716
PF3D7_0218400	ATP-dependent RNA helicase DDX47, putative	Yes	Yes	Yes	
PF3D7_1200600	Erythrocyte membrane protein 1, PfEMP1	No	No	No	20194779, 22570492, 16025132, 15520249

Table 2.3. List of primers used in the study to generate the cell lines SBP1^{TbID}, VAC^{apt} and GAPM1$^{mNG\text{-}apt}$.

Primer	Amplicon	Sequence (5' – 3')
P1	SBP1-Cterm	CCCTCACTAAAGGGACTAGTCTTTGTTATTAACATATTATTGTTCATCAACTTTTACAAC
P2	SBP1-Cterm	TAGATCTGTTAACGGATCCGGTTTCTCTAGCAACTGTTTTTGTCGTTGATTTGGTTGTGG
P3	SBP1-3'UTR	TGGACAGCACCTAAGAATTCAGATAAATTATTATAAATCAATTGTGCCAACAATAATGAG
P4	SBP1-3'UTR	TAGCGGCCGCGAATTCGTTGTGAACGTTTTTAATTATGTATGCATACAAAAAATATAC
P5	TurboID	CCCTCACTAAAGGGACTAGTGCTCGGGATCCACCGGTCGCCACCATG
P6	TurboID	TAGCGGCCGCGAATTCTTAGGTGCTGTCCAGGCCCAGCAGGGGGTTG
P7	VAC-Cterm	TGCAGAAAGGTGTGGATATCATCCCGAGTAATAAACACTTTTATGGATCC
P8	VAC-Cterm	CGTCATAAGGGTATCCGGAGACGTCTGATTTTAAATAAAGTTTCATTCCAAATTTGGTG
P9	VAC-3'UTR	TCCAATGGCCCCTTTCCGGGCGCGCCTCTTATTTGTTTTTATTTATTAAGGAAGAATTAG
P10	VAC-3'UTR	TTATTACTCGGGATGATATCCACACCTTTCTGCACCTTATATATAC
P11	GAPM1-Cterm	TGGTGCTAGGTAGGGATATCGAACTGTATCATGGAGCTTGTCCCTTATATGTTTG
P12	GAPM1-Cterm	AAACGGTGGCGACCGGTGGATCCCGAGCACATTGTTTGCATGCTGCAATATTTTCGGTAG
P13	GAPM1-3'UTR	TCCAATGGCCCCTTTCCGGGCGCGCCCCTACAAATTAACAAATTCGAAGAATACAAAAG
P14	GAPM1-3'UTR	CCATGATACAGTTCGATATCCCTACCTAGCACCACATTTTAACATTG
P15	mNeonGreen	ATGTGCTCGGGATCCACCGGTCGCCACCGTTTCTAAGGGTGAAGAAGATAACATGGCTTC
P16	mNeonGreen	CGTCATAAGGGTATCCGGAGACGTCCTTGTATAATTCATCCATACCCATAACATCAGTG
P17	SBP1 gRNA	TAAGTATATAATATTTCTAGCAACTGTTTTTGTTGGTTTTAGAGCTAGAA
P18	SBP1 gRNA	TTCTAGCTCTAAAACCAACAAAAACAGTTGCTAGAAATATTATATACTTA
P19	VAC gRNA	CATATTAAGTATATAATATTTACTGTCTATAATTAAACAAGTTTTAGAGCTAGAAATAGC
P20	GAPM1 gRNA	CATATTAAGTATATAATATTATGCAAACAATGTTAAAAAGGTTTTAGAGCTAGAAATAGC

2.9. Figures

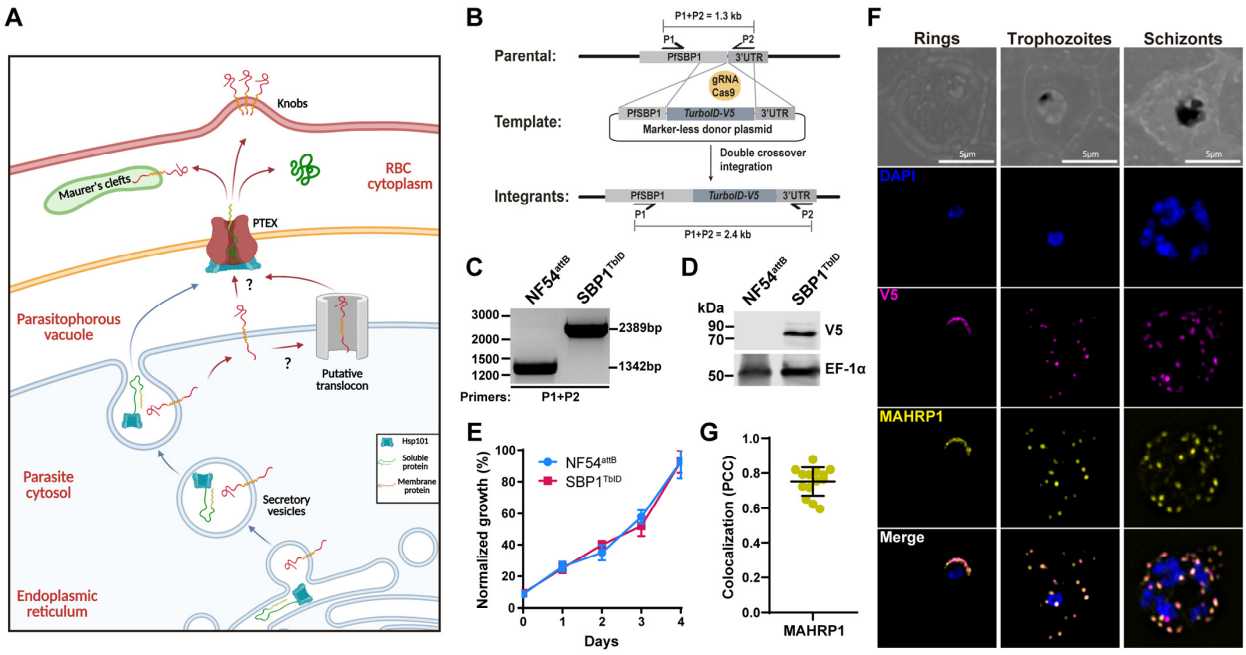

Figure 2.1. Generation of SBP1^{TbID} mutants. (A) Schematic of protein export. Membrane and soluble proteins are transported from the ER into the PV by secretory vesicles. Soluble proteins are released into the PV lumen after fusion of the secretory vesicle to the PPM. Membrane proteins, on the other hand, are inserted into the PPM and need to be extracted from the membrane by a putative translocon (PTEM) for further transport through the PV membrane to the RBC cytoplasm by the PTEX complex. Soluble and membrane proteins are transported to their final location in the infected RBC. (B) Schematic showing the integration of the repair plasmid used to tag the genomic loci of SBP1 with TurboID-V5. Cas9 introduces a double-stranded break at the C-terminus of the SBP1 locus. The repair plasmid provides homology regions for double-crossover homologous recombination, introducing TurboID and the V5 tag sequences. (C) PCR test confirming integration at the SBP1 locus. Amplicons were amplified from genomic DNA isolated from mutant and wild-type parasites. Primers were designed to amplify the region between the C-terminus and the 3'UTR of SBP1. (D) Western blot of parasite lysates isolated from the parental line (NF54^{attB})

(Nkrumah et al., 2006) and a clone of SBP1^{TbID} (D10) probed with antibodies against V5 and EF1α (loading control). The protein marker sizes are shown on the left. (E) Growth of asynchronous SBP1^{TbID} parasites, compared to the parental line NF54^{attB}, over 4 days via flow cytometry. 100% represents the highest value of calculated parasitemia. Representative of three biological replicates shown for each growth curve. Each data point represents the mean of three technical replicates; error bars represent the standard deviation. (F) IFA showing that SBP1^{TbID} localizes to the parasite periphery in the early-ring stage (left) and is exported to the MC in trophozoite (center) and schizont (right) stages. Asynchronous SBP1^{TbID} parasites were fixed with acetone and stained with specific antibodies. Images from left to right are phase-contrast, DAPI (nucleus, blue), anti-V5 (magenta), anti-MAHRP (yellow), and fluorescence merge. Z stack images were deconvolved and projected as a combined single image. (G) Quantification of the colocalization of SBP1^{TbID} with MAHRP as determined by the Pearson's correlation coefficient. Three biological replicates were represented with 4 late-stage-parasite images from each replicate. Error bars represent standard deviation. All results are representative of three experimental repeats.

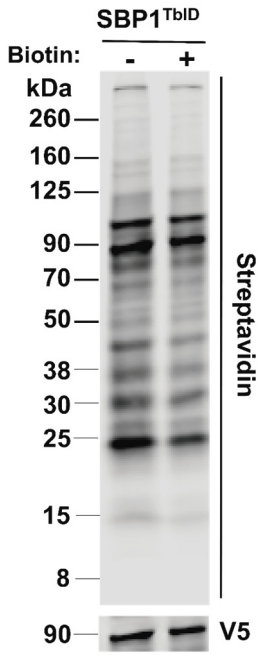

Figure 2.2. Biotinylation of proximal proteins by TurboID$_{V5}$-tagged SBP1. Western blot of parasite lysates isolated from the mutant line SBP1^{TbID} grown in complete RPMI medium, incubated with or without biotin (50 μM) for 2 h. Samples were probed with antibodies against V5 (loading control) and fluorescent dye-labeled streptavidin. The protein marker sizes are shown on the left.

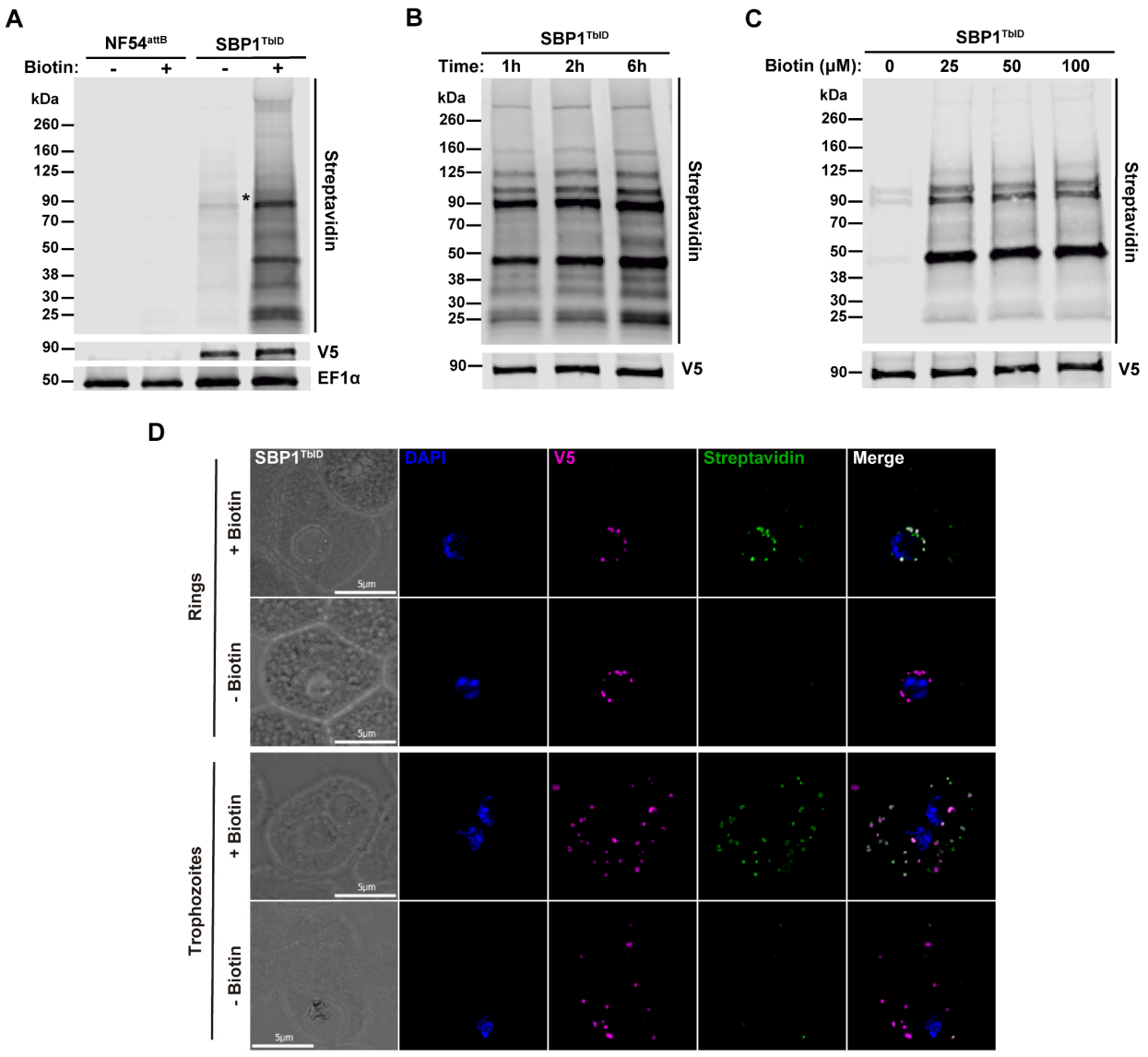

Figure 2.3. Biotinylation of proximal proteins by TurboID$_{V5}$-tagged SBP1. (A) Western blot of parasite lysates isolated from the parental line NF54^{attB} and the mutant line SBP1^{TbID} incubated with or without biotin (50 μM) for 2 h. Samples were probed with antibodies against V5, EF1α (loading control), and fluorescent dye-labeled streptavidin. The protein marker sizes are shown on the left. (B) Western blot of parasite lysates isolated from the mutant line SBP1^{TbID} incubated with biotin (50 μM) for 1 h, 2h, and 6h. Samples were probed with antibodies against V5 (loading control) and fluorescent dye-labeled streptavidin. The protein marker sizes are shown on the left.

(C) Western blot of parasite lysates isolated from the mutant line SBP1^{TbID} incubated with different concentrations of biotin (0, 25, 50, and 100 μM) for 1 h. Samples were probed with antibodies against V5 (loading control) and fluorescent dye-labeled streptavidin. The protein marker sizes are shown on the left. (D) IFA showing SBP1^{TbID} biotinylated proteins during their export out of the parasite (top panels) and at their final location at the Maurer's clefts (Bottom panels). Synchronous SBP1^{TbID} parasites were fixed with acetone after 2 h of incubation with biotin (50 μM) and stained with specific antibodies. Images from left to right are phase contrast, DAPI (nucleus, blue), anti-V5 (magenta), streptavidin (green), and fluorescence merge. Z stack images were deconvolved and projected as a combined single image.

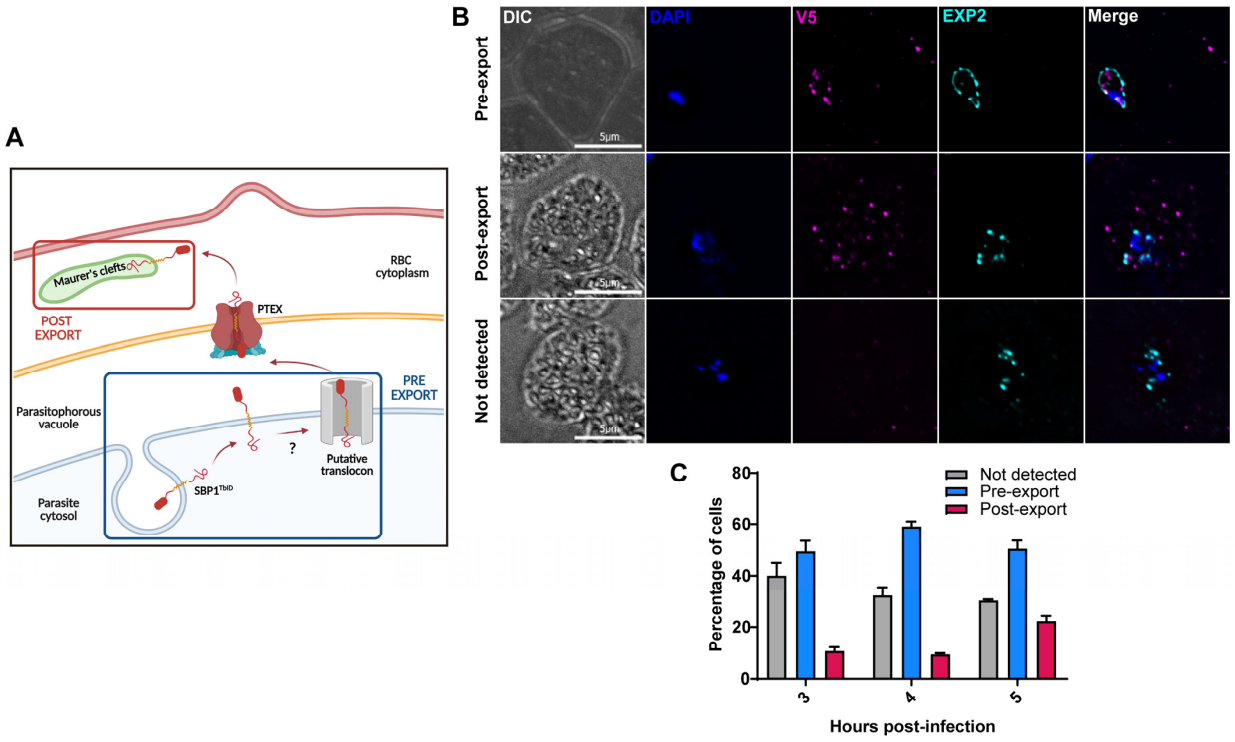

Figure 2.4. SBP1^{TbID} localizes at the host-parasite interface before exporting to the RBC. (A) Schematic of the export of proteins in P. falciparum highlighting the locations where proteins biotinylated by SBP1^{TbID} will be harvested. Created with BioRender.com. (B) IFA showing the different localizations of SBP1^{TbID} during its export at early ring stages (3-5 hpi). Tightly synchronous SBP1^{TbID} parasites were fixed with acetone at 3 h, 4h, and 5 h post-infection, and stained with specific antibodies. Images from left to right are phase-contrast, DAPI (nucleus, blue), anti-V5 (magenta), EXP2 (PV marker, cyan), and fluorescence merge. Z stack images were deconvolved and projected as a combined single image. (C) Quantification of the events observed in (B). Events were scored based on the localization of SBP1^{TbID} with respect to the PV marker EXP2. A total of 50 parasites were scored for each time point. n= 3 biological replicates; error bars represent standard deviation.

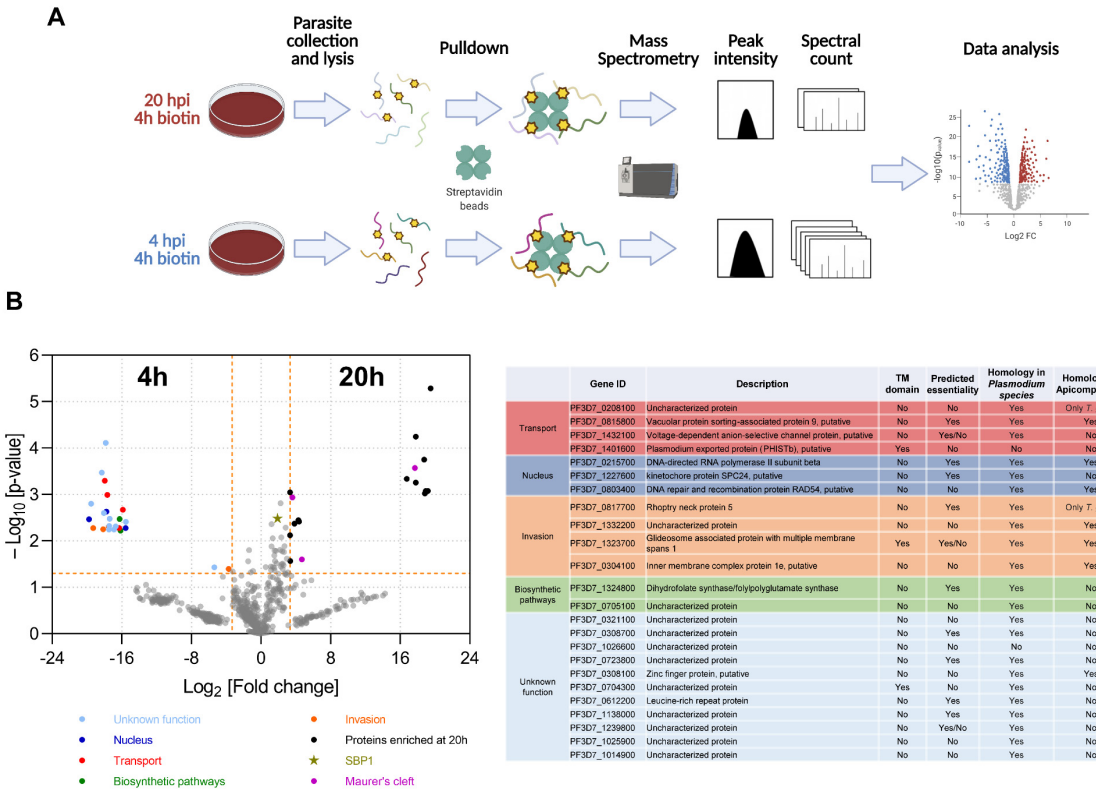

	Gene ID	Description	TM domain	Predicted essentiality	Homology in *Plasmodium* species	Homology in Apicomplexans	References (PMID)
Transport	PF3D7_0208100	Uncharacterized protein	No	No	Yes	Only *T. gondi*	
	PF3D7_0815800	Vacuolar protein sorting-associated protein 9, putative	No	Yes	Yes	Yes	25640905
	PF3D7_1432100	Voltage-dependent anion-selective channel protein, putative	No	Yes/No	Yes	No	
	PF3D7_1401600	Plasmodium exported protein (PHISTb), putative	Yes	No	No	No	21908595
Nucleus	PF3D7_0215700	DNA-directed RNA polymerase II subunit beta	No	Yes	Yes	Yes	25373614
	PF3D7_1227600	kinetochore protein SPC24, putative	No	Yes	Yes	No	32501284
	PF3D7_0803400	DNA repair and recombination protein RAD54, putative	No	No	Yes	Yes	23631919
Invasion	PF3D7_0817700	Rhoptry neck protein 5	No	Yes	Yes	Only *T. gondi*	25102354, 21185360, 20228060
	PF3D7_1332200	Uncharacterized protein	No	No	Yes	Yes	
	PF3D7_1323700	Glideosome associated protein with multiple membrane spans 1	Yes	Yes/No	Yes	Yes	19561073, 22389454, 19465059
	PF3D7_0304100	Inner membrane complex protein 1e, putative	No	No	Yes	Yes	15533999, 18359944, 25185663
Biosynthetic pathways	PF3D7_1324800	Dihydrofolate synthase/folylpolyglutamate synthase	No	Yes	Yes	No	11223131, 11197757, 20350571
	PF3D7_0705100	Uncharacterized protein	No	No	Yes	No	
Unknown function	PF3D7_0321100	Uncharacterized protein	No	No	Yes	No	
	PF3D7_0308700	Uncharacterized protein	No	Yes	Yes	No	
	PF3D7_1026600	Uncharacterized protein	No	No	No	No	
	PF3D7_0723800	Uncharacterized protein	No	Yes	Yes	No	
	PF3D7_0308100	Zinc finger protein, putative	No	No	Yes	Yes	
	PF3D7_0704300	Uncharacterized protein	Yes	No	Yes	No	
	PF3D7_0612200	Leucine-rich repeat protein	No	Yes	Yes	No	
	PF3D7_1138000	Uncharacterized protein	No	Yes	Yes	No	
	PF3D7_1239800	Uncharacterized protein	No	Yes/No	Yes	No	
	PF3D7_1025900	Uncharacterized protein	No	No	Yes	No	
	PF3D7_1014900	Uncharacterized protein	No	No	Yes	No	

Figure 2.5. SBP1^{TbID} interacting partners at 4 hpi. (A) Schematic of the experimental design for time-resolved biotinylation (with 50 µM biotin) and proteomics to identify pre-export and post-export interactors of SBP1^{TbID}**.** Created with BioRender.com. (B) Interactors enriched at 4 hpi (p-value plotted as function of fold change between the two conditions). Proteins with p-value ≤0.05 and more than 10-fold change are identified as SBP1^{TbID} interactors. n= 3 biological replicates. (C) A summary table of the putative interactors of SBP1^{TbID} at 4hpi grouped by their putative functions is shown. All proteins identified are in Appendix A.

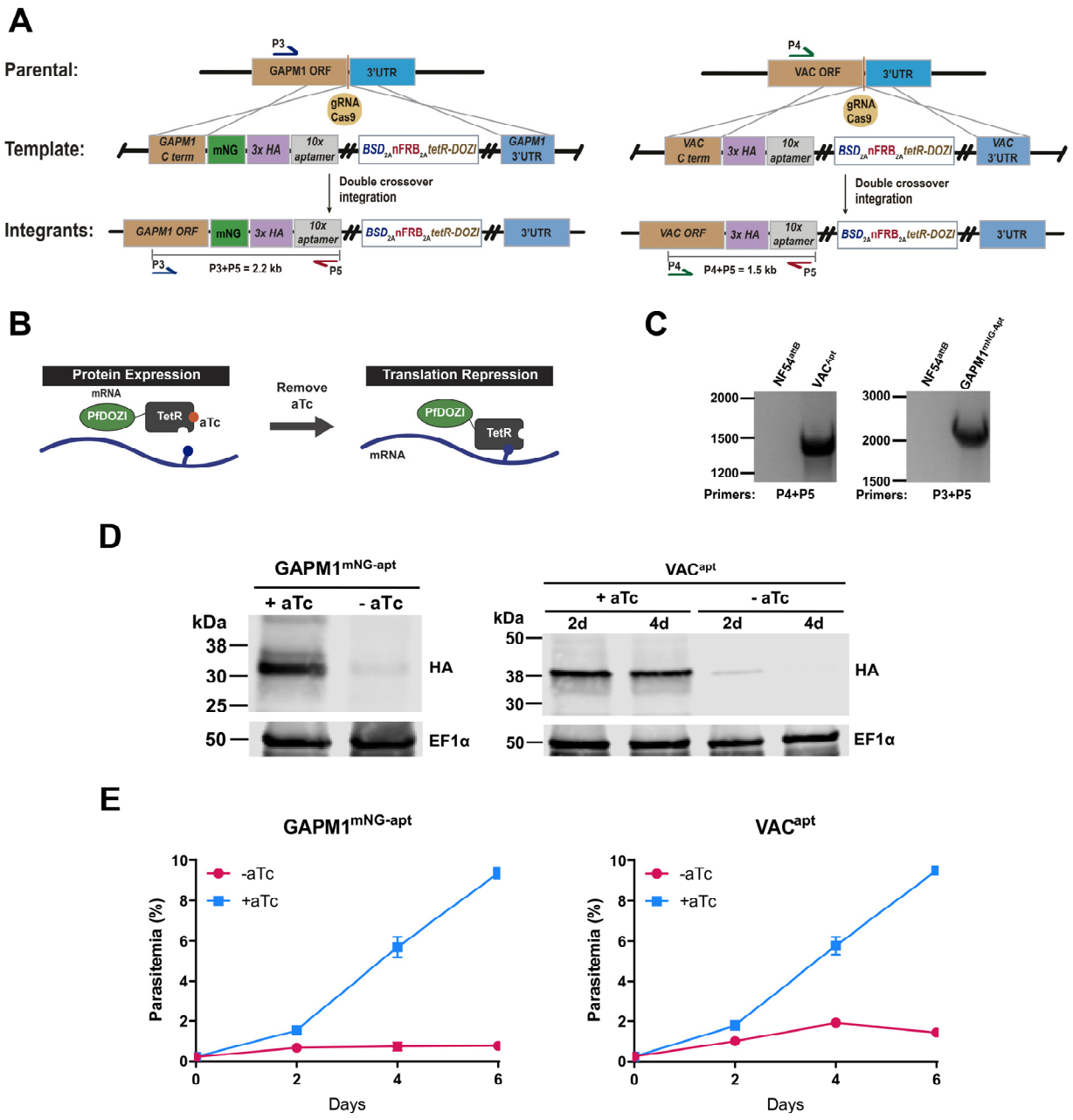

Figure 2.6. Characterization of parasite lines VAC^{apt} and GAPM1$^{mNG-apt}$. (A) Schematic showing the integration of the repair plasmid to modify the genomic loci of Pf3D7_1432100 (VAC) and Pf3D7_1323700 (GAPM1). Cas9 introduces a double-stranded break at the C-terminus of the VAC and GAPM1 locus. The repair plasmid provides homology regions for double-crossover homologous recombination, introducing the HA-tag and the TetR-Aptamer system. For

GAPM1$^{mNG\text{-}apt}$, a fluorescent tag mNeonGreen was introduced between the C-terminus and the HA-tag. (B) Regulation of protein expression using the TetR-Aptamer knockdown system. TetR binds to aptamer repeats in the mRNA, while PfDOZI localizes the complex to sites of mRNA sequestration, causing a repression in translation of the gene of interest. Anhydrous tetracycline (aTc) binds to TetR, blocking its interaction with the aptamers. (C) PCR test confirming integration at the VAC and GAPM1 locus. Amplicons were amplified from genomic DNA isolated from mutant and wild-type parasites. Primers were designed to amplify the region between the C-terminus and the tandem of 10X aptamer repeats. (D) Western blot of parasite lysates isolated from the mutant lines VAC^{apt} and GAPM1$^{mNG\text{-}apt}$ probed with antibodies against HA and EF1α (loading control). The protein marker sizes are shown on the left. GAPM1$^{mNG\text{-}apt}$ parasites were collected after incubation for 48 h in the presence or absence of aTc. VAC^{apt} parasites were collected after incubation for 48 and 96 h in presence or absence of aTc. (E) Growth of synchronous VAC^{apt} and GAPM1$^{mNG\text{-}apt}$ parasites over 6 days after removal of aTc from the medium via flow cytometry. Representative of three biological replicates shown for each growth curve. Each data point represents the mean of three technical replicates; error bars represent standard deviation.

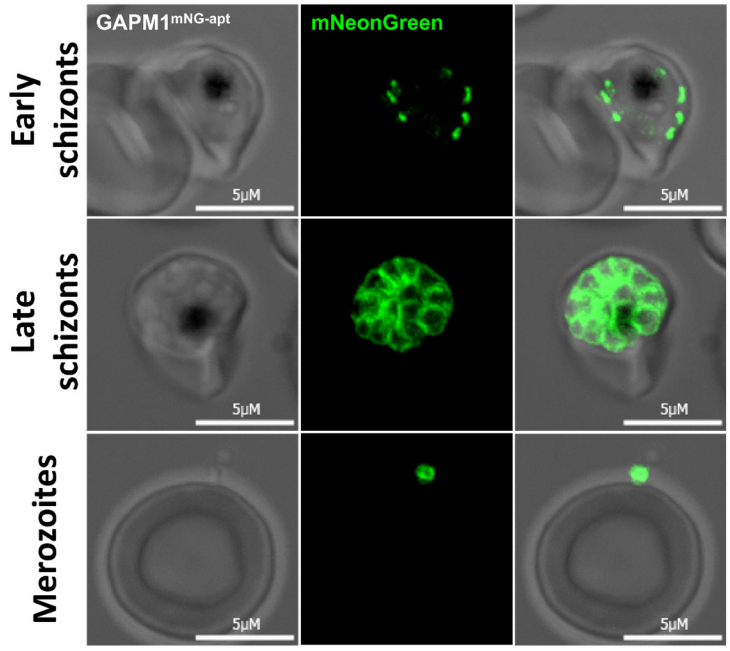

Figure 2.7. Localization of GAPM1 at late stages in the GAPM1$^{mNG\text{-}apt}$ cell line. Representative live images showing GAPM1$^{mNG\text{-}apt}$ localization at early and late schizonts, and merozoites. Images of GAPM1$^{mNG\text{-}apt}$ from left to right are phase-contrast, mNeonGreen (green), and fluorescence merge. Z stack images were deconvolved and projected as a combined single image.

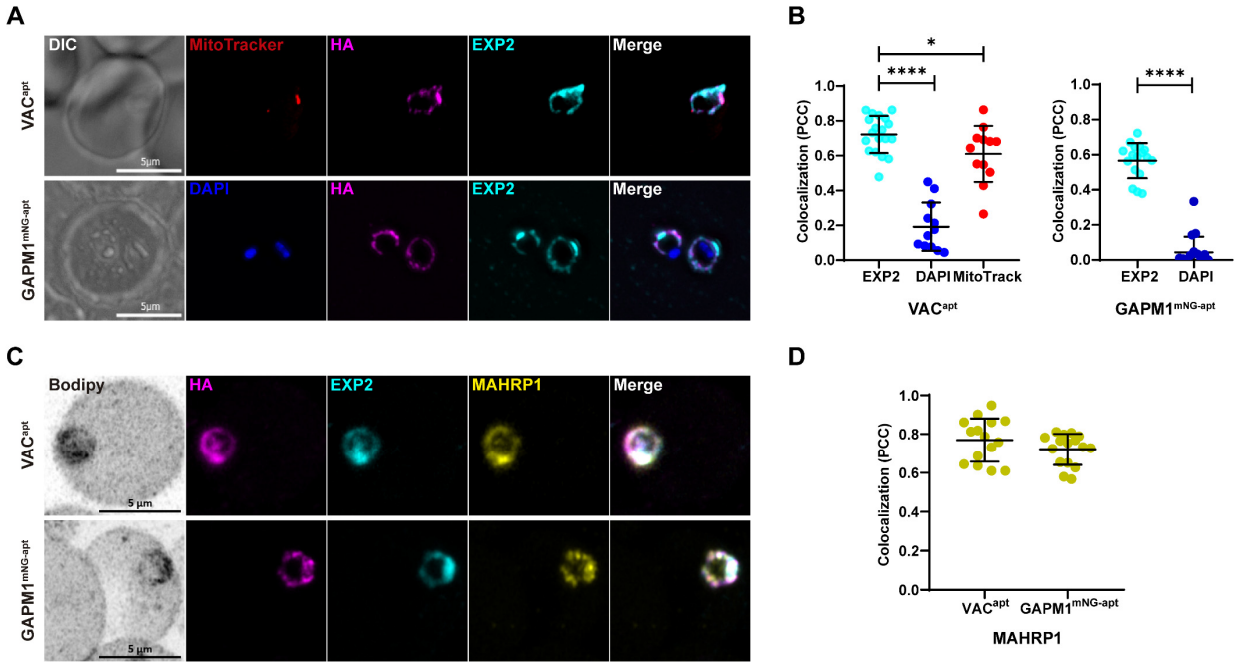

Figure 2.8. VAC^{apt} and GAPM1$^{mNG\text{-}apt}$ localize to the host-parasite interface. (A) Representative IFAs showing VAC^{apt} and GAPM1$^{mNG\text{-}apt}$ localization in early-ring stages (4 hpi). Tightly synchronous parasites were fixed with PFA (VAC^{apt}) and acetone (GAPM1$^{mNG\text{-}apt}$) and stained with specific antibodies. Images of VAC^{apt} from left to right are phase-contrast, anti-HA (magenta), anti-EXP2 (PV, cyan), MitoTracker (mitochondria, red), and fluorescence merge. Images of GAPM1$^{mNG\text{-}apt}$ from left to right are phase-contrast, DAPI (nucleus, blue), anti-HA (magenta), anti-EXP2 (PV, cyan), and fluorescence merge. Z stack images were deconvolved and projected as a combined single image. (B) Quantifying the colocalization of VAC and GAPM1^{mNG} with respect to EXP2, MitoTracker (Mitochondrial marker) and DAPI, and to EXP2 and DAPI, respectively, determined by the Pearson's correlation coefficient. Three biological replicates were represented with 6 parasite images from each replicate for EXP2, and 3 parasite images for MitoTracker and DAPI. Error bars represent standard deviation. ****$p<0.05$ (unpaired two-tailed Student's *t*-test). (C) Representative IFAs imaged by Airyscan microscopy showing VAC^{apt} and

GAPM1$^{mNG\text{-}apt}$ localization in early-ring stages (4 hpi). Tightly synchronous parasites were fixed with PFA and stained with BODIPY TRc (greyscale), anti-HA (magenta), anti-EXP2 (cyan), and anti-MAHRP1 (yellow). Z stack images were projected as a combined single image. (D) Quantifying the colocalization of VAC and GAPM1^{mNG} with respect to MAHRP1 as determined by Pearson's correlation coefficient. Three biological replicates were represented with 5 parasite images from each replicate. Error bars represent standard deviation. ns, non-significant (unpaired two-tailed Student's *t*-test).

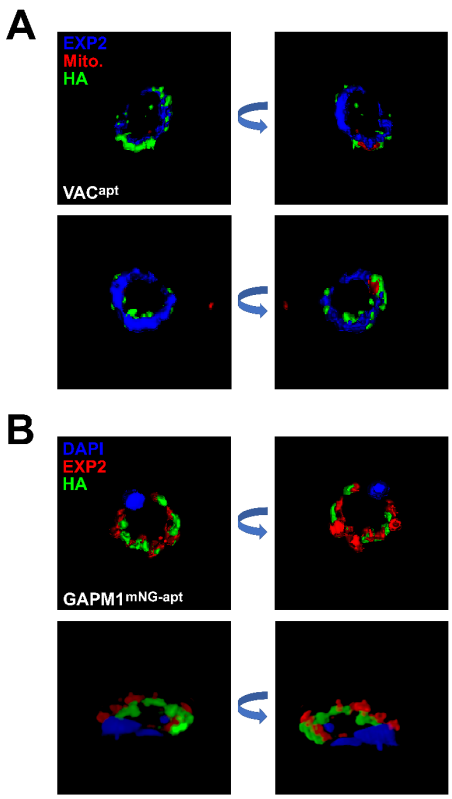

Figure 2.9. Localization of VAC and GAPM1 at early-stage parasites. 3D reconstruction based on structured illumination microscopy images captured from (A) VAC^{apt} and (B) GAPM1$^{mNG\text{-}apt}$ ring-stage parasites at 4 hpi and stained with the antibodies as in Fig 2.8A.

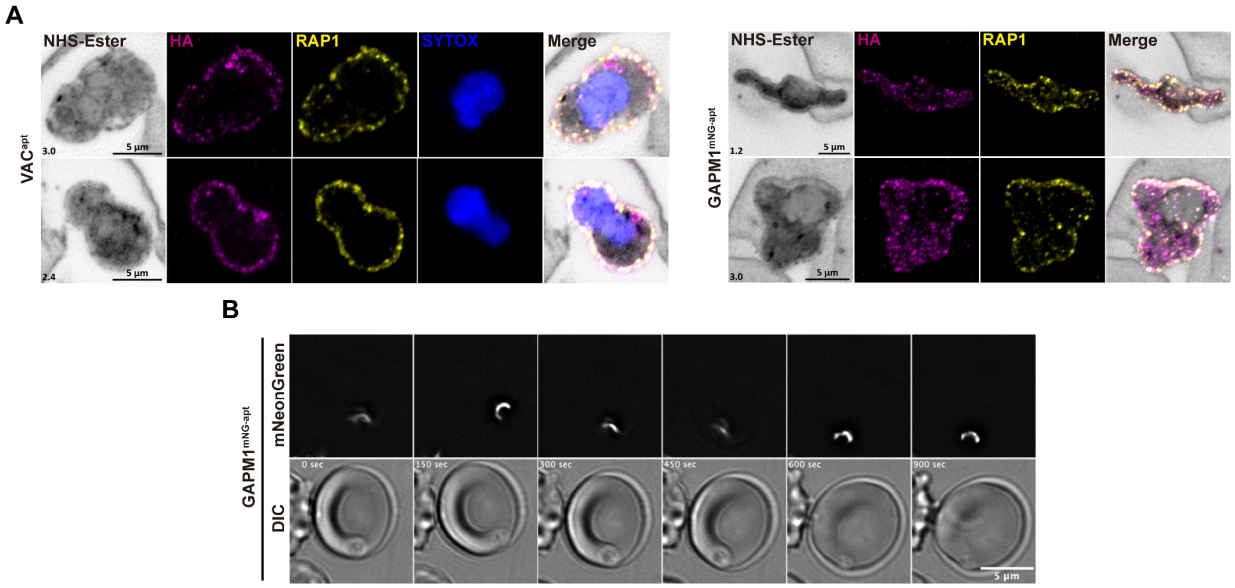

Figure 2.10. VAC^{apt} and GAPM1$^{mNG\text{-}apt}$ localize to the host-parasite interface. (A) Representative images of VAC^{apt} and GAPM1$^{mNG\text{-}apt}$ parasites showing their localization in early-ring stages (4 hpi). Tightly synchronous parasites were expanded by U-ExM, fixed with PFA, and stained with NHS-Ester (greyscale), anti-HA (magenta), and anti-RAP1 (yellow). Selected Z stack images were projected as a combined single image. Number on image = Z-axis thickness of projection in µm. (B) Time course images showing GAPM1$^{mNG\text{-}apt}$ localization after invasion of red blood cells. Images of GAPM1$^{mNG\text{-}apt}$ from left to right are phase-contrast and mNeonGreen (white). Video captions were deconvolved and projected as a combined single image. All results are representative of three experimental repeats.

CHAPTER 3

3. *PLASMODIUM FALCIPARUM* REQUIRES TWO RHOPTRIES TO INVADE RED BLOOD CELLS

David Anaguano, James Blauwkamp, Manuel Fierro, Sabrina Absalon, Vasant Muralidharan. To be submitted to eLife

3.1. Abstract

Malaria is a global and deadly human disease caused by the apicomplexan parasites of the genus *Plasmodium*. The disease's clinical manifestations are closely linked to the proliferation of parasites within human red blood cells (RBCs). Establishment of infection within the human host begins with the invasion of RBCs by *P. falciparum*. This invasion is mediated by the secretion of effectors from specialized secretory organelles, most notably a pair of club-shaped organelles localized to the apical end of merozoite-stage parasites, termed rhoptries. In my research, I investigated the function of one of these effectors, namely Rhoptry Neck Protein 11 (RON11). RON11 contains seven transmembrane domains and a putative single calcium-binding EF-hand domain, localized towards the parasite's cytoplasm. By generating RON11 conditional knockdown mutants, I demonstrated that the reduction of RON11 inhibits parasite growth by preventing merozoite invasion of red RBCs. Using ultrastructure expansion microscopy (U-ExM), I observed a unique phenotype in the absence of RON11, characterized by fully developed merozoites featuring single rhoptries. More intriguingly, RON11 depletion does not hinder merozoite attachment, nor does it impede the release of rhoptry effectors into the RBC during invasion. However, it does block internalization of merozoites. When observing RON11 during rhoptry biogenesis, I noted RON11's participation in the formation of the second rhoptry pair in the final stages of schizogony, which coincided with merozoite segregation. In summary, these data collectively suggest that RON11 plays a pivotal role in generating two rhoptries and is crucial for completing the process of merozoite internalization into the RBC.

3.2. Introduction

Malaria remains a devastating disease that affected approximately 247 million people worldwide in 2021, with the African region accounting for over 95% of the cases (World Health Organization 2022). The main causative agent of malaria is the unicellular protozoan parasite *Plasmodium falciparum*, which belongs to the apicomplexan phylum, along with other medically important organisms such as *Toxoplasma gondii* and *Cryptosporidium parvum*. Clinical symptoms of malaria in humans are associated with the continuous cycle of invasion of red blood cells (RBCs), development and replication through within them, and egress from them to release new merozoites that perpetuate the cycle. Invasion is a process that has been targeted by multiple vaccination and antibody treatment strategies (Beeson et al. 2016; González-Sanz, Berzosa, and Norman 2023), which underscores the importance of understanding this process for the development of clinical interventions.

Invasion is a rapid and complex process involving multiple steps (reviewed in Chapter 1). Newly egressed merozoites initiate an early attachment, leading to RBC deformation and merozoite reorientation (Groomes, Kanjee, and Duraisingh 2022; Hart et al. 2023; Weiss et al. 2015). Once its apical end is reoriented towards the RBC, the merozoite seems to form a pore in the RBC membrane, secretes proteins from the micronemes and rhoptries to form an irreversible tight junction at the interface merozoite-RBC (Geoghegan et al. 2021; Riglar et al. 2011; Vulliez-Le Normand et al. 2012; Weiss et al. 2015). Subsequently, the merozoite utilizes its actinomyosin motor to push through the tight junction and internalize within the newly formed parasitophorous vacuole (PV) (Blake, Haase, and Baum 2020; Geoghegan et al. 2021; Perrin Abigail J. et al. 2018; Yahata et al. 2021). Within the PV, merozoites develop into their ring stage, progressing into their metabolically active forms, trophozoites, and finally into their replicative form, schizonts, which

make 16-32 daughter merozoites. The parasite then initiates a cascade of events leading to the rupture of the RBC and PV membranes, resulting in the egress of merozoites.

Rhoptries, together with micronemes, are two specialized secretory organelles localized to the apical end in apicomplexans known to be essential for parasite proliferation. Even though they carry conserved roles among apicomplexans, they vary in numbers according to species, for instance *Cryptosporidium spp*. have a single rhoptry, *Plasmodium spp*. have two, and *Toxoplasma spp.* can have from eight to twelve rhoptries (Mageswaran et al. 2021; Martinez et al. 2022; Segev-Zarko et al. 2022). In *P. falciparum*, rhoptries are a pair of club-shaped secretory organelles located at the apical end of the merozoite that secrete proteins facilitating different steps during invasion. Rhoptries are internally compartmentalized into two regions: the neck and bulb, storing specific groups of proteins that are secreted sequentially at each step of invasion (Counihan et al. 2013; Liffner et al. 2021). Rhoptry neck proteins are released first, primarily mediating attachment to RBCs and the formation of the tight junction through secretion of proteins from the RON complex (Weiss et al. 2015). In contrast, rhoptry bulb proteins are secreted after tight junction formation and are associated with proper development within the PV, such as RAP1 and RAP2, which form the RAP complex (Ghosh et al. 2017; Riglar et al. 2011).

During invasion, rhoptries fuse their necks and bulbs to form a single rhoptry (Hanssen et al. 2013). After invasion is completed, this single rhoptry is assumed to be disassembled, as rhoptries become absent during early ring stages. During schizogony, rhoptries are then formed *de novo* by the fusion of Golgi-derived vesicles (Bannister et al. 2000; Krai, Dalal, and Klemba 2014). Rhoptry biogenesis begins early during schizogony, where the rhoptries remain associated with the cytoplasmic extensions of the MTOCs in a 1:1 ratio with each new rhoptry appearing to be formed *de novo* through each remaining mitotic event, until the last event where this ratio is broken

and each MTOC is observed with 2 rhoptries (Rudlaff et al. 2020; Liffner et al. 2023). Rhoptries maintain a bulb shape throughout most of their biogenesis process, adopting their final shape only after merozoite segmentation, with the formation of the neck in each rhoptry (Bannister et al. 2000; Liffner et al. 2023). Nevertheless, the factors triggering rhoptry biogenesis and regulating their structure and internal compartmentalization are still poorly understood.

Rhoptry neck protein 11, or RON11 (PF3D7_1463900), is a protein putatively localized to the rhoptries during intraerythrocytic life stages. RON11 is highly conserved among apicomplexans and contains seven transmembrane domains with a pair of calcium-binding EF-hand domains predicted to localize in the cytoplasm. Initial attempts to disrupt *P. berghei* RON11 were unsuccessful (Lasonder et al. 2008; van Ooij et al. 2008), while a recent knockdown showed a potential role in sporozoite invasion and gliding motility (Bantuchai et al. 2019). In contrast, RON11 disruption in *T. gondii* showed only a minor fitness defect, suggesting a non-essential role (Wang et al. 2016). However, nothing is known about the role of RON11 in *P. falciparum*. In this study, we employed the tetR-DOZI conditional knockdown system to investigate the role of RON11 in the process of rhoptry biogenesis and RBC invasion by *P. falciparum*. Our findings revealed that RON11 knockdown results in fully developed merozoites with a single rhoptry, with no effect on the trafficking and processing of the rhoptry proteins RON4 and RAP1. Intriguingly, these single rhoptry merozoites are unable to complete invasion, even though they are capable of attaching and secreting proteins to RBCs. Our data suggest that RON11 plays a role in regulating the *de novo* formation of the second rhoptry during merozoite segmentation.

3.3. Results

3.3.1. RON11 is essential for *P. falciparum* intraerythrocytic life cycle

To investigate the role of RON11 in *P. falciparum*, we generated a RON11 conditional knockdown parasite line employing the tetR-DOZI aptamer system, termed as RON11^{apt} (Rajaram, Liu, and Prigge 2020). Using CRISPR/Cas9 technology, we integrated the tetR-DOZI system into the endogenous loci of RON11, leading to the expression of a hemagglutinin (HA)-tagged protein under the regulation of anhydrotetracycline (aTc) (Fig. 3.1A). PCR analysis of genomic DNA from RON11^{apt} parasites showed correct integration at the endogenous loci (Fig. 3.1B). To test the efficiency of the knockdown system, we evaluated protein expression both in the presence (+RON11) and absence (-RON11) of aTc via Western blotting. Lysates from parasites cultured without aTc since ring stages exhibited a clear reduction in protein expression (Fig. 3.1C), confirming the system's suitability for studying RON11 function. Growth analysis using flow cytometry showed us that the knockdown of RON11 knockdown proved lethal for parasite expansion, as RON11^{apt} parasites failed to progress past their first life cycle when aTc was absent (Fig. 3.1D).

Furthermore, we assessed the putative subcellular localization of RON11 to the rhoptries, as it was previously observed in *P. berghei* schizonts (Bantuchai et al. 2019), by exploring its localization in comparison with two well-known markers of the rhoptry neck (RON4) and rhoptry bulb (RAP1). Employing immunofluorescence microscopy (IFA), we confirmed the presence of RON11 in the rhoptry neck of schizonts, as suggested by its high degree of colocalization with RON4 (Fig. 3.1E, top panels, and 3.1F). RON11 did not colocalize with RAP1, suggesting that RON11 is confined solely to the neck region (Fig. 3.1E, bottom panels, and 3.1F). Additionally, we observed RON11 at the parasite periphery of newly invaded ring-stage parasites (Fig. 3.2),

suggesting that RON11 might localize to the parasitophorous vacuole (PV) after invasion, in a similar way to RAP1 (Anaguano et al. 2023; Liffner et al. 2023; Riglar et al. 2011). It could also indicate a fusion event between the rhoptries and the parasite plasma membrane (PPM) happening after merozoite invasion. In summary, our results show RON11 localizes to the rhoptry neck in schizonts, and in early-ring-stage parasites, it localizes at the parasite periphery.

3.3.2. RON11 is required for the formation of two rhoptries in fully developed merozoites

Rhoptries are critical secretory organelles conserved among apicomplexans, with differences in numbers depending on the species. During *P. falciparum* intraerythrocytic development, rhoptries are initially observed forming *de novo* during early schizogony (Liffner et al. 2023). Then, rhoptries replicate throughout multiple mitotic events until each merozoite contains two rhoptries by the end of the cycle. In contrast, *T. gondii* can have as many as 8-12 rhoptries, but only two are known to release their contents during invasion (Mageswaran et al. 2021).

Given previous observations that other rhoptry membrane-associated proteins, such as RAMA, play a role in rhoptry formation and rhoptry protein localization (Sherling et al. 2019), we sought to determine whether RON11 shares a similar function. Therefore, due to the limited resolution provided by conventional microscopy to visualize rhoptry structures, we employed Ultrastructural expansion microscopy (UExM) to investigate this matter. We combined UExM with the application of NHS-ester staining, to analyze ML10-synchronized schizonts that were cultured in the presence or absence of aTc. Through this assay, we observed fully formed rhoptries exhibiting their distinctive structures: a slender and elongated neck at the apex, connected to an

apical ring, and a distal rotund bulb (Fig. 3.3A, top panels), as previously reported (Liffner and Absalon 2021). Most notably, we discovered that the knockdown of RON11 resulted in merozoites with only one rhoptry (Fig. 3.3A and 3.3B). These single rhoptries displayed no discernible structural alterations, as all three, the neck, the bulb, and apical ring, were still present in the proper orientation in each merozoite (Fig. 3.3A, bottom panels). Intriguingly, the absence of RON11 also resulted in a marginal number of schizonts with several rhoptries amassed in regions that appeared to be located outside of merozoites (Fig. 3.4A). Basal complexes were visible at their maximum contraction at the basal end of the analyzed merozoites (Liffner et al. 2023), discarding any impact of RON11 knockdown on merozoite segmentation, and confirming that the analyzed merozoites were fully developed (Fig. 3.3A and 3.4A). To validate this finding, we quantified the number of merozoites per schizont and found that the absence of RON11 did not affect the total number of merozoites, even though the number of rhoptries was reduced by half (Fig. 3.4B). To our knowledge, this marks the first observation of such a unique phenotype in *Plasmodium spp.* parasites.

To further investigate the impact of RON11 knockdown on rhoptry structures, we analyzed the localization of other subcellular markers in ML10-arrested schizonts using UExM. We confirmed RON11's localization at the neck of fully formed rhoptries, along with its colocalization with RON4 (Fig. 3.3A, top panels, and 3.5A, top panels). Furthermore, the localization of RON4 and RAP1 remained unaltered in the single rhoptries resulting from RON11 knockdown (Fig. 3.5A). Similarly, RON4 and RAP1 retained their localization in rhoptries of free merozoites lacking RON11 (Fig. 3.6A).

To independently confirm our previous observations, we assessed the effect of RON11 knockdown on the expression of RON4 and RAP1 in fully matured schizonts, previously treated

with the egress inhibitor, E64, through Western blotting. The total amount of RON4 and RAP1 was reduced by approximately half in the absence of RON11 (Fig. 3.5B). This finding could be attributed to the reduction of the number of rhoptries by half, aligning with recent findings suggesting that rhoptry pairs form *de novo* during schizogony rather than through duplication from a single mother rhoptry (Liffner et al. 2023).

Finally, we aimed to study if the absence of RON11 has any impact on the expression of markers of other subcellular compartments, such as the micronemes (AMA1) and merozoite surface (MSP1). We used IFAs and Western blotting on fully mature E64-treated schizonts cultured in the absence of RON11. We observed no effect on protein content or secretion of MSP1 to the merozoite surface under RON11 knockdown (Fig. 3.7A and B). Similarly, AMA1 retained its micronemal and secreted locations in the absence of RON11 (Fig. 3.7C), however we failed to detect AMA1 by Western blotting with our available antibody.

In summary, our data suggests that RON11 plays a crucial role in maintaining rhoptry duality during rhoptry biogenesis, yet RON11 loss does not appear to affect the secretion and production of rhoptry proteins.

3.3.3. RON11 knockdown impairs merozoite internalization

As RON11 is known to be highly expressed in schizont stages (Bozdech et al. 2003; Llinás et al. 2006), and we showed its knockdown inhibits parasite growth (Fig. 3.1D), we sought to investigate whether RON11 is necessary for schizont development, egress or merozoite invasion. To this end, we monitored the progression of RON11^{apt} parasites through their different life stages, both in the presence and absence of aTc. We collected samples at different time points, starting with tightly synchronized schizonts, using Hema3-stained smears and light microscopy. Our

findings indicate that, regardless of the presence of RON11, parasites developed normally from rings through schizonts, and egressed without issues (Fig. 3.8A). However, in the absence of RON11, the egressed merozoites did not progress into rings as the +RON11 parasites did, and instead, they appeared to accumulate around the RBCs (Fig. 3.8A). To validate our observations, we employed flow cytometry to measure parasite development over an 8-hour period following the removal of ML10 from arrested mature schizonts. Even though schizonts egressed normally in the absence of RON11, rings were not detected at any time point after egress (Fig. 3.8B). Together these findings suggest that the knockdown of RON11 prevents merozoite invasion, while having no effect on intracellular development or egress of merozoites. These data aligns with our previous findings using UExM (Fig. 3.3 and 3.5).

Merozoite invasion is a complex multistep process, which involves the participation of multiple regulatory factors. In general terms, invasion can be divided in 4 main events: attachment and RBC deformation, apical end reorientation and pore formation, rhoptry secretion and tight junction formation, and internalization and PVM sealing (Cowman et al. 2017; Groomes, Kanjee, and Duraisingh 2022). To dissect the role RON11 might play during merozoite invasion, we investigated two specific events in the absence of RON11: merozoite attachment to RBCs, and secretion of rhoptry proteins into RBCs. Since invasion is a very rapid process (Gilson and Crabb 2009), we used a cytochalasin-D-based strategy to observe specific steps. Cytochalasin D is an actin polymerization inhibitor that disrupts the activity of the merozoite actinomyosin motor, preventing internalization, but not affecting the previous steps on merozoite invasion (Boyle et al. 2010; Geoghegan et al. 2021; Riglar et al. 2011).Samples for analysis were collected from ML-10 treated mature schizonts that were allowed to invade fresh RBCs in the presence of cytochalasin D (Fig. 3.8C).

First, we used Hema3-stained smears and light microscopy to blindly score the percentage of merozoites attached to RBCs with and without RON11. No significant difference in the percentage of attached merozoites grown in the presence or absence of RON11 was observed (Fig. 3.8D). And, when merozoites were allowed to invade without the inhibitor, we found that a higher percentage of attached merozoites in the absence of RON11, comparable to the cytochalasin-D-treated parasites grown without RON11 (Fig. 3.9). Also, the percentage of +RON11 attached merozoites dropped significantly when cytochalasin D was removed, as they were able to normally invade RBCs and form rings (Fig. 3.9). Altogether, these data demonstrated that RON11 is not required for merozoite attachment to RBCs.

Next, we used IFAs to analyze the secretion of rhoptry proteins from cytochalasin-D-treated merozoites into RBCs in the presence or absence of RON11. RAP1 was selected as our secretion marker because it has been previously shown to be secreted into RBCs cytoplasm in the presence of cytochalasin D (Riglar et al. 2011). We found that merozoites lacking RON11 were able to secrete RAP1 into RBCs similarly to merozoites with RON11 (Fig. 3.8E). And, when comparing the number of attached merozoites capable of secreting versus the ones who did not, no significant differences were observed based on RON11 presence (Fig. 3.8F). These results show that RON11 does not play a role in secretion of rhoptry proteins during invasion.

In summary, our results showed that RON11 is dispensable for merozoite attachment and rhoptry discharge, however it is necessary for the completion of merozoite invasion.

3.3.4. RON11 is required for the biogenesis of the last rhoptry pair

Given that rhoptries can be first observed early during schizogony (Mahajan et al. 2008; Liffner et al. 2023) and that we showed that RON11 loss generates fully developed single-rhoptry merozoites, we aimed to understand the exact role of RON11 during rhoptry biogenesis.

Because schizogony is known to lasts approximately 15 hours (Voß et al. 2023), we designed a rescue assay to define the window of time within schizogony where RON11 might act. We measured by flow cytometry the formation of rings in cultures that had "aTc" added back at different time points during their previous schizogony cycle. Supplementation of schizonts with "aTc" as late as 44 hpi showed partial to complete rescue of the RON11-knockdown phenotype. However, supplementation after 46 hpi was unable to rescue the phenotype (Fig. 3.10). These findings suggested that RON11 has an essential role during the last hours of schizont development.

As we have shown that RON11 acts during the last hours of schizogony, we hypothesized it might have a role in regulating the formation of the last rhoptry pair during late schizogony. To test our premise, we employed UExM in combination with NHS-ester to follow the development of rhoptry biogenesis during schizogony in the presence and absence of RON11. It has been previously shown that during their biogenesis, rhoptries associate with the cytoplasmic extensions of microtubule organization centers (MTOC) in a ratio of one rhoptry per branch during the early mitotic events of schizogony. Once merozoite segmentation starts, each MTOC branch accommodates two rhoptries, which will form the final rhoptry pair within each merozoite (Liffner et al. 2023). By analyzing at 44-48 hour synchronized schizonts, we found that the formation and segregation of rhoptries during the mitotic events was not affected by the removal of RON11 (Fig. 3.11). Nevertheless, we also discovered that the loss of RON11 impaired the *de novo* formation of the second rhoptry after the last mitotic event (Fig. 3.11). Initiation of merozoite segmentation on

those events was confirmed by the presence of basal complex rings in association with the MTOC/rhoptry-complex densities (Fig. 3.11).

Altogether this data confirms our thesis that RON11 regulates the *de novo* formation of the second rhoptry after the last mitotic event during schizogony.

3.4. Materials and methods

3.4.1. Construction of RON11 plasmids

Genomic DNA was isolated from *P. falciparum* NF54^{attB} cultures using the QIAamp DNA blood kit (Qiagen). PCR products were inserted into the respective plasmids using the NEBuilder HiFi DNA Assembly system (NEB). All constructs used in this study were confirmed by sequencing. All primers used in this study are in Table 3.1.

For generation of the plasmid pKD-RON11-Apt, sequences of approximately 500 bp of homology to the RON11 (Pf3D7_1463900) C-terminus and 3'UTR were amplified using primer pairs P3-P4 and P5-P6, respectively (Table 3.1). Amplicons were then inserted into pKD (Anaguano et al. 2023; Rajaram, Liu, and Prigge 2020) digested by with AatII and AscI. For expression of a RON11 gRNA, oligo P7 was inserted into cut pUF1-Cas9 (Table 3.1).

3.4.2. Parasite culture and transfections

Plasmodium parasites were cultured in RPMI 1640 medium (NF54^{attB}, RON11^{apt}) supplemented with AlbuMAX I (Gibco), and transfected as described earlier (Kudyba et al. 2018).

For generation of RON11^{Apt} parasites, a mix of two plasmids (50 µg each) were transfected into NF54^{attB} parasites in duplicate. The plasmid mix contained the plasmid pUF1-Cas9-SBP1gRNA, which contains the DHOD resistance gene, and the marker-free plasmid pTOPO-SBP1-TbID. Drug pressure was applied 48 h after transfection, using 1µM DSM1 (Ganesan et al. 2011) and selecting for Cas9 expression. After parasites grew back from transfection, integration was confirmed by PCR, and then cloned using limiting dilution. After clonal selection, cultures were transferred to biotin-free medium without DSM1.

For generation of RON11^{apt} parasites, the pKD-RON11-Apt plasmid (20 µg) and the respective pUF1-Cas9 plasmid (50 µg) were transfected into NF54^{attB} parasites in duplicate. Before transfection pKD plasmids were digested overnight with EcoRV (NEB). The enzyme was then subjected to heat inactivation for 20 min at 65 °C and then mixed with the pUF1-Cas9 plasmid. Transfected parasites were grown in 0.5 µM anhydrous tetracycline (aTc) (Cayman Chemical). Drug pressure was applied 48 h after transfection, using blasticidin (BSD) (Gibco) at a concentration of 2.5 µg/mL, selecting for pKD-RON11-Apt expression. After parasites grew back from transfection, integration was confirmed by PCR, and then cloned using limiting dilution. Clones were maintained in mediums containing 0.5 µM aTc and 2.5 µg/mL BSD.

3.4.3. Growth assays

For all assays, aliquots of parasite cultures were incubated in 8 µM Hoechst 33342 (ThermoFisher Scientific) for 20 min at room temperature and then fluorescence was measured using a CytoFlex S (Beckman Coulter) flow-cytometer. Flow cytometry data were analyzed using FlowJo software (Tree Star, Inc.) and plotted using Prism (GraphPad Software Inc.).

For the growth assay, synchronous ring-stage parasites were washed five times with RPMI 1640 medium and split into two cultures, one resuspended in medium containing 0.5 µM aTc and 2.5 µg/mL BSD (+RON11), and the other one in medium containing only 2.5 µg/mL BSD (-RON11). Cultures were then transferred to a 96-well plate at 0.2% parasitemia and grown for 6 days. Parasitemia was monitored every 48 h.

For the invasion vs egress assay, synchronous ring-stage parasites were washed and split into two cultures with and without aTc, as previously described. Parasites were then allowed to develop into mature schizonts to be isolated using a Percoll gradient (Genesee Scientific). Enriched parasites were then incubated for 4 hours at 37 °C in pre-warmed RPMI media supplemented with

the PKG inhibitor, ML10 compound (25 nM) (obtained from S. Osborne, BEI resources) (Ressurreição et al. 2020). After incubation, parasites were washed twice with pre-warmed RPMI media and transferred immediately to pre-warmed RBCs at 2% hematocrit. Parasitemia was monitored every two hours, for eight hours.

For the rescue assay, parasites were synchronized to a 1-hour window. Synchronized ring-stage parasites were washed and split into six cultures in a 6-well plate (+ RON11, - RON11, 44h, 46h, 48h and 50h). Culture "+RON11" was grown in the presence of aTc, while the others were grown in absence of aTc. Parasites were allowed to develop into schizonts and aTc was supplemented back into cultures at their corresponding time point, except for the "-RON11" culture. Parasitemia was monitored at 44 and 56 hours post infection (hpi).

3.4.4. Western blotting

Parasites were synchronized, washed, and split into two cultures with and without aTc, as previously described. Synchronous parasites were then allowed to develop into mature schizonts to be then incubated with E64 for 4 hours at 37 °C. After treatment, culture pellets were treated with ice-cold 0.04% saponin in 1x PBS to isolate parasites from host cells. The parasite pellets were subsequently solubilized in protein loading dye with Beta-mercaptoethanol (LI-COR Biosciences) and used for SDS-PAGE.

Primary antibodies used in this study included mouse-anti-HA (6E2; Cell Signaling Technology; 1:2000), rabbit-anti-PfEF1α (from Daniel Goldberg, 1:2000), mouse-anti-RAP1 (2.29; from Jana McBride via the European Malaria Reagent Repository; 1:500) (Hall et al. 1983), mouse-anti-RON4 (10H11; from Alan Cowman; 1:500) (Richard et al. 2010), mouse-anti-MSP1 (12.4; from Jana McBride via the European Malaria Reagent Repository; 1:500) (McBride, Newbold, and Anand 1985). Secondary antibodies used were IRDye 680 CW goat-anti-rabbit IgG

and IRDye 800CW goat-anti-mouse IgG (Li-COR Biosciences; 1:20 000). Membranes were imaged using the Odyssey Clx Li-COR infrared imaging system (Li-COR Biosciences). Images were processed and analyzed using ImageStudio (Li-COR Biosciences).

3.4.5. Microscopy and image analysis

For all microscopy assays, parasites were synchronized, washed, and split into two cultures with and without aTc, as previously described.

For IFAs, cells were fixed following the previously described protocol (Cobb et al. 2017).

For localization assays, schizont-stage parasites were smeared onto a slide, fixed and permeabilized with acetone for 10 min at room temperature.

For rhoptry secretion assays, synchronous parasites were allowed to develop into mature schizonts to be isolated using a Percoll gradient (Genesee Scientific). Enriched parasites were then incubated for 4 hours at 37 °C in pre-warmed RPMI media supplemented with 25 nM ML10 compound. After incubation, parasites were washed twice with pre-warmed RPMI media and transferred immediately to RBCs at 1% hematocrit. Cultures were then allowed to egress for 30 min at 37 °C in media supplemented with 1 µM cytochalasin D (Invitrogen). After incubation, parasites were fixed with 4% paraformaldehyde (PFA) (Electron Microscopy Sciences) and 0.03% glutaraldehyde, before being permeabilized with 0.1% Triton-X100.

Primary antibodies used in the IFAs included rabbit-anti-HA (SG77; ThermoFisher Scientific; 1:100), mouse-anti-RAP1 (2.29; from Jana McBride via the European Malaria Reagent Repository; 1:500) (Hall et al. 1983), mouse-anti-RON4 (10H11; from Alan Cowman; 1:200) (Richard et al. 2010). Secondary antibodies used were Alexa Fluor 488 and Alexa Fluor 546 (Life Technologies, 1:1000).

After mounting the cells using ProLong Diamond with 4',6'-diamidino-2-phenylindole (DAPI) (Invitrogen), they were imaged using a DeltaVision II microscope system with an Olympus Ix-71 inverted microscope. Images were collected as a Z-stack and deconvolved using SoftWorx (GE HealthCare), then displayed as a maximum intensity projection. Adjustments to brightness and contrast were made for display purposes using Adobe Photoshop. Colocalization was analyzed using the Pearson's correlation coefficient calculated by the Cell Profiler software (Broad Institute Inc.).

For growth assays, synchronous schizont-stage parasites were washed five times and split into two cultures, one without and one with aTc. Parasites were allowed to develop during two life cycles and sample aliquots were collected at different time points.

For attachment assays, parasites were collected as previously described in the rhoptry secretion assay with a slight change. After ML10 removal, schizont-stage parasites were allowed to egress during 2 h at 37 °C in the presence and absence of 1 μM cytochalasin D. Samples were collected after incubation.

For light microscopy imaging, aliquots were smeared into glass slides and stained using Hema3 Fixative solutions (Fischer Healthcare). Slides were imaged using a Zeiss Axio Scope A1 microscope with a Zeiss Axiocam 305 color camera. Images were processed using Adobe Photoshop.

3.4.6. Ultrastructural expansion microscopy (U-ExM)

Cultures for U-ExM were synchronized to mature schizont parasites, following the previously described methods. Ultrastructure expansion microscopy (U-ExM) was performed as described previously (Liffner and Absalon 2021), with minor modifications.

To start, 12 mm round coverslips were treated with poly-D-lysine for 1 hour at 37 °C. They were then washed three times with MilliQ water and placed in a 24-well plate. Parasite cultures with approximately 5% parasitemia were adjusted to 0.5% hematocrit. Then, 1 mL of parasite culture was added to the well containing the treated coverslip and incubated for 1 h at 37 °C.

After the incubation, the supernatant was carefully removed, and a fixative solution (4% v/v PFA in PBS) was added, followed by a 20 min incubation at 37 °C. The coverslips were washed three times with 1X PBS and incubated overnight at 37 °C in 500 µL of 1.4% formaldehyde/2% acrylamide (FA/AA) in PBS.

The monomer solution (19% sodium acrylate, 10% acrylamide, 0.1% N,N'-methylenebisacrylamide in PBS) was prepared a day prior and stored at -20 °C. Before gelation, coverslips were removed from FA/AA solution and washed three times in 1X PBS.

For gelation, 5 µL of 10% tetramethylenediamine (TEMED) and 5 µL of 10% ammonium persulfate (APS) were added to 90 µL of the monomer solution, briefly vortexed, and 35 µL of the monomer mixture were pipetted onto parafilm. The coverslips were placed on top with the cell-side facing down, and the gels were incubated at 37 °C for 30 min.

Next, the gels were transferred into a 6-well plate containing denaturing buffer (200 mM sodium dodecyl sulfate (SDS), 200 mM NaCl, 50 mM Tris, pH 9) and incubated for 15 min incubation at room temperature. Afterward, the gels were separated from the coverslips and transferred to 1.5 mL tubes with the denaturing buffer for 90-min incubation at 95 °C.

Subsequently, the gels were incubated with secondary antibodies diluted in 1X PBS for 2.5 hours. After denaturation, gels were transferred to Petri dishes containing 25 mL of MilliQ water and incubated three times for 30 min at room temperature with shaking, changing the water in between. The gels were measured and subsequently shrunk using two washes with 1X PBS. They

were then transferred to a 24-well plate for blocking in 3% BSA in PBS at room temperature for 30 min. After blocking gels were incubated with primary antibodies diluted in 3% BSA overnight at room temperature.

Following primary antibody incubation, the gels were washed three times in 0.5% PBS-Tween 20 for 10 min before incubation with secondary antibodies diluted in 1X PBS for 2.5 hours.

After secondary antibody staining, the gels were washed three times with 0.5% PBS-Tween 20. Then, gels were transferred back to 10 cm Petri dishes for the second round of expansion, involving three incubations with MilliQ water. After re-expansion, the gels were either imaged immediately or stored in 0.2% propyl gallate in water until imaging.

The primary antibodies used were rat-anti-HA 3F10 (Roche, 1:50), mouse-anti-RAP1 (2.29; from Jana McBride via the European Malaria Reagent Repository; 1:500) (Hall et al. 1983), mouse-anti-RON4 (10H11; from Alan Cowman; 1:200) (Richard et al. 2010). The secondary antibodies used were Alexa Fluor 488 and Alexa Fluor 546 (Life Technologies, 1:500), NHS-ester 405 (Thermofisher, 1:250). The gels were imaged using a Zeiss LSM 980 microscope with Airyscan 2. Images were collected as a Z-stack, processed by Airyscan, and then displayed as a maximum intensity projection. Adjustments to brightness and contrast were made using ZEN Blue software for display purposes.

3.5. References

Anaguano, David, Watcharatip Dedkhad, Carrie F. Brooks, David W. Cobb, and Vasant Muralidharan. 2023. "Time-Resolved Proximity Biotinylation Implicates a Porin Protein in Export of Transmembrane Malaria Parasite Effectors." *Journal of Cell Science*, September. https://doi.org/10.1242/jcs.260506.

Bannister, L. H., J. M. Hopkins, R. E. Fowler, S. Krishna, and G. H. Mitchell. 2000. "Ultrastructure of Rhoptry Development in Plasmodium Falciparum Erythrocytic Schizonts." *Parasitology* 121 (Pt 3) (September): 273–87.

Bantuchai, Sirasate, Mamoru Nozaki, Amporn Thongkukiatkul, Natcha Lorsuwannarat, Mayumi Tachibana, Minami Baba, Kazuhiro Matsuoka, Takafumi Tsuboi, Motomi Torii, and Tomoko Ishino. 2019. "Rhoptry Neck Protein 11 Has Crucial Roles during Malaria Parasite Sporozoite Invasion of Salivary Glands and Hepatocytes." *International Journal for Parasitology* 49 (9): 725–35.

Beeson, James G., Damien R. Drew, Michelle J. Boyle, Gaoqian Feng, Freya J. I. Fowkes, and Jack S. Richards. 2016. "Merozoite Surface Proteins in Red Blood Cell Invasion, Immunity and Vaccines against Malaria." *FEMS Microbiology Reviews* 40 (3): 343–72.

Blake, Thomas C. A., Silvia Haase, and Jake Baum. 2020. "Actomyosin Forces and the Energetics of Red Blood Cell Invasion by the Malaria Parasite Plasmodium Falciparum." *PLoS Pathogens* 16 (10): e1009007.

Boyle, Michelle J., Danny W. Wilson, Jack S. Richards, David T. Riglar, Kevin K. A. Tetteh, David J. Conway, Stuart A. Ralph, Jake Baum, and James G. Beeson. 2010. "Isolation of Viable *Plasmodium Falciparum* Merozoites to Define Erythrocyte Invasion Events and

Advance Vaccine and Drug Development." *Proceedings of the National Academy of Sciences of the United States of America* 107 (32): 14378–83.

Bozdech, Zbynek, Manuel Llinás, Brian Lee Pulliam, Edith D. Wong, Jingchun Zhu, and Joseph L. DeRisi. 2003. "The Transcriptome of the Intraerythrocytic Developmental Cycle of Plasmodium Falciparum." *PLoS Biology* 1 (1): E5.

Cobb, David W., Anat Florentin, Manuel A. Fierro, Michelle Krakowiak, Julie M. Moore, and Vasant Muralidharan. 2017. "The Exported Chaperone PfHsp70x Is Dispensable for the Plasmodium Falciparum Intraerythrocytic Life Cycle." *MSphere* 2 (5): e00363-17.

Counihan, Natalie A., Ming Kalanon, Ross L. Coppel, and Tania F. de Koning-Ward. 2013. "Plasmodium Rhoptry Proteins: Why Order Is Important." *Trends in Parasitology* 29 (5): 228–36.

Cowman, Alan F., Christopher J. Tonkin, Wai-Hong Tham, and Manoj T. Duraisingh. 2017. "The Molecular Basis of Erythrocyte Invasion by Malaria Parasites." *Cell Host & Microbe* 22 (2): 232–45.

Ganesan, Suresh M., Joanne M. Morrisey, Hangjun Ke, Heather J. Painter, Kamal Laroiya, Margaret A. Phillips, Pradipsinh K. Rathod, Michael W. Mather, and Akhil B. Vaidya. 2011. "Yeast Dihydroorotate Dehydrogenase as a New Selectable Marker for Plasmodium Falciparum Transfection." *Molecular and Biochemical Parasitology* 177 (1): 29–34.

Geoghegan, Niall D., Cindy Evelyn, Lachlan W. Whitehead, Michal Pasternak, Phoebe McDonald, Tony Triglia, Danushka S. Marapana, et al. 2021. "4D Analysis of Malaria Parasite Invasion Offers Insights into Erythrocyte Membrane Remodeling and Parasitophorous Vacuole Formation." *Nature Communications* 12 (1): 1–16.

Ghosh, Sreejoyee, Kit Kennedy, Paul Sanders, Kathryn Matthews, Stuart A. Ralph, Natalie A. Counihan, and Tania F. de Koning-Ward. 2017. “The Plasmodium Rhoptry Associated Protein Complex Is Important for Parasitophorous Vacuole Membrane Structure and Intraerythrocytic Parasite Growth.” *Cellular Microbiology* 19 (8). https://doi.org/10.1111/cmi.12733.

Gilson, Paul R., and Brendan S. Crabb. 2009. “Morphology and Kinetics of the Three Distinct Phases of Red Blood Cell Invasion by Plasmodium Falciparum Merozoites.” *International Journal for Parasitology* 39 (1): 91–96.

González-Sanz, Marta, Pedro Berzosa, and Francesca F. Norman. 2023. “Updates on Malaria Epidemiology and Prevention Strategies.” *Current Infectious Disease Reports*, June, 1–9.

Groomes, Patrice V., Usheer Kanjee, and Manoj T. Duraisingh. 2022. “RBC Membrane Biomechanics and Plasmodium Falciparum Invasion: Probing beyond Ligand-Receptor Interactions.” *Trends in Parasitology* 38 (4): 302–15.

Hall, Roger, Jana McBride, Gillian Morgan, Andrew Tait, J. Werner Zolg, David Walliker, and John Scaife. 1983. “Antigens of the Erythrocytic Stages of the Human Malaria Parasite Plasmodium Falciparum Detected by Monoclonal Antibodies.” *Molecular and Biochemical Parasitology* 7 (3): 247–65.

Hanssen, Eric, Chaitali Dekiwadia, David T. Riglar, Melanie Rug, Leandro Lemgruber, Alan F. Cowman, Marek Cyrklaff, et al. 2013. “Electron Tomography of Plasmodium Falciparum Merozoites Reveals Core Cellular Events That Underpin Erythrocyte Invasion.” *Cellular Microbiology* 15 (9): 1457–72.

Hart, Melissa N., Franziska Mohring, Sophia M. DonVito, James A. Thomas, Nicole Muller-Sienerth, Gavin J. Wright, Ellen Knuepfer, Helen R. Saibil, and Robert W. Moon. 2023.

"Sequential Roles for Red Blood Cell Binding Proteins Enable Phased Commitment to Invasion for Malaria Parasites." *Nature Communications* 14 (1): 4619.

Krai, Priscilla, Seema Dalal, and Michael Klemba. 2014. "Evidence for a Golgi-to-Endosome Protein Sorting Pathway in Plasmodium Falciparum." *PloS One* 9 (2): e89771.

Kudyba, Heather M., David W. Cobb, Anat Florentin, Michelle Krakowiak, and Vasant Muralidharan. 2018. "CRISPR/Cas9 Gene Editing to Make Conditional Mutants of Human Malaria Parasite P. Falciparum." *Journal of Visualized Experiments: JoVE*, no. 139 (January): 1–10.

Lasonder, Edwin, Chris J. Janse, Geert-Jan van Gemert, Gunnar R. Mair, Adriaan M. W. Vermunt, Bruno G. Douradinha, Vera van Noort, et al. 2008. "Proteomic Profiling of Plasmodium Sporozoite Maturation Identifies New Proteins Essential for Parasite Development and Infectivity." *PLoS Pathogens* 4 (10): e1000195.

Liffner, Benjamin, and Sabrina Absalon. 2021. "Expansion Microscopy Reveals Plasmodium Falciparum Blood-Stage Parasites Undergo Anaphase with A Chromatin Bridge in the Absence of Mini-Chromosome Maintenance Complex Binding Protein." *Microorganisms* 9 (11): 2306.

Liffner, Benjamin, Juan Miguel Balbin, Jan Stephan Wichers, Tim-Wolf Gilberger, and Danny W. Wilson. 2021. "The Ins and Outs of Plasmodium Rhoptries, Focusing on the Cytosolic Side." *Trends in Parasitology* 37 (7): 638–50.

Liffner, Benjamin, Ana Karla Cepeda Diaz, James Blauwkamp, David Anaguano, Sonja Frölich, Vasant Muralidharan, Danny W. Wilson, Jeffrey Dvorin, and Sabrina Absalon. 2023. "Atlas of Plasmodium Falciparum Intraerythrocytic Development Using Expansion Microscopy." https://doi.org/10.7554/elife.88088.1.

Llinás, Manuel, Zbynek Bozdech, Edith D. Wong, Alex T. Adai, and Joseph L. DeRisi. 2006. "Comparative Whole Genome Transcriptome Analysis of Three Plasmodium Falciparum Strains." *Nucleic Acids Research* 34 (4): 1166–73.

Mageswaran, Shrawan Kumar, Amandine Guérin, Liam M. Theveny, William David Chen, Matthew Martinez, Maryse Lebrun, Boris Striepen, and Yi-Wei Chang. 2021. "In Situ Ultrastructures of Two Evolutionarily Distant Apicomplexan Rhoptry Secretion Systems." *Nature Communications* 12 (1): 4983.

Mahajan, Babita, Angamuthu Selvapandiyan, Noel J. Gerald, Victoria Majam, Hong Zheng, Thilan Wickramarachchi, Jawahar Tiwari, et al. 2008. "Centrins, Cell Cycle Regulation Proteins in Human Malaria Parasite Plasmodium Falciparum." *The Journal of Biological Chemistry* 283 (46): 31871–83.

Martinez, Matthew, William David Chen, Marta Mendonça Cova, Petra Molnár, Shrawan Kumar Mageswaran, Amandine Guérin, Audrey R. Odom John, Maryse Lebrun, and Yi-Wei Chang. 2022. "Rhoptry Secretion System Structure and Priming in Plasmodium Falciparum Revealed Using in Situ Cryo-Electron Tomography." *Nature Microbiology*. https://doi.org/10.1038/s41564-022-01171-3.

McBride, J. S., C. I. Newbold, and R. Anand. 1985. "Polymorphism of a High Molecular Weight Schizont Antigen of the Human Malaria Parasite Plasmodium Falciparum." *The Journal of Experimental Medicine* 161 (1): 160–80.

Nkrumah, Louis J., Rebecca A. Muhle, Pedro A. Moura, Pallavi Ghosh, Graham F. Hatfull, William R. Jacobs Jr, and David A. Fidock. 2006. "Efficient Site-Specific Integration in Plasmodium Falciparum Chromosomes Mediated by Mycobacteriophage Bxb1 Integrase." *Nature Methods* 3 (8): 615–21.

Ooij, Christiaan van, Pamela Tamez, Souvik Bhattacharjee, N. Luisa Hiller, Travis Harrison, Konstantinos Liolios, Taco Kooij, et al. 2008. “The Malaria Secretome: From Algorithms to Essential Function in Blood Stage Infection.” *PLoS Pathogens* 4 (6): e1000084.

Perrin Abigail J., Collins Christine R., Russell Matthew R. G., Collinson Lucy M., Baker David A., and Blackman Michael J. 2018. “The Actinomyosin Motor Drives Malaria Parasite Red Blood Cell Invasion but Not Egress.” *MBio* 9 (4): 10.1128/mbio.00905-18.

Rajaram, Krithika, Hans B. Liu, and Sean T. Prigge. 2020. “Redesigned TetR-Aptamer System To Control Gene Expression in Plasmodium Falciparum.” *MSphere* 5 (4). https://doi.org/10.1128/mSphere.00457-20.

Ressurreição, Margarida, James A. Thomas, Stephanie D. Nofal, Christian Flueck, Robert W. Moon, David A. Baker, and Christiaan van Ooij. 2020. “Use of a Highly Specific Kinase Inhibitor for Rapid, Simple and Precise Synchronization of Plasmodium Falciparum and Plasmodium Knowlesi Asexual Blood-Stage Parasites.” *PloS One* 15 (7): e0235798.

Richard, Dave, Christopher A. MacRaild, David T. Riglar, Jo-Anne Chan, Michael Foley, Jake Baum, Stuart A. Ralph, Raymond S. Norton, and Alan F. Cowman. 2010. “Interaction between Plasmodium Falciparum Apical Membrane Antigen 1 and the Rhoptry Neck Protein Complex Defines a Key Step in the Erythrocyte Invasion Process of Malaria Parasites.” *The Journal of Biological Chemistry* 285 (19): 14815–22.

Riglar, David T., Dave Richard, Danny W. Wilson, Michelle J. Boyle, Chaitali Dekiwadia, Lynne Turnbull, Fiona Angrisano, et al. 2011. “Super-Resolution Dissection of Coordinated Events during Malaria Parasite Invasion of the Human Erythrocyte.” *Cell Host & Microbe* 9 (1): 9–20.

Rudlaff, Rachel M., Stephan Kraemer, Jeffrey Marshman, and Jeffrey D. Dvorin. 2020. “Three-Dimensional Ultrastructure of Plasmodium Falciparum throughout Cytokinesis.” *PLoS Pathogens* 16 (6): e1008587.

Segev-Zarko, Li-Av, Peter D. Dahlberg, Stella Y. Sun, Daniël M. Pelt, Chi Yong Kim, Elizabeth S. Egan, James A. Sethian, Wah Chiu, and John C. Boothroyd. 2022. “Cryo-Electron Tomography with Mixed-Scale Dense Neural Networks Reveals Key Steps in Deployment of Toxoplasma Invasion Machinery.” *PNAS Nexus* 1 (4): gac183.

Sherling, Emma S., Abigail J. Perrin, Ellen Knuepfer, Matthew R. G. Russell, Lucy M. Collinson, Louis H. Miller, and Michael J. Blackman. 2019. “The Plasmodium Falciparum Rhoptry Bulb Protein RAMA Plays an Essential Role in Rhoptry Neck Morphogenesis and Host Red Blood Cell Invasion.” *PLoS Pathogens* 15 (9): e1008049.

Voß, Yannik, Severina Klaus, Julien Guizetti, and Markus Ganter. 2023. “Plasmodium Schizogony, a Chronology of the Parasite’s Cell Cycle in the Blood Stage.” *PLoS Pathogens* 19 (3): e1011157.

Vulliez-Le Normand, Brigitte, Michelle L. Tonkin, Mauld H. Lamarque, Susann Langer, Sylviane Hoos, Magali Roques, Frederick A. Saul, et al. 2012. “Structural and Functional Insights into the Malaria Parasite Moving Junction Complex.” *PLoS Pathogens* 8 (6): e1002755.

Wang, Kevin, Eric D. Peng, Amy S. Huang, Dong Xia, Sarah J. Vermont, Gaelle Lentini, Maryse Lebrun, Jonathan M. Wastling, and Peter J. Bradley. 2016. “Identification of Novel O-Linked Glycosylated Toxoplasma Proteins by Vicia Villosa Lectin Chromatography.” *PloS One* 11 (3): e0150561.

Weiss, Greta E., Paul R. Gilson, Tana Taechalertpaisarn, Wai-Hong Tham, Nienke W. M. de Jong, Katherine L. Harvey, Freya J. I. Fowkes, et al. 2015. "Revealing the Sequence and Resulting Cellular Morphology of Receptor-Ligand Interactions during Plasmodium Falciparum Invasion of Erythrocytes." *PLoS Pathogens* 11 (2): e1004670.

World Health Organization. 2022. *World Malaria Report 2022*. World Health Organization.

Yahata, Kazuhide, Melissa N. Hart, Heledd Davies, Masahito Asada, Samuel C. Wassmer, Thomas J. Templeton, Moritz Treeck, Robert W. Moon, and Osamu Kaneko. 2021. "Gliding Motility of *Plasmodium* Merozoites." *Proceedings of the National Academy of Sciences of the United States of America* 118 (48). https://doi.org/10.1073/pnas.2114442118.

3.6. Tables

Table 3.1. List of primers used in the study to generate the cell lines RON11^{apt}.

Amplicon	Primer	Sequence (5' – 3')
RON11-Cterm integration	P1	TGTTTAGGAATTTTTGGAGGTATTTGATAG
Apt integration	P2	CTAGACTAGGTTCCAAGATCTCCC
RON11-Cterm	P3	ATTGTGTATCCCGATATCGATGTTAATAGTTTAAAAAAAATACTAACAGAAGTAAGATG
	P4	CGTCATAAGGGTATCCGGAGACGTCTTTCGAATCAGATGCTGACTGTAAATAAG
RON11-3'UTR	P5	CCAATGGCCCCTTTCCGGGCGCGCCCTTTTTTGTTTGAAATTGGCAAAAATATTAGTAG
	P6	ACTATTAACATCGATATCGGGATACACAATAGAATATTAATTAAGTGTATTATTAAGTG
RON11 gRNA	P7	CATATTAAGTATATAATATTGATATGGATGTCGAAAGAAAGTTTTAGAGCTAGAAATAGC

3.7. Figures

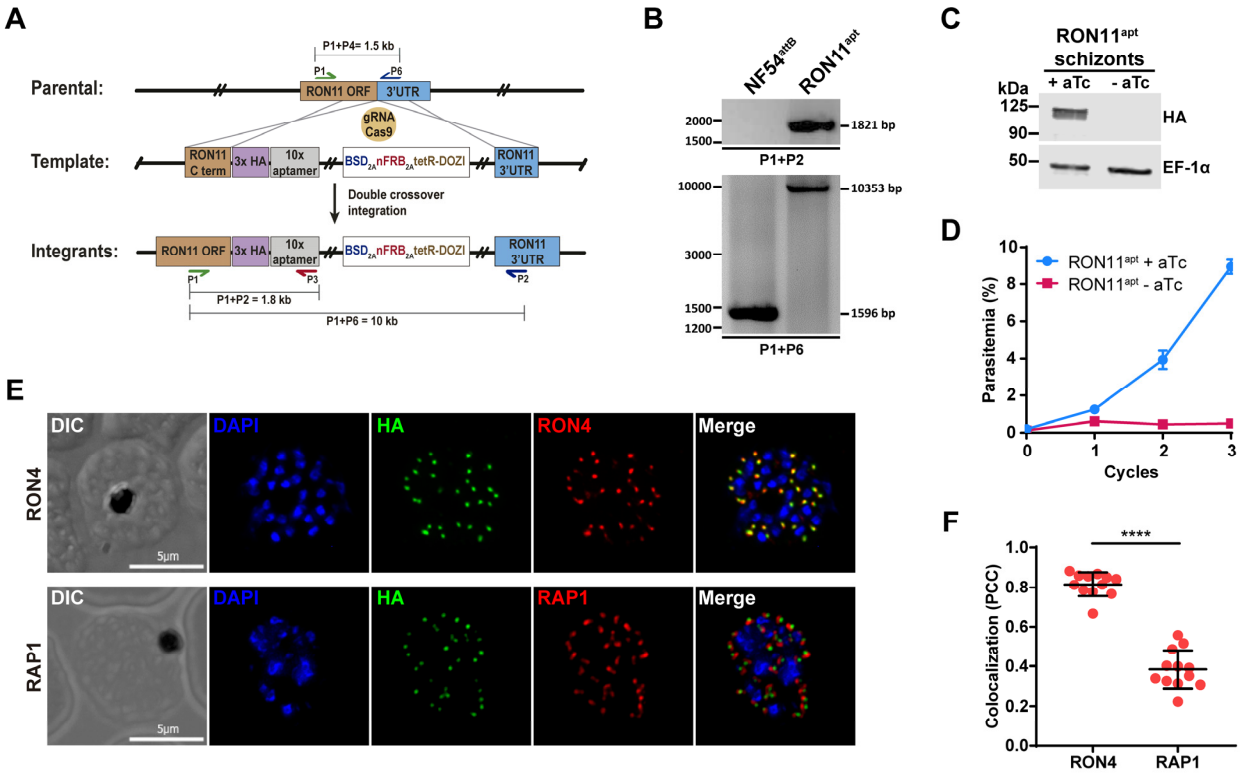

Figure 3.1. RON11 is essential for intraerythrocytic growth. (A) Schematic showing the integration of the repair plasmid used to introduce the tetR-DOZI system in the genomic loci of RON11. Cas9 introduces a double-stranded break at the C-terminus of the RON11 locus. The repair plasmid provides homology regions for double-crossover homologous recombination, introducing the system and providing a new 3'UTR to the gene. **(B)** PCR test confirming integration at the RON11 locus. Amplicons were amplified from genomic DNA isolated from mutant and the parental line ($NF54^{attB}$) (Nkrumah et al. 2006). Primers were designed to amplify two regions: between the C-terminus and the 3'UTR of RON11, and between the C-terminus of RON11 and the new aptamer tandem. **(C)** Western blot of $RON11^{apt}$ schizont lysates growth in the presence and absence of 0.5 µM aTc. Lysates were probed with antibodies against HA

(RON11) and EF1α (loading control). The protein marker sizes are shown on the left. (n = 4 biological replicates). **(D)** Growth of RON11^{apt} parasites over 3 life cycles in the presence and absence of 0.5 μM aTc. Synchronous parasites were collected every 48 hours, stained with the DNA dye Hoechst 33342, and measured via flow cytometry. One representative data set of three biological replicates shown. (n = 3 technical replicates; error bars = SD; *p < 0.05; ****p < 0.0001 by 2-way ANOVA). **(E)** IFAs showing the localization of RON11 in RON11^{apt} schizont with respect to two rhoptry markers: RON4 (neck) and RAP1 (bulb). Synchronous parasites were fixed with acetone and stained with specific antibodies. Images from left to right are phase-contrast, DAPI (nucleus, blue), anti-HA (green), anti-RON4 or RAP1 (red), and fluorescence merge. Z stack images were deconvolved and projected as a combined single image. Representative images of 3 biological replicates. **(F)** Quantification of colocalization of RON11^{apt} with RON4 and RAP1 as determined by the Pearson's correlation coefficient (PCC). (n = 3 biological replicates, 4 schizonts per replicate. Error bars = SD; ****p < 0.0001 by unpaired two-tailed t-test.

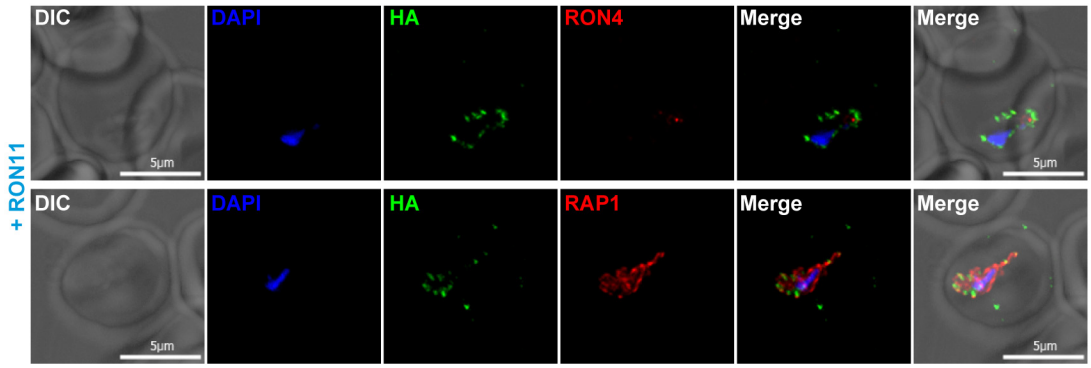

Figure 3.2. RON11 localizes to the parasite periphery during early-ring stages. IFAs showing the localization of RON11 in RON11^{apt} rings with respect to the rhoptry markers RON4 and RAP1. Synchronous parasites were fixed with PFA and stained with specific antibodies. Images from left to right are phase-contrast, DAPI (nucleus, blue), anti-HA (RON11, green), anti-RON4 or RAP1 (red), and fluorescence merge. Z stack images were deconvolved and projected as a combined single image. Representative images of 2 biological replicates.

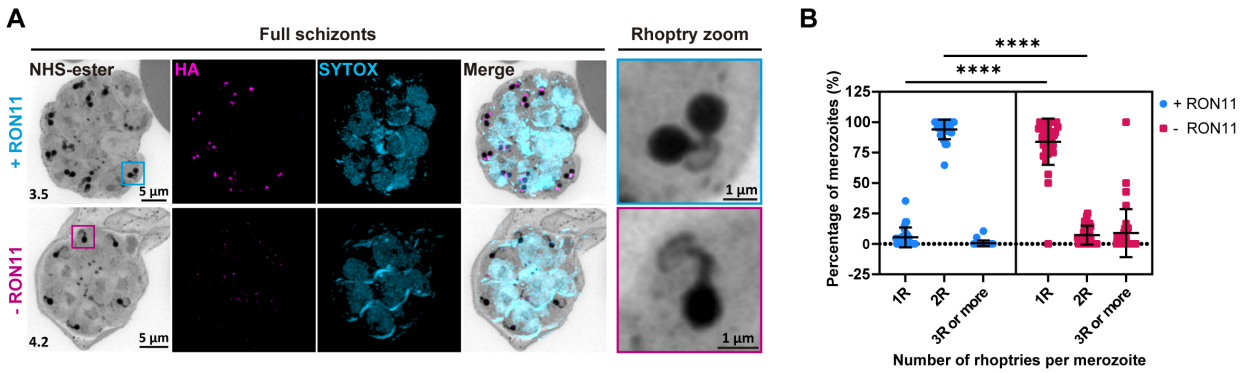

Figure 3.3. RON11 knockdown generates merozoites with single rhoptries. (A) Representative images of RON11^{apt} parasite showing the structure of rhoptries within fully developed merozoites in the presence and absence of 0.5 µM aTc. ML10-arrested parasites were expanded by U-ExM, fixed with PFA, and stained with NHS-Ester (greyscale), anti-HA (magenta), and the DNA dye SYTOX (cyan). Selected Z stack images were projected as a combined single image. Number on image = Z-axis thickness of projection in µm. **(B)** Quantification of the percentage of merozoites with single, dual or multiple rhoptries in the presence and absence of 0.5 µM aTc. (n = 4 biological replicates, 9 schizonts per replicate; error bars = SD; ****p < 0.0001 by unpaired two-tailed *t*-test)

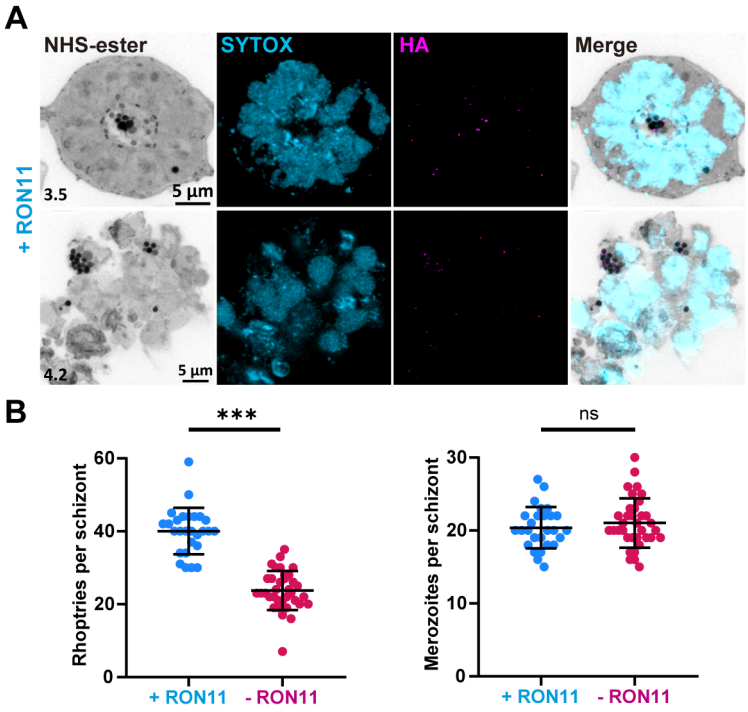

Figure 3.4. RON11 knockdown can generate multiple rhoptries but does not affect the number of merozoites. (A) Representative images of RON11^{apt} parasite showing multiple rhoptries accumulating within fully developed schizonts in the absence of aTc. ML10-arrested parasites were expanded by U-ExM, fixed with PFA, and stained with NHS-Ester (greyscale), anti-HA (magenta), and the DNA dye SYTOX (cyan). Selected Z stack images were projected as a combined single image. Number on image = Z-axis thickness of projection in µm. **(B)** Quantification of the percentage of rhoptries per merozoites and merozoites per schizont in the presence and absence of aTc. (n = 4 biological replicates, 9 schizonts per replicate; error bars = SD; ns = non-significant; ***$p < 0.001$ by unpaired two-tailed *t*-test)

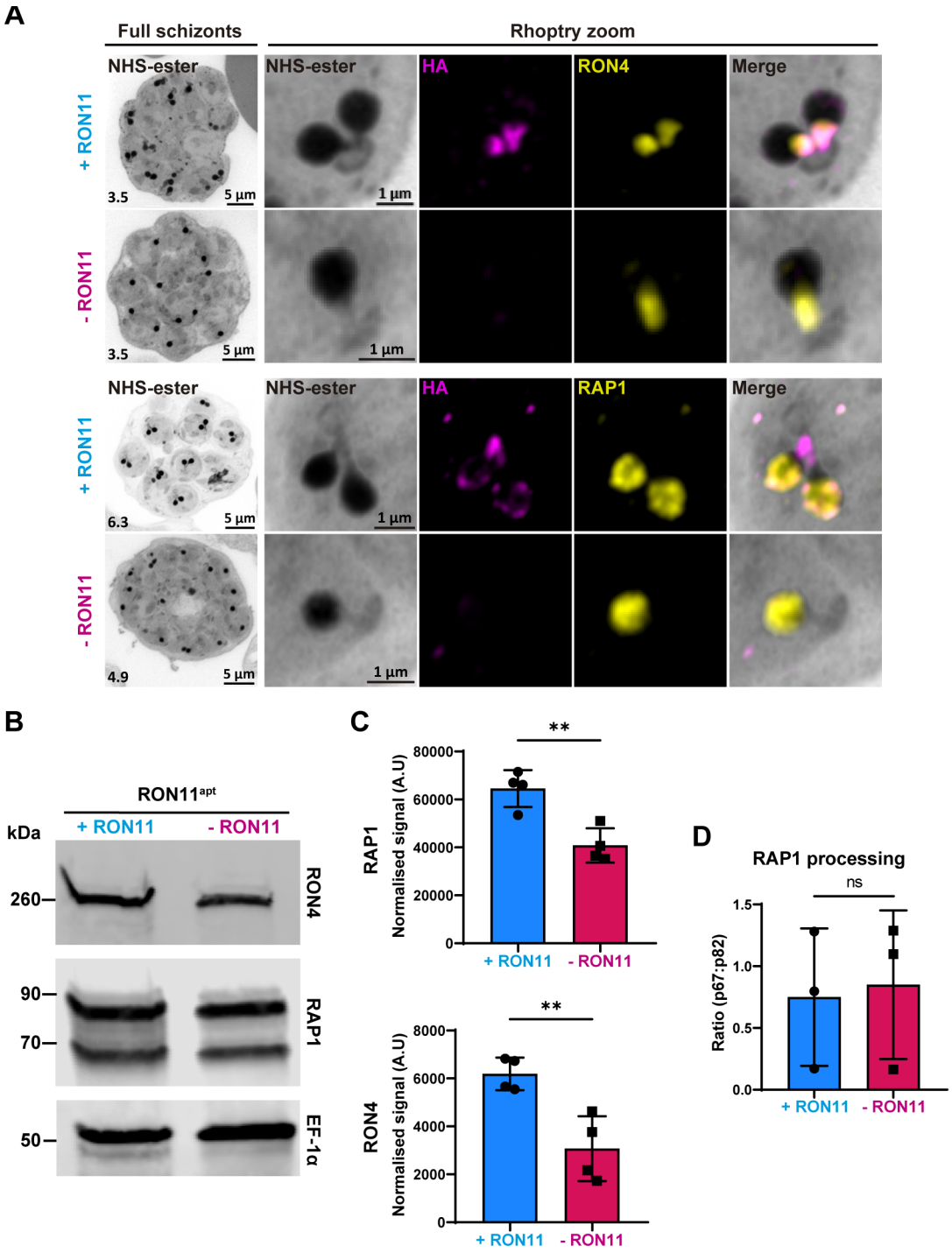

Figure 3.5. RON11 knockdown does not affect the localization and processing of other rhoptry proteins. (A) Representative images of RON11^{apt} parasite showing the localization of RON11 with respect to RON4 and RAP1 in the presence and absence of aTc. E64-arrested

parasites were expanded by U-ExM, fixed with PFA, and stained with NHS-Ester (greyscale), anti-HA (magenta), and RON4 or RAP1 (yellow). Selected Z stack images were projected as a combined single image. Number on image = Z-axis thickness of projection in μm. **(B)** Western blot of parasite lysates isolated from E64-arrested RON11^{apt} parasites in the presence and absence of aTc. Samples were probed with antibodies against RON4, RAP1 and EF1α (loading control). The protein marker sizes are shown on the left. Representative blot of 4 biological replicates shown. **(C)** Quantification of the relative level of RON4 and RAP1 total protein content in E64-arrested RON11^{apt} parasites in the presence and absence of aTc. Band intensities were normalized to the loading control, EF1α, and are presented as normalized arbitrary units (A.U.) (n = 4 biological replicates; error bars = SD; **p < 0.01 by unpaired two-tailed *t*-test). **(D)** Quantification of RAP1 processing in E64-arrested RON11^{apt} parasites in the presence and absence of aTc. Band intensities were normalized to the ratio of processed RAP1 (p67/p82) (n = 3 biological replicates; error bars = SD; ns = non-significant by unpaired two-tailed *t*-test).

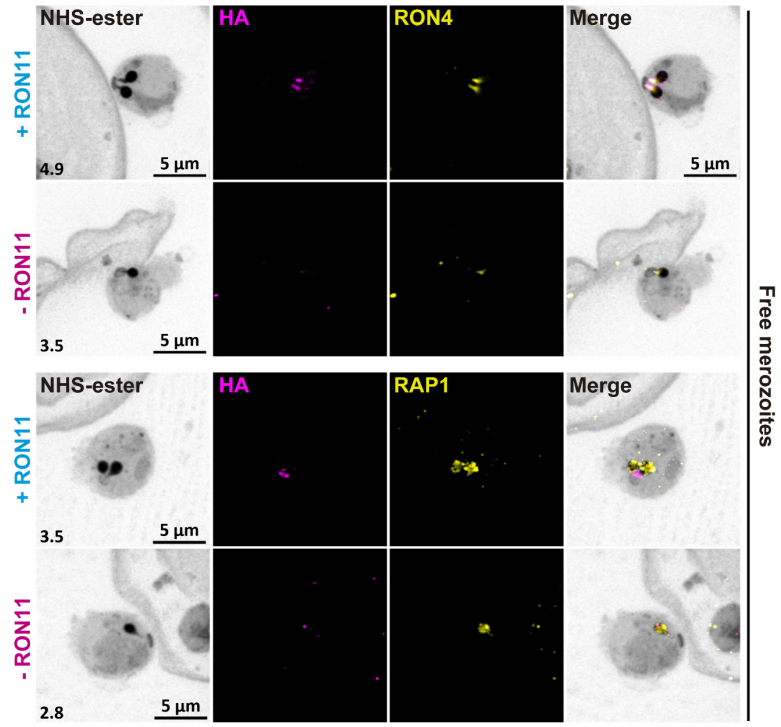

Figure 3.6. RON11 knockdown does not affect the localization of other rhoptry proteins. Representative images of RON11^{apt} free merozoites showing the localization of RON11 with respect to RON4 and RAP1 in the presence and absence of aTc. Late-schizonts were expanded by U-ExM, fixed with PFA, and stained with NHS-Ester (greyscale), anti-HA (magenta), and anti-RON4 or RAP1 (yellow). Selected Z stack images were projected as a combined single image. Number on image = Z-axis thickness of projection in µm.

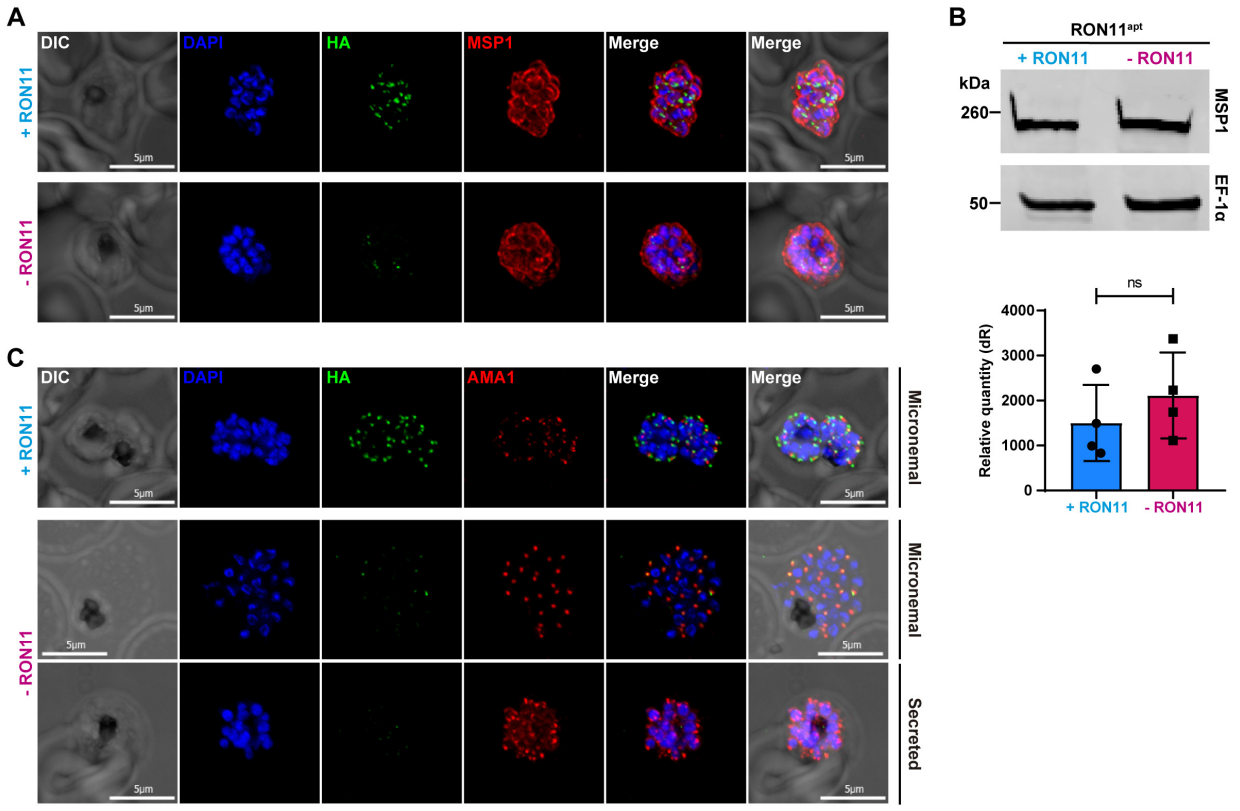

Figure 3.7. RON11 knockdown does not impact the expression and secretion of MSP1 and AMA1. (A) Representative IFAs of RON11^{apt} schizonts showing secretion of MSP1 proteins in the presence or absence of aTc. E64-arrested schizonts were fixed with PFA and stained with specific antibodies. Images from left to right are phase-contrast, DAPI (nucleus, blue), anti-HA (RON11, green), anti-MSP1 (red), and fluorescence merges. Z stack images were deconvolved and projected as a combined single image. Representative images of 3 biological replicates. **(B)** (Top) Western blot of parasite lysates isolated from E64-arrested RON11^{apt} parasites in the presence and absence of aTc. Samples were probed with antibodies against MSP1 and EF1α (loading control). The protein marker sizes are shown on the left. Representative blot of 4 biological replicates shown. (Bottom) Quantification of the relative level of MSP1 total protein content in E64-arrested RON11^{apt} parasites in the presence and absence of aTc. Band intensities

were normalized to the loading control, EF1α, and are presented as normalized arbitrary units (A.U.) (n = 4 biological replicates; error bars = SD; ns = non-significant by unpaired two-tailed t-test). **(C)** Representative IFAs of RON11^{apt} schizonts showing AMA1 localization in the presence or absence of aTc. E64-arrested schizonts were fixed with PFA and stained with specific antibodies. Images from left to right are phase-contrast, DAPI (nucleus, blue), anti-HA (RON11, green), anti-AMA1 (red), and fluorescence merges. Z stack images were deconvolved and projected as a combined single image. Representative images of 3 biological replicates.

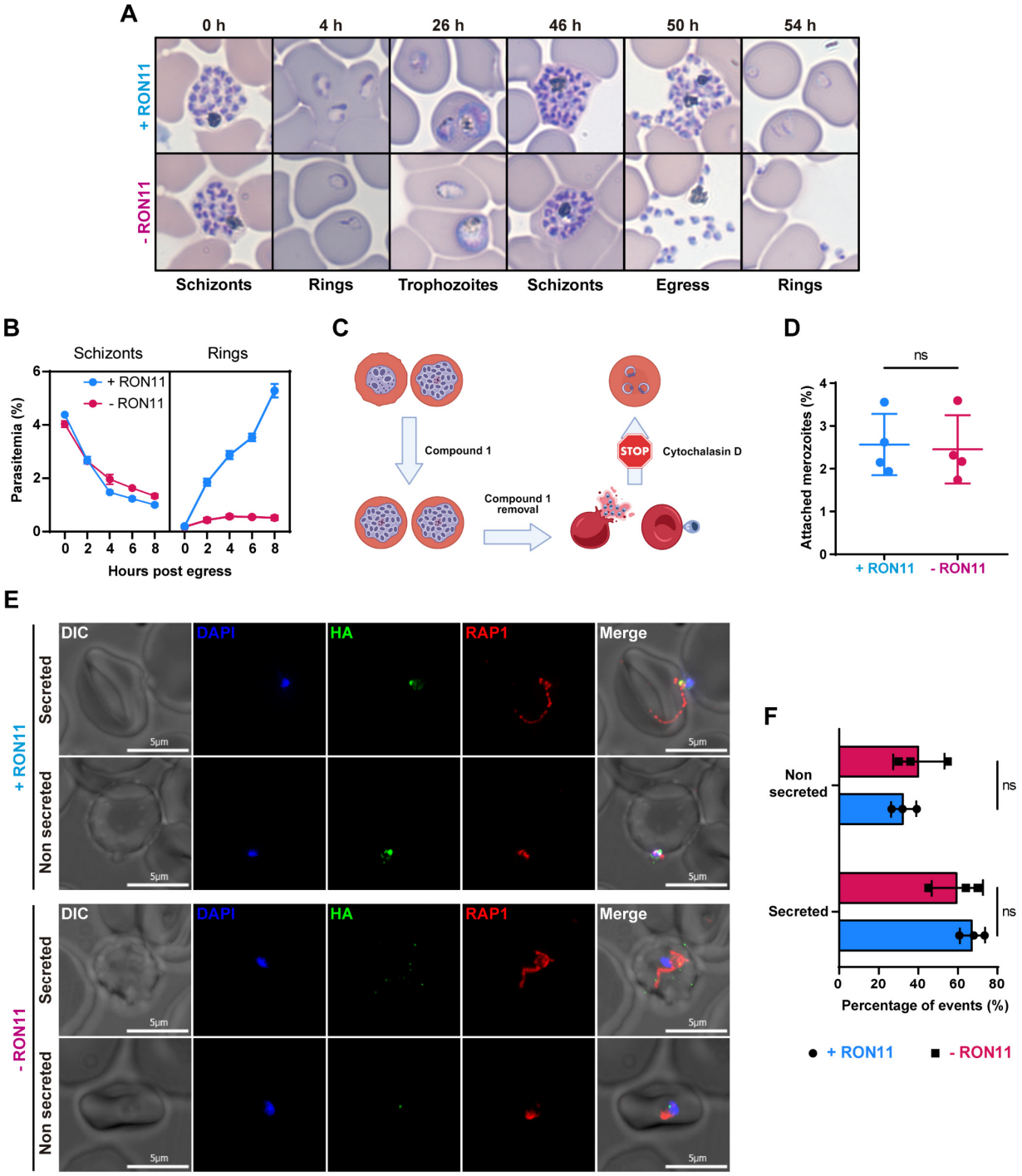

Figure 3.8. RON11 is required for merozoite invasion but not for merozoite attachment nor rhoptry secretion. (A) Representative Hema-3-stained blood-smears showing the development of RON11^{apt} parasites over a life cycle in the presence and absence of 0.5 µM aTc. Synchronous parasites were smeared, stained, and imaged at different time points by lightf microscopy. **(B)**

Tracking of the development of synchronous RON11^{apt} parasites over 8 hours post-egress in the presence and absence of 0.5 μM aTc. Tightly synchronized parasites were collected every 2 hours, stained with Hoechst 33342, and measured via flow cytometry to distinguish between rings and schizonts. One representative data set of three biological replicates shown. (n = 3 technical replicates; error bars = SD; ****p < 0.0001 by 2-way ANOVA). **(C)** Schematic of the actin-polymerization inhibitor assay. Schizonts were tightly synchronized incubating for 4 hours with the PKG inhibitor, Compound 1. After incubation, schizonts were washed twice and then transferred to fresh red blood cells in the presence of the actin inhibitor, cytochalasin D, for 30 minutes. Created with BioRender.com. **(D)** Quantification of the number of RON11^{apt} merozoites attached to RBCs in the presence or absence of aTc, after incubation with cytochalasin D. Parasites were smeared, stained with Hema 3, and observed by light microscopy. Attached-merozoites were blindly scored and represented as the percentage of events per 100 RBCs (n = 4 biological replicates; error bars = SD; ns = non-significant by unpaired two-tailed t-test). **(C)** IFAs showing RON11^{apt} attached-merozoites secreting RAP1 into RBCs in the presence or absence of aTc, after incubation with cytochalasin D. Parasites were fixed with PFA and stained with specific antibodies. Images from left to right are phase-contrast, DAPI (nucleus, blue), anti-HA (green), anti-RAP1 (red), and fluorescence merge. Z stack images were deconvolved and projected as a combined single image. Representative images of 3 biological replicates. **(E)** Quantification of the number of RON11^{apt} attached-merozoites secreting or not RAP1 into RBCs. Secreting events were blindly scored and represented as the percentage of events per 50 attached merozoites (n = 3 biological replicates, 50 events per replicate. Error bars = SD; ns = non-significant by unpaired two-tailed t-test).

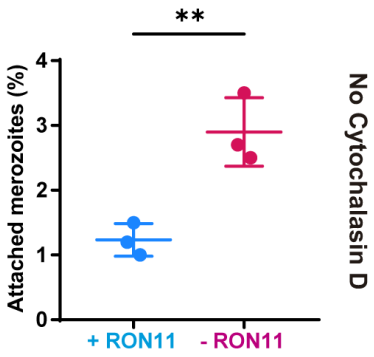

Figure 3.9. RON11^{apt} merozoites attached to RBCs in the presence or absence of aTc. Parasites were smeared 2 hours after ML10 removal, stained with Hema 3, and observed by light microscopy. Attached-merozoites were blindly scored and represented as the percentage of events per 100 RBCs (n = 3 biological replicates; error bars = SD; **p < 0.01 by unpaired two-tailed t-test).

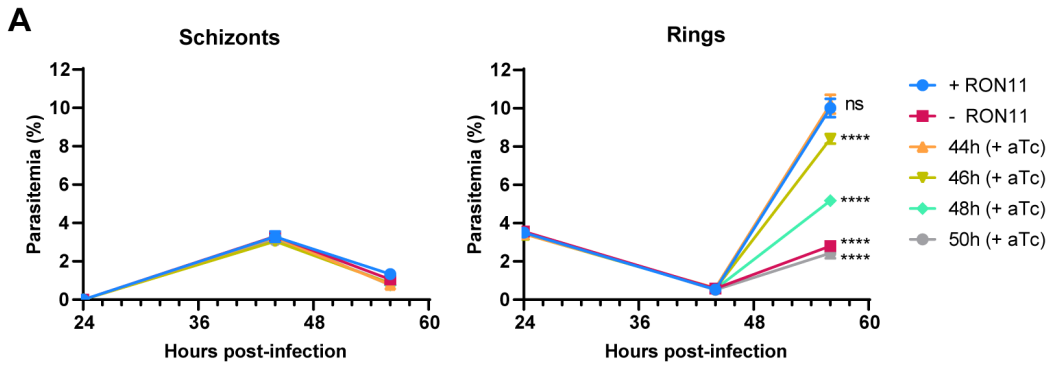

Figure 3.10. RON11 knockdown phenotype is rescued by addition of aTc during the last 2 hours of the asexual life cycle. Growth of RON11^{apt} parasites over a life cycle in the presence and absence of aTc. Tightly synchronous parasites were grown for 44 hpi and aTc was added back every two hours. Samples were collected at 24, 44 and 56 hpi, fixed in PFA, stained with the DNA dye Hoechst 33342, and measured via flow cytometry to differentiate between rings and schizonts. One representative data set of three biological replicates shown. (n = 3 technical replicates; error bars = SD; *ns = non-significant; ****$p < 0.0001$ by 2-way ANOVA compared to + RON11).

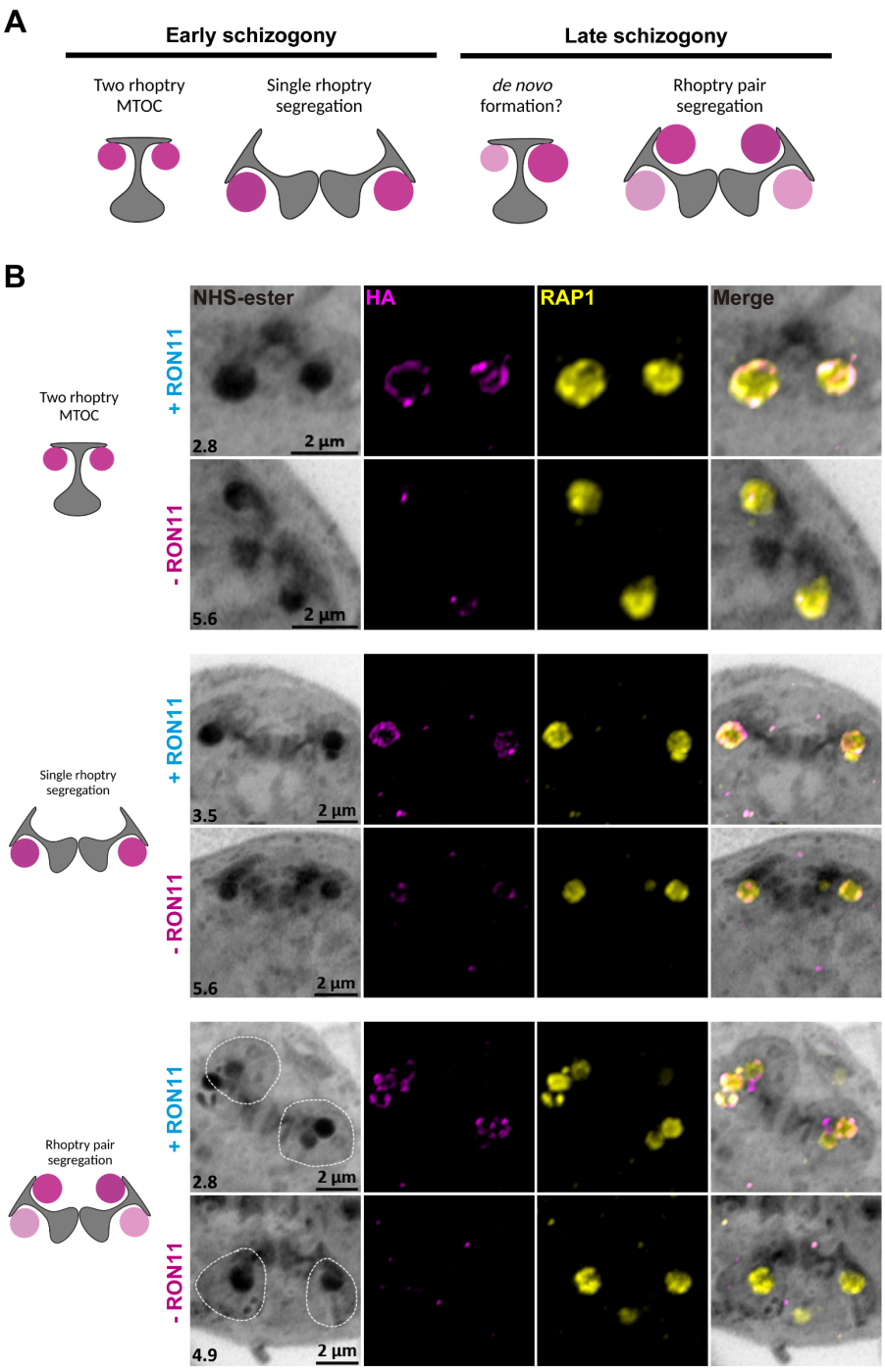

Figure 3.11. RON11 is required for the *de novo* formation of the last rhoptry pair during merozoite segmentation. (A) Schematic of the current model for *de novo* formation of rhoptries during schizogony. **(B)** Representative images of RON11^{apt} late schizonts during the different steps of rhoptry biogenesis in the presence and absence of aTc. Late-schizont parasites were expanded

by U-ExM, fixed with PFA, and stained with NHS-Ester (greyscale), anti-HA (magenta), and anti-RAP1 (yellow). Selected Z stack images were projected as a combined single image. Number on image = Z-axis thickness of projection in μm.

CHAPTER 4

4. CONCLUSIONS AND DISCUSSION

In this dissertation, I introduce a manuscript and preliminary data in which I applied molecular and cellular biological approaches to study specific regulatory factors in two secretory pathways essential for intraerythrocytic development of *P. falciparum* parasites. The first manuscript unveils the utilization of proximity-labeling-based proteomics to identify two proteins, VAC and GAPM1, which may play a role in the export of transmembrane proteins during intracellular growth. Meanwhile, the other chapter provides new insights into the crucial role that the rhoptry protein, RON11, might have during the biogenesis of rhoptries and its importance for merozoite invasion.

In Chapter 2, I describe the application of an improved version of the biotin ligase BirA, TurboID, to identify protein interactors of the membrane-associated protein SBP1 during its transport through the PV. Using CRISPR-Cas9, we tagged SBP1 at its C-terminus end with TurboID, demonstrating that its integration did not influence SBP1's trafficking or its final localization to the MCs. Then, capitalizing on TurboID's efficient labeling radius and time of action (Branon et al. 2018; May et al. 2020), we successfully labeled protein partners of SBP1 during its traffic at the PV-PPM interphase, to be subsequently analyzed by label-free proteomics in comparison with labeled interactors of SBP1 at the MCs. Through this analysis, we identified a group of putative interactors, and we focused on two specific proteins for further study. The first one, VAC, a soluble protein containing a TOM40 domain, which has not been characterized in *P. falciparum*. The second one, GAPM1, is an IMC protein shown to be essential for merozoite invasion (Bullen et al. 2009; Kono et al. 2012, 2013). We confirmed the localization of both proteins to the parasite periphery during early rings, as well as their colocalization with EXP2

(PVM) and MAHRP1 (exported membrane protein). However, despite the use of UExM we were unsuccessful in delimiting their specific localization to the PPM or PV, which might be related to the constricted space of the PV at such an early time during ring-stage development. Discerning their specific localization might require the application of recently develop expansion microscopy approaches that allow the observation of structures at a higher resolution (Louvel et al. 2022) or that better preserve membranous structures (Klimas et al. 2023).

Despite our efforts to establish a presumptive role in protein export using the tetR-DOZI conditional knockdown system, we could not definitely prove such a role due to the dynamics and essential nature of both proteins. Designing an alternative knockdown system with faster kinetics could help to obtain a definitive answer regarding the role of both proteins in protein export.

Even though our approach to identify interactors at the PPM-PV interface proved to be successful, one of the disadvantages of the system to identify protein export participants was the high number of proteins identified. Most TurboID-based approaches in *Plasmodium spp*. had the goal of identifying proteomes of different organelles or structures (Ambekar Sushma V., Beck Josh R., and Mair Gunnar R. 2022; Clements et al. 2022; Davies et al. 2023; Lamb et al. 2022), but no study has focused on identifying specific interactors in time and space-dependent scenarios. An alternative to improving our model could be the application of quantitative proteomics analysis using isotopically labeled biotin (Kim et al. 2018), to reduce the number of candidates by contrasting the interactors of SBP1, with those from other soluble proteins, or proteins that are exported through uncharacterized pathways, such as EMP1.

Our work also highlights the successful application of protein labeling for the study of biological events that occur within short windows of time, a novel approach in our field. Additionally, our results introduce two proteins with potential multiple, albeit unrelated, roles and

localizations. While proteins with two unrelated roles during protein export have been previously reported (Charnaud et al. 2018; Elsworth et al. 2016; Gabriela et al. 2022; Garten et al. 2018; Sherling et al. 2017), we could not definitely classify GAPM1 and VAC in the same category due to our inability to study their role in protein export using our knockdown approach. Regarding our hypothesis and not directly aligned with the objective of our study, our results raise an intriguing question regarding the fate of the IMC after merozoite invasion. Earlier studies indicated that IMC proteins are not visible around 15 minutes post-invasion (Riglar et al. 2013), yet our data strongly suggests that the IMC protein GAPM1 remains detectable at least until 4 hours post-invasion.

In Chapter 3, I present the characterization of the essential role of RON11 in merozoite invasion and propose a role of RON11 during rhoptry biogenesis. Similar to most rhoptry proteins studied to date in RBC stages (Liffner et al. 2021), we have demonstrated that RON11 is indispensable for parasite development, particularly merozoite invasion of RBCs. This aligns with previous failed attempts to disrupt RON11 in *P. berghei* which suggested essentiality of RON11 in blood stages (Llinás et al. 2006; Bozdech et al. 2003). A more recent study successfully generated a RON11 knockdown in *P. berghei* and demonstrated RON11's requirement for sporozoite invasion, although it did not investigate its role during intraerythrocytic life stages (Bantuchai et al. 2019), making our study the first to describe RON11's essential role during blood stages.

Rhoptry biogenesis remains a poorly understood process, primarily due to the small size of *P. falciparum*'s rhoptries, which, coupled with the limited resolution offered by conventional microscopy, has made their study challenging. Recent advances in microscopy techniques, such as UExM, have opened new possibilities for exploring these micron-sized secretory organelles (Liffner and Absalon 2023). Through the application of this tool, we found RON11 is required for

the proper biogenesis of rhoptry pairs, as its absence led to merozoites with single rhoptries, an unprecedented phenotype not associated with any other apicomplexan protein studied to date. Only three parasite proteins, Sortilin, RAMA and CERLI2, have been shown to have a role in the biogenesis of rhoptries in *P. falciparum* (Hallée et al. 2018; Liffner et al. 2022; Sherling et al. 2019). None of them share any structural similarities, localize to the same region within rhoptries, or generate a knockdown phenotype analogous to RON11. For instance, RAMA and CERLI2 loss causes morphological alterations in the rhoptry necks (Liffner et al. 2022; Sherling et al. 2019), while RON11's single rhoptries did not display any apparent structural change. However, only carrying out volumetric measures of the rhoptries observed by UExM would discard that assumption.

Our data strongly suggests that RON11 performs its role during rhoptry biogenesis only by the end of schizogony. This thesis is supported by our initial observations by UExM that rhoptries are formed and segregated with the MTOCs without issues in the absence of RON11 during the asynchronous mitotic events of schizogony. These observations align with our findings that RON11 knockdown phenotype cannot be rescued by the addition of aTc after 46 hours post invasion.

In contrast, we observed that the *de novo* formation of the last rhoptry pairs was disrupted by the knockdown of RON11 during merozoite segmentation. Specifically, we noticed that one rhoptry was being distributed along with the dividing MTOC into a nascent merozoite, instead of two rhoptries as observed in the presence of RON11. These observations are in agreement with our findings of a roughly 50% reduction in the number of rhoptries per schizont. In conclusion, even though quantification of these observations needs to be carried out, our preliminary data enabled us to outline a timeline of action of RON11, which we hypothesize begins at the initiation

of merozoite segmentation, where RON11 might respond to unidentified factors triggering the formation of merozoites.

Also, as part of our work, we have shown that merozoite invasion initiates normally in absence of RON11 but appears to be required for the completion of merozoite internalization into RBCs. While the actinomyosin motor and its components are well-established as being involved in merozoite internalization (Blake, Haase, and Baum 2020; Perrin et al. 2018), no rhoptry protein has been associated with a role in this final stage of invasion. Although our current data strongly suggests a role in internalization, we cannot rule out the possibility that the invasion phenotype might be a consequence of the defect in rhoptry formation. The second possibility could be explained by the reduction in the amount of rhoptry proteins within each merozoite upon deletion of RON11. Characterizing proteins with roles in invasion are based on efficient knockdowns or knockouts, so no information regarding protein titration is available to understand the amount of protein necessary to complete invasion. For instance, measuring amounts of proteins secreted into RBCs could help us to initially test our hypothesis. So, further research is needed to elucidate the precise contribution of RON11 to internalization.

In the near future, we aspire to investigate further the role of RON11 in rhoptry biogenesis. At first, we aim to understand whether RON11 binds to calcium through its EF-hand domain as part of its role in rhoptry formation. To dissect the role of the highly conserved EF-hand domain in RON11, we will generate a cell line to specifically knockout the domain, maintaining the rest of the protein. The characterization of this cell line, under the presence or absence of the EF-hand domain would help us understand better the role of RON11 and calcium in rhoptry biogenesis. Also, we aim to identify the unknown signals that putatively activate the segmentation of merozoites. To do this, we will use immunoprecipitation assays to pull-down protein interactors

of RON11 during the last hours of schizogony and rhoptry formation. Finding these interactors could give us a better idea of the cascade of events that lead to the start of merozoite segmentation, which are currently unexplored.

In summary, this dissertation represents the application of state-of-the-art tools in the field of malaria research to investigate two fundamental aspects of parasite intraerythrocytic development, protein export and merozoite invasion. In the first body of work, I demonstrate the applicability of proximity labelling to study biological events with narrow timeframes, a novel approach in this field. In the second body of work, I employ various microscopy techniques to characterize a protein with a novel role in rhoptry biogenesis, an area of that remains largely unexplored.

4.1. References

Ambekar Sushma V., Beck Josh R., and Mair Gunnar R. 2022. "TurboID Identification of Evolutionarily Divergent Components of the Nuclear Pore Complex in the Malaria Model Plasmodium Berghei." *MBio* 13 (5): e01815-22.

Bantuchai, Sirasate, Mamoru Nozaki, Amporn Thongkukiatkul, Natcha Lorsuwannarat, Mayumi Tachibana, Minami Baba, Kazuhiro Matsuoka, Takafumi Tsuboi, Motomi Torii, and Tomoko Ishino. 2019. "Rhoptry Neck Protein 11 Has Crucial Roles during Malaria Parasite Sporozoite Invasion of Salivary Glands and Hepatocytes." *International Journal for Parasitology* 49 (9): 725–35.

Blake, Thomas C. A., Silvia Haase, and Jake Baum. 2020. "Actomyosin Forces and the Energetics of Red Blood Cell Invasion by the Malaria Parasite Plasmodium Falciparum." *PLoS Pathogens* 16 (10): e1009007.

Bozdech, Zbynek, Manuel Llinás, Brian Lee Pulliam, Edith D. Wong, Jingchun Zhu, and Joseph L. DeRisi. 2003. "The Transcriptome of the Intraerythrocytic Developmental Cycle of Plasmodium Falciparum." *PLoS Biology* 1 (1): E5.

Branon, Tess C., Justin A. Bosch, Ariana D. Sanchez, Namrata D. Udeshi, Tanya Svinkina, Steven A. Carr, Jessica L. Feldman, Norbert Perrimon, and Alice Y. Ting. 2018. "Efficient Proximity Labeling in Living Cells and Organisms with TurboID." *Nature Biotechnology* 36 (9): 880–87.

Bullen, Hayley E., Christopher J. Tonkin, Rebecca A. O'Donnell, Wai-Hong Tham, Anthony T. Papenfuss, Sven Gould, Alan F. Cowman, Brendan S. Crabb, and Paul R. Gilson. 2009. "A Novel Family of Apicomplexan Glideosome-Associated Proteins with an Inner Membrane-Anchoring Role." *Journal of Biological Chemistry*. https://doi.org/10.1074/jbc.m109.036772.

Charnaud, Sarah C., Rasika Kumarasingha, Hayley E. Bullen, Brendan S. Crabb, and Paul R. Gilson. 2018. “Knockdown of the Translocon Protein EXP2 in Plasmodium Falciparum Reduces Growth and Protein Export.” *PloS One* 13 (11): e0204785.

Clements, Rebecca L., Alexander A. Morano, Francesca M. Navarro, James P. McGee, Esrah W. Du, Vincent A. Streva, Scott E. Lindner, and Jeffrey D. Dvorin. 2022. “Identification of Basal Complex Protein That Is Essential for Maturation of Transmission-Stage Malaria Parasites.” *Proceedings of the National Academy of Sciences* 119 (34): e2204167119.

Davies, Heledd, Hugo Belda, Malgorzata Broncel, Jill Dalimot, and Moritz Treeck. 2023. “PerTurboID, a Targeted in Situ Method Reveals the Impact of Kinase Deletion on Its Local Protein Environment in the Cytoadhesion Complex of Malaria-Causing Parasites.” *ELife* 12 (September): e86367.

Elsworth, Brendan, Paul R. Sanders, Thomas Nebl, Steven Batinovic, Ming Kalanon, Catherine Q. Nie, Sarah C. Charnaud, et al. 2016. “Proteomic Analysis Reveals Novel Proteins Associated with the Plasmodium Protein Exporter PTEX and a Loss of Complex Stability upon Truncation of the Core PTEX Component, PTEX150.” *Cellular Microbiology* 18 (11): 1551–69.

Gabriela, Mikha, Kathryn M. Matthews, Cas Boshoven, Betty Kouskousis, Thorey K. Jonsdottir, Hayley E. Bullen, Joyanta Modak, et al. 2022. “A Revised Mechanism for How Plasmodium Falciparum Recruits and Exports Proteins into Its Erythrocytic Host Cell.” *PLoS Pathogens* 18 (2): e1009977.

Garten, Matthias, Armiyaw S. Nasamu, Jacquin C. Niles, Joshua Zimmerberg, Daniel E. Goldberg, and Josh R. Beck. 2018. “EXP2 Is a Nutrient-Permeable Channel in the

Vacuolar Membrane of Plasmodium and Is Essential for Protein Export via PTEX." *Nature Microbiology* 3 (10): 1090–98.

Hallée, Stéphanie, Natalie A. Counihan, Kathryn Matthews, Tania F. de Koning-Ward, and Dave Richard. 2018. "The Malaria Parasite Plasmodium Falciparum Sortilin Is Essential for Merozoite Formation and Apical Complex Biogenesis." *Cellular Microbiology* 20 (8): e12844.

Kim, Dae In, Jevon A. Cutler, Chan Hyun Na, Sina Reckel, Santosh Renuse, Anil K. Madugundu, Raiha Tahir, et al. 2018. "BioSITe: A Method for Direct Detection and Quantitation of Site-Specific Biotinylation." *Journal of Proteome Research* 17 (2): 759–69.

Klimas, Aleksandra, Brendan R. Gallagher, Piyumi Wijesekara, Sinda Fekir, Emma F. DiBernardo, Zhangyu Cheng, Donna B. Stolz, et al. 2023. "Magnify Is a Universal Molecular Anchoring Strategy for Expansion Microscopy." *Nature Biotechnology*, January, 1–12.

Kono, Maya, Susann Herrmann, Noeleen B. Loughran, Ana Cabrera, Klemens Engelberg, Christine Lehmann, Dipto Sinha, et al. 2012. "Evolution and Architecture of the Inner Membrane Complex in Asexual and Sexual Stages of the Malaria Parasite." *Molecular Biology and Evolution* 29 (9): 2113–32.

Kono, Maya, Dhaneswar Prusty, John Parkinson, and Tim W. Gilberger. 2013. "The Apicomplexan Inner Membrane Complex." *Frontiers in Bioscience* 18 (3): 982–92.

Lamb, Ian M., Kelly T. Rios, Anurag Shukla, Avantika I. Ahiya, Joanne M. Morrisey, Joshua C. Mell, Scott E. Lindner, Michael W. Mather, and Akhil B. Vaidya. 2022.

"Mitochondrially Targeted Proximity Biotinylation and Proteomic Analysis in Plasmodium Falciparum." *BioRxiv*. https://doi.org/10.1101/2022.05.30.494025.

Liffner, Benjamin, and Sabrina Absalon. 2023. "Expansion Microscopy of Apicomplexan Parasites." *Molecular Microbiology*, August. https://doi.org/10.1111/mmi.15135.

Liffner, Benjamin, Juan Miguel Balbin, Gerald J. Shami, Ghizal Siddiqui, Jan Strauss, Sonja Frölich, Gary K. Heinemann, et al. 2022. "Cell Biological Analysis Reveals an Essential Role for Pfcerli2 in Erythrocyte Invasion by Malaria Parasites." *Communications Biology* 5 (1): 1–17.

Liffner, Benjamin, Juan Miguel Balbin, Jan Stephan Wichers, Tim-Wolf Gilberger, and Danny W. Wilson. 2021. "The Ins and Outs of Plasmodium Rhoptries, Focusing on the Cytosolic Side." *Trends in Parasitology* 37 (7): 638–50.

Llinás, Manuel, Zbynek Bozdech, Edith D. Wong, Alex T. Adai, and Joseph L. DeRisi. 2006. "Comparative Whole Genome Transcriptome Analysis of Three Plasmodium Falciparum Strains." *Nucleic Acids Research* 34 (4): 1166–73.

Louvel, Vincent, Romuald Haase, Olivier Mercey, Marine H. Laporte, Dominique Soldati-Favre, Virginie Hamel, and Paul Guichard. 2022. "Nanoscopy of Organelles and Tissues with Iterative Ultrastructure Expansion Microscopy (IU-ExM)." *BioRxiv*. https://doi.org/10.1101/2022.11.14.516383.

May, Danielle G., Kelsey L. Scott, Alexandre R. Campos, and Kyle J. Roux. 2020. "Comparative Application of BioID and TurboID for Protein-Proximity Biotinylation." *Cells* 9 (5). https://doi.org/10.3390/cells9051070.

Perrin, Abigail J., Christine R. Collins, Matthew R. G. Russell, Lucy M. Collinson, David A. Baker, and Michael J. Blackman. 2018. "The Actinomyosin Motor Drives Malaria

Parasite Red Blood Cell Invasion but Not Egress." *MBio* 9 (4). https://doi.org/10.1128/mBio.00905-18.

Riglar, David T., Kelly L. Rogers, Eric Hanssen, Lynne Turnbull, Hayley E. Bullen, Sarah C. Charnaud, Jude Przyborski, et al. 2013. "Spatial Association with PTEX Complexes Defines Regions for Effector Export into Plasmodium Falciparum-Infected Erythrocytes." *Nature Communications* 4: 1415.

Sherling, Emma S., Ellen Knuepfer, Joseph A. Brzostowski, Louis H. Miller, Michael J. Blackman, and Christiaan van Ooij. 2017. "The Plasmodium Falciparum Rhoptry Protein RhopH3 Plays Essential Roles in Host Cell Invasion and Nutrient Uptake." *ELife* 6 (March). https://doi.org/10.7554/eLife.23239.

Sherling, Emma S., Abigail J. Perrin, Ellen Knuepfer, Matthew R. G. Russell, Lucy M. Collinson, Louis H. Miller, and Michael J. Blackman. 2019. "The Plasmodium Falciparum Rhoptry Bulb Protein RAMA Plays an Essential Role in Rhoptry Neck Morphogenesis and Host Red Blood Cell Invasion." *PLoS Pathogens* 15 (9): e1008049.

APPENDIX A

MASS SPECTROMETRY DATA OF SBP1^{TbID}

Data from mass spectrometry analysis of SBP1^{TbID} biotinylation assays. Results were ranked by the fold change ratio of 4hpi:20hpi. Those that were >10-fold enriched above 20hpi and with a p-value <0.05 are marked by bold face and asterisks. Those that were >10-fold enriched above 4hpi and with a p-value <0.05 are marked by bold italics and asterisks.

PlasmoDB ID	p-value	Fold change (4hpi vs 20hpi)
PF3D7_0215700*	0.003415	904196.4
PF3D7_0321100*	0.000335	328124.1
PF3D7_0308700*	0.002502	274388.3
PF3D7_0208100*	0.000505	257115.3
PF3D7_1026600*	7.73E-05	239351.6
PF3D7_1227600*	0.002318	227704.4
PF3D7_0723800*	0.005325	191237
PF3D7_1323700*	0.004949	186339.9
PF3D7_0308100*	0.005634	184311.7
PF3D7_0704300*	0.003321	175428.8
PF3D7_0612200*	0.005658	122590.1
PF3D7_1138000*	0.004867	108757.5
PF3D7_0815800*	0.005264	81888.85
PF3D7_1324800*	0.003378	78313.69
PF3D7_0705100*	0.005964	72902.32
PF3D7_1239800*	0.008168	67991.43
PF3D7_1432100*	0.002114	60845.32
PF3D7_0803400*	0.00527	48347.02
PF3D7_0919900	0.117329	21394.57
PF3D7_1332200	0.109896	20174.89
PF3D7_1128900	0.102074	19623.29
PF3D7_1312500	0.124742	19219.16
PF3D7_0822600	0.170779	17798.51
PF3D7_1409400	0.170809	16014.59
PF3D7_1228600	0.173089	15858.92
PF3D7_1435600	0.079562	12729.45
PF3D7_1203900	0.186633	12486.8
PF3D7_1401600	0.137472	11616.29
PF3D7_1414500	0.161761	11309.56
PF3D7_1116000	0.120179	9331.756
PF3D7_1340700	0.15414	9155.899
PF3D7_0508900	0.115553	7662.936
PF3D7_1330600	0.182679	6858.166
PF3D7_0303000	0.170958	6564.442
PF3D7_1027700.1	0.172082	6480.986
PF3D7_1031200	0.185182	5729.763

PF3D7_1003800	0.205392	5686.715
PF3D7_1436200	0.116538	5247.45
PF3D7_1126700	0.157585	4761.331
PF3D7_0803700	0.168227	4700.158
PF3D7_0204200	0.187669	4666.99
PF3D7_1467900	0.184858	4636.334
PF3D7_0214100	0.189668	4553.866
PF3D7_1001600	0.148057	4476.707
PF3D7_1427500	0.163645	4260.599
PF3D7_0912900	0.209913	4231.6
PF3D7_1419000	0.183759	4089.454
PF3D7_0217500	0.191131	3991.628
PF3D7_0109000	0.202753	3905.766
PF3D7_0312400	0.19274	3751.097
PF3D7_0709700	0.185504	3731.348
PF3D7_1143400	0.203886	3664.482
PF3D7_0320800	0.191995	3540.042
PF3D7_0420600	0.172238	3494.166
PF3D7_1142300	0.183532	3481.325
PF3D7_1438400	0.146702	3419.766
PF3D7_1227700	0.167674	3393.766
PF3D7_0932100	0.185268	3269.752
PF3D7_0309500	0.209521	3176.822
PF3D7_1450100	0.21082	3170.941
PF3D7_1406700	0.198508	3048.897
PF3D7_1033600	0.191608	3005.251
PF3D7_0419600	0.219883	2979.35
PF3D7_1455400	0.196723	2974.731
PF3D7_0214000	0.228954	2966.62
PF3D7_1225200	0.185543	2917.136
PF3D7_0828900	0.188108	2833.008
PF3D7_0513600	0.211047	2826.057
PF3D7_1213600	0.169007	2714.343
PF3D7_0606900	0.195133	2686.016
PF3D7_0317200	0.184589	2573.194
PF3D7_0935200	0.176847	2568.234
PF3D7_1107400	0.193445	2363.54
PF3D7_1004500	0.175138	2286.998
PF3D7_1458400	0.22276	2213.431
PF3D7_1322200	0.152559	2213.277
PF3D7_1426700	0.207912	2171.855
PF3D7_1350100	0.239322	2129.204
PF3D7_0618700	0.184712	2126.626
PF3D7_0511000	0.233395	2112.59
PF3D7_1124300	0.191843	2109.211
PF3D7_1304900	0.196883	2101.746
PF3D7_1367600	0.202254	2024.193
PF3D7_0308300	0.18644	1883.033
PF3D7_1008500	0.154538	1837.276
PF3D7_0310700	0.197771	1807.074
PfNF54_100026900	0.186044	1795.754
PF3D7_1015200.1	0.218426	1686.298
PF3D7_1212000	0.216275	1561.155
PF3D7_0810000	0.211913	1560.569
PF3D7_0918700	0.18539	1533.829
PF3D7_1211200	0.170803	1499.254
PF3D7_1243000	0.188428	1341.492
PF3D7_0914500	0.170641	1245.44
PF3D7_0111500	0.23871	1171.717

PF3D7_1405800	0.151078	1113.857
PF3D7_0609000	0.21154	957.8436
PF3D7_1308600	0.239234	847.4636
PF3D7_0527100	0.207775	799.4489
PF3D7_1003600	0.3094	659.6165
PF3D7_1351700	0.265848	399.1397
PF3D7_1141300	0.263828	331.5063
PF3D7_0618000	0.304182	298.8956
PF3D7_1317100	0.326009	237.8285
PF3D7_0810800	0.340214	222.9816
PF3D7_1014900	0.317581	218.8666
PF3D7_0722200	0.360803	214.6497
PF3D7_1457300	0.362936	212.6577
PF3D7_0212300	0.361533	189.714
PF3D7_1017900	0.364512	188.2018
PF3D7_1437200	0.311259	187.0775
PF3D7_1419700	0.361679	181.6588
PF3D7_1417800	0.365852	180.3426
PF3D7_1332800	0.342148	177.3669
PF3D7_1220900	0.35873	165.1085
PF3D7_0934500	0.352792	164.6349
PF3D7_1461400	0.307441	163.8455
PF3D7_1352400	0.347568	156.4413
PF3D7_0505500	0.351073	155.8733
PF3D7_1466300	0.364624	153.2615
PF3D7_1246800	0.347564	152.0824
PF3D7_1311900	0.399626	151.7463
PF3D7_1225800	0.352682	151.1774
PF3D7_0620000	0.363701	150.3611
PF3D7_1450000	0.324006	149.965
PF3D7_0803200	0.339503	147.1013
PF3D7_0627800	0.369338	145.6626
PF3D7_0422300	0.469032	140.3954
PF3D7_1123400	0.369377	138.5727
PF3D7_1251200	0.37347	130.5424
PF3D7_1237000	0.347133	129.6325
PF3D7_1329100	0.337945	127.9686
PF3D7_0304100	0.342167	127.5947
PF3D7_1115300	0.375516	126.8914
PF3D7_0206800	0.259134	126.514
PF3D7_1238100	0.38881	125.3125
PF3D7_0318200	0.355002	123.1479
PF3D7_0714500	0.363285	122.0239
PF3D7_0213100	0.397127	119.4001
PF3D7_1318800	0.414005	117.906
PF3D7_1429800	0.35394	116.2936
PF3D7_1015600	0.414273	113.3774
PF3D7_0616200	0.476223	112.5764
PF3D7_1439800	0.407076	111.2706
PF3D7_0932200	0.388134	109.9426
PF3D7_0320100	0.370326	109.6518
PF3D7_1129400	0.42265	106.4166
PF3D7_0529400.2	0.358734	104.5713
PF3D7_0212500	0.42265	104.4768
PF3D7_1362600	0.42265	101.037
PF3D7_0703600	0.474949	99.26866
PF3D7_0807900	0.404519	99.22826
PF3D7_0923000	0.377986	98.48276
PF3D7_1123900	0.431387	96.98113

PF3D7_1447700	0.382681	96.96742
PF3D7_1412300	0.430922	96.71105
PF3D7_1446700	0.42265	96.31519
PF3D7_0316500	0.474228	96.25473
PF3D7_1428300	0.398229	96.25366
PF3D7_1442300	0.420448	95.08005
PF3D7_1459400	0.371032	90.78402
PF3D7_0917600	0.42265	89.59547
PF3D7_1135100	0.346833	89.22105
PF3D7_1136400	0.469983	86.27851
PF3D7_0414900	0.42265	84.34106
PF3D7_0505900	0.42265	84.09653
PF3D7_0413500	0.457197	83.66647
PF3D7_0822800	0.476406	83.42314
PF3D7_1312900	0.410342	82.86752
PF3D7_1105700	0.504285	81.93421
PF3D7_0926700	0.42265	81.74113
PF3D7_0107000.1	0.42265	81.67491
PF3D7_1356900	0.42265	80.15969
PF3D7_1108500	0.42265	79.02769
PF3D7_1129200	0.539695	78.71132
PF3D7_0817600	0.358902	77.35817
PF3D7_1111100	0.42265	76.97174
PF3D7_1247400	0.552433	76.46339
PF3D7_0704800	0.42265	76.25734
PF3D7_0515000	0.42265	74.79387
PF3D7_0816600	0.530834	74.39987
PF3D7_0821000	0.514837	73.88425
PF3D7_0207800	0.42265	73.65558
PF3D7_0304200	0.49856	72.63469
PF3D7_1129000	0.461164	71.7973
PF3D7_0704100	0.42265	71.67446
PF3D7_0617000	0.42265	71.5505
PF3D7_0312300	0.432871	71.19351
PF3D7_1373500	0.420803	70.98877
PF3D7_0528100	0.377657	70.95576
PF3D7_1449500	0.503872	70.65095
PF3D7_0311300	0.355758	70.61345
PF3D7_0918900	0.52381	70.04484
PF3D7_0317800	0.42265	70.02457
PF3D7_1474800	0.410321	69.88016
PF3D7_1457000	0.432941	69.67974
PF3D7_1202600	0.395954	69.60354
PF3D7_0932800	0.394103	69.24509
PF3D7_0933500	0.42265	69.21561
PF3D7_1249100	0.423132	69.0823
PF3D7_0413900	0.42265	68.8235
PF3D7_0527500	0.400441	67.49455
PF3D7_1118300	0.411043	66.63467
PF3D7_1304000	0.42265	66.47196
PF3D7_1143200	0.368979	65.84011
PF3D7_0319100	0.42265	65.59724
PF3D7_1336900	0.42265	63.67565
PF3D7_1211700	0.436326	63.49843
PF3D7_0308000	0.405472	62.66405
PF3D7_0527000	0.538423	62.49448
PF3D7_0509000	0.370644	62.10383
PF3D7_1305300	0.490129	62.09723
PF3D7_1207000	0.42265	62.08854

PF3D7_0905900	0.395576	61.74944
PF3D7_1447800	0.42265	61.69834
PF3D7_1364800	0.421279	61.5443
PF3D7_0422700	0.532808	61.00204
PF3D7_0807800	0.541757	60.97138
PF3D7_1128100	0.538076	60.68746
PF3D7_1401800	0.42265	60.65403
PF3D7_1118100	0.40596	59.74854
PF3D7_1347700	0.43849	59.67153
PF3D7_0316600	0.423113	59.28855
PF3D7_1338100	0.531077	59.25271
PF3D7_0530900	0.479715	58.33706
PF3D7_0613900	0.42265	57.90358
PF3D7_0310400	0.369154	57.73698
PF3D7_0518200	0.3747	57.63091
PF3D7_0109400	0.39989	56.92013
PF3D7_0110900	0.42265	56.79232
PF3D7_1425900	0.42265	56.2291
PF3D7_1211900	0.411332	55.63389
PF3D7_0510100	0.42265	55.39801
PF3D7_1119300	0.544108	55.18238
PF3D7_1363400	0.42265	54.74317
PF3D7_1014600	0.535708	53.58921
PF3D7_1103600	0.42265	53.44167
PF3D7_0415300	0.510223	53.19297
PF3D7_1405600	0.523574	52.7017
PF3D7_1241200	0.499363	52.6938
PF3D7_1358200	0.442258	52.47049
PF3D7_1317000	0.42265	52.17085
PF3D7_1453800	0.547822	51.89549
PF3D7_0422500	0.429546	51.81448
PF3D7_1104000	0.532936	51.76468
PF3D7_0405400	0.543487	51.14983
PF3D7_0907600	0.42265	50.67164
PF3D7_1332900	0.417961	50.38833
PF3D7_1358500	0.515002	50.28241
PF3D7_1009000	0.42265	50.02273
PF3D7_1324700	0.42265	49.94368
PF3D7_0306200	0.524725	49.4345
PF3D7_0413700	0.556827	48.94558
PF3D7_0919100	0.425821	48.42752
PF3D7_1032800	0.506587	47.72386
PF3D7_0721800	0.527085	47.59052
PF3D7_1334200	0.539302	45.5313
PF3D7_0716300	0.543933	44.25318
PF3D7_0807500	0.532148	44.11696
PF3D7_1215000	0.513922	44.05919
PF3D7_1313600	0.42265	42.76757
PF3D7_1412800	0.527131	41.88417
PF3D7_1025900*	0.036837	41.71483
PF3D7_0726500	0.42265	41.54703
PF3D7_0920900	0.572557	40.28981
PF3D7_1350200	0.560854	40.20145
PF3D7_1415300	0.545728	40.11305
PF3D7_1420600	0.536702	38.92827
PF3D7_1401400	0.434832	38.59202
PF3D7_0621800	0.454146	37.29016
PF3D7_1333400	0.556272	35.31975
PF3D7_0720400	0.572864	34.89624

PF3D7_1369500	0.552491	34.73448
PF3D7_1304100	0.537068	33.86523
PF3D7_1110200	0.42265	33.7943
PF3D7_1104100	0.450857	33.54988
PF3D7_1245100	0.528334	33.08594
PF3D7_0810200	0.438036	32.14743
PF3D7_1343900	0.554064	31.61091
PF3D7_1124700	0.578104	31.56751
PF3D7_1417500	0.515136	29.39899
PF3D7_1429600	0.435953	28.7854
PF3D7_1028600	0.541413	28.09542
PF3D7_0501800	0.513791	27.91793
PF3D7_0819900	0.562331	27.88437
PF3D7_0812100	0.589087	27.24939
PF3D7_0703200	0.42265	23.59477
PF3D7_1474900	0.506825	22.85358
PF3D7_1227800	0.456909	22.52025
PF3D7_1455300	0.059427	20.98991
PF3D7_1147300	0.585798	17.0884
PF3D7_0817700*	0.046046	13.13373
PF3D7_1008100*	0.045561	9.74276
PF3D7_1459000	0.242274	9.671982
PF3D7_0219600	0.161754	9.192916
PF3D7_1410400	0.130096	9.170126
PF3D7_1412500	0.377778	8.512841
PF3D7_1446600	0.068575	8.459478
PF3D7_1463200	0.134039	8.274563
PF3D7_0617900	0.135458	7.198469
PF3D7_0918000	0.165215	6.904608
PF3D7_0218000	0.24382	6.802669
PF3D7_1311800	0.275492	6.742903
PF3D7_0728000	0.376976	6.363984
PF3D7_0802000	0.301281	6.15747
PF3D7_0610400	0.121379	6.067196
PF3D7_1136500.2	0.185597	6.058224
PF3D7_1310700	0.182262	5.969289
PF3D7_1437000	0.206791	5.938546
PF3D7_1252100	0.111503	5.86109
PF3D7_0705400	0.306264	5.841058
PF3D7_1452000	0.215905	5.678166
PF3D7_1231100	0.26228	5.522484
PF3D7_1345600	0.294377	5.437724
PF3D7_1343700	0.250503	5.409271
PF3D7_0525800	0.215568	5.293855
PF3D7_0416800	0.217309	5.265954
PF3D7_1304500	0.264296	5.228307
PF3D7_1342600	0.124001	5.027061
PF3D7_1105000	0.192004	4.93247
PF3D7_1223100	0.353319	4.830993
PF3D7_1219100	0.273368	4.824544
PF3D7_1206000	0.055691	4.766841
PF3D7_0525100	0.275381	4.61356
PF3D7_0918300	0.400057	4.525084
PF3D7_1453700	0.319607	4.4627
PF3D7_1361100	0.281325	4.435645
PF3D7_0503400	0.307564	4.348579
PF3D7_1343000	0.314187	4.345693
PF3D7_1368200	0.338665	4.252191
PF3D7_1320600	0.28759	4.239682

PF3D7_0904800	0.329752	4.163604
PF3D7_0209800	0.262389	4.141325
PF3D7_0501600	0.117721	4.138924
PF3D7_0721400	0.295638	4.10137
PF3D7_0922200	0.303108	4.095667
PF3D7_1142100	0.315031	4.082183
PF3D7_1012400	0.41993	4.045373
PF3D7_0320900	0.277614	4.035532
PF3D7_0515700	0.312932	4.024197
PF3D7_1124600	0.3602	4.002791
PF3D7_0423500	0.141626	4.002246
PF3D7_0619400	0.415354	3.997409
PF3D7_1361800	0.413808	3.995535
PF3D7_0822900	0.144537	3.939386
PF3D7_0930300	0.35293	3.926278
PF3D7_1020900	0.335913	3.911136
PF3D7_1409800	0.406997	3.892006
PF3D7_1105100	0.17349	3.879841
PF3D7_0617800	0.242294	3.826569
PF3D7_1241700	0.281318	3.805897
PF3D7_1237700	0.316212	3.761424
PF3D7_1306400	0.318102	3.710896
PF3D7_1355100	0.355038	3.708625
PF3D7_1104400	0.459122	3.697152
PF3D7_0501500	0.191351	3.695612
PF3D7_1473200	0.349809	3.689383
PF3D7_0922500	0.371076	3.656719
PF3D7_1368100	0.403092	3.643224
PF3D7_1205600	0.421643	3.61167
PF3D7_1354500	0.45472	3.599653
PF3D7_1011800	0.407446	3.591221
PF3D7_1437900	0.446391	3.587507
PF3D7_1136300	0.35674	3.554219
PF3D7_1145400	0.264337	3.540085
PF3D7_0714000	0.239683	3.513329
PF3D7_1149200	0.229414	3.466215
PF3D7_0207600	0.366785	3.455473
PF3D7_1338300	0.385987	3.44215
PF3D7_1462300	0.369987	3.424437
PF3D7_1116700	0.348543	3.416591
PF3D7_0104300	0.158485	3.402818
PF3D7_1238800	0.273403	3.355654
PF3D7_1427900	0.494259	3.332052
PF3D7_1008700	0.3621	3.328138
PF3D7_1030500	0.385302	3.327967
PF3D7_1033400	0.455817	3.326264
PF3D7_0628300.1	0.27148	3.293885
PF3D7_1471100	0.302123	3.290292
PF3D7_1416100	0.285736	3.282327
PF3D7_0319600	0.541368	3.228781
PF3D7_1352500	0.490819	3.217577
PF3D7_0706000	0.26531	3.211393
PF3D7_0915400	0.378133	3.169715
PF3D7_1341200	0.12271	3.152173
PF3D7_1402300	0.207316	3.111794
PF3D7_0624600	0.42142	3.105856
PF3D7_0627700	0.143315	3.105749
PF3D7_0807300	0.288574	3.085325
PF3D7_1226300	0.217154	3.074412

PF3D7_0707200	0.485495	3.052241
PF3D7_0812400	0.429463	3.039417
PF3D7_0813400	0.388962	3.030599
PF3D7_0315100	0.434221	3.024903
PF3D7_0415900	0.275566	3.018117
PF3D7_1235700	0.21522	3.010271
PF3D7_0629100	0.372528	3.00932
PF3D7_0708400	0.409941	2.98745
PF3D7_0524400	0.507215	2.983961
PF3D7_1447900	0.42359	2.913394
PF3D7_1134800	0.365578	2.897255
PF3D7_0500800	0.504546	2.890733
PF3D7_0920800	0.478117	2.848854
PF3D7_1410600	0.485068	2.837993
PF3D7_1133800*	0.02747	2.828779
PF3D7_1414400	0.324296	2.826255
PF3D7_1341300	0.086568	2.820414
PF3D7_0517400	0.311548	2.796868
PF3D7_1105800	0.420622	2.728357
PF3D7_1324900	0.508485	2.715179
PF3D7_0410800	0.872963	2.707323
PF3D7_0621200	0.534408	2.70612
PF3D7_0413600	0.423368	2.703859
PF3D7_0606700	0.431045	2.703578
PF3D7_1357000; PF3D7_1357100	0.416668	2.701815
PF3D7_1037500	0.399655	2.690849
PF3D7_1024800*	0.015712	2.623357
PF3D7_1232100	0.446715	2.597148
PF3D7_1342400	0.510726	2.582537
PF3D7_0716800	0.536177	2.581777
PF3D7_0621900	0.379153	2.569936
PF3D7_1460600	0.316026	2.531582
PF3D7_1457500	0.128196	2.526816
PF3D7_1349200	0.421154	2.520755
PF3D7_0929400	0.272102	2.520436
PF3D7_0811400	0.436695	2.503539
PF3D7_1408000	0.433473	2.495566
PF3D7_0903200	0.487768	2.483389
PF3D7_0629200	0.887773	2.479668
PF3D7_1468700	0.417279	2.44843
PF3D7_0302900	0.439216	2.447532
PF3D7_1246200	0.368142	2.445372
PF3D7_0608500	0.5327	2.424165
PF3D7_0528200	0.483299	2.422039
PF3D7_0818900	0.438989	2.419375
PF3D7_1007700	0.541613	2.409419
PF3D7_1023900	0.369098	2.409332
PF3D7_0527200	0.468635	2.403523
PF3D7_1360900.1	0.453455	2.397492
PF3D7_0302500	0.304081	2.386534
PF3D7_1414800	0.496348	2.382822
PF3D7_0523000	0.469895	2.382423
PF3D7_1130400	0.432962	2.379172
PF3D7_1445100	0.4466	2.374292
PF3D7_1357800	0.546901	2.362675
PF3D7_0810600	0.568478	2.334961
PF3D7_1446200	0.540297	2.328806
PF3D7_0424600	0.389048	2.321226

PF3D7_0608800	0.539483	2.307858
PF3D7_0517700	0.539959	2.294073
PF3D7_1204300	0.532936	2.289107
PF3D7_1351400*	0.047366	2.285433
PF3D7_0306800	0.532233	2.260644
PF3D7_1212700	0.054041	2.221261
PF3D7_1236100	0.631748	2.21527
PF3D7_1353900	0.536119	2.21319
PF3D7_0407800	0.512313	2.212876
PF3D7_0308200	0.560625	2.202209
PF3D7_1129100	0.531584	2.201592
PF3D7_0813300	0.600997	2.194779
PF3D7_1441200	0.451429	2.180353
PF3D7_1451100	0.568751	2.179153
PF3D7_1132800	0.226234	2.174841
PF3D7_1222300	0.534578	2.173168
PF3D7_0320300	0.554257	2.168811
PF3D7_1117700	0.450316	2.158974
PF3D7_0512600	0.3714	2.158829
PF3D7_1224000	0.439474	2.156098
PF3D7_1203700	0.519014	2.154604
PF3D7_1108600	0.620291	2.148314
PF3D7_1206200	0.533758	2.144565
PF3D7_1325100	0.458776	2.142059
PF3D7_0102200	0.501993	2.140303
PF3D7_1347500	0.546273	2.136767
PF3D7_1125500	0.540458	2.134968
PF3D7_1345100	0.122648	2.130135
PF3D7_1311500	0.384621	2.112086
PF3D7_1104200	0.564727	2.104183
PF3D7_1436000	0.90071	2.099921
PF3D7_0303200	0.57203	2.097408
PF3D7_0106300	0.457458	2.093801
PF3D7_0827900	0.593881	2.090694
PF3D7_0524000	0.534212	2.081414
PF3D7_1420400	0.607959	2.07679
PF3D7_1248900	0.442268	2.06721
PF3D7_0102900	0.585081	2.065593
PF3D7_0627500	0.576983	2.056962
PF3D7_0815600	0.568908	2.054877
PF3D7_1108700	0.909022	2.05448
PF3D7_0925900	0.545551	2.052626
PF3D7_1106000	0.552378	2.043305
PF3D7_0608700	0.573256	2.038194
PF3D7_1144900	0.461952	2.037441
PF3D7_1434800	0.576796	2.021641
PF3D7_1118200	0.494764	2.015318
PF3D7_1469200	0.096826	2.013333
PF3D7_1110100	0.908054	2.005728
PF3D7_0108300	0.55153	2.00412
PF3D7_0903700	0.364096	1.99756
PF3D7_0909800	0.631849	1.987047
PF3D7_0307100	0.593873	1.97622
PF3D7_0826700	0.645759	1.975802
PF3D7_1218500	0.491387	1.974501
PF3D7_0626800	0.624996	1.968718
PF3D7_0418200	0.547309	1.959174
PF3D7_1431700	0.11813	1.958989
PF3D7_0708800	0.513875	1.95821

PF3D7_0935800	0.477682	1.953221
PF3D7_0611400	0.510103	1.935916
PF3D7_0513100	0.605222	1.934219
PF3D7_1116800	0.455652	1.922538
PF3D7_1444800	0.615471	1.916519
PF3D7_0821700	0.044164	1.904816
PF3D7_1004000	0.530486	1.899333
PF3D7_1328300	0.91523	1.894969
PF3D7_1108400	0.545555	1.864042
PF3D7_1034900	0.698692	1.854625
PF3D7_0205900	0.543789	1.841406
PF3D7_0917900	0.662276	1.801344
PF3D7_1342800	0.540257	1.791366
PF3D7_1216900	0.723923	1.778655
PF3D7_0208700.2	0.158177	1.774581
PF3D7_1142600	0.273303	1.77361
PF3D7_1426100	0.537697	1.772602
PF3D7_0504800	0.343481	1.772441
PF3D7_0600200	0.929934	1.77058
PF3D7_0212900	0.497249	1.768025
PF3D7_1123500	0.435585	1.766387
PF3D7_1012900	0.166363	1.746628
PF3D7_0708300	0.273733	1.744488
PF3D7_1367100	0.107313	1.737831
PF3D7_1365900	0.596066	1.734477
PF3D7_1248700	0.744747	1.729327
PF3D7_1468800	0.513526	1.725103
PF3D7_0914700	0.452274	1.717694
PF3D7_1352700	0.928656	1.716331
PF3D7_1027800	0.187708	1.716102
PF3D7_0817900	0.35725	1.715824
PF3D7_0529800	0.922732	1.714903
PF3D7_0813000	0.406026	1.713471
PF3D7_0818200	0.628659	1.712264
PF3D7_0214700	0.93843	1.710392
PF3D7_0919000	0.701484	1.705013
PF3D7_0812000	0.24417	1.699323
PF3D7_1229400	0.93105	1.695591
PF3D7_0727400	0.599535	1.689787
PFNF54_00314	0.636745	1.687849
PF3D7_1309200	0.10722	1.684747
PF3D7_0310600.1	0.516731	1.683554
PF3D7_1008400	0.482712	1.659422
PF3D7_1206700	0.72178	1.656184
PF3D7_0602200	0.613577	1.651379
PF3D7_1121100	0.744881	1.622874
PF3D7_1460700	0.510229	1.622245
PF3D7_0424200	0.577055	1.600144
PF3D7_1026800	0.710237	1.580597
PF3D7_1021900	0.311094	1.579446
PF3D7_1229500	0.670479	1.578038
PF3D7_1245800	0.214561	1.577427
PF3D7_0309600	0.718769	1.575763
PF3D7_0308600	0.94309	1.572238
PF3D7_0929200	0.632535	1.569848
PF3D7_1130200	0.706693	1.569789
PF3D7_0831600	0.935166	1.563389
PF3D7_0319400	0.02955	1.546656
PF3D7_1357500	0.936064	1.546116

PF3D7_1007900	0.811993	1.540235
PF3D7_0103200	0.585244	1.539601
PF3D7_0420300	0.936675	1.537992
PF3D7_1107800	0.716324	1.530868
PF3D7_1016800	0.63838	1.529438
PF3D7_0832200.2	0.78137	1.528352
PF3D7_0307200	0.584768	1.525648
PF3D7_1211400	0.738599	1.512341
PF3D7_0710600	0.434949	1.492613
PF3D7_1463900	0.944529	1.492275
PF3D7_0912000	0.054134	1.484679
PF3D7_1340600	0.94934	1.481942
PF3D7_0612100	0.79045	1.479261
PF3D7_1019400	0.607176	1.475173
PF3D7_0927600	0.949412	1.467584
PF3D7_1458100	0.254084	1.462388
PF3D7_1233000	0.948306	1.460896
PF3D7_0508500	0.951818	1.457442
PF3D7_1132200	0.615659	1.452027
PF3D7_1362200	0.782568	1.44452
PF3D7_0802200	0.791015	1.443302
PF3D7_1037300	0.749139	1.442217
PF3D7_0610900	0.716637	1.436799
PF3D7_1435500	0.954816	1.434775
PF3D7_0905100	0.955535	1.431839
PF3D7_1224300	0.82961	1.427023
PF3D7_1134000	0.594693	1.418986
PF3D7_1346300	0.765676	1.402259
PF3D7_0811300	0.949045	1.399342
PF3D7_1308300	0.706391	1.398036
PF3D7_1464900	0.956271	1.391574
PF3D7_1103100	0.832695	1.381799
PF3D7_1305100	0.956119	1.376764
PF3D7_0507500	0.960606	1.366834
PF3D7_1331700	0.963806	1.366064
PF3D7_1213700	0.960434	1.360388
PF3D7_0410600	0.567117	1.352237
PF3D7_0823800	0.603498	1.348009
PF3D7_1424400	0.672818	1.347176
PF3D7_1468100	0.749801	1.342317
PF3D7_1407800	0.762503	1.342297
PF3D7_1359600	0.957	1.336233
PF3D7_1407300	0.715521	1.333934
PF3D7_1030100	0.267331	1.331614
PF3D7_1126900	0.96311	1.331488
PF3D7_0814000	0.435841	1.329486
PF3D7_1217500	0.306406	1.32484
PF3D7_1404900	0.963774	1.320504
PF3D7_0722400	0.752637	1.31998
PF3D7_0614500	0.424595	1.318505
PF3D7_0305600	0.855965	1.31726
PF3D7_1233600	0.964216	1.316612
PF3D7_1212300	0.095702	1.314393
PF3D7_1441400	0.778248	1.312032
PF3D7_1353800	0.963636	1.31037
PF3D7_1423700	0.870239	1.304355
PF3D7_1436600	0.965098	1.30381
PF3D7_0605100	0.968523	1.301294
PF3D7_0218500	0.969328	1.296935

PF3D7_0704600	0.966551	1.288243
PF3D7_1202900	0.636555	1.287919
PF3D7_1415200	0.968587	1.281226
PF3D7_1301700	0.819498	1.280581
PF3D7_0301600	0.683004	1.280147
PF3D7_1008800	0.608565	1.279775
PF3D7_0711000	0.970639	1.278791
PF3D7_1466400	0.791653	1.277387
PF3D7_1359400	0.968327	1.274727
PF3D7_1472200	0.967269	1.271798
PF3D7_0801800	0.793763	1.267173
PF3D7_1341900	0.971046	1.262124
PF3D7_0513300	0.967801	1.261908
PF3D7_1235600	0.745087	1.26119
PF3D7_0406100	0.971602	1.257967
PF3D7_1456700	0.971308	1.257941
PF3D7_1327800	0.970569	1.257472
PF3D7_1231600	0.694173	1.256907
PF3D7_0707400	0.795971	1.252936
PF3D7_0507100	0.497563	1.251853
PF3D7_0921000.2	0.973297	1.248982
PF3D7_0529500	0.971717	1.24775
PF3D7_1011400	0.971678	1.246107
PF3D7_1138500	0.620773	1.241587
PF3D7_0906600	0.686597	1.241308
PF3D7_1010600	0.643153	1.240021
PF3D7_1308200	0.853055	1.232275
PF3D7_1461900	0.971967	1.225237
PF3D7_0914400	0.845106	1.223805
PF3D7_1461300	0.879748	1.219782
PF3D7_1006600	0.870167	1.217232
PF3D7_0807700	0.146491	1.215749
PF3D7_0206700	0.975005	1.215343
PF3D7_1323100	0.664039	1.214355
PF3D7_1358700	0.806015	1.209785
PF3D7_1344200	0.97509	1.207712
PF3D7_1144000	0.730853	1.205696
PF3D7_0911400	0.732302	1.201296
PF3D7_0202400	0.90075	1.200197
PF3D7_1015900	0.796735	1.199458
PF3D7_0624000	0.979637	1.196271
PF3D7_0627100	0.152878	1.196164
PF3D7_1032100	0.840942	1.195007
PF3D7_0306300	0.976464	1.192279
PF3D7_1465900	0.808709	1.190981
PF3D7_0513200	0.97611	1.188971
PF3D7_0706400	0.40717	1.188861
PF3D7_0109500	0.976604	1.186935
PF3D7_0618200	0.980237	1.183902
PF3D7_0311100	0.591734	1.176206
PF3D7_1216200	0.977829	1.1747
PF3D7_0211800	0.979372	1.171484
PF3D7_0520900	0.890625	1.170984
PF3D7_0507600	0.981039	1.161591
PF3D7_1417200	0.98155	1.148632
PF3D7_1445900	0.88945	1.147855
PF3D7_0501100.2	0.983631	1.145829
PF3D7_0517000	0.903118	1.145215
PF3D7_0831700	0.879864	1.143153

PF3D7_1462800	0.904023	1.131128
PF3D7_0718500	0.985155	1.126417
PF3D7_1223400	0.849435	1.120332
PF3D7_1331800	0.852641	1.116136
PF3D7_0924700	0.835411	1.11426
PF3D7_1340300	0.812351	1.112225
PF3D7_1438900	0.913028	1.110353
PF3D7_0300700	0.797551	1.109215
PF3D7_0913200	0.691445	1.105254
PF3D7_0719700	0.926318	1.102723
PF3D7_1006200	0.955319	1.081424
PF3D7_1016300	0.955448	1.073545
PF3D7_1001200	0.991427	1.071959
PF3D7_0709000	0.945451	1.071352
PF3D7_1355700	0.827693	1.067294
PF3D7_0706500	0.965392	1.063037
PF3D7_1302800	0.934677	1.057441
PF3D7_1433500	0.954652	1.055322
PF3D7_0617200	0.970571	1.053574
PF3D7_0905400	0.937317	1.050779
PF3D7_1346100	0.951025	1.049135
PF3D7_0916700	0.975432	1.042426
PF3D7_0311800	0.995306	1.039554
PF3D7_1441100	0.996059	1.035952
PF3D7_1116200.1	0.996519	1.024831
PF3D7_0511500	0.996831	1.023566
PF3D7_0317600	0.977299	1.015782
PF3D7_0719600	0.999184	1.000564
PF3D7_0106800	0.99871	0.988813
PF3D7_0931100	0.975973	0.981405
PF3D7_0811600	0.963603	0.981041
PF3D7_1022400	0.985103	0.980774
PF3D7_0212100	0.996324	0.972348
PF3D7_1143300	0.996423	0.970102
PF3D7_1407900	0.979225	0.96288
PF3D7_1466800	0.958288	0.960322
PF3D7_1326300	0.99387	0.957367
PF3D7_0819100	0.882936	0.952123
PF3D7_1140800	0.991451	0.939677
PF3D7_1216300	0.925741	0.937317
PF3D7_1447000	0.903784	0.932764
PF3D7_1338200	0.908896	0.925329
PF3D7_1414300	0.829924	0.923107
PF3D7_0823200	0.946396	0.920134
PF3D7_0903900	0.855579	0.918695
PF3D7_0721600	0.889271	0.910912
PF3D7_0516900	0.781503	0.906422
PF3D7_0704200	0.550017	0.890027
PF3D7_1202200	0.901814	0.881536
PF3D7_1319300	0.663448	0.879092
PF3D7_1149000	0.793347	0.87564
PF3D7_1114200	0.835133	0.873467
PF3D7_0312800	0.751698	0.862425
PF3D7_1422700	0.664448	0.858899
PF3D7_0923900	0.893133	0.854166
PF3D7_1003500	0.828941	0.849428
PF3D7_1400200	0.796497	0.842648
PF3D7_0508600	0.411651	0.837067
PF3D7_1407100	0.822972	0.835949

PF3D7_1009400	0.975636	0.827384
PF3D7_0516200	0.844371	0.827112
PF3D7_0316800	0.620058	0.826674
PF3D7_0607000	0.877173	0.823897
PF3D7_1027300	0.873932	0.819805
PF3D7_1330800	0.928637	0.81924
PF3D7_1200700	0.089827	0.811738
PF3D7_1016400	0.734231	0.808352
PF3D7_0202000	0.681183	0.79779
PF3D7_0422400	0.548105	0.793256
PF3D7_1452700	0.287836	0.788029
PF3D7_0936800	0.803724	0.785583
PF3D7_0821300	0.41666	0.743215
PF3D7_0604500	0.807786	0.741906
PF3D7_0414100	0.521001	0.7407
PF3D7_0318900	0.688761	0.731671
PF3D7_1118500	0.824301	0.727951
PF3D7_0501200	0.684837	0.688833
PF3D7_1407500	0.719047	0.686223
PF3D7_1137300	0.714999	0.682736
PF3D7_0828200	0.780928	0.677034
PF3D7_0527900	0.256081	0.657495
PF3D7_0720100	0.936516	0.651948
PF3D7_1242700	0.309831	0.628264
PF3D7_0520000	0.231245	0.625992
PF3D7_0814200	0.683133	0.60853
PF3D7_0708500	0.070218	0.593013
PF3D7_0418300	0.144317	0.591995
PF3D7_1409600	0.085804	0.586343
PF3D7_1309100	0.354003	0.578259
PF3D7_1006800	0.703832	0.577597
PF3D7_1235300	0.924115	0.576707
PF3D7_1317800	0.079603	0.557319
PF3D7_1424100	0.449156	0.546779
PF3D7_1305900	0.436801	0.54372
PF3D7_1342000	0.259037	0.542317
PF3D7_1323400	0.197504	0.541139
PF3D7_1120100	0.51015	0.540167
PF3D7_1445400	0.331337	0.523743
PF3D7_0818000	0.094054	0.511838
PF3D7_1220400	0.201491	0.494812
PF3D7_0913000	0.314509	0.488387
PF3D7_0210100.1	0.059069	0.472419
PF3D7_1109900	0.133118	0.465568
PF3D7_0322900*	0.047405	0.463141
PF3D7_1149400*	0.035708	0.457192
PF3D7_0502100	0.187419	0.457101
PF3D7_1307800*	0.039349	0.44811
PF3D7_0830500*	0.004259	0.436859
PF3D7_0705700*	0.013091	0.432009
PF3D7_0603000*	0.007188	0.430142
PF3D7_0201800	0.391752	0.429592
PF3D7_0503800	0.192327	0.421699
PF3D7_0310300	0.262178	0.417904
PF3D7_0730800.1*	0.008761	0.398615
PF3D7_0623100	0.190865	0.394661
PF3D7_1120000	0.69412	0.394323
PF3D7_0517300	0.325939	0.392907
PF3D7_1002100	0.060717	0.389309

PF3D7_0612900	0.184644	0.389291
PF3D7_0202200*	0.036126	0.389066
PF3D7_1353200	0.115138	0.388165
PF3D7_1002000	0.119739	0.381984
PF3D7_0803000	0.139734	0.37718
PF3D7_0606100*	0.012302	0.360932
PF3D7_0306900	0.298253	0.357998
PF3D7_0519400*	0.020429	0.348924
PF3D7_1217200	0.106919	0.340864
PF3D7_0702300	0.053266	0.337329
PF3D7_0523400	0.406692	0.332575
PF3D7_1107700*	0.02177	0.327664
PF3D7_1126200	0.224297	0.322893
PF3D7_0424500*	0.016223	0.306397
PF3D7_0924100	0.153886	0.301545
PF3D7_1426000	0.108581	0.295611
PF3D7_0618300*	0.033285	0.294978
PF3D7_1408600	0.067338	0.288996
PF3D7_1209300	0.787412	0.285737
PF3D7_1205400	0.191637	0.279896
PF3D7_1314700	0.065126	0.276049
PF3D7_1008900	0.346059	0.268043
PF3D7_0501300*	0.003354	0.267626
PF3D7_1130100	0.106036	0.264752
PF3D7_0831400	0.068543	0.255753
PF3D7_0935900*	0.048193	0.254649
PF3D7_0801000	0.079635	0.247541
PF3D7_0501000	0.100034	0.242905
PF3D7_0702500	0.121267	0.239615
PF3D7_0210900	0.268814	0.238338
PF3D7_1001400	0.168018	0.229825
PF3D7_1301400	0.100383	0.22233
PF3D7_0304400.1	0.110585	0.222299
PF3D7_0813900*	0.015517	0.220904
PF3D7_1402500	0.082064	0.213605
PF3D7_0804000	0.170556	0.209241
PF3D7_1001900*	0.004824	0.199424
PF3D7_1445700	0.360575	0.199085
PF3D7_1105400*	0.036055	0.198786
PF3D7_0403200*	0.031842	0.198313
PF3D7_1421200	0.136744	0.194646
PF3D7_1354300	0.065251	0.191073
PF3D7_0415500	0.130676	0.188085
PF3D7_1200600*	0.035234	0.18159
PF3D7_1401200*	0.030662	0.178766
PF3D7_1004400	0.27536	0.176453
PF3D7_0730900*	0.015037	0.170828
PF3D7_1358800*	0.001393	0.170539
PF3D7_0611700*	0.035372	0.169457
PF3D7_0508700	0.266933	0.165199
PF3D7_1110400*	0.029096	0.164843
PF3D7_1302000*	0.007283	0.161415
PF3D7_1036900	0.275912	0.157453
PF3D7_1370300	0.062978	0.156104
PF3D7_0936300	0.154472	0.154179
PF3D7_0702400	0.052121	0.148036
PF3D7_1408500*	0.049797	0.14681
PF3D7_0705500*	0.005903	0.14097
PF3D7_0601900*	0.026383	0.133174

PF3D7_1124900	0.054086	0.131621
PF3D7_0217800	0.105473	0.121997
PF3D7_0812500	0.058132	0.116272
PF3D7_1018200	0.656087	0.115751
PF3D7_1142500*	0.007541	0.099962
PF3D7_1134200*	0.000901	0.099812
PF3D7_1460300*	0.026969	0.098463
PF3D7_1109400*	0.001477	0.097428
PF3D7_1451900	0.13721	0.097131
PF3D7_0218400*	0.031754	0.09426
PF3D7_0731100*	0.000639	0.083626
PF3D7_0506100	0.103068	0.07428
PF3D7_0519700*	0.004227	0.070377
PF3D7_0201900	0.093247	0.065535
PF3D7_0731500	0.504273	0.064711
PF3D7_0727800	0.624448	0.064076
PF3D7_1113400	0.66776	0.057204
PF3D7_0401800	0.514627	0.054408
PF3D7_0528800	0.053453	0.053859
PF3D7_0113000*	0.003554	0.051285
PF3D7_1416900	0.554938	0.04653
PF3D7_1459600	0.592598	0.044783
PF3D7_0711500	0.454575	0.044109
PF3D7_1431300	0.600469	0.04343
PF3D7_1357700	0.568301	0.043138
PF3D7_1242500	0.482651	0.042701
PF3D7_1134100	0.481931	0.040499
PF3D7_0700100	0.597021	0.040202
PF3D7_1355800	0.496833	0.039818
PF3D7_1234800	0.633198	0.039709
PF3D7_0731300*	0.025013	0.038537
PF3D7_0907200	0.540615	0.037235
PF3D7_0907700	0.495851	0.033444
PF3D7_1126000	0.538111	0.03336
PF3D7_1434300	0.512077	0.032709
PF3D7_1135400	0.570621	0.031856
PF3D7_0720700	0.455765	0.026605
PF3D7_1438000	0.501677	0.026239
PF3D7_1001100.1	0.42265	0.025816
PF3D7_1336800	0.42265	0.023808
PF3D7_1107300	0.454177	0.019163
PF3D7_0522300	0.44012	0.01788
PF3D7_1461600	0.432596	0.017603
PF3D7_1033700	0.42265	0.017522
PF3D7_0821200	0.387063	0.017139
PF3D7_0322000	0.439854	0.016416
PF3D7_1415400	0.42265	0.015929
PF3D7_1133700	0.072808	0.014452
PF3D7_0317700	0.413183	0.013795
PF3D7_0105200	0.418841	0.01258
PF3D7_0936000	0.374294	0.009636
PF3D7_0202100	0.368527	0.009101
PF3D7_0615300	0.432105	0.009056
PF3D7_1317400	0.347919	0.00826
PF3D7_1230800	0.369583	0.006953
PF3D7_1133100	0.332755	0.00673
PF3D7_0409800	0.312709	0.006028
PF3D7_0804700	0.383297	0.0052
PF3D7_1022100	0.338397	0.004743

PF3D7_0417800	0.323044	0.003938
PF3D7_0615700	0.301104	0.002496
PF3D7_0722000	0.25086	0.002312
PF3D7_1353100	0.289806	0.002135
PF3D7_0503300	0.283958	0.001965
PF3D7_1239700	0.184385	0.001788
PF3D7_0707900	0.228019	0.001769
PF3D7_1002400.2	0.287238	0.001614
PF3D7_0109700	0.208103	0.001327
PF3D7_1366300	0.250748	0.001165
PF3D7_1018600	0.181794	0.001112
PF3D7_1200610	0.184125	0.000759
PF3D7_1213800	0.246489	0.000644
PF3D7_0721300	0.183792	0.000643
PF3D7_0518500	0.228069	0.000503
PF3D7_1021500	0.183504	0.000456
PF3D7_1469300	0.128854	0.000345
PF3D7_1026000	0.169533	0.000342
PF3D7_0521000	0.177664	0.000306
PF3D7_0803100	0.144146	0.000304
PF3D7_0723400	0.203372	0.000254
PF3D7_0723900	0.163363	0.000233
PF3D7_0528600	0.170121	0.000152
PF3D7_0113300	0.173266	0.000151
PF3D7_0818400	0.15814	0.000126
PF3D7_1132600	0.157458	0.000104
PF3D7_1464200	0.148595	8.23E-05
PF3D7_1110300	0.13758	6.61E-05
PF3D7_1423000	0.150262	5.65E-05
PF3D7_1354600	0.13627	5.12E-05
PF3D7_0827000*	0.000459	9.17E-06
PF3D7_0113700*	0.000269	4.77E-06
PF3D7_1348200*	5.67E-05	4.43E-06
PF3D7_1247900*	0.000835	2.01E-06
PF3D7_0420100*	5.14E-06	1.37E-06
PF3D7_0915600*	0.000498	1.21E-06